

Wilfrid Laurier University

Scholars Commons @ Laurier

Theses and Dissertations (Comprehensive)

2016

Theoretical investigations of Zinc Blende and Wurtzite semiconductor quantum wells on the rotated substrates

Igor Ivashev

Wilfrid Laurier University, ivas5210@mylaurier.ca

Follow this and additional works at: <https://scholars.wlu.ca/etd>



Part of the [Condensed Matter Physics Commons](#)

Recommended Citation

Ivashev, Igor, "Theoretical investigations of Zinc Blende and Wurtzite semiconductor quantum wells on the rotated substrates" (2016). *Theses and Dissertations (Comprehensive)*. 1833.

<https://scholars.wlu.ca/etd/1833>

This Thesis is brought to you for free and open access by Scholars Commons @ Laurier. It has been accepted for inclusion in Theses and Dissertations (Comprehensive) by an authorized administrator of Scholars Commons @ Laurier. For more information, please contact scholarscommons@wlu.ca.

Masters Thesis

Theoretical investigations of Zinc Blende and Wurtzite semiconductor quantum wells on the rotated substrates

By

Igor IVASHEV

ivas5210@mylaurier.ca

Supervisor: Dr. Marek WARTAK

May 2016

This thesis is submitted in partial fulfillment of the requirement of
MSc in Mathematics

Department of Mathematics
Wilfrid Laurier University
Waterloo, ON

“Thanks to my solid academic training, today I can write hundreds of words on virtually any topic without possessing a shred of information, which is how I got a good job in journalism.”

Dave Barry

Acknowledgements

I would like to acknowledge all who have made this work possible. I am especially grateful to Professor Marek Stanislaw Wartak, for his invaluable contribution to research on my thesis. I also benefited from courses read by Professor Roderick Melnik and Professor Connell McCluskey, who shared their knowledge with me on instruments, used in my research. Special thanks to University members: Lynda Clarke, Trevor Saunderson, Hasan Shodiev and my colleague Ben Skinner, who kept me busy and shared experience with me.

I acknowledge the ASPIRE and NSERC for a very crucial financial support, and making possible my travel to Nova Scotia.

I am deeply indebted to my brother and father for their unconditional financial and moral support. I am grateful to my family and my beloved lady Ziyoda for their love and dedication. Without their constant support this work would be impossible.

Abstract

We present a comprehensive set of computations of effective mass theory for both the Kane's parabolic band approximation and Luttinger-Kohn's valence band mixing approximation. We generalize the $k \cdot p$ method to be able to evaluate band structures for the materials such as zincblende InGaAsN and GaAsBi compounds used in long wavelength lasers and wurtzite materials used in short wavelength lasers. We investigate methodology to study band structure of semiconductors that are grown away from natural direction. The strain influence is introduced via Bir and Pikus model. It is expected that band structure is strongly dependent on direction of crystal growth and the strain plays here an important role. The energy levels, and consequently the optical matrix elements, change with orientation. The optical matrix elements are directly involved in optical gain calculations, so the growth orientation provides a tool, to control gain in semiconductor laser.

Contents

Acknowledgements	ii
Abstract	iii
Contents	iv
List of Figures	viii
List of Tables	x
Abbreviations	xi
Physical Constants	xii
Symbols	xiii
1 Introduction	1
1.1 Studies of cubic systems	3
1.2 Studies of hexagonal systems	5
1.3 Novel methods of band structure calculations	6
1.4 About the thesis	7
2 Construction of Kane's model Hamiltonian	8
2.1 Hamiltonian for Schrödinger equation and basis functions	9
2.2 Explicit calculations of matrix elements of \mathbf{H}	13
2.2.1 Matrix element \mathbf{H}_{11}	13
2.2.2 Matrix element \mathbf{H}_{12}	14
2.2.3 Matrix element \mathbf{H}_{13}	17
2.2.4 Matrix element \mathbf{H}_{22}	17
2.2.5 Matrix element \mathbf{H}_{23}	19
2.2.6 Matrix element \mathbf{H}_{33}	21

2.3	Explicit Kane's matrix Hamiltonian	21
2.4	Corrections to basis functions	22
3	Construction of Luttinger-Kohn's model Hamiltonian	27
3.1	Cubic symmetry (Zincblende)	27
3.1.1	The Hamiltonian and the basis functions	27
3.1.2	Matrix in $ X\rangle Y\rangle Z\rangle$ basis	31
3.1.3	Matrix in $u_{n0}(\vec{r})$ basis	34
3.1.4	Strain effects on band structures	36
3.2	Hexagonal symmetry (Wurtzite)	45
3.2.1	The Hamiltonian and the Basis functions	45
3.2.2	Hamiltonian matrix in $ X\rangle Y\rangle Z\rangle$ basis	49
3.2.3	Matrix in u_n basis	50
3.2.4	Strain effects on band structures	52
4	Luttinger-Kohn's model Hamiltonian for semiconductors on arbitrary-oriented substrates	56
4.1	Rotation of Luttinger-Kohn's Hamiltonian for hole states using angular momentum matrices (4×4) for zincblende crystal	56
4.1.1	Explanation of transformations	56
4.1.2	Coordinate transformations	57
4.1.3	Solution for rotated Hamiltonian	59
4.1.4	Explicit form of rotated Luttinger effective-mass Hamiltonian	60
4.2	Rotation of Luttinger-Kohn's Hamiltonian for hole states using rotation matrix (4×4) for zincblende crystal	61
4.2.1	Introduction	61
4.2.2	Rotation matrix	63
4.2.3	Basis functions for arbitrary growth direction	66
4.2.4	Matrix elements for rotated Luttinger-Kohn Hamiltonian	67
4.3	Generalization of rotated (4×4) Hamiltonian to rotated (6×6) Hamiltonian for zincblende crystal	69
4.4	Rotation of Luttinger-Kohn's Hamiltonian for conduction, hole and spin split off states using rotation matrix (8×8) for zincblende crystal	70
4.4.1	Basis functions and notation	70
4.4.2	(8×8) Luttinger-Kohn Hamiltonian for arbitrary growth direction	71
4.4.3	Hamiltonian matrix	73
4.5	Generalization of (8×8) Hamiltonian rotations to (10×10) Hamiltonian for zincblende crystal	75
4.6	Strain effects on band structures for arbitrary oriented zincblende crystal	76
4.7	Rotation of Luttinger-Kohn's Hamiltonian for hole states using rotation matrix (6×6) for wurtzite crystal	84
4.7.1	Introduction	84

4.7.2	Basis functions	85
4.7.3	Matrix elements for rotated Luttinger-Kohn Hamiltonian	85
4.8	Strain effects on band structures for arbitrary oriented wurtzite crystal	87
5	Numerical method for band structure calculations	94
5.1	Plane wave expansion method for 4×4 Hamiltonian	96
5.1.1	Reading initial data	96
5.1.2	Material parameters	96
5.1.3	Fourier transform and matrix of Fourier coefficients	98
5.2	Generalization plane wave expansion for 4×4 Hamiltonian to 6 - 14 band Hamiltonians	99
5.2.1	6×6 Hamiltonian	100
5.2.2	8×8 Hamiltonian	100
5.2.3	10×10 Hamiltonian	101
5.2.4	14×14 Hamiltonian	101
6	Band structure calculations results	102
6.1	Band structures for zincblende semiconductors	102
6.1.1	4×4 Hamiltonian	102
6.1.2	6×6 Hamiltonian	102
6.1.3	8×8 Hamiltonian	104
6.1.4	10×10 Hamiltonian	106
6.1.5	14×14 Hamiltonian	108
7	Optical applications	113
7.1	Matrix elements in optical transitions	113
7.1.1	Wave functions	113
7.1.2	Optical momentum matrix element	115
7.1.3	Application of the optical momentum matrix element	118
7.1.4	Expressions for matrix elements $\mathbf{M}_{c-hh, lh, so}$	119
7.1.5	Cell periodic functions part for bulk semiconductor	121
7.1.6	Cell periodic functions part for quantum well	123
8	Conclusions	127
A	Maple 16 code used in calculations of rotated Luttinger effective-mass Hamiltonian	129
B	Maple 16 code used in matrix elements rotations 4×4 zincblende and 6×6 wurtzite	132
B.1	Zincblende	132

B.2 Wurtzite	134
C Maple 16 code used in matrix elements calculations 8×8	137
D Basis functions for 6×6 LKH for arbitrary orientation	142
D.1 Zincblende	142
D.2 Wurtzite	143
E Tables of material parameters for various semiconductor materials	145
F Notes on point group theory	148
Bibliography	154

List of Figures

2.1	The $k \cdot p$ method in (a) Kane's model: only a conduction, a heavy hole, a light hole and a spin-orbit split-off bands with double degeneracy are considered, all other bands discarded; (b) LKM: the heavy hole, light hole and spin split-off bands in double degeneracy are of interest and called as class A, all other bands are denoted as class B. The effect of class B on class A is taken into account.	10
2.2	Evolution of atomic s - and p -states, to form conduction and valence zone exists in semiconductors; E_F - Fermi level; four zones on the right hand of the figure are (from top to bottom): conduction bands formed by antibonding p - and s -states and below Fermi level are valence bands formed by bonding p - and s -states.	12
3.1	T_d^2 symmetry group has main symmetry axis, which is a diagonal of cube, and rotation of coordinate system around this axis for each 120° degree causes the axes to convert as such: $x \rightarrow y, y \rightarrow z, z \rightarrow x$	33
3.2	Positions of vectors \vec{r} and \vec{r}' for atom A in (a) unstrained and (b) strained lattice.	37
4.1	Rotation of coordinate system: a) x, y and z are axes of Cartesian coordinate system where z axis is perpendicular to (001) plane; 1, 2 and 3 are axes of rotated coordinate system; axis 2 is perpendicular to 1-3 plane which is parallel to $(\bar{1}10)$ plane; crystal is growing along axis 3; the system is rotated about axis 2 for angle θ ; b) side view of x - z and 1-3 planes; c) upside down view of x - y and 1-2 planes, coordinate system rotated to $\pi/4$ angle.	57
4.2	Growth surfaces in Miller indices notation: a - (110), b - (111), c - (112), d - (113), e - (11 ∞). Growth direction is perpendicular to plane which is colored gray.	58
4.3	General transformation for arbitrary rotation from old to new rectangular coordinate system: a) axes x, y, z correspond to axes 1, 2, 3 respectively, which are perpendicular to each other; x - y, x - z and 1-3 planes are indicated; angle ϕ is the angle between x - z plane and 1-3 plane; angle θ is the angle between z axis and 3 axis; both of the angles run from 0 to $\pi/2$; b) side view of x - z and 1-3 planes, angle of rotation θ indicated; c) upside down view of x - y and 1-2 planes, coordinate system rotated to angle ϕ	62

4.4	The Cartesian coordinate system in wurtzite primitive cell.	84
5.1	QW profiles for the conduction and valence bands of a GaAs/AlGaAs system.	95
6.1	Hole subband for unstrained superlattices grown on (11N)-oriented substrates with (a) $N = \infty$, (b) $N = 0$, (c) $N = 1$. [44]	103
6.2	Hole subband for unstrained superlattices grown on (11N)-oriented substrates with (a) $N = \infty$, (b) $N = 0$, (c) $N = 1$. [this work]	104
6.3	Hole subband for (111)-oriented superlattices under the uniaxial stresses $T = 2.0$ and 2.5 kbar. [44]	105
6.4	Hole subband for (111)-oriented superlattices under the uniaxial stresses (a) $T = 2.0$ and (b) 2.5 kbar. [this work]	105
6.5	Hole subband for unstrained superlattices grown on (11N)-oriented substrates with (a) $N = \infty$, (b) $N = 0$, (c) $N = 1$. [45]	106
6.6	Hole subband for unstrained superlattices grown on (11N)-oriented substrates with (a) $N = \infty$, (b) $N = 0$, (c) $N = 1$. [this work]	106
6.7	Hole subband for (111)-oriented superlattices under the uniaxial stresses (a) $T = 1.0 \cdot 10^9 Pa$ and (b) $T = 2.0 \cdot 10^9 Pa$. [45]	107
6.8	Hole subband for (111)-oriented superlattices under the uniaxial stresses (a) $T = 1.0 \cdot 10^9 Pa$ and (b) $T = 2.0 \cdot 10^9 Pa$. [this work]	107
6.9	Band structure for unstrained AlGaAs/InGaAs QWs grown on (11N)-oriented substrates with (a) $N = \infty$, (b) $N = 0$, (c) $N = 1$	108
6.10	Electron and hole energy dispersion curves of the unstrained (110)-, (111)-, (113), and (001)-oriented QWs. [46]	109
6.11	Band structure for unstrained InGaAsN/GaAs QWs grown on (a) (110)-, (b) (111)-, (c) (113), and (d) (001)-oriented QWs. [this work]	110
6.12	Band structure for unstrained InGaAsN/GaAs QWs grown on (a) (001)-, (b) (110)-, (c) (111), (d) (112), and (e) (113)-oriented QWs. [this work]	111
6.13	Band structure for unstrained GaAsBi/GaAs QWs grown on (11N)-oriented substrates with (a) $N = \infty$, (b) $N = 0$, (c) $N = 1$, (d) $N = 2$	112

List of Tables

E.1	Important band structure parameters for zincblende GaAs, AlAs, InAs, InP and GaP [61](p. 803)	146
E.2	Important band structure parameters for wurtzite GaN, AlN and InN [61](p. 807)	147
F.1	Representations for cubic crystals	152
F.2	Representations for wurtzite crystals	152

Abbreviations

LKH	L uttinger K ohn's H amiltonian
BPH	B ir and P ikus H amiltonian
LKM	L uttinger K ohn's M odel
BAC	B and A nti C rossing
QW	Q uantum W ell
RHEED	R eflection H igh E nergy E lectron D iffraction

Physical Constants

Speed of Light $c = 2.997\,924\,58 \times 10^8 \text{ ms}^{-\text{S}}$ (exact)

Planck constant $\hbar = 1.054\,571\,726(47) \times 10^{-34} \text{ Js}$

Planck constant $\hbar = 6.582\,119\,28(15) \times 10^{-16} \text{ eVs}$

Electron mass $m_e = 9.10938356 \cdot 10^{-31} \text{ kg}$

Electron charge $e_0 = -1.6021766209 \cdot 10^{-19} \text{ C}$

Symbols

m^*	effective mass	m_e
x, y, z	Cartesian coordinate system axes	
X, Y, Z	spherical harmonics (wave functions)	
Y_{lm}	general expression for spherical harmonics	
$ i\rangle$	Kane's basis	$i = 1, 2, 3, 4, \bar{1}, \bar{2}, \bar{3}, \bar{4}$
$ u_i\rangle$ or $ u_{0i}\rangle$	Luttinger-Kohn's basis	$i = 1, 2, 3, 4, 5, 6$
\vec{k}	wave vector	
\vec{p}	momentum operator	

Dedicated to my family, with love

Chapter 1

Introduction

At present time many consumer and industrial technologies are based on lasers¹, MOS-FETs, bipolar transistors, diodes, semiconductor sensors of various types and other low power semiconductor devices, of which the important parameters are: size, shock resistance, reliability etc. The most commonly used lasers are made of solid state semiconductor materials. There are several ways to produce a laser diode out of semiconductor material. The present work will concentrate on quantum wells (QWs).

The laser diode is a device, similar to what is known as rectifier diode, but with some important differences. Rectifier diode has two regions: p-type and n-type on each side of the device, whereas the laser diode has a third region in the middle of these two that is made of another material, as a variant: p-type doped, undoped intrinsic and n-type doped semiconductors. When electric current is applied to this semiconductor pie, the carriers are pumped into the middle of the undoped region: electrons from n-type side and holes from p-type side. The goal of pumping the carriers is to make them to recombine² and produce photons. The use of direct bandgap semiconductors makes the recombination process to convert all the energy into radiation.

There are two types of radiative emission: spontaneous and stimulated. Spontaneous emission events occur randomly whereas the stimulated emission is driven by external factors. Stimulated emission is important for lasers while spontaneous emission dominates in light emitting diodes (LEDs). The stimulated emission generates pack of photons with

¹laser - acronym for “light amplification by stimulated emission of radiation”.

²Recombinations means disappearance of one pair of carriers in semiconductor with the energy output.

the same frequency, phase and polarization. To produce a laser beam this pack should increase in its magnitude. This process creates an optical gain. Gain in laser crystal may be achieved by polishing it on two sides to form mirrors: one is fully reflective and one is semi-reflective. This structure is known as a Fabry-Pérot resonator. The laser beam propagates through the semi-reflective mirror. Size of the active³ region is relatively small, thus the laser beam is coming out through the slot of the size $20\text{-}100 \text{ \AA} = 2\text{-}10 \text{ nm}$, whereas the light wavelengths vary from $\approx 400 \text{ nm}$ to 3000 nm which results in a significant diffraction effect on the output laser beam. Thus the semiconductor laser usually requires the optical system at the output, focused on a particular point.

Semiconductor laser has many advantages including size, efficiency in terms of consuming electricity, etc. Also, variety of semiconductor materials allow to fabricate lasers with many different wavelengths which are required by different applications. Gas lasers, such as the widely used Helium-Neon laser in comparison with the semiconductor lasers, are costly to change its operational wavelength. Typical wavelength emitted by Helium-Neon laser is 633 nm , while the semiconductor lasers have a variety of operational wavelengths.

QW used in semiconductor laser is formed by at least two materials with different bandgap energies to make a potential barrier. The value of bandgap energy has a significant influence on the operational wavelength of the resulting laser. Apart from that, the probabilities of the populations of energy bands depend on band structure, which affect the laser output. The external factors which have an influence on band structures are: well width, barriers width, material compositions, strain and crystal orientation.

Further research in scientific methods was attempted to improve properties of semiconductor lasers. The well thickness and strain may not be the only ways to improve their properties. A possible method to consider is QW grown on the substrate oriented away from natural direction, which is (001) when using Miller indices notation. Over the last twenty years there has been increased interest in analyzing the properties of semiconductor structures at arbitrary oriented substrates; first for cubic crystals and then for hexagonal crystals. Research is done mostly for a practical reason: how to improve the properties of devices. It is expected that many properties of crystal lattices will depend on the growth orientation. As of now most studies were done for cubic crystals, with only a limited amount of work performed for hexagonal semiconductors.

³The active region's material responsible for the optical gain.

1.1 Studies of cubic systems

Typical materials which exhibit cubic⁴ symmetry, known as zincblende sometimes called as sphalerite⁵, are *GaAs*, *CdTe*, *InAs*, *InP*, *GaP*, *AlAs*, *GaBi* and many other compounds (including not only semiconductor materials) such as *AlGaAs* and *InGaAsN* which are used in photonics applications.

Early studies of non (001)-oriented substrates began from considering the (11 N)-oriented growth of *GaAs*. It has been shown that for some particular orientations, such as (110) and (112), the nucleation and morphology are better than (001) orientation. Chang [1] reported successful fabrication by molecular beam epitaxy of high quality *Ge-GaAs* superlattices on (100) oriented *GaAs* substrate at 400°C, and provided experimental data for orientation differences obtained by reflection high energy electron diffraction (RHEED). Later, he provided in [2] similar experimental data for surface of *Ge-GaAs* systems for differently oriented substrates. Wright et al. [3] discussed *GaP* grown on (211) oriented *Si* substrate and provided experimental data for reflection electron diffraction and Hall effect voltages. He also constructed p-n junction for different orientations with this material. Uppal et al. [4] provided similar work for *GaAs* grown on *Si* substrate.

With the semiconductor devices' aspect in mind, McKenna et al. [5] considered p-n junction diode made of *GaP* material. They discussed orientational dependence of power requirements of the diode prepared by liquid beam epitaxy, made of *AlGaAs* grown of *GaAs* substrate, and concluded that the orientation of growth is very important. Pearsall et al. [6] presented first systematic study of the dependence of impact ionization by electrons and holes on the details of the electronic band structure. They considered *GaAs* and determined that the ionization rate strongly depended on composition of the material (*GaAsSb*) and the orientation of growth.

By early 1991 there were already many reports about successful growth of high quality *GaAs/Al_xGa_{1-x}As* superlattices with (11 N) orientation which had very promising optical and electronic properties as compared to the usual (001) orientation. For instance, Wang [7] reported on the experiments with (11 N)-oriented *GaAs/Al_xGa_{1-x}As* with $N = 2, 3, 5, 7, 9$. His experiments confirm that the *Si* inserted into *GaAs* acts as p-

⁴The cubic symmetry also means rock-salt and diamond, but in the context of this work the cubic means particularly zincblende.

⁵The mineral Sphalerite is a wide band gap semiconductor with chemical structure ZnS.

or n-type dopant depending on orientation and surface index. The two-dimensional carrier mobility in modulation-doped heterostructures grown on $(11N)$ planes varies from $\sim 6.3 \cdot 10^4$ up to $\sim 6.4 \cdot 10^5$ $\text{cm}^2 \text{V}^{-1} \text{s}^{-1}$ (10 times difference!) at low temperatures (4.2 K). In addition, Subbanna et al. [8] presented first detailed study of the *AlGaAs* grown on (211) oriented *GaAs* substrate and provided photoluminescence spectra of *A* and *B* faces of (211) grown material, which are ~ 30 times different (*B* is stronger than *A*) and both much stronger than the same spectra for (100) orientation. Besides, Allen et al. [9] showed that at low temperatures (4 K), the (110) orientation leads to strong exciton photoluminescence emission and at room temperature the electron mobility is as high as $5700 \text{cm}^2 \text{V}^{-1} \text{s}^{-1}$ (lower than for (100) orientation) for carrier concentration $n \sim 4 \cdot 10^{15} \text{cm}^{-2}$. Hayakawa et al. [10] discovered that for (111) oriented structure the photoluminescence emission efficiency is higher than for (001) orientation and the threshold current for quantum well lasers is smaller for (111) than for (001) oriented crystals. Many groups [11][12][13][14] investigated variation of the binding energy of the $1s$ exciton for (001), (110), (111), (113) and (310) orientations and it was found that the binding energy of the light-hole exciton is more sensitive to the substrate orientation than the heavy-hole exciton.

By 2001 there were many reports of successful high quality grown substrates of various high index substrates of many semiconductor materials with cubic crystal structure besides *GaAs* (*InP*, *ZnSe*, *ZnS* etc.). Xu et al. [15] studied the exciton-localization effect of *AlAs* grown on (311) oriented *GaAs* substrates and obtained the redshift compared to the exciton emission of (100) oriented samples. To understand the formation and self-organization of quantum dots on novel index surfaces Henini et al. [16] investigated structural and optical properties of *InAs* layers grown on high index *GaAs* surfaces. Polimeni et al. [17] carried out a systematic study of optical and microscopic properties of self-assembled quantum dots of *InGaAs/GaAs* heterostructures and obtained that orientation of growth is important in the dots self-aggregation process. Nötzel et al. [18] reviewed the unique self-organizing growth mechanisms on planar and patterned high-index substrates leading to wire and quantum dot arrays with unprecedented structural and electronic properties. Li et al. [19] investigated the effects of *InP* substrate orientation on self-assembled *InAs* quantum dots and showed dependence of the infrared luminescence on the substrate orientation of *InAs* dots deposited on *InP* substrates. Freire et al. [20] performed theoretical calculations for *InGaAs* QWs grown on oriented

substrates, including strain effects and explained strong relation between strain, growth direction and blueshift of the photoluminescence emission.

Since 2011, there have been attempts to investigate properties of dilute nitride semiconductors, because long wavelength (1.3 and 1.5 μm) lasers can be manufactured out of narrow band gap dilute nitride materials and used in fiber optics. Most researchers focused on (001) oriented *InGaAsN* and a few reported the results for other orientations. Tomić et al. [21][22] presented a comprehensive theoretical and experimental analysis of ideal and real 1.3- μm *InGaAsN/GaAs* lasers grown on natural (001) substrates and compared their gain characteristics. Ibáñez et al. [23] used photorefectance and high resolution x-ray diffraction measurements to assess the composition of *InGaAsN* thin films grown on *GaAs* substrates with different growth orientations and determined corrections to interpolated values for deformation potentials. Blanc et al. [24] and Miguel-Sánchez et al. [25] considered (111) oriented *InGaAsN/GaAs* QW and demonstrated photoluminescence emission at wavelength as long as 1.42 μm at 16 K and also observed blueshift and other optical properties of *GaAsN* and *InGaAsN* QWs. Miguel-Sánchez et al. [26][27] reported successful growth of (111)-oriented *InGaAsN* laser diode structures by molecular beam epitaxy and room-temperature laser emission above 1.2 μm under pulsed current conditions. Latkowska et al. [28] applied low temperature micro-photoluminescence to study *InGaAsN* bulklike layers grown on various oriented *GaAs* substrates.

1.2 Studies of hexagonal systems

In the early 1990s, the semiconductors with hexagonal⁶ crystal lattice received considerable attention due to the use of materials containing wide bandgap *GaN*, *AlN* and *InN* compounds in blue LEDs and lasers⁷. There was considerable amount of publications related to experiments and theory of band structure and optical gain for wurtzite semiconductors for (0001) oriented substrates. Based on cubic models, Chuang and Chang [29][30] established theoretical base for band structure calculation for wurtzite

⁶Hexagonal symmetry is known as wurtzite, by the mineral ZnS - wurtzite (ZnS is zinc sulfide which in nature may be found both in cubic - zincblende and hexagonal - wurtzite crystals).

⁷Apart from *GaN*, *AlN* and *InN* there are several materials which have both cubic and hexagonal forms.

bulk and QW semiconductors including strain effects. Then, Chuang [31] presented a theory for the free-carrier optical gain of strained wurtzite QW lasers.

For non (0001)-oriented substrates, many properties of semiconductors are still not understood. Park and Chuang [32] investigated crystal orientation effects of GaN wurtzite semiconductors including band structure, piezoelectric field, strain effects, momentum matrix elements for optical transitions, band gap and wave functions for bulk and QW structures. Mireles and Ulloa [33] presented derivation of Hamiltonian which is valid for general (h0il) oriented wurtzite strained substrates and band structure for various oriented GaN/InAlN QWs. Park and Chuang [34] investigated crystal orientation effects on optical gain of GaN/AlGaIn QW lasers and obtained the maximum gain around 60° inclined substrate. Park and Ahn [35] investigated band structure and gain for arbitrary oriented wurtzite ZnO/MgZnO QWs and compared to GaN-based QW structures. Park, Ahn and Chuang [36] obtained optical gain and electronic properties of natural planes of wurtzite InGaIn/GaN QW structures. Yoo et al. [37] presented simple approach to the evaluation of strain in zincblende and wurtzite structure for arbitrary orientations.

In recent years, there were also published investigations of particular non-(0001) oriented wurtzite semiconductors with special properties. Waltereit et al. [38] discuss consequences of very large electrostatic fields along the wurtzite QW structure. Sun et al. [39] considered particular (1 $\bar{1}$ 00) orientation and discovered improvements of photoluminescence characteristics. Reports include the results of various oriented wurtzite multiple quantum wells grown on lithium aluminate and sapphire substrates. Ng [40] reported on multiple AlGaIn QWs grown on non (0001) sapphire substrates, showing 30 times higher photoluminescence intensity than (0001) oriented QW. Craven et al. [41] investigated a-plane *AlGaIn* multiple QWs. Chitnis et al. [42] reported blue-purple pn-junction light-emitting diodes with a-plane *InGaIn* multiple QWs active region grown on r-plane sapphire substrates. Domen et al. [43] analyzed specific strained orientation of *GaN* QW which may reduce carrier density to create optical gain and generate laser radiation.

1.3 Novel methods of band structure calculations

Commonly used effective mass or $k \cdot p$ method is one of the methods of describing band structure around the extremum Γ point. The band structures of *GaAs/Al_xGa_{1-x}As*

QWs are described by the effective mass theory for cubic (zinc-blende) crystals, which was obtained for (11 N) orientation first by Xia [44] for hole subband structure (4×4 Hamiltonian) and with spin-orbit split-off influence by Seo and Donegan [45] (6×6 Hamiltonian) for $In_xGa_{1-x}As/InP$ QWs. For dilute nitride semiconductors, $InGaAsN$, the influence of nitrogen concentration on band structures is not negligible and is described by ten band $k \cdot p$ model which was obtained for (11 N)-oriented substrates by Fan [46]. Broderick et al. [47] introduced tight binding analysis of band anticrossing in $GaBiAs$, 12-band $k \cdot p$ model for dilute bismide alloys and 14-band $k \cdot p$ Hamiltonian for $GaBiNAs$ compound grown on (001) oriented substrates. Gladysiewicz et al. [48] derived 8- and 14-band $k \cdot p$ models for $GaInAsBi$ QWs grown on (001) oriented GaAs and InP substrates. There are no reports in literature on the band structure of Bi containing semiconductors grown on non-(001) oriented substrates.

1.4 About the thesis

In the present thesis we discuss $k \cdot p$ method of semiconductor band structure calculations based on Kane's and Luttinger-Kohn's models for zincblende and wurtzite semiconductors. The presented work shows fully detailed calculations and explanation in the area of $k \cdot p$ method. The strain has a significant influence on band structure and is introduced using Bir and Pikus model. The purpose of the work is to obtain the method of calculating band structure of semiconductors on arbitrary oriented substrates. There is very limited literature on the band structure of the semiconductors grown on rotated substrates. In the present work we aimed at fulfilling that gap. In addition, we introduce the numerical implementation of the theory. We provide, as examples, results of calculations band structures for a number of materials for the models that we discuss.

Chapter 2

Construction of Kane's model Hamiltonian

To understand optical properties of semiconductors we have to know the electronic band structure including energy bands and corresponding wave functions. For applications in optical devices, one needs semiconductors with direct band gaps, as main transitions occur near the band edges. There are various methods of calculating band structure of semiconductors:

1. Free electron approximation.
2. Pseudo potential method.
3. Tight binding model.
4. Green function model (Korringa, Kohn and Rostocker model).
5. Density-functional theory.
6. Kronig–Penney model.
7. $k \cdot p$ perturbation theory.

Our main focus is on the conduction and valence band structures near the band edges, where the $k \cdot p$ method is very useful. This theory has been applied specifically in the

framework of the Kane model (after Evan O. Kane), and of the Luttinger–Kohn model (LKM) (after Joaquin Mazdak Luttinger and Walter Kohn). We consider the case when extremum point of band structure occurs at the zone center where $k_0 = 0$, here k_0 is a particular point in k space (k is a wave vector). This is a very useful case for III-V direct band gap semiconductors. Kane model is unrealistic, but it is necessary to find basis functions, which are going to be used in LKM. Kane model gives incorrect energy for heavy holes band, due to discarding all but four bands. LKM uses the result of Kane model and provides realistic results.

2.1 Hamiltonian for Schrödinger equation and basis functions

In Kane's model [49] the spin-orbit interaction is taken into account and four bands are considered (Fig. 2.1): conduction, heavy hole, light hole and the spin orbit split-off band, while each band is double degenerate with their spin counterparts. Hamiltonian near $\vec{k}_0 = 0$ is expressed in the form:

$$H = H_0 + \frac{\hbar}{4m_0^2c^2} \left[\vec{\nabla}V \times \vec{p} \right] \cdot \vec{\sigma} \quad (2.1)$$

$$H_0 = \frac{p^2}{2m_0} + V(\vec{r}) \quad (2.2)$$

where H_0 consists of kinetic and potential energies, the second term in (2.1) is the spin-orbit interaction, and the $\vec{\sigma}$ is the vector of Pauli spin matrices with components:

$$\sigma_x = \begin{bmatrix} 0 & 1 \\ 1 & 0 \end{bmatrix} \quad \sigma_y = \begin{bmatrix} 0 & -i \\ i & 0 \end{bmatrix} \quad \sigma_z = \begin{bmatrix} 1 & 0 \\ 0 & -1 \end{bmatrix} \quad (2.3)$$

Relations for Pauli spin matrices (2.3) operating on the spins are:

$$\begin{array}{lll} \sigma_x \uparrow = \downarrow & \sigma_y \uparrow = i \downarrow & \sigma_z \uparrow = \uparrow \\ \sigma_x \downarrow = \uparrow & \sigma_y \downarrow = -i \uparrow & \sigma_z \downarrow = -\downarrow \end{array} \quad (2.4)$$

where spins orthonormality relations are:

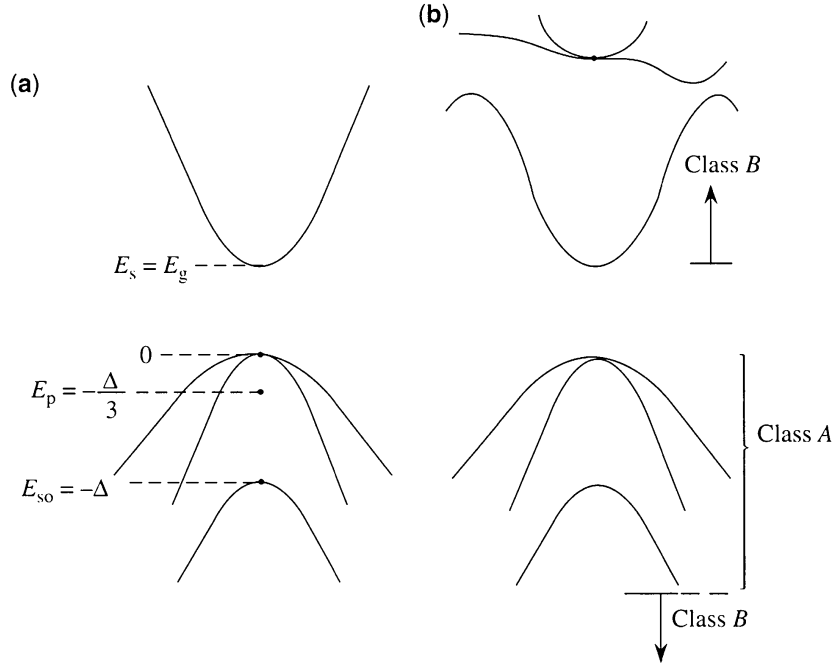


FIGURE 2.1: The $k \cdot p$ method in (a) Kane's model: only a conduction, a heavy hole, a light hole and a spin-orbit split-off bands with double degeneracy are considered, all other bands discarded; (b) LKM: the heavy hole, light hole and spin split-off bands in double degeneracy are of interest and called as class A, all other bands are denoted as class B. The effect of class B on class A is taken into account.

$$\uparrow \equiv \begin{bmatrix} 1 \\ 0 \end{bmatrix} \quad \downarrow \equiv \begin{bmatrix} 0 \\ 1 \end{bmatrix} \quad \langle \uparrow | \uparrow \rangle = \langle \downarrow | \downarrow \rangle = 1 \quad \langle \uparrow | \downarrow \rangle = \langle \downarrow | \uparrow \rangle = 0 \quad (2.5)$$

From the original equation for the Bloch function $\psi_{n\vec{k}}$:

$$\left\{ H_0 + \frac{\hbar}{4m_0^2c^2} [\vec{\nabla}V \times \vec{p}] \cdot \vec{\sigma} \right\} \psi_{n\vec{k}}(\vec{r}) = E_n(\vec{k}) \psi_{n\vec{k}}(\vec{r}) \quad (2.6)$$

the Schrödinger equation for cell periodic function $u_{n\vec{k}}(\vec{r})$ (also known as Bloch periodic amplitude) is obtained:

$$\left\{ H_0 + \frac{\hbar}{m_0} \vec{k} \vec{p} + \frac{\hbar}{4m_0^2c^2} [\vec{\nabla}V \times \vec{p}] \cdot \vec{\sigma} + \frac{\hbar^2}{4m_0^2c^2} [\vec{\nabla}V \times \vec{k}] \cdot \vec{\sigma} \right\} u_{n\vec{k}}(\vec{r}) = E' u_{n\vec{k}}(\vec{r}) \quad (2.7)$$

where

$$E' = E_n(\vec{k}) - \frac{\hbar^2 k^2}{2m_0} \quad (2.8)$$

The relation between Bloch function and periodic function is $\psi_{n\vec{k}}(\vec{r}) = e^{i\vec{k}\vec{r}} u_{n\vec{k}}(\vec{r})$ and the last term in (2.7) is a \vec{k} dependent spin-orbit interaction which is relatively small and can be neglected. Thus, Hamiltonian near \vec{k}_0 operating on cell periodic function is expressed in the form:

$$H = H_0 + H_1 + H_2 = H_0 + \frac{\hbar}{m_0} \vec{k} \vec{p} + \frac{\hbar}{4m_0^2 c^2} [\vec{\nabla} V \times \vec{p}] \cdot \vec{\sigma} \quad (2.9)$$

Here H_1 appears due to the transition from Bloch function to cell periodic function and H_2 is a p dependent spin-orbit interaction. The band edge functions, $u_{n0}(\vec{r})$ (corresponding to $k_0 = 0$) are: $|iS \uparrow\rangle, |iS \downarrow\rangle$ - for conduction band and $|X \uparrow\rangle, |X \downarrow\rangle, |Y \uparrow\rangle, |Y \downarrow\rangle, |Z \uparrow\rangle, |Z \downarrow\rangle$ - for valence band with corresponding eigenenergies E_s and E_p respectively, which are defined as $H_0 |S\rangle = E_c |S\rangle, H_0 |X\rangle = E_p |X\rangle$, etc., see Fig. 2.1. Basis functions are chosen in a convenient form:

$$|1\rangle = |iS \downarrow\rangle, |2\rangle = \left| \frac{X - iY}{\sqrt{2}} \uparrow \right\rangle, |3\rangle = |Z \downarrow\rangle, |4\rangle = \left| -\frac{X + iY}{\sqrt{2}} \uparrow \right\rangle \quad (2.10)$$

$$|\bar{1}\rangle = |iS \uparrow\rangle, |\bar{2}\rangle = \left| -\frac{X + iY}{\sqrt{2}} \downarrow \right\rangle, |\bar{3}\rangle = |Z \uparrow\rangle, |\bar{4}\rangle = \left| \frac{X - iY}{\sqrt{2}} \downarrow \right\rangle \quad (2.11)$$

where the conduction band wave function is the s -state wave function and the valence band basis functions are taken from the p -state wave functions of hydrogen atom model. Basis functions are related to spherical harmonics as:

$$\begin{aligned} Y_{00} &= \frac{1}{\sqrt{4\pi}} \equiv |S\rangle \\ Y_{10}(\theta, \phi) &= \sqrt{\frac{3}{4\pi}} \cos \theta = \sqrt{\frac{3}{4\pi}} \frac{z}{r} \equiv |Z\rangle \\ Y_{1\pm 1}(\theta, \phi) &= \mp \sqrt{\frac{3}{4\pi}} \sin \theta e^{\pm i\phi} = \mp \sqrt{\frac{3}{4\pi}} \frac{x \pm iy}{r} \equiv \mp \frac{1}{\sqrt{2}} |X \pm iY\rangle \end{aligned} \quad (2.12)$$

Spherical harmonics are obtained by the following expression:

$$Y_{lm}(\theta, \phi) = (-1)^{\frac{m+|m|}{2}} \sqrt{\frac{2l+1}{4\pi} \frac{(l-|m|)!}{(l+|m|)!}} P_l^m(\cos \theta) e^{im\phi} \quad (2.13)$$

where $P_l^m(\cos \theta)$ are Legendre polynomials. The Legendre polynomials in explicit form are:

$$P_l^m(\cos \theta) = \sin^m \theta \frac{d^m}{d(\cos \theta)^m} P_l(\cos \theta) \quad (2.14)$$

where P_l for $l = 1$ is:

$$P_1 = \cos \theta \quad (2.15)$$

The spherical harmonics do not include spin. Basis functions which including spin are discussed at the end of this chapter. The reason of this choice [50](p.68-96) is that in the crystal potentials of atoms overlap with each other and forming bands, as it is shown on Fig. 2.2. Due to the fact that our main interest is around band gap, we should use the highest valence bands and the lowest conduction band. As it is seen, the highest valence bands are atomic p -states and the lowest conduction bands are atomic s -states. The p - and s -states originate from the fine structure of energy levels in atomic physics. Each state with principal quantum number n is degenerate with respect to fine structure (s -, p -, d -, f -sub-states) due to electron spin and relativistic corrections to Schrödinger equation. Explicit degenerations are shown at the end of this chapter. For convenience,

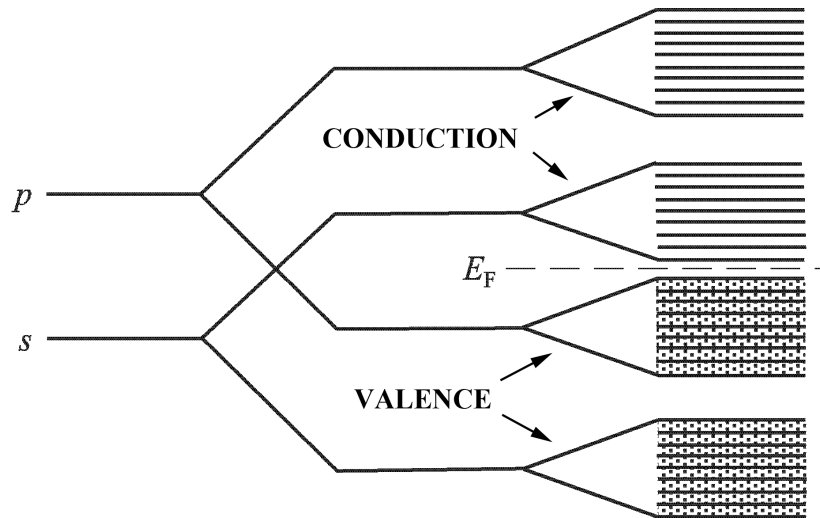


FIGURE 2.2: Evolution of atomic s - and p -states, to form conduction and valence zone exists in semiconductors; E_F - Fermi level; four zones on the right hand of the figure are (from top to bottom): conduction bands formed by antibonding p - and s -states and below Fermi level are valence bands formed by bonding p - and s -states.

assume that the wave vector is $\vec{k} = k\hat{z}$ and Kane's parameter P and spin-orbit split off

energy Δ are defined as:

$$\begin{aligned} P &\equiv -i \frac{\hbar}{m_0} \langle S | p_z | Z \rangle \\ \Delta &\equiv i \frac{3\hbar}{4m_0^2 c^2} \left\langle X \left| \frac{\partial V}{\partial x} p_y - \frac{\partial V}{\partial y} p_x \right| Y \right\rangle \end{aligned} \quad (2.16)$$

2.2 Explicit calculations of matrix elements of H

In this section we will determine matrix elements of the Hamiltonian H as given by Eq. (2.9) within basis functions (2.10) and (2.11). We will calculate only half of the matrix elements due to the fact that matrix is symmetric. Matrix elements are evaluated for upper block between states (2.10)¹. The resulting structure of the Hamiltonian matrix is as follows:

$$H = \begin{bmatrix} \tilde{H} & 0 \\ 0 & \tilde{H} \end{bmatrix} \quad (2.17)$$

with the upper and lower blocks of the form:

$$\tilde{H} = \begin{bmatrix} H_{11} & H_{12} & H_{13} & H_{14} \\ H_{21} & H_{22} & H_{23} & H_{24} \\ H_{31} & H_{32} & H_{33} & H_{34} \\ H_{41} & H_{42} & H_{43} & H_{44} \end{bmatrix} \quad (2.18)$$

In the following we evaluate the relevant matrix elements.

2.2.1 Matrix element \mathbf{H}_{11}

Matrix element is defined below along with its value.

$$\mathbf{H}_{11} = \langle 1 | H | 1 \rangle = \langle -iS \downarrow | H | iS \downarrow \rangle = E_s \quad (2.19)$$

¹For lower block, the matrix elements should be evaluated between states (2.11), but it will give same results.

The evaluation is done as follows. Consider evaluation of each term of Hamiltonian separately:

$$\langle -iS \downarrow | H_0 | iS \downarrow \rangle = \langle S | E_s | S \rangle = E_s \quad (2.20)$$

$$\langle -iS \downarrow | H_1 | iS \downarrow \rangle = \left\langle S \left| \frac{\hbar k}{m_0} p_z \right| S \right\rangle = 0 \quad (2.21)$$

where $p_z \equiv -i\hbar \frac{\partial}{\partial z}$.

$$\begin{aligned} \langle -iS \downarrow | H_2 | iS \downarrow \rangle &= \underbrace{\langle \downarrow | \sigma_x | \downarrow \rangle}_{=0} \langle S | H_2 | S \rangle_x + \underbrace{\langle \downarrow | \sigma_y | \downarrow \rangle}_{=0} \langle S | H_2 | S \rangle_y + \underbrace{\langle \downarrow | \sigma_z | \downarrow \rangle}_{=-1} \langle S | H_2 | S \rangle_z \\ &= -\langle S | H_2 | S \rangle_z = -\left\langle S \left| \frac{\hbar}{4m_0^2 c^2} \left(\frac{\partial V}{\partial x} p_y - \frac{\partial V}{\partial y} p_x \right) \right| S \right\rangle = 0 \end{aligned} \quad (2.22)$$

where matrix elements are zero due to the fact that derivative of a constant number is zero.

2.2.2 Matrix element \mathbf{H}_{12}

Matrix element is defined below in the same way as before.

$$\mathbf{H}_{12} = \langle 1 | H | 2 \rangle = \left\langle -iS \downarrow \left| H \right| \frac{X - iY}{\sqrt{2}} \uparrow \right\rangle = 0 \quad (2.23)$$

Due to spin relations (2.5), the only non zero terms are:

$$\left\langle -iS \downarrow \left| H \right| \frac{X - iY}{\sqrt{2}} \uparrow \right\rangle = \left\langle -iS \downarrow \left| H_2 \right| \frac{X - iY}{\sqrt{2}} \downarrow \right\rangle_x + i \left\langle -iS \downarrow \left| H_2 \right| \frac{X - iY}{\sqrt{2}} \downarrow \right\rangle_y \quad (2.24)$$

where subscripts x and y mean the term in H_2 which contains σ_x and σ_y respectively. The explicit form of the above and another matrix elements, evaluated in next sections, contains typical integrals which we evaluate here. The first type of typical integrals do not contain the potential related terms and have the form²:

$$\int_{-\infty}^{\infty} \frac{x}{r^n} d\vec{r} = \int_{-\infty}^{\infty} \frac{x^3}{r^n} d\vec{r} = 0 \quad (2.25)$$

²Not to be confused by r and \vec{r} , here $r = \sqrt{x^2 + y^2 + z^2}$ and $d\vec{r} = dx dy dz$.

where $n = 1, 2, 3, 4, 5, \dots$. Here the functions are integrated over the entire space. It is not necessary to perform the integration, it is enough to consider the parity of such integral: if the integrand has odd parity, the integral vanishes. We check the above functions:

$$f(-x) = \frac{-x}{r^n} = -\frac{x}{r^n} = -f(x) \quad (2.26)$$

$$f(-x) = \frac{(-x)^3}{r^n} = -\frac{x^3}{r^n} = -f(x) \quad (2.27)$$

and find out that functions have odd parity, so the integrals of the form (2.25) vanish. Other typical integrals, which do not contain the potential are the following:

$$\int_{-\infty}^{\infty} \frac{x^2}{r^n} d\vec{r} \neq 0 \neq \int_{-\infty}^{\infty} \frac{x^4}{r^n} d\vec{r} \quad (2.28)$$

The functions of the above integrals:

$$f(-x) = \frac{(-x)^2}{r^n} = \frac{x^2}{r^n} = f(x) \quad (2.29)$$

have even parity so the integrals of the form (2.28) do not vanish (same arguments applies to y and z).

The second type of typical integrals has the form where the integrand has the same functions as above with a multiplier of the form $\frac{\partial V}{\partial x}$ with odd function:

$$\int_{-\infty}^{\infty} \frac{\partial V}{\partial x} \frac{x}{r^n} d\vec{r} \neq 0 \neq \int_{-\infty}^{\infty} \frac{\partial V}{\partial x} \frac{x^3}{r^n} d\vec{r} \quad (2.30)$$

The $\frac{\partial V}{\partial x}$ may be rewritten, assuming that V is spherically symmetric, i.e. depends only on r and is even, i.e. $V(r) = V(-r)$:

$$\frac{\partial V}{\partial x} = \frac{dV(r)}{dr} \frac{\partial r}{\partial x} = \frac{dV(r)}{dr} \frac{\partial}{\partial x} \sqrt{x^2 + y^2 + z^2} = \frac{dV(r)}{dr} \frac{x}{\sqrt{x^2 + y^2 + z^2}} = \frac{dV(r)}{dr} \frac{x}{r} \quad (2.31)$$

Using (2.31) in one of the integrals³ in Eq. (2.30), we can write explicitly:

$$\int_{-\infty}^{\infty} \frac{\partial V}{\partial x} \frac{x}{r^3} d\vec{r} = \int_{-\infty}^{\infty} \frac{dV(r)}{dr} \frac{x}{r} \frac{x}{r^3} d\vec{r} = \frac{dV(r)}{dr} \int_{-\infty}^{\infty} dy \int_{-\infty}^{\infty} dz \int_{-\infty}^{\infty} \frac{x^2}{r^4} dx \neq 0 \quad (2.32)$$

Here, it is obvious that the influence of $\frac{\partial V}{\partial x}$ term lies in the fact that the additional term changes integrand function's parity from odd ($\frac{x}{r^n}$) to even ($\frac{x^2}{r^n}$), while as shown above, the integral of even functions in the infinite limits does not vanish. The integral with potential and even function converts to:

$$\int_{-\infty}^{\infty} \frac{\partial V}{\partial x} \frac{x^2}{r^3} d\vec{r} = \int_{-\infty}^{\infty} \frac{dV(r)}{dr} \frac{x}{r} \frac{x^2}{r^3} d\vec{r} = \frac{dV(r)}{dr} \int_{-\infty}^{\infty} dy \int_{-\infty}^{\infty} dz \int_{-\infty}^{\infty} \frac{x^3}{r^4} dx = 0 \quad (2.33)$$

the integral with odd integrand function, and therefore vanishes. The other integral has the form of:

$$\int_{-\infty}^{\infty} \frac{\partial V}{\partial x} \frac{y}{r^3} d\vec{r} = \int_{-\infty}^{\infty} \frac{dV(r)}{dr} \frac{x}{r} \frac{y}{r^3} d\vec{r} = \frac{dV(r)}{dr} \int_{-\infty}^{\infty} y dy \int_{-\infty}^{\infty} dz \int_{-\infty}^{\infty} \frac{x}{r^4} dx = 0 \quad (2.34)$$

Here it is clear that integrand functions do not interact with each other so the property (2.25) applies directly, and the integral (2.34) disappears.

The equation (2.24) contains two vanishing terms of the form:

$$\begin{aligned} \left\langle -iS \left| \frac{\hbar}{4m_0^2 c^2} \left(\frac{\partial V}{\partial z} p_x - \frac{\partial V}{\partial x} p_z \right) \right| \frac{Y}{\sqrt{2}} \right\rangle_y &= C \int_{-\infty}^{\infty} \left(\frac{\partial V}{\partial z} \frac{-xy}{r^3} - \frac{\partial V}{\partial x} \frac{-yz}{r^3} \right) d\vec{r} = 0 \\ \left\langle -iS \left| \frac{\hbar}{4m_0^2 c^2} \left(\frac{\partial V}{\partial y} p_z - \frac{\partial V}{\partial z} p_y \right) \right| \frac{X}{\sqrt{2}} \right\rangle_x &= C \int_{-\infty}^{\infty} \left(\frac{\partial V}{\partial y} \frac{-xz}{r^3} - \frac{\partial V}{\partial z} \frac{-xy}{r^3} \right) d\vec{r} = 0 \end{aligned} \quad (2.35)$$

The two non vanishing terms in (2.24) are⁴:

$$\begin{aligned} \left\langle -S \left| \frac{\hbar}{4m_0^2 c^2} \left(\frac{\partial V}{\partial y} p_z - \frac{\partial V}{\partial z} p_y \right) \right| \frac{Y}{\sqrt{2}} \right\rangle_x &= C \int_{-\infty}^{\infty} \left(\frac{\partial V}{\partial y} \frac{-yz}{r^3} - \frac{\partial V}{\partial z} \frac{x^2 + z^2}{r^3} \right) d\vec{r} \\ &= -C \int_{-\infty}^{\infty} \frac{\partial V}{\partial z} \frac{x^2}{r^3} d\vec{r} \end{aligned} \quad (2.36)$$

³The other gives very similar result.

⁴Taking into account (2.25), (2.28) and (2.30).

$$\begin{aligned}
\left\langle -S \left| \frac{\hbar}{4m_0^2c^2} \left(\frac{\partial V}{\partial z} p_x - \frac{\partial V}{\partial x} p_z \right) \right| \frac{X}{\sqrt{2}} \right\rangle_y &= C \int_{-\infty}^{\infty} \left(\frac{\partial V}{\partial z} \frac{y^2 + z^2}{r^3} - \frac{\partial V}{\partial x} \frac{-xz}{r^3} \right) d\vec{r} \\
&= C \int_{-\infty}^{\infty} \frac{\partial V}{\partial z} \frac{y^2}{r^3} d\vec{r}
\end{aligned} \tag{2.37}$$

where all constants are denoted as C for convenience. Last two terms (2.36) and (2.37) are non zero, but due to the fact that in cubic crystals x , y and z axes are crystallographically equivalent, they are equal to each other and they have opposite signs. Thus, sum of (2.36) and (2.37) cancel each other.

2.2.3 Matrix element \mathbf{H}_{13}

This matrix element is defined below, along with its value.

$$\mathbf{H}_{13} = \langle 1 | H | 3 \rangle = \langle -iS \downarrow | H | Z \downarrow \rangle = kP \tag{2.38}$$

Consider evaluation of each term of Hamiltonian separately:

$$\langle -iS \downarrow | H_0 | Z \downarrow \rangle = \langle -iS | E_p | Z \rangle = \frac{\sqrt{3}E_p}{4\pi} \int_0^{2\pi} \cos \theta d\theta = \frac{\sqrt{3}E_p}{4\pi} \cdot \sin \theta \Big|_0^{2\pi} = 0 \tag{2.39}$$

Other terms are:

$$\langle -iS \downarrow | H_1 | Z \downarrow \rangle = \left\langle -iS \left| \frac{\hbar k}{m_0} p_z \right| Z \right\rangle = -ik \frac{\hbar}{m_0} \langle S | p_z | Z \rangle = kP \tag{2.40}$$

Due to spin relations (2.5) the only term left is:

$$\langle -iS | H_2 | Z \rangle_z = \left\langle -iS \left| \frac{\hbar}{4m_0^2c^2} \left(\frac{\partial V}{\partial x} p_y - \frac{\partial V}{\partial y} p_x \right) \right| Z \right\rangle = C \int_{-\infty}^{\infty} \left(\frac{\partial V}{\partial x} \frac{-zy}{r^3} - \frac{\partial V}{\partial y} \frac{-zx}{r^3} \right) d\vec{r} = 0 \tag{2.41}$$

where all constants are denoted as C for convenience and the property (2.34) is used.

2.2.4 Matrix element \mathbf{H}_{22}

The second diagonal matrix element is defined below along with its value.

$$\mathbf{H}_{22} = \langle 2 | H | 2 \rangle = \left\langle \frac{X + iY}{\sqrt{2}} \uparrow \left| H \right| \frac{X - iY}{\sqrt{2}} \uparrow \right\rangle = E_p - \frac{\Delta}{3} \quad (2.42)$$

Consider evaluation of each term of Hamiltonian separately:

$$\begin{aligned} \left\langle \frac{X + iY}{\sqrt{2}} \left| H_0 \right| \frac{X - iY}{\sqrt{2}} \right\rangle &= \frac{1}{2} \langle X | H_0 | X \rangle - \frac{1}{2} \langle iY | H_0 | iY \rangle - \frac{1}{2} \langle X | H_0 | iY \rangle + \frac{1}{2} \langle iY | H_0 | X \rangle \\ &= \frac{1}{2} E_p + \frac{1}{2} E_p - i \langle X | E_p | Y \rangle + i \langle Y | E_p | X \rangle = E_p \end{aligned} \quad (2.43)$$

where last two terms are equal⁵ and cancel each other. Using the properties (2.25) and (2.28) one evaluates part H_1 of the Hamiltonian:

$$\begin{aligned} \left\langle \frac{X + iY}{\sqrt{2}} \uparrow \left| H_1 \right| \frac{X - iY}{\sqrt{2}} \uparrow \right\rangle &= \left\langle \frac{X + iY}{\sqrt{2}} \left| \frac{\hbar k}{m_0} p_z \right| \frac{X - iY}{\sqrt{2}} \right\rangle \\ &= Ck \cdot \int_{-\infty}^{\infty} \left(\frac{x}{r} \cdot \frac{-xz}{r^3} + i \frac{x}{r} \cdot \frac{yz}{r^3} + i \frac{y}{r} \cdot \frac{xz}{r^3} + \frac{-y}{r} \cdot \frac{yz}{r^3} \right) d\vec{r} = 0 \end{aligned} \quad (2.44)$$

The last part is evaluated as follows:

$$\begin{aligned} \left\langle \frac{X + iY}{\sqrt{2}} \left| H_2 \right| \frac{X - iY}{\sqrt{2}} \right\rangle &= C \left\{ \left\langle X \left| \frac{\partial V}{\partial x} p_y - \frac{\partial V}{\partial y} p_x \right| X \right\rangle - \left\langle X \left| \frac{\partial V}{\partial x} p_y - \frac{\partial V}{\partial y} p_x \right| iY \right\rangle \right. \\ &\quad \left. + \left\langle iY \left| \frac{\partial V}{\partial x} p_y - \frac{\partial V}{\partial y} p_x \right| X \right\rangle - \left\langle iY \left| \frac{\partial V}{\partial x} p_y - \frac{\partial V}{\partial y} p_x \right| iY \right\rangle \right\} \end{aligned} \quad (2.45)$$

It is convenient to consider each of the terms in (2.45) separately⁶ (taking into account properties (2.25)-(2.34)):

$$\begin{aligned} \langle X | \dots | X \rangle &= C \int_{-\infty}^{\infty} \frac{x}{r} \left(\frac{\partial V}{\partial x} \frac{-xy}{r^3} - \frac{\partial V}{\partial y} \frac{y^2 + z^2}{r^3} \right) d\vec{r} = 0 \\ \langle Y | \dots | Y \rangle &= C \int_{-\infty}^{\infty} \frac{y}{r} \left(\frac{\partial V}{\partial x} \frac{x^2 + z^2}{r^3} - \frac{\partial V}{\partial y} \frac{xy}{r^3} \right) d\vec{r} = 0 \end{aligned} \quad (2.46)$$

⁵As soon as the E_p is a constant value we have the right to interchange “bra”-term X and “ket”-term Y inside the matrix element.

⁶... in each expression corresponds to $\frac{\partial V}{\partial x} p_y - \frac{\partial V}{\partial y} p_x$.

$$\begin{aligned}
\langle iY | \dots | X \rangle &= C \int_{-\infty}^{\infty} \frac{y}{r} \left(\frac{\partial V}{\partial x} \frac{-xy}{r^3} - \frac{\partial V}{\partial y} \frac{y^2 + z^2}{r^3} \right) d\vec{r} \\
&= C \int_{-\infty}^{\infty} \left(\frac{\partial V}{\partial x} \frac{-xy^2}{r^3} - \frac{\partial V}{\partial y} \frac{y^3 + yz^2}{r^3} \right) d\vec{r} \\
-\langle X | \dots | iY \rangle &= C \int_{-\infty}^{\infty} \frac{x}{r} \left(\frac{\partial V}{\partial x} \frac{x^2 + z^2}{r^3} - \frac{\partial V}{\partial y} \frac{-xy}{r^3} \right) d\vec{r} \\
&= C \int_{-\infty}^{\infty} \left(\frac{\partial V}{\partial x} \frac{x^3 + xz^2}{r^3} - \frac{\partial V}{\partial y} \frac{-x^2y}{r^3} \right) d\vec{r}
\end{aligned} \tag{2.47}$$

where all constants are denoted as C for convenience. Next, instead of C in (2.47) we write all constants explicitly, take into account the property of equivalent axes in cube (interchange y to x and as a result multiplier 2 appears in front of the integral) and combine non-zero terms (2.43) and (2.47):

$$\begin{aligned}
E_p - \frac{\hbar^2 i}{4m_0^2 c^2} \cdot \frac{3}{8\pi} \int_{-\infty}^{\infty} \left[\left(\frac{\partial V}{\partial x} \frac{-xy^2}{r^3} - \frac{\partial V}{\partial y} \frac{y^3 + yz^2}{r^3} \right) - \left(\frac{\partial V}{\partial x} \frac{x^3 + xz^2}{r^3} - \frac{\partial V}{\partial y} \frac{-x^2y}{r^3} \right) \right] d\vec{r} \\
= E_p - \frac{\hbar^2 i}{4m_0^2 c^2} \cdot \frac{3 \cdot 2}{8\pi} \int_{-\infty}^{\infty} \left(\frac{\partial V}{\partial x} \frac{x^3 + xz^2}{r^4} - \frac{\partial V}{\partial y} \frac{-x^2y}{r^4} \right) d\vec{r} \equiv E_p - \frac{\Delta}{3}
\end{aligned} \tag{2.48}$$

In order to prove the last equivalence in (2.48) we write the definition of Δ (2.16) and expand it in explicit form:

$$\begin{aligned}
\Delta \equiv \frac{3\hbar i}{4m_0^2 c^2} \left\langle X \left| \frac{\partial V}{\partial x} p_y - \frac{\partial V}{\partial y} p_x \right| Y \right\rangle &= \frac{3\hbar i}{4m_0^2 c^2} \cdot \hbar \cdot \frac{3}{8\pi} \cdot 2 \cdot \int_{-\infty}^{\infty} \frac{x}{r} \left(\frac{\partial V}{\partial x} \frac{x^2 + z^2}{r^3} - \frac{\partial V}{\partial y} \frac{-xy}{r^3} \right) d\vec{r} \\
&= 3 \cdot \frac{\hbar^2 i}{4m_0^2 c^2} \cdot \frac{3 \cdot 2}{8\pi} \int_{-\infty}^{\infty} \left(\frac{\partial V}{\partial x} \frac{x^3 + xz^2}{r^4} - \frac{\partial V}{\partial y} \frac{-x^2y}{r^4} \right) d\vec{r}
\end{aligned} \tag{2.49}$$

where the property (2.32) applied.

2.2.5 Matrix element \mathbf{H}_{23}

The off-diagonal matrix element.

$$\mathbf{H}_{23} = \langle 2 | H | 3 \rangle = \left\langle \frac{X + iY}{\sqrt{2}} \uparrow \left| H \right| Z \downarrow \right\rangle = \frac{\sqrt{2}}{3} \Delta \tag{2.50}$$

Due to spin properties (2.5) we consider only non zero terms of Hamiltonian:

$$\left\langle \frac{X+iY}{\sqrt{2}} \middle| H_2 \middle| Z \right\rangle = \left\langle \frac{X+iY}{\sqrt{2}} \middle| H_2 \middle| Z \right\rangle_x - i \left\langle \frac{X+iY}{\sqrt{2}} \middle| H_2 \middle| Z \right\rangle_y \quad (2.51)$$

where

$$\left\langle \frac{X+iY}{\sqrt{2}} \middle| H_2 \middle| Z \right\rangle_x = \left\langle \frac{X}{\sqrt{2}} \middle| H_2 \middle| Z \right\rangle_x + \left\langle \frac{iY}{\sqrt{2}} \middle| H_2 \middle| Z \right\rangle_x \quad (2.52)$$

$$-i \left\langle \frac{X+iY}{\sqrt{2}} \middle| H_2 \middle| Z \right\rangle_y = - \left\langle \frac{iX}{\sqrt{2}} \middle| H_2 \middle| Z \right\rangle_y + \left\langle \frac{Y}{\sqrt{2}} \middle| H_2 \middle| Z \right\rangle_y \quad (2.53)$$

It is convenient to consider each of the terms in (2.52) and (2.53) separately and using the relations (2.32), (2.33) and (2.34):

$$\langle X | \dots | Z \rangle_x = C \int_{-\infty}^{\infty} \frac{x}{r} \left(\frac{\partial V}{\partial y} \frac{x^2 + y^2}{r^3} - \frac{\partial V}{\partial z} \frac{-zy}{r^3} \right) d\vec{r} = 0 \quad (2.54)$$

$$\begin{aligned} \langle iY | \dots | Z \rangle_x &= iC \int_{-\infty}^{\infty} \frac{y}{r} \left(\frac{\partial V}{\partial y} \frac{x^2 + y^2}{r^3} - \frac{\partial V}{\partial z} \frac{-zy}{r^3} \right) d\vec{r} \\ &= iC \int_{-\infty}^{\infty} \left(\frac{\partial V}{\partial y} \frac{yx^2 + y^3}{r^4} - \frac{\partial V}{\partial z} \frac{-zy^2}{r^4} \right) d\vec{r} \end{aligned} \quad (2.55)$$

$$\begin{aligned} \langle iX | \dots | Z \rangle_y &= -iC \int_{-\infty}^{\infty} \frac{x}{r} \left(\frac{\partial V}{\partial z} \frac{-xz}{r^3} - \frac{\partial V}{\partial x} \frac{x^2 + y^2}{r^3} \right) d\vec{r} \\ &= -iC \int_{-\infty}^{\infty} \left(\frac{\partial V}{\partial z} \frac{-x^2z}{r^4} - \frac{\partial V}{\partial x} \frac{x^3 + xy^2}{r^4} \right) d\vec{r} \end{aligned} \quad (2.56)$$

$$- \langle Y | \dots | Z \rangle_y = C \int_{-\infty}^{\infty} \frac{y}{r} \left(\frac{\partial V}{\partial z} \frac{-zx}{r^3} - \frac{\partial V}{\partial x} \frac{x^2 + y^2}{r^3} \right) d\vec{r} = 0 \quad (2.57)$$

where all constants are denoted as C for convenience. The only terms left (2.55) and (2.56) (write C explicitly and interchange x and y):

$$\begin{aligned} & \frac{\hbar^2 i}{4m_0^2 c^2} \cdot \frac{3}{4\sqrt{2}\pi} \left[\int_{-\infty}^{\infty} \left(\frac{\partial V}{\partial y} \frac{yx^2 + y^3}{r^4} - \frac{\partial V}{\partial z} \frac{-zy^2}{r^4} \right) d\vec{r} + \int_{-\infty}^{\infty} \left(\frac{\partial V}{\partial z} \frac{-x^2z}{r^4} - \frac{\partial V}{\partial x} \frac{x^3 + xy^2}{r^4} \right) d\vec{r} \right] \\ &= 2 \cdot \frac{\hbar^2 i}{4m_0^2 c^2} \cdot \frac{3}{4\sqrt{2}\pi} \int_{-\infty}^{\infty} \left(\frac{\partial V}{\partial x} \frac{x^3 + xz^2}{r^4} - \frac{\partial V}{\partial y} \frac{-x^2y}{r^4} \right) d\vec{r} \equiv \frac{\sqrt{2}}{3} \Delta \end{aligned} \quad (2.58)$$

where the last equivalence can be found from Δ expression (2.49) in section 2.2.4.

2.2.6 Matrix element \mathbf{H}_{33}

The third diagonal matrix element is defined.

$$\mathbf{H}_{33} = \langle 3 | H | 3 \rangle = \langle Z \downarrow | H | Z \downarrow \rangle = E_p \quad (2.59)$$

Consider evaluation of each term of Hamiltonian separately:

$$\langle Z \downarrow | H_0 | Z \downarrow \rangle = \langle Z | E_p | Z \rangle = E_p \quad (2.60)$$

The term below is obtained using property (2.25):

$$\langle Z \downarrow | H_1 | Z \downarrow \rangle = \left\langle Z \left| \frac{\hbar k}{m_0} p_z \right| Z \right\rangle = C \int_{-\infty}^{\infty} \frac{z}{r} \cdot \frac{x^2 + y^2}{r^3} d\vec{r} = C \int_{-\infty}^{\infty} \frac{z}{r^4} \cdot (x^2 + y^2) d\vec{r} = 0 \quad (2.61)$$

Due to spin relations (2.5), the only term left is (using property (2.34)):

$$\langle Z | H_2 | Z \rangle_z = \left\langle Z \left| \frac{\hbar}{4m_0^2 c^2} \left(\frac{\partial V}{\partial x} p_y - \frac{\partial V}{\partial y} p_x \right) \right| Z \right\rangle = C \int_{-\infty}^{\infty} \frac{z}{r} \left(\frac{\partial V}{\partial x} \frac{-zy}{r^3} - \frac{\partial V}{\partial y} \frac{-zx}{r^3} \right) d\vec{r} = 0 \quad (2.62)$$

where all constants combined denoted as C for convenience.

2.3 Explicit Kane's matrix Hamiltonian

After the evaluation of all matrix elements, a complete upper matrix Hamiltonian, evaluated for states (2.10), has the explicit form:

$$\tilde{H} = \begin{bmatrix} E_s & 0 & kP & 0 \\ 0 & E_p - \Delta/3 & \sqrt{2}\Delta/3 & 0 \\ kP & \sqrt{2}\Delta/3 & E_p & 0 \\ 0 & 0 & 0 & E_p + \Delta/3 \end{bmatrix} \quad (2.63)$$

The lower part is identical and evaluated for states (2.11).

2.4 Corrections to basis functions

In order to simplify 4×4 matrix (2.63) to 3×3 matrix we define the zero of energy on the top of valence band and define reference energy to be $E_p = -\Delta/3$, so the conduction band minimum is $E_s = E_g$, where E_g is a band gap as it is shown on Fig. 2.1. The Hamiltonian in (2.63) becomes:

$$\mathbf{H} = \begin{bmatrix} E_g & 0 & kP & 0 \\ 0 & -2\Delta/3 & \sqrt{2}\Delta/3 & 0 \\ kP & \sqrt{2}\Delta/3 & -\Delta/3 & 0 \\ 0 & 0 & 0 & 0 \end{bmatrix} \quad (2.64)$$

The determinantal equation $|\mathbf{H} - E'\mathbf{I}| = 0$ gives four eigenvalues for E' :

$$E' = 0 \quad (2.65)$$

$$E'(E' - E_g)(E' + \Delta) - k^2 P^2 \left(E' + \frac{2}{3}\Delta \right) = 0 \quad (2.66)$$

Due to the fact that k^2 is very small, the equation (2.66) can be written as:

$$E'(E' - E_g)(E' + \Delta) \approx 0 \quad (2.67)$$

From the above it is clear that roots of this equation are going to be very close to the three band edges $E' = E_g$, $E' = 0$ and $E' = -\Delta$. Going back to original equation (2.66) we should add a very small k^2 dependent ε , where $\varepsilon \ll \Delta$ and E_g , which leads to three possible solutions:

1. $E' = E_g + \varepsilon(k^2)$
2. $E' = 0 + \varepsilon(k^2)$
3. $E' = -\Delta + \varepsilon(k^2)$

Substituting the above relations into the equation (2.66), one obtains the explicit form of ε for each case:

1.

$$\varepsilon E_g(E_g + \Delta) - k^2 P^2 \left(E_g + \frac{2}{3} \Delta \right) = 0$$

$$\varepsilon = \frac{k^2 P^2 \left(E_g + \frac{2}{3} \Delta \right)}{E_g(E_g + \Delta)}$$

2.

$$\varepsilon E_g \Delta - k^2 P^2 \frac{2}{3} \Delta = 0$$

$$\varepsilon = -\frac{2k^2 P^2}{3E_g}$$

3.

$$-\varepsilon \Delta (-E_g - \Delta) - k^2 P^2 \left(-\frac{1}{3} \Delta \right) = 0$$

$$\varepsilon = -\frac{k^2 P^2}{3(\Delta + E_g)}$$

At this point it is easy to obtain eigenvalues using the relation (2.8):

$$E' = E_n(\vec{k}) - \frac{\hbar^2 k^2}{2m_0}$$

$$E_n(\vec{k}) = E' + \frac{\hbar^2 k^2}{2m_0}$$
(2.68)

By substituting the values for E' , the energies for conduction and valence bands are:

$$E_c(\vec{k}) = E_g + \frac{\hbar^2 k^2}{2m_0} + \frac{k^2 P^2 \left(E_g + \frac{2}{3} \Delta \right)}{E_g(E_g + \Delta)}$$

$$E_{hh}(\vec{k}) = \frac{\hbar^2 k^2}{2m_0}$$

$$E_{lh}(\vec{k}) = \frac{\hbar^2 k^2}{2m_0} - \frac{2k^2 P^2}{3E_g}$$

$$E_{so}(\vec{k}) = -\Delta + \frac{\hbar^2 k^2}{2m_0} - \frac{k^2 P^2}{3(\Delta + E_g)}$$
(2.69)

As it was mentioned above, this result gives an incorrect effective mass for the heavy hole band. To obtain eigenfunctions, which are useful in LKM, it is necessary to improve

Kane basis functions for the upper (2.63) matrix (here $n = c, lh$, so and α, β are used to indicate the basis states for upper and lower block matrix in (2.17) respectively):

$$\begin{aligned} \phi_{hh,\alpha} &= \left| -\frac{X+iY}{\sqrt{2}} \uparrow \right\rangle \\ \phi_{n,\alpha} &= a_n |iS \downarrow\rangle + b_n \left| \frac{X-iY}{\sqrt{2}} \uparrow \right\rangle + c_n |Z \downarrow\rangle \end{aligned} \quad (2.70)$$

and the lower matrix:

$$\begin{aligned} \phi_{hh,\beta} &= \left| \frac{X-iY}{\sqrt{2}} \downarrow \right\rangle \\ \phi_{n,\beta} &= a_n |iS \uparrow\rangle + b_n \left| -\frac{X+iY}{\sqrt{2}} \downarrow \right\rangle + c_n |Z \uparrow\rangle \end{aligned} \quad (2.71)$$

by solving the eigenequation:

$$\begin{bmatrix} E_g - E'_n & 0 & kP \\ 0 & -2\Delta/3 - E'_n & \sqrt{2}\Delta/3 \\ kP & \sqrt{2}\Delta/3 & -\Delta/3 - E'_n \end{bmatrix} \begin{bmatrix} a_n \\ b_n \\ c_n \end{bmatrix} = 0 \quad (2.72)$$

We obtain values for eigenvector column $[a_n, b_n, c_n]$ by substituting each eigenvalue into the eigenequation, and assume limit $k^2 \rightarrow 0$:

1.

$$n = c \quad \begin{bmatrix} 0 & 0 & 0 \\ 0 & -2\Delta/3 - E_g & \sqrt{2}\Delta/3 \\ 0 & \sqrt{2}\Delta/3 & -\Delta/3 - E_g \end{bmatrix} \begin{bmatrix} a_c \\ b_c \\ c_c \end{bmatrix} = 0$$

From the above, it is clear that this system has infinite number of solutions with respect to a_c , whereas b_c and c_c can be only 0. To find a_c we use normalization such that $(a_n^2 + b_n^2 + c_n^2)^{1/2} = 1$ and obtain $a_c = 1$. Then the values are:

$$n = c \quad a_c \simeq 1, b_c \simeq 0, c_c \simeq 0$$

2.

$$n = lh \quad \begin{bmatrix} E_g & 0 & 0 \\ 0 & -2\Delta/3 & \sqrt{2}\Delta/3 \\ 0 & \sqrt{2}\Delta/3 & -\Delta/3 \end{bmatrix} \begin{bmatrix} a_{lh} \\ b_{lh} \\ c_{lh} \end{bmatrix} = 0$$

From the above, it is clear that $a_{lh} = 0$ and $c_{lh} = \sqrt{2}b_{lh}$ and it has infinite number of solutions with respect to c_{lh} and b_{lh} . Using the same normalization as above, we obtain $(b_{lh}^2 + c_{lh}^2)^{1/2} = 1$ which leads to:

$$3b_{lh}^2 = 1 \quad b_{lh}^2 = \frac{1}{3} \quad b_{lh} = \frac{1}{\sqrt{3}} \quad c_{lh} = \sqrt{\frac{2}{3}}$$

Then the values are:

$$n = lh \quad a_{lh} \simeq 0, b_{lh} = \frac{1}{\sqrt{3}}, c_{lh} = \sqrt{\frac{2}{3}}$$

3.

$$n = so \quad \begin{bmatrix} E_g + \Delta & 0 & 0 \\ 0 & \Delta/3 & \sqrt{2}\Delta/3 \\ 0 & \sqrt{2}\Delta/3 & 2\Delta/3 \end{bmatrix} \begin{bmatrix} a_{so} \\ b_{so} \\ c_{so} \end{bmatrix} = 0$$

From the above, it is clear that $a_{so} = 0$ and $b_{so} = -\sqrt{2}c_{so}$ and it has infinite number of solutions with respect to b_{so} and c_{so} . Using the same normalization as above, we obtain $(b_{so}^2 + c_{so}^2)^{1/2} = 1$ which leads to:

$$\frac{3b_{so}^2}{2} = 1 \quad b_{so}^2 = \frac{2}{3} \quad b_{so} = \sqrt{\frac{2}{3}} \quad c_{so} = -\frac{1}{\sqrt{3}}$$

Then the values are:

$$n = so \quad a_{so} \simeq 0, b_{so} = \sqrt{\frac{2}{3}}, c_{so} = \frac{1}{\sqrt{3}}$$

From the above results we obtain improved basis functions which are going to be used in LKM:

$$\begin{aligned}
\phi_{c\alpha} &= |iS \downarrow\rangle \\
\phi_{c\beta} &= |iS \uparrow\rangle \\
\phi_{hh,\alpha} &= \frac{-1}{\sqrt{2}} |(X + iY) \uparrow\rangle = \left| \frac{3}{2}, \frac{3}{2} \right\rangle \\
\phi_{hh,\beta} &= \frac{1}{\sqrt{2}} |(X - iY) \downarrow\rangle = \left| \frac{3}{2}, \frac{-3}{2} \right\rangle \\
\phi_{lh,\alpha} &= \frac{1}{\sqrt{6}} |(X - iY) \uparrow\rangle + \sqrt{\frac{2}{3}} |Z \downarrow\rangle = \left| \frac{3}{2}, \frac{-1}{2} \right\rangle \\
\phi_{lh,\beta} &= \frac{-1}{\sqrt{6}} |(X + iY) \downarrow\rangle + \sqrt{\frac{2}{3}} |Z \uparrow\rangle = \left| \frac{3}{2}, \frac{1}{2} \right\rangle \\
\phi_{so,\alpha} &= \frac{1}{\sqrt{3}} |(X - iY) \uparrow\rangle - \frac{1}{\sqrt{3}} |Z \downarrow\rangle = \left| \frac{1}{2}, \frac{-1}{2} \right\rangle \\
\phi_{so,\beta} &= \frac{1}{\sqrt{3}} |(X + iY) \downarrow\rangle + \frac{1}{\sqrt{3}} |Z \uparrow\rangle = \left| \frac{1}{2}, \frac{1}{2} \right\rangle
\end{aligned} \tag{2.73}$$

where α, β are used to indicate the basis for upper and lower block matrix in (2.17) respectively and Dirac's notation for wave functions is used for simplicity:

$$|j, m\rangle$$

Here j is total angular momentum, which is determined as $j = l + s$, where l is the angular momentum and s is the spin, and m is the magnetic quantum number or z component of j . For p -states $l = 1$ and spin is always $1/2$ for electrons, thus j can be $j = l + s$ and $j = l - s$ or $3/2$ and $1/2$. m has $2j + 1$ values: $j, j - 1, \dots, -j + 1, -j$ and for the case when $j = 3/2$ m takes four values: $3/2, 1/2, -1/2, -3/2$ and for $j = 1/2$ - two values: $1/2$ and $-1/2$. The spin orbit interaction is responsible for the spin-orbit split-off Δ between $j = 1/2$ and $j = 3/2$ states and it's value is almost constant for most of the materials.

The states (2.73) are labeled with respect to corresponding quantum number. As an example we consider $\phi_{hh,\alpha}$:

$$\phi_{hh,\alpha} = Y_{11} \uparrow$$

where \uparrow represents the spin up $s = 1/2$, thus following the above explanations we have $j = 1 + 1/2 = 3/2$ and $m = 3/2$ due to spin up condition which is used above. For the spin down $m = -3/2$.

Chapter 3

Construction of Luttinger-Kohn's model Hamiltonian

Kane model does not provide a complete result because the effects of distant bands are neglected and only four bands are considered. In addition to this, it gives incorrect result for a heavy hole band. Those difficulties were eliminated by LKM, which considered all bands: bands of main interest considered exactly and the influence of all other bands treated as perturbation. In this case, it is convenient to use Löwdin's perturbation method [51] and treat the six valence bands as a class of states of main interest A and put the rest of the bands in class B (Fig. 2.1).

3.1 Cubic symmetry (Zincblende)

3.1.1 The Hamiltonian and the basis functions

We write the total Hamiltonian in (2.7) which operates on $u_{\vec{k}}(\vec{r})$ as:

$$H = H_0 + \frac{\hbar^2 k^2}{2m_0} + \frac{\hbar}{4m_0^2 c^2} \left[\vec{\nabla} V \times \vec{p} \right] \cdot \vec{\sigma} + H' \quad (3.1)$$

where

$$H_0 = \frac{p^2}{2m_0} + V(\vec{r}) \quad (3.2)$$

$$H' = \frac{\hbar}{m_0} \vec{k} \cdot \vec{\Pi} \quad (3.3)$$

where

$$\vec{\Pi} = \vec{p} + \frac{\hbar}{2m_0c^2} \vec{\sigma} \times \vec{\nabla}V \quad (3.4)$$

The last term in (3.4) can be neglected, due to the fact that k dependent term (crystal momentum) is much smaller than the p dependent term (atomic momentum) $\hbar k \ll p$.

Thus we are left with:

$$H' \cong \frac{\hbar}{m_0} \vec{k} \cdot \vec{p} \quad (3.5)$$

This is the only term which is responsible for the coupling class A to class B states. According to Löwdin's perturbation method, we expand eigenfunctions of the Schrödinger equation with the Hamiltonian (3.1):

$$u_{\vec{k}}(\vec{r}) = \sum_j^A a_j(\vec{k}) u_{j0}(\vec{r}) + \sum_\gamma^B a_\gamma(\vec{k}) u_{\gamma 0}(\vec{r}) \quad (3.6)$$

where the first summation with index $j = 1, \dots, 6$ refers to states in class A and the second index γ to states in class B. Explicitly basis functions in class A are taken from improvements of Kane's model (2.73) for Heavy-hole (u_{10}, u_{40}), Light-hole (u_{20}, u_{30}) and Spin Split-off (u_{50}, u_{60}) bands:

$$\begin{aligned} u_{10}(\vec{r}) &= \left| \frac{3}{2}, \frac{3}{2} \right\rangle = \frac{-1}{\sqrt{2}} |(X + iY) \uparrow\rangle \\ u_{20}(\vec{r}) &= \left| \frac{3}{2}, \frac{1}{2} \right\rangle = \frac{-1}{\sqrt{6}} |(X + iY) \downarrow\rangle + \sqrt{\frac{2}{3}} |Z \uparrow\rangle \\ u_{30}(\vec{r}) &= \left| \frac{3}{2}, \frac{-1}{2} \right\rangle = \frac{1}{\sqrt{6}} |(X - iY) \uparrow\rangle + \sqrt{\frac{2}{3}} |Z \downarrow\rangle \\ u_{40}(\vec{r}) &= \left| \frac{3}{2}, \frac{-3}{2} \right\rangle = \frac{1}{\sqrt{2}} |(X - iY) \downarrow\rangle \\ u_{50}(\vec{r}) &= \left| \frac{1}{2}, \frac{1}{2} \right\rangle = \frac{1}{\sqrt{3}} |(X + iY) \downarrow\rangle + \frac{1}{\sqrt{3}} |Z \uparrow\rangle \\ u_{60}(\vec{r}) &= \left| \frac{1}{2}, \frac{-1}{2} \right\rangle = \frac{1}{\sqrt{3}} |(X - iY) \uparrow\rangle - \frac{1}{\sqrt{3}} |Z \downarrow\rangle \end{aligned} \quad (3.7)$$

At $\vec{k} = 0$, the above band-edge functions satisfy:

$$H(0)u_{j0}(\vec{r}) = E_j(0)u_{j0}(\vec{r}) \quad (3.8)$$

where

$$E_j(0) = 0 \text{ for } j = 1, 2, 3, 4$$

$$E_j(0) = -\Delta \text{ for } j = 5, 6$$

as we set $E_p = -\Delta/3$.

Matrix elements of LKH are obtained using Löwdin's perturbation method [51] by solving the eigenequation ($H_{jj'}^{LK}$ is associated with class A states):

$$\sum_{j'}^A (H_{jj'}^{LK} - E\delta_{jj'}) a_{j'}(\vec{k}) = 0 \quad (3.9)$$

where

$$H_{jj'}^{LK} = H_{jj'} + \sum_{\gamma}^B \frac{H'_{j\gamma} H'_{\gamma j'}}{E_0 - E_{\gamma}} \quad (3.10)$$

where $j, j' = 1, \dots, 6$ indicate states (3.7), $\gamma \neq j, j'$. First (unperturbed) term corresponds to coupling between states in class A and the second (perturbed) term corresponds to coupling between states in class A and states in class B; only coupling between states in class B is neglected:

$$H_{jj'} = \langle u_{j0} | H | u_{j'0} \rangle = \left[E_j(0) + \frac{\hbar^2 k^2}{2m_0} \right] \delta_{jj'} \quad (3.11)$$

$$H'_{j\gamma} \cong \left\langle u_{j0} \left| \frac{\hbar}{m_0} \vec{k} \cdot \vec{p} \right| u_{\gamma 0} \right\rangle = \sum_{\alpha} \frac{\hbar k_{\alpha}}{m_0} p_{j\gamma}^{\alpha} \quad (3.12)$$

where $\alpha = x, y, z$, $p_{jj'}^{\alpha} = 0$ for $j, j' \in A$ (i.e. the perturbed part has no effect on class A states) and $p_{j\gamma}^{\alpha} \neq 0$ for $\gamma \notin A$ where the following notation is used:

$$p_{j\gamma}^{\alpha} \equiv \langle u_{j0} | p_{\alpha} | u_{\gamma 0} \rangle \quad (3.13)$$

where operator $p_{\alpha} \equiv -i\hbar \frac{\partial}{\partial \alpha}$. Here equation (3.11) describes the unperturbed part and (3.12) describes perturbed part. By substituting (3.11) and (3.12) into (3.10) we obtain:

$$H_{jj'}^{LK} = \left[E_j(0) + \frac{\hbar^2 k^2}{2m_0} \right] \delta_{jj'} + \frac{\hbar^2}{m_0^2} \sum_{\gamma}^B \sum_{\alpha, \beta} \frac{k_{\alpha} k_{\beta} p_{j\gamma}^{\alpha} p_{\gamma j'}^{\beta}}{E_0 - E_{\gamma}} \quad (3.14)$$

where $\alpha, \beta = x, y, z$ and $\delta_{jj'}$ is a Kronecker symbol. In a simplified form this expression is:

$$H_{jj'}^{LK} = E_j(0)\delta_{jj'} + \sum_{\alpha,\beta} D_{jj'}^{\alpha\beta} k_\alpha k_\beta \quad (3.15)$$

where

$$D_{jj'}^{\alpha\beta} = \frac{\hbar^2}{2m_0} \left\{ \delta_{jj'}\delta_{\alpha\beta} + \sum_{\gamma} \frac{p_{j\gamma}^\alpha p_{\gamma j'}^\beta + p_{j\gamma}^\beta p_{\gamma j'}^\alpha}{m_0(E_0 - E_\gamma)} \right\} \quad (3.16)$$

To prove the above equivalence, we substitute equation (3.16) into (3.15) and obtain:

$$\begin{aligned} H_{jj'}^{LK} &= E_j(0)\delta_{jj'} + \frac{\hbar^2}{2m_0} \sum_{\alpha,\beta} k_\alpha k_\beta \left\{ \delta_{jj'}\delta_{\alpha\beta} + \sum_{\gamma} \frac{p_{j\gamma}^\alpha p_{\gamma j'}^\beta + p_{j\gamma}^\beta p_{\gamma j'}^\alpha}{m_0(E_0 - E_\gamma)} \right\} \\ &= \left[E_j(0) + \frac{\hbar^2 k^2}{2m_0} \right] \delta_{jj'} + \frac{\hbar^2}{2m_0} \sum_{\gamma} \sum_{\alpha,\beta} k_\alpha k_\beta \frac{p_{j\gamma}^\alpha p_{\gamma j'}^\beta + p_{j\gamma}^\beta p_{\gamma j'}^\alpha}{m_0(E_0 - E_\gamma)} \\ &= \left[E_j(0) + \frac{\hbar^2 k^2}{2m_0} \right] \delta_{jj'} + \frac{\hbar^2}{m_0} \sum_{\gamma} \sum_{\alpha,\beta} \frac{k_\alpha k_\beta p_{j\gamma}^\alpha p_{\gamma j'}^\beta}{m_0(E_0 - E_\gamma)} \end{aligned}$$

where the last term was obtained by the following relation:

$$p_{j\gamma}^\alpha p_{\gamma j'}^\beta + p_{j\gamma}^\beta p_{\gamma j'}^\alpha \equiv \langle u_{j0} | p_\alpha | u_{\gamma 0} \rangle \langle u_{\gamma 0} | p_\beta | u_{j'0} \rangle + \langle u_{j0} | p_\beta | u_{\gamma 0} \rangle \langle u_{\gamma 0} | p_\alpha | u_{j'0} \rangle \equiv 2p_{j\gamma}^\alpha p_{\gamma j'}^\beta$$

In the last step we interchanged α and β . It is convenient to introduce the short notation which is based on the fact that each basis function consists of $|X\rangle$, $|Y\rangle$ and $|Z\rangle$ and we are able to split all matrix elements into the parts containing only one of these basis functions. Based on those statements the following short notation is used:

$$\begin{aligned} A &= \frac{\hbar^2}{2m_0} + \frac{\hbar^2}{m_0^2} \sum_{\gamma} \frac{p_{X\gamma}^x p_{\gamma X}^x}{E_0 - E_\gamma} \\ B &= \frac{\hbar^2}{2m_0} + \frac{\hbar^2}{m_0^2} \sum_{\gamma} \frac{p_{X\gamma}^y p_{\gamma X}^y}{E_0 - E_\gamma} \\ C &= \frac{\hbar^2}{m_0^2} \sum_{\gamma} \frac{p_{X\gamma}^x p_{\gamma Y}^y + p_{X\gamma}^y p_{\gamma Y}^x}{E_0 - E_\gamma} \end{aligned} \quad (3.17)$$

Here A and B describe coupling of the A class states to all other states, and C relates to the anisotropy of the band structure around extremum point (Γ point). The above notation is used to introduce experimental band structure (or Luttinger) parameters γ_i

for cubic crystals, and in a convenient form they are defined as:

$$\begin{aligned} -\frac{\hbar^2}{2m_0}\gamma_1 &= \frac{1}{3}(A + 2B) \\ -\frac{\hbar^2}{2m_0}\gamma_2 &= \frac{1}{6}(A - B) \\ -\frac{\hbar^2}{2m_0}\gamma_3 &= \frac{C}{6} \end{aligned} \quad (3.18)$$

The definitions are made on the assumption that the right hand side relations are invariant under operations of cubic point group (Appendix F). The relations were labeled by Luttinger as γ_i for convenience.

3.1.2 Matrix in $|X\rangle |Y\rangle |Z\rangle$ basis

The evaluation of matrix elements of Hamiltonian in $|X\rangle |Y\rangle |Z\rangle$ basis helps to obtain matrix elements in u_{j0} basis. In this section indices $a, b = |X\rangle, |Y\rangle, |Z\rangle$ and indices $\alpha, \beta = x, y, z$ are used.

In this section the following notation for matrix elements is used (the same as in the expression (3.17) and similar to (3.13) where u_j are replaced by $|X\rangle |Y\rangle |Z\rangle$):

$$\begin{aligned} \langle X | p_y | \gamma \rangle &\equiv p_{X\gamma}^y \\ |\langle X | p_y | \gamma \rangle|^2 &\equiv p_{X\gamma}^y p_{\gamma X}^y \end{aligned} \quad (3.19)$$

where X represents $|X\rangle, |Y\rangle$ or $|Z\rangle$ states, p_y is the operator $-i\hbar\frac{\partial}{\partial y}$ and γ labels states from class B. The property that operator Hamiltonian should be Hermitian¹ requires the following relation (the definition of Hermitian conjugation):

$$\begin{aligned} p_{X\gamma}^y &= (p_{\gamma X}^y)^* \\ (D_{ab}^{\alpha\beta})^* &= D_{ba}^{\beta\alpha} \end{aligned} \quad (3.20)$$

where “*” means complex conjugation. The symmetry of cube allows us to write the following:

$$p_{X\gamma}^y p_{\gamma X}^y = p_{X\gamma}^z p_{\gamma X}^z \neq p_{X\gamma}^x p_{\gamma X}^x \quad (3.21)$$

¹Hermitian conjugation means complex conjugation and transpose, which is shown as eq. (3.20).

which means that the properties of materials along all axes in cubic crystal are equal to each other. To simplify calculations we use the following notation:

$$\begin{aligned} A &= D_{XX}^{xx} \\ B &= D_{XX}^{yy} \\ C &= D_{XY}^{xy} + D_{XY}^{yx} \end{aligned} \quad (3.22)$$

where A, B, C are given by (3.17). $D_{ab}^{\alpha\beta}$ is defined by (3.16) with indices a, b instead of j, j' and explicitly can be written as:

$$\begin{aligned} A = D_{XX}^{xx} &= \frac{\hbar^2}{2m_0} \left\{ \delta_{XX} \delta_{xx} + \sum_{\gamma}^B \frac{p_{X\gamma}^x p_{\gamma X}^x + p_{X\gamma}^x p_{\gamma X}^x}{m_0(E_0 - E_{\gamma})} \right\} = \frac{\hbar^2}{2m_0} \left\{ 1 + 2 \sum_{\gamma}^B \frac{p_{X\gamma}^x p_{\gamma X}^x}{m_0(E_0 - E_{\gamma})} \right\} \\ &= \frac{\hbar^2}{2m_0} + \frac{\hbar^2}{m_0^2} \sum_{\gamma}^B \frac{p_{X\gamma}^x p_{\gamma X}^x}{E_0 - E_{\gamma}} \end{aligned}$$

The other terms are obtained in the same way. We also define:

$$\langle X | H | Y \rangle \equiv D_{XY} \quad (3.23)$$

where D_{ab} has the following form:

$$D_{ab} = \sum_{\alpha\beta} D_{ab}^{\alpha\beta} k_{\alpha} k_{\beta} \quad (3.24)$$

or in a matrix form the same expression has the following structure:

$$D = \begin{bmatrix} D_{XX} & D_{XY} & D_{XZ} \\ D_{YX} & D_{YY} & D_{YZ} \\ D_{ZX} & D_{ZY} & D_{ZZ} \end{bmatrix} \quad (3.25)$$

By writing the summation in equation (3.24) explicitly, we obtain the following matrix elements:

$$\begin{aligned} D_{XX} &= \sum_{\alpha\beta} D_{XX}^{\alpha\beta} k_{\alpha} k_{\beta} = D_{XX}^{xx} k_x^2 + 2D_{XX}^{xy} k_x k_y + D_{XX}^{yy} k_y^2 + 2D_{XX}^{xz} k_x k_z + D_{XX}^{zz} k_z^2 + 2D_{XX}^{yz} k_y k_z \\ &= D_{XX}^{xx} k_x^2 + D_{XX}^{yy} k_y^2 + D_{XX}^{zz} k_z^2 = A k_x^2 + B(k_y^2 + k_z^2) \end{aligned}$$

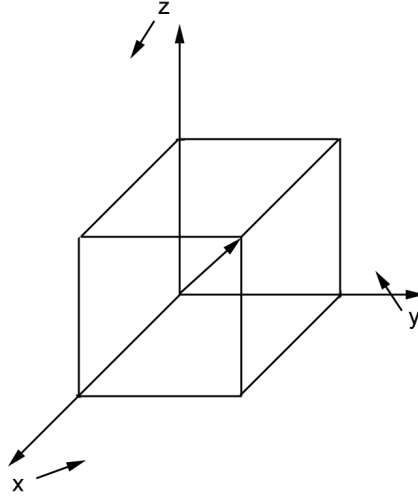


FIGURE 3.1: T_d^2 symmetry group has main symmetry axis, which is a diagonal of cube, and rotation of coordinate system around this axis for each 120° degree causes the axes to convert as such: $x \rightarrow y, y \rightarrow z, z \rightarrow x$.

$$D_{YY} = D_{YY}^{xx}k_x^2 + D_{YY}^{yy}k_y^2 + D_{YY}^{zz}k_z^2 = Ak_y^2 + B(k_x^2 + k_z^2)$$

$$D_{ZZ} = D_{ZZ}^{xx}k_x^2 + D_{ZZ}^{yy}k_y^2 + D_{ZZ}^{zz}k_z^2 = Ak_z^2 + B(k_x^2 + k_y^2)$$

$$D_{XY} = \sum_{\alpha\beta} D_{XY}^{\alpha\beta}k_\alpha k_\beta =$$

$$= D_{XY}^{xx}k_x^2 + D_{XY}^{xy}k_x k_y + D_{XY}^{yx}k_y k_x + D_{XY}^{yy}k_y^2 + 2D_{XY}^{xz}k_x k_z + D_{XY}^{zz}k_z^2 + 2D_{XY}^{yz}k_y k_z$$

$$= D_{XY}^{xy}k_x k_y + D_{XY}^{yx}k_y k_x = Ck_x k_y$$

$$D_{XZ} = D_{XZ}^{xz}k_x k_z + D_{XZ}^{zx}k_z k_x = Ck_x k_z$$

$$D_{YZ} = D_{YZ}^{yz}k_y k_z + D_{YZ}^{zy}k_z k_y = Ck_y k_z$$

where the following properties (Fig. 3.1), allowed by T_d group² symmetry, are used:

$$D_{XX}^{xx} = D_{YY}^{yy} = D_{ZZ}^{zz}$$

$$D_{XX}^{yy} = D_{XX}^{zz} = D_{YY}^{xx} = D_{YY}^{zz} = D_{ZZ}^{xx} = D_{ZZ}^{yy}$$

$$D_{XY}^{xy} = D_{YX}^{yx} = D_{XZ}^{xz} = D_{ZX}^{zx} = D_{YZ}^{yz} = D_{ZY}^{zy}$$

$$D_{XY}^{yx} = D_{YX}^{xy} = D_{XZ}^{zx} = D_{ZX}^{xz} = D_{YZ}^{zy} = D_{ZY}^{yz}$$

²More details on T_d group is provided in Appendix F.

According to Fig. 3.1, as we exchange the axes with each other the result is going to have the same form. Matrix elements of the form (with different upper and lower indices):

$$D_{XY}^{zx} = D_{XX}^{zx} = D_{ZZ}^{xy} = 0$$

are equal to zero [52](p. 74). For example, matrix element $p_{XZ}^y = \langle X|p_y|Z\rangle$ has part $\langle X|p_y$ with odd parity with respect to x and y so only functions with odd parity with respect x or y will contribute. The function $|Z\rangle$ has odd parity with respect to z and even with respect to x and y so the matrix elements of the form $p_{XZ}^y = 0$ vanish.

The explicit form of matrix Hamiltonian in $|X\rangle |Y\rangle |Z\rangle$ basis is the following:

$$D = \begin{bmatrix} Ak_x^2 + B(k_y^2 + k_z^2) & Ck_xk_y & Ck_xk_z \\ Ck_xk_y & Ak_y^2 + B(k_x^2 + k_z^2) & Ck_yk_z \\ Ck_xk_z & Ck_yk_z & Ak_z^2 + B(k_x^2 + k_y^2) \end{bmatrix} \begin{matrix} |X\rangle \\ |Y\rangle \\ |Z\rangle \end{matrix} \quad (3.26)$$

3.1.3 Matrix in $u_{n0}(\vec{r})$ basis

It is necessary to express Hamiltonian in the basis u_{j0} , Eq. (3.7). Matrix elements of Hamiltonian in (3.7) basis are combinations of matrix elements in $|X\rangle |Y\rangle |Z\rangle$ basis, Eq. (3.26). In this section, the following notation for matrix elements is introduced:

$$\begin{aligned} P_k &= \frac{\hbar^2}{2m_0} \gamma_1 (k_x^2 + k_y^2 + k_z^2) \\ Q_k &= \frac{\hbar^2}{2m_0} \gamma_2 (k_x^2 + k_y^2 - 2k_z^2) \\ R_k &= \frac{\hbar^2}{2m_0} [-\sqrt{3}\gamma_2 (k_x^2 - k_y^2) + i2\sqrt{3}\gamma_3 k_x k_y] \\ S_k &= \frac{\hbar^2}{m_0} \gamma_3 \sqrt{3} (k_x - ik_y) k_z \end{aligned} \quad (3.27)$$

where subscript k means “kinetic”. The following matrix elements are calculated using the results of Sec. 3.1.2, Eq. (3.26). Hamiltonian H is given by Eq. (3.1). $H_{jj'}^{LK} \equiv \langle u_{j0} | H | u_{j'0} \rangle$ with $j, j' = 1, \dots, 6$ which are the indices of basis functions (3.7):

$$H_{11}^{LK} = \langle u_{10} | H | u_{10} \rangle = \frac{1}{2} \langle (X - iY) \uparrow | H | (X + iY) \uparrow \rangle$$

$$\begin{aligned}
&= \frac{1}{2}[\langle X | H | X \rangle + i \langle X | H | Y \rangle - i \langle Y | H | X \rangle + \langle Y | H | Y \rangle] = \frac{1}{2}[D_{XX} + iD_{XY} - iD_{YX} + D_{YY}] \\
&= \frac{1}{2}[A(k_x^2 + k_y^2) + B(k_x^2 + k_y^2 + 2k_z^2)] = -(P_k + Q_k)
\end{aligned}$$

where definitions (3.22)-(3.24) are used. Explicitly the above relation is:

$$\begin{aligned}
-(P_k + Q_k) &= -\frac{\hbar^2}{2m_0}\gamma_1(k_x^2 + k_y^2 + k_z^2) - \frac{\hbar^2}{2m_0}\gamma_2(k_x^2 + k_y^2 - 2k_z^2) \\
&= \frac{1}{3}(A + 2B)(k_x^2 + k_y^2 + k_z^2) + \frac{1}{6}(A - B)(k_x^2 + k_y^2 - 2k_z^2) \\
&= \frac{2Ak_x^2 + 2Ak_y^2 + 2Ak_z^2 + 4Bk_x^2 + 4Bk_y^2 + 4Bk_z^2 + Ak_x^2 + Ak_y^2 - 2Ak_z^2 - Bk_x^2 - Bk_y^2 + 2Bk_z^2}{6} \\
&= \frac{3Ak_x^2 + 3Ak_y^2 + 3Bk_x^2 + 3Bk_y^2 + 6Bk_z^2}{6} = \frac{A(k_x^2 + k_y^2) + B(k_x^2 + k_y^2 + 2k_z^2)}{2}
\end{aligned}$$

Due to spin relations (2.5) terms with opposite spins vanish:

$$H_{14}^{LK} = H_{41}^{LK} = \langle u_{10} | H | u_{40} \rangle = \frac{1}{2} \langle (X - iY) \uparrow | H | (X - iY) \downarrow \rangle = 0$$

The other terms are also calculated in a similar way:

$$\begin{aligned}
H_{12}^{LK} &= \langle u_{10} | H | u_{20} \rangle = -\frac{1}{\sqrt{3}} \langle (X - iY) \uparrow | H | Z \uparrow \rangle = -\frac{1}{\sqrt{3}}[D_{XZ} - iD_{YZ}] \\
&= -\frac{1}{\sqrt{3}}[C(k_x k_z) - iC(k_y k_z)] = -\frac{C}{\sqrt{3}}(k_x - ik_y)k_z = S_k \\
H_{21}^{LK} &= \langle u_{20} | H | u_{10} \rangle = -\frac{1}{\sqrt{3}} \langle Z \uparrow | H | (X + iY) \uparrow \rangle = -\frac{1}{\sqrt{3}}[D_{ZX} + iD_{ZY}] \\
&= -\frac{1}{\sqrt{3}}[C(k_x k_z) + iC(k_y k_z)] = -\frac{C}{\sqrt{3}}(k_x + ik_y)k_z = S_k^+ \\
H_{13}^{LK} &= \langle u_{10} | H | u_{30} \rangle = -\frac{1}{\sqrt{12}} \langle (X - iY) \uparrow | H | (X - iY) \uparrow \rangle \\
&= -\frac{1}{\sqrt{12}}[D_{XX} - iD_{XY} - iD_{YX} - D_{YY}] = -\frac{1}{\sqrt{12}}[(A - B)(k_x^2 - k_y^2) - 2iCk_x k_y] = -R_k \\
H_{31}^{LK} &= \langle u_{30} | H | u_{10} \rangle = -\frac{1}{\sqrt{12}} \langle (X + iY) \uparrow | H | (X + iY) \uparrow \rangle \\
&= -\frac{1}{\sqrt{12}}[D_{XX} + iD_{XY} + iD_{YX} - D_{YY}] = -\frac{1}{\sqrt{12}}[(A - B)(k_x^2 - k_y^2) + 2iCk_x k_y] = -R_k^+
\end{aligned}$$

where superscript “+” means Hermitian conjugation.

Full explicit Luttinger Kohn Hamiltonian, denoted as \mathbf{H}^{LK} can be expressed in the following form:

$$\mathbf{H}^{LK} = - \begin{bmatrix} P_k + Q_k & -S_k & R_k & 0 & -\frac{S_k}{\sqrt{2}} & \sqrt{2}R_k \\ -S_k^+ & P_k - Q_k & 0 & R_k & -\sqrt{2}Q_k & \sqrt{\frac{3}{2}}S_k \\ R_k^+ & 0 & P_k - Q_k & S_k & \sqrt{\frac{3}{2}}S_k^+ & \sqrt{2}Q_k \\ 0 & R_k^+ & S_k^+ & P_k + Q_k & -\sqrt{2}R_k^+ & -\frac{S_k^+}{\sqrt{2}} \\ -\frac{S_k^+}{\sqrt{2}} & -\sqrt{2}Q_k^+ & \sqrt{\frac{3}{2}}S_k & -\sqrt{2}R_k & P_k + \Delta & 0 \\ \sqrt{2}R_k^+ & \sqrt{\frac{3}{2}}S_k^+ & \sqrt{2}Q_k^+ & -\frac{S_k}{\sqrt{2}} & 0 & P_k + \Delta \end{bmatrix} \quad (3.28)$$

where the above notation (3.27) is used.

3.1.4 Strain effects on band structures

In this section, we derive the Bir and Pikus Hamiltonian (BPH) for strained semiconductors [53], [54], [55]. In general the strain may be arbitrary. However, practical cases are the axial strain, in other words strain along the axes. Following this definition, below we discuss uniaxial (along one of the axes at a time) and biaxial (along two axes at the same time with the same value) strain. Strain is defined by strain tensor ε :

$$\varepsilon = \begin{bmatrix} \varepsilon_{xx} & \varepsilon_{xy} & \varepsilon_{xz} \\ \varepsilon_{yx} & \varepsilon_{yy} & \varepsilon_{yz} \\ \varepsilon_{zx} & \varepsilon_{zy} & \varepsilon_{zz} \end{bmatrix} \quad (3.29)$$

where the subscripts indicate axes along which the lattice is strained. Axial strain leaves non zero terms only along main diagonal.

The strain influence on band structure is relatively large and cannot be treated as perturbation directly. However, there is a method, developed by Bir and Pikus, of treating the strain influence as perturbation. Consider the crystal before (Fig. 3.2.a) and after

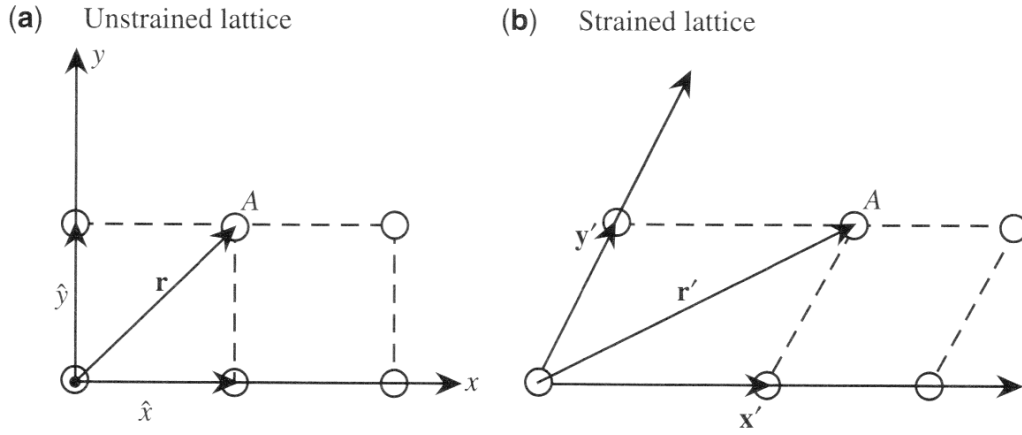


FIGURE 3.2: Positions of vectors \vec{r} and \vec{r}' for atom A in (a) unstrained and (b) strained lattice.

(Fig. 3.2.b) deformation. In the undeformed, crystal unit vectors \hat{x}, \hat{y} can be assumed as basis vectors for coordinate system. The relations between the unit vectors in the undeformed and uniformly deformed crystal are the following:

$$\begin{aligned}
 \mathbf{x}' &= (1 + \varepsilon_{xx})\hat{x} + \varepsilon_{xy}\hat{y} + \varepsilon_{xz}\hat{z} \\
 \mathbf{y}' &= \varepsilon_{yx}\hat{x} + (1 + \varepsilon_{yy})\hat{y} + \varepsilon_{yz}\hat{z} \\
 \mathbf{z}' &= \varepsilon_{zx}\hat{x} + \varepsilon_{zy}\hat{y} + (1 + \varepsilon_{zz})\hat{z}
 \end{aligned} \tag{3.30}$$

\mathbf{x}', \mathbf{y}' and \mathbf{z}' are not unit vectors anymore. We define six strain components assuming a homogeneous³ strain and $\varepsilon_{\alpha\beta} = \varepsilon_{\beta\alpha}$:

$$\begin{aligned}
 e_1 &= \varepsilon_{xx} & e_2 &= \varepsilon_{yy} & e_3 &= \varepsilon_{zz} \\
 e_4 &= \mathbf{x}' \cdot \mathbf{y}' = \varepsilon_{xy} + \varepsilon_{yx} \\
 e_5 &= \mathbf{y}' \cdot \mathbf{z}' = \varepsilon_{yz} + \varepsilon_{zy} \\
 e_6 &= \mathbf{z}' \cdot \mathbf{x}' = \varepsilon_{zx} + \varepsilon_{xz}
 \end{aligned} \tag{3.31}$$

keeping only the linear terms in strain. Fig. 3.2 shows how the position of A (atom A) is labeled in undeformed crystal:

$$\vec{r} = x\hat{x} + y\hat{y} + z\hat{z} \equiv (x, y, z) \tag{3.32}$$

³Homogeneous means that the forces exerted across the faces of a given volume depend only on the shape and orientation of the volume, not on its location within the solid.

The same atom in the deformed crystal can be labeled either using the new basis vectors:

$$\vec{r}' = x\mathbf{x}' + y\mathbf{y}' + z\mathbf{z}' \approx (1 - \varepsilon) \cdot \vec{r} \quad (3.33)$$

or using the original (undeformed) basis vectors:

$$\vec{r}' = x'\hat{x} + y'\hat{y} + z'\hat{z} \equiv (x', y', z') \quad (3.34)$$

The change of the volume Ω due to deformation in the linear strain regime:

$$\frac{\Omega + \delta\Omega}{\Omega} = |\mathbf{x}' \cdot (\mathbf{y}' \times \mathbf{z}')| = 1 + (\varepsilon_{xx} + \varepsilon_{yy} + \varepsilon_{zz}) \quad (3.35)$$

From the above expression it is clear that the fractional change of the volume $\delta\Omega/\Omega$ of the crystal under uniform deformation is the trace of matrix ε :

$$\frac{\delta\Omega}{\Omega} = \varepsilon_{xx} + \varepsilon_{yy} + \varepsilon_{zz} \quad (3.36)$$

Change of the \vec{r} vector leads to changes in all \vec{r} dependent operators, especially operators \vec{p} and p^2 :

$$\vec{p} = -i\hbar \frac{\partial}{\partial \vec{r}} = -i\hbar \frac{\partial}{\partial \vec{r}'} \frac{\partial \vec{r}'}{\partial \vec{r}} \quad (3.37)$$

or the same in component form:

$$p_\alpha = -i\hbar \frac{\partial}{\partial r_\alpha} = -i\hbar \frac{\partial}{\partial r'_\beta} \frac{\partial r'_\beta}{\partial r_\alpha} \quad (3.38)$$

Eq. (3.33) in a component form:

$$r'_\beta = (\delta_{\alpha\beta} - \varepsilon_{\alpha\beta})r_\alpha \quad (3.39)$$

Eq. (3.38) contains derivative of the form:

$$\frac{\partial r'_\beta}{\partial r_\alpha} = \delta_{\alpha\beta} - \varepsilon_{\alpha\beta} \quad (3.40)$$

Substituting (3.40) into (3.38) yields the following relation for p_α :

$$p_\alpha = -i\hbar \frac{\partial}{\partial r'_\beta} (\delta_{\alpha\beta} - \varepsilon_{\alpha\beta}) = -i\hbar \frac{\partial}{\partial r'_\alpha} + i\hbar \frac{\partial}{\partial r'_\beta} \varepsilon_{\beta\alpha} \quad (3.41)$$

Momentum operator in the deformed system is:

$$p'_\alpha \equiv -i\hbar \frac{\partial}{\partial r'_\alpha} \quad (3.42)$$

thus p_α (3.41) may be written in terms of p'_α :

$$p_\alpha = p'_\alpha - \varepsilon_{\beta\alpha} p'_\beta \quad (3.43)$$

Using (3.43) and the homogeneous strain assumption $\varepsilon_{\alpha\beta} = \varepsilon_{\beta\alpha}$, the $p^2 = p_\alpha p_\alpha$ may be obtained⁴:

$$\begin{aligned} p^2 &= (p'_\alpha - \varepsilon_{\beta\alpha} p'_\beta)(p'_\alpha - \varepsilon_{\alpha\zeta} p'_\zeta) \\ &= p'^2 - 2p'_\alpha \varepsilon_{\alpha\beta} p'_\beta + p'_\alpha \varepsilon_{\alpha\beta} \varepsilon_{\beta\zeta} p'_\zeta \\ &\approx p'^2 - 2p'_\alpha \varepsilon_{\alpha\beta} p'_\beta \end{aligned} \quad (3.44)$$

where the second order effects of ε are neglected. The strain changes the period of the lattice and consequently changes the \vec{r} dependent potential from V_0 to V :

$$V(\vec{r}') = V_0 + V_{\alpha\beta} \varepsilon_{\alpha\beta} \quad (3.45)$$

where

$$V_{\alpha\beta} = \frac{\partial \delta V}{\partial \varepsilon_{\alpha\beta}} \quad (3.46)$$

where δV is a perturbing potential, which is dependent on ε . Perturbing potential is a very complicated object. The explicit form of δV is more difficult to obtain than the unperturbed potential V_0 , as it requires to solve exactly self consistent problem in deformed crystal, which will show the differences between deformed and undeformed potentials under small deformations. There are theoretical models [56](p.426) for obtaining the perturbing potential, however the theoretical results for perturbing potential were completely different from the experimental measurements. To avoid using explicit form of perturbing potential, the experimental deformation potentials have been introduced, which are described below. The strain effects are included in the unstrained Hamiltonian (3.1) by substitution transformed expressions for p^2 , \vec{p} , \vec{r} , \vec{k} and V :

$$H = H_0 + H_1 + H_2 \quad (3.47)$$

⁴Components of p commute.

where

$$\begin{aligned}
H_0 &= \frac{p^2}{2m_0} + V(\vec{r}) \\
H_1 &= \frac{\hbar}{m_0} \vec{k} \cdot \vec{p} + \left(-\frac{1}{m_0} p_\alpha p_\beta + V_{\alpha\beta} \right) \varepsilon_{\alpha\beta} - 2 \frac{\vec{k} \cdot \varepsilon \cdot \vec{p}}{m_0} \\
H_2 &= \frac{\hbar^2 k^2}{2m_0} - \frac{\vec{k} \cdot \varepsilon \cdot \vec{k}}{m_0}
\end{aligned} \tag{3.48}$$

In addition to k -dependent perturbations the strain effects are added. The above strain can be assumed small and treated as perturbation as we now work in the deformed crystal. The effects of \vec{k} are treated to second order and the effects of ε are treated to first order, thus the terms containing $\vec{k} \cdot \varepsilon$ can be neglected because ε is much larger than $\vec{k} \cdot \varepsilon$. Then the approximate relations may be written as:

$$\begin{aligned}
H_1 &\approx \frac{\hbar}{m_0} \vec{k} \cdot \vec{p} + \left(-\frac{1}{m_0} p_\alpha p_\beta + V_{\alpha\beta} \right) \varepsilon_{\alpha\beta} \\
H_2 &\approx \frac{\hbar^2 k^2}{2m_0}
\end{aligned} \tag{3.49}$$

Combining the value $V_{\alpha\beta}$ with the $\vec{p} \cdot \varepsilon \cdot \vec{p}$ in H_1 we define the deformation potential operator:

$$\hat{D} \cdot \varepsilon = \left(-\frac{1}{m_0} p_\alpha p_\beta + V_{\alpha\beta} \right) \varepsilon_{\alpha\beta} \tag{3.50}$$

In unstrained semiconductor the LKH is given by (3.15) and in explicit matrix form by (3.28):

$$H_{jj'}^{LK} = E_j(0) \delta_{jj'} + \sum_{\alpha,\beta} D_{jj'}^{\alpha\beta} k_\alpha k_\beta \tag{3.51}$$

For strained semiconductor the extra terms to Eq. (3.51) are added⁵:

$$(H_\varepsilon)_{jj'} = \sum_{\alpha,\beta} \hat{D}_{jj'}^{\alpha\beta} \varepsilon_{\alpha\beta} \tag{3.52}$$

due to the linear strain, where \hat{D} transforms as a second-rank tensor under the operations of crystal point group. At this point, it is clear (by comparing eq. (3.16) and (3.50)) that the relation $\hat{D} \cdot \varepsilon$ has similar behavior as $D \cdot \vec{k} \cdot \vec{k}$. Thus, matrix may be constructed, similar to (3.26), which will include the matrix elements of the form $\langle u | \hat{D} \varepsilon | u \rangle$ for conduction

⁵In this section strain effects on 6×6 LKH are considered. Strain effects on conduction and nitrogen level matrix elements are discussed in section 4.6.

band:

$$\begin{aligned}
\langle S | \left(-\frac{1}{m_0} p_\alpha p_\beta + V_{\alpha\beta} \right) \varepsilon_{\alpha\beta} | S \rangle &= \langle S | -\frac{1}{m_0} p_x p_x + V_{xx} | S \rangle \varepsilon_{xx} \\
&+ \langle S | -\frac{1}{m_0} p_y p_y + V_{yy} | S \rangle \varepsilon_{yy} + \langle S | -\frac{1}{m_0} p_z p_z + V_{zz} | S \rangle \varepsilon_{zz} \\
&= a_c (\varepsilon_{xx} + \varepsilon_{yy} + \varepsilon_{zz}) = a_c \text{Tr}(\varepsilon)
\end{aligned} \tag{3.53}$$

where $a_c = \langle S | \hat{D}_{xx} | S \rangle = \langle S | \hat{D}_{yy} | S \rangle = \langle S | \hat{D}_{zz} | S \rangle$ and off-diagonal terms in \hat{D} vanish because $|S\rangle$ is odd function in all coordinates. The same for $|X\rangle$ from valence band:

$$\begin{aligned}
\langle X | \left(-\frac{1}{m_0} p_\alpha p_\beta + V_{\alpha\beta} \right) \varepsilon_{\alpha\beta} | X \rangle &= \langle X | -\frac{1}{m_0} p_x p_x + V_{xx} | X \rangle \varepsilon_{xx} \\
&+ \langle X | -\frac{1}{m_0} p_y p_y + V_{yy} | X \rangle \varepsilon_{yy} + \langle X | -\frac{1}{m_0} p_z p_z + V_{zz} | X \rangle \varepsilon_{zz} \\
&= l_\varepsilon \varepsilon_{xx} + m_\varepsilon (\varepsilon_{yy} + \varepsilon_{zz})
\end{aligned} \tag{3.54}$$

where $l_\varepsilon = \langle X | \hat{D}_{xx} | X \rangle$ and $m_\varepsilon = \langle X | \hat{D}_{yy} | X \rangle = \langle X | \hat{D}_{zz} | X \rangle$ and off-diagonal terms in \hat{D} vanish, due to $|X\rangle$ is even in x , but odd in y and z . The typical off-diagonal term:

$$\langle X | \left(-\frac{1}{m_0} p_\alpha p_\beta + V_{\alpha\beta} \right) \varepsilon_{\alpha\beta} | Y \rangle = \langle X | -\frac{1}{m_0} p_x p_y + V_{xy} | Y \rangle \varepsilon_{xy} = n_\varepsilon \varepsilon_{xy} \tag{3.55}$$

where $n_\varepsilon = \langle X | \hat{D}_{xy} | Y \rangle$ and all terms in \hat{D} except \hat{D}_{xy} vanish due to the fact that \hat{D} terms should be odd in x , odd in y and even in z . The $l_\varepsilon, m_\varepsilon$ and n_ε are different deformation potentials. The total matrix may be expressed as:

$$H_\varepsilon = \begin{bmatrix} a_c \text{Tr}(\varepsilon) & 0 & 0 & 0 \\ 0 & l_\varepsilon \varepsilon_{xx} + m_\varepsilon (\varepsilon_{yy} + \varepsilon_{zz}) & n_\varepsilon \varepsilon_{xy} & n_\varepsilon \varepsilon_{xz} \\ 0 & n_\varepsilon \varepsilon_{yx} & l_\varepsilon \varepsilon_{yy} + m_\varepsilon (\varepsilon_{xx} + \varepsilon_{zz}) & n_\varepsilon \varepsilon_{yz} \\ 0 & n_\varepsilon \varepsilon_{zx} & n_\varepsilon \varepsilon_{zy} & l_\varepsilon \varepsilon_{zz} + m_\varepsilon (\varepsilon_{xx} + \varepsilon_{yy}) \end{bmatrix} \begin{matrix} |S\rangle \\ |X\rangle \\ |Y\rangle \\ |Z\rangle \end{matrix} \tag{3.56}$$

This is the BPH in $|S\rangle, |X\rangle, |Y\rangle, |Z\rangle$ basis. By inspecting the hole part of the (3.56), the following equivalences between (3.26) and (3.56) are found:

$$\begin{aligned}
k_\alpha k_\beta &\rightarrow \varepsilon_{\alpha\beta} \\
A &\rightarrow l_\varepsilon \\
B &\rightarrow m_\varepsilon \\
C &\rightarrow n_\varepsilon
\end{aligned} \tag{3.57}$$

Both equations are written in the same basis, the parameters A, B and C are linked to Luttinger parameters by invariant relations (3.18) with respect to spin-orbit coupling, thus, intuitively, parameters $l_\varepsilon, m_\varepsilon$ and n_ε should have similar invariant link with measurable valence band deformation potentials:

$$\begin{aligned} a_v &= \frac{l_\varepsilon + 2m_\varepsilon}{3} \\ b &= \frac{l_\varepsilon - m_\varepsilon}{3} \\ d &= \frac{n_\varepsilon}{\sqrt{3}} \end{aligned} \quad (3.58)$$

The similarities between Luttinger parameters and deformation potentials lead to the following equivalences:

For conduction band

$$\frac{\hbar^2}{2m_e^*} \rightarrow a_c \quad (3.59)$$

where a_c is the conduction deformation potential. Thus, the conduction band edge dispersion is:

$$E(k) = E_c(0) + \frac{\hbar^2}{2m_e^*} k^2 + a_c \text{Tr}(\varepsilon) \quad (3.60)$$

For valence band

$$\frac{\hbar^2 \gamma_1}{2m_0} \rightarrow D_v^d \equiv a_v \quad (3.61)$$

$$\frac{\hbar^2 \gamma_2}{2m_0} \rightarrow \frac{D_u}{3} \equiv -\frac{b}{2} \quad (3.62)$$

$$\frac{\hbar^2 \gamma_3}{2m_0} \rightarrow \frac{D'_u}{3} \equiv -\frac{d}{2\sqrt{3}} \quad (3.63)$$

The total Hamiltonian is obtained as a sum of \mathbf{H}^{LK} (3.28) and the strain counterpart H_ε ⁶:

$$\mathbf{H} = - \begin{bmatrix} P+Q & -S & R & 0 & -\frac{S}{\sqrt{2}} & \sqrt{2}R \\ -S^+ & P-Q & 0 & R & -\sqrt{2}Q & \sqrt{\frac{3}{2}}S \\ R^+ & 0 & P-Q & S & \sqrt{\frac{3}{2}}S^+ & \sqrt{2}Q \\ 0 & R^+ & S^+ & P+Q & -\sqrt{2}R^+ & -\frac{S^+}{\sqrt{2}} \\ -\frac{S^+}{\sqrt{2}} & -\sqrt{2}Q^+ & \sqrt{\frac{3}{2}}S & -\sqrt{2}R & P+\Delta & 0 \\ \sqrt{2}R^+ & \sqrt{\frac{3}{2}}S^+ & \sqrt{2}Q^+ & -\frac{S}{\sqrt{2}} & 0 & P+\Delta \end{bmatrix} \quad (3.64)$$

where

$$\begin{aligned} P &= P_k + P_\varepsilon & Q &= Q_k + Q_\varepsilon \\ R &= R_k + R_\varepsilon & S &= S_k + S_\varepsilon \\ P_k &= \frac{\hbar^2}{2m_0} \gamma_1 (k_x^2 + k_y^2 + k_z^2) & Q_k &= \frac{\hbar^2}{2m_0} \gamma_2 (k_x^2 + k_y^2 - 2k_z^2) \\ R_k &= \frac{\hbar^2}{2m_0} [-\sqrt{3}\gamma_2 (k_x^2 - k_y^2) + i2\sqrt{3}\gamma_3 k_x k_y] \\ S_k &= \frac{\hbar^2}{m_0} \gamma_3 \sqrt{3} (k_x - ik_y) k_z \\ P_\varepsilon &= -a_v (\varepsilon_{xx} + \varepsilon_{yy} + \varepsilon_{zz}) & Q_\varepsilon &= -\frac{b}{2} (\varepsilon_{xx} + \varepsilon_{yy} - 2\varepsilon_{zz}) \\ R_\varepsilon &= \frac{\sqrt{3}b}{2} (\varepsilon_{xx} - \varepsilon_{yy}) - id\varepsilon_{xy} \\ S_\varepsilon &= -d (\varepsilon_{xz} - i\varepsilon_{yz}) \end{aligned} \quad (3.65)$$

The Hamiltonian \mathbf{H} in (3.64) is written for an arbitrary strain. In the case of a biaxial strain, the problem can be simplified as:

$$\begin{aligned} \varepsilon_{xx} &= \varepsilon_{yy} \neq \varepsilon_{zz} \\ \varepsilon_{xy} &= \varepsilon_{yz} = \varepsilon_{zx} = 0 \end{aligned} \quad (3.66)$$

By substitution (3.66) into definition of matrix elements we obtain⁷:

$$R_\varepsilon = S_\varepsilon = 0$$

⁶Here kinetic terms correspond to LKH and strain terms correspond to BPH.

⁷For arbitrary grown substrate the terms R_ε and S_ε are not zero.

The above case covers three strained systems: (001) oriented substrate, bulk semiconductor under external uniaxial stress along the z -direction and external biaxial in-plane stress along x - y -directions.

For cubic systems, stress tensor is related to strain by the elastic stiffness tensor with elements C_{ij} (Hooke's law⁸):

$$\begin{bmatrix} \tau_{xx} \\ \tau_{yy} \\ \tau_{zz} \\ \tau_{xy} \\ \tau_{yz} \\ \tau_{zx} \end{bmatrix} = \begin{bmatrix} C_{11} & C_{12} & C_{12} & 0 & 0 & 0 \\ C_{12} & C_{11} & C_{12} & 0 & 0 & 0 \\ C_{12} & C_{12} & C_{11} & 0 & 0 & 0 \\ 0 & 0 & 0 & C_{44} & 0 & 0 \\ 0 & 0 & 0 & 0 & C_{44} & 0 \\ 0 & 0 & 0 & 0 & 0 & C_{44} \end{bmatrix} \begin{bmatrix} \varepsilon_{xx} \\ \varepsilon_{yy} \\ \varepsilon_{zz} \\ 0 \\ 0 \\ 0 \end{bmatrix} \quad (3.67)$$

The tensor C is expressed using Voigt notation [58], which is convenient due to the fact that the original stiffness tensor C is a four rank tensor with elements C_{ijkl} . The explicit form of Voigt notation converts four indices $ijkl$ into two indices ab (original indices $ijkl$ are run from 1 to 3, whereas Voigt indices ab run from 1 to 6):

$$11 \rightarrow 1, \quad 22 \rightarrow 2, \quad 33 \rightarrow 3, \quad 23, 32 \rightarrow 4, \quad 31, 13 \rightarrow 5, \quad 12, 21 \rightarrow 6$$

where indices are splitted into pairs as $ij = 11$ and $kl = 11$ etc ($ij \rightarrow a$ and $kl \rightarrow b$).

Here, the most important two cases for (001) orientation should be considered:

a: The case of lattice-mismatched strain:

$$\varepsilon_{xx} = \varepsilon_{yy} = \frac{a_0 - a}{a} \quad \varepsilon_{zz} = -\frac{2C_{12}}{C_{11}}\varepsilon_{xx} \quad (3.68)$$

where a_0 and a are the lattice constants of the substrate and the well layer material, and C_{11} and C_{12} are the elastic stiffness constants. The terms $\tau_{xy} = \tau_{yz} = \tau_{zx} = 0$ as there are no diagonal stresses. There should be no stress in the z -direction due to the fact that the lattice mismatch exists only in x - y plane, but not along growth direction:

$$0 = \tau_{zz} = C_{12}(\varepsilon_{xx} + \varepsilon_{yy}) + C_{11}\varepsilon_{zz}$$

⁸In general stiffness tensor C is a four-rank tensor and discussed in detail in [55](p. 98-107), complete discussions of tensor properties for Hooke's law are found in [57](chapter VIII).

From the above relation:

$$\varepsilon_{zz} = -\frac{2C_{12}}{C_{11}}\varepsilon_{xx}$$

b: The case of an external uniaxial stress T along the z axis⁹. One has $\tau_{zz} = T$ and $\tau_{xx} = \tau_{yy} = 0$, and by substitution τ terms to (3.67) we obtain the system of equations:

$$\begin{cases} T &= 2C_{12}\varepsilon_{xx} + C_{11}\varepsilon_{zz} \\ 0 &= (C_{11} + C_{12})\varepsilon_{xx} + C_{12}\varepsilon_{zz} \end{cases} \quad (3.69)$$

From the second equation we obtain:

$$\varepsilon_{zz} = -\frac{C_{11} + C_{12}}{C_{12}}\varepsilon_{xx}$$

Substitution of the last expression to the first equation in the system (3.69) leads to:

$$\begin{aligned} 2C_{12}\varepsilon_{xx} - C_{11}\frac{C_{11} + C_{12}}{C_{12}}\varepsilon_{xx} &= T \Rightarrow \\ \varepsilon_{xx} = \varepsilon_{yy} &= \frac{-C_{12}}{C_{11}^2 + C_{11}C_{12} - 2C_{12}^2}T \end{aligned} \quad (3.70)$$

Substituting the above into the equation for ε_{zz} we obtain:

$$\varepsilon_{zz} = \frac{C_{11} + C_{12}}{C_{11}^2 + C_{11}C_{12} - 2C_{12}^2}T$$

The ε_{xx} term is positive for tensile strain and negative for compressive strain¹⁰. The elastic stiffness constants C_{ij} have pressure units and Bir and Pikus deformation constants a_v, b and d - energy units.

3.2 Hexagonal symmetry (Wurtzite)

3.2.1 The Hamiltonian and the Basis functions

The method of obtaining LKH for wurtzite crystal is the same as expressed in section 3.1.1, but the basis functions in class A for Heavy-hole (u_1, u_5), Light-hole (u_2, u_4)

⁹i.e. external pressure on the crystal.

¹⁰ ε_{xx} is the percentage change in lattice constant.

and Crystal-field Split-off (u_3, u_6) bands are the same as (2.10) and (2.11) and ordered as:

$$\begin{aligned}
 u_1 &= \frac{-1}{\sqrt{2}} |(X'' + iY'') \uparrow\rangle \\
 u_2 &= \frac{1}{\sqrt{2}} |(X'' - iY'') \uparrow\rangle \\
 u_3 &= |Z \uparrow\rangle \\
 u_4 &= \frac{1}{\sqrt{2}} |(X'' - iY'') \downarrow\rangle \\
 u_5 &= \frac{-1}{\sqrt{2}} |(X'' + iY'') \downarrow\rangle \\
 u_6 &= |Z \downarrow\rangle
 \end{aligned} \tag{3.71}$$

The basis is chosen according to C_{6v}^{411} symmetry group [56](p. 97, 285-289) which makes properties in $x - y$ plane different from along z axis. In other words, the wave functions $|X''\rangle$ and $|Y''\rangle$ for hexagonal systems are not the same as for cubic systems. The Hamiltonian is invariant under 60° rotations around the vertical axis z (i.e. c - in hexagonal crystal vertical axis). Thus, the hexagonal wave functions have the following form (obtained in eq. (F.7)):

$$\begin{aligned}
 |X''\rangle &= \frac{1}{2} |X\rangle + \frac{\sqrt{3}}{2} |Y\rangle \\
 |Y''\rangle &= -\frac{\sqrt{3}}{2} |X\rangle + \frac{1}{2} |Y\rangle
 \end{aligned} \tag{3.72}$$

where double primed wave functions create basis for hexagonal system, and unprimed wave functions are (2.12). Starting here the basis X'' used to define experimental parameters, but for convenience we drop the double prime index.

The basis (3.71) is given by the inner product of $|l, m\rangle \left| \frac{1}{2}, s \right\rangle$ with $l = 1, m = 0, \pm 1$ and $s = \pm 1$ for each spin (The details about Dirac notation were explained in section 2.4). In this basis the Hamiltonian is nearly block diagonal. Schrödinger equation is expressed as:

$$H u_{\vec{k}}(\vec{r}) = E(\vec{k}) u_{\vec{k}}(\vec{r}) \tag{3.73}$$

$$H = H_0 + \frac{\hbar^2}{2m_0} + H_{so} + H' \tag{3.74}$$

¹¹More details on C_{6v} group is provided in Appendix F.

where

$$H_{so} = \frac{\hbar}{4m_0^2c^2} \nabla V \times \vec{p} \cdot \vec{\sigma} = H_{sx}\sigma_x + H_{sy}\sigma_y + H_{sz}\sigma_z \quad (3.75)$$

$$H' = \frac{\hbar}{m_0} \vec{k} \cdot \vec{\Pi} \quad (3.76)$$

$$\vec{\Pi} = \vec{p} + \frac{\hbar}{4m_0c^2} \vec{\sigma} \times \vec{\nabla} V \simeq \vec{p} \quad (3.77)$$

where the last term is neglected because it is much smaller than p dependent term. The matrix elements of LKH in general form are expressed as the sum of band edge contribution and a \vec{k} -dependent contribution (in details expressed in section 3.1.1):

$$H_{jj'}^{LK} = H_{jj'}(\vec{k} = 0) + \sum_{\alpha\beta} D_{jj'}^{\alpha\beta} k_\alpha k_\beta \quad (3.78)$$

where the matrix $D_{jj'}$ at $\vec{k} \neq 0$:

$$D_{jj'}^{\alpha\beta} = \frac{\hbar^2}{2m_0} \left\{ \delta_{jj'} \delta_{\alpha\beta} + \sum_{\gamma} \frac{p_{j\gamma}^\alpha p_{\gamma j'}^\beta + p_{j\gamma}^\beta p_{\gamma j'}^\alpha}{m_0(E_0 - E_\gamma)} \right\} \quad (3.79)$$

where the indices $j, j' = 1, 2, 3, 4, 5, 6 \in A, \gamma \in B$, and $\alpha, \beta = x, y, z$.

The band-edge Hamiltonian matrix has been obtained from Kane's model[29]:

$$\mathbf{H}(\vec{k} = 0) = \begin{bmatrix} E_v + \Delta_1 + \Delta_2 & 0 & 0 & 0 & 0 & 0 \\ 0 & E_v + \Delta_1 - \Delta_2 & 0 & 0 & 0 & \sqrt{2}\Delta_3 \\ 0 & 0 & E_v & 0 & \sqrt{2}\Delta_3 & 0 \\ 0 & 0 & 0 & E_v + \Delta_1 + \Delta_2 & 0 & 0 \\ 0 & 0 & \sqrt{2}\Delta_3 & 0 & E_v + \Delta_1 - \Delta_2 & 0 \\ 0 & \sqrt{2}\Delta_3 & 0 & 0 & 0 & E_v \end{bmatrix} \quad (3.80)$$

where the energies have the following definitions:

$$\begin{aligned} \langle X | H_0 | X \rangle &= \langle Y | H_0 | Y \rangle = E_v + \Delta_1 \\ \langle X | H_0 | Y \rangle &= 0 \\ \langle Z | H_0 | Z \rangle &= E_v \\ \langle X | H_{sz} | Y \rangle &= -i\Delta_2 \\ \langle Y | H_{sx} | Z \rangle &= \langle Z | H_{sy} | X \rangle = -i\Delta_3 \end{aligned} \quad (3.81)$$

The sample calculation of Kane's model band edge matrix element is the following (spin properties (2.3), (2.4) and (2.5) are used):

$$\begin{aligned}
\langle u_1 | H(\vec{k} = 0) | u_1 \rangle &= \frac{1}{2} \langle (X - iY) \uparrow | H(\vec{k} = 0) | (X + iY) \uparrow \rangle \\
&= \frac{1}{2} (\langle X | H_0 | X \rangle + \langle Y | H_0 | Y \rangle + i \langle X | H_{sz} | Y \rangle - i \langle Y | H_{sz} | X \rangle) \\
&= \frac{1}{2} [E_v + \Delta_1 + E_v + \Delta_1 + i \langle X | H_{sz} | Y \rangle + i (\langle Y | H_{sz} | X \rangle)^+] \\
&= \frac{1}{2} [2(E_v + \Delta_1) + 2\Delta_2] = E_v + \Delta_1 + \Delta_2
\end{aligned} \tag{3.82}$$

where u_1 is defined as (3.71) with double prime “''” dropped and “+” is Hermitian conjugation. For hexagonal crystals the short notation is used based on the same idea as for cubic systems, but using sixfold rotation symmetry. Thus the following terms, similar to (3.17) $L_1, L_2, M_1, M_2, M_3, N_1, N_2$ are introduced by substitution $\alpha, \beta = x, y, z$ and $a, b = X, Y, Z$ instead of j, j' into (3.79):

$$\begin{aligned}
L_1 &= \frac{\hbar^2}{2m_0} \left[1 + \sum_{\gamma}^B \frac{2p_{X\gamma}^x p_{\gamma X}^x}{m_0(E_0 - E_{\gamma})} \right] = \frac{\hbar^2}{2m_0} \left[1 + \sum_{\gamma}^B \frac{2p_{Y\gamma}^y p_{\gamma Y}^y}{m_0(E_0 - E_{\gamma})} \right] \\
L_2 &= \frac{\hbar^2}{2m_0} \left[1 + \sum_{\gamma}^B \frac{2p_{Z\gamma}^z p_{\gamma Z}^z}{m_0(E_0 - E_{\gamma})} \right] \\
M_1 &= \frac{\hbar^2}{2m_0} \left[1 + \sum_{\gamma}^B \frac{2p_{X\gamma}^y p_{\gamma X}^y}{m_0(E_0 - E_{\gamma})} \right] = \frac{\hbar^2}{2m_0} \left[1 + \sum_{\gamma}^B \frac{2p_{Y\gamma}^x p_{\gamma Y}^x}{m_0(E_0 - E_{\gamma})} \right] \\
M_2 &= \frac{\hbar^2}{2m_0} \left[1 + \sum_{\gamma}^B \frac{2p_{X\gamma}^z p_{\gamma X}^z}{m_0(E_0 - E_{\gamma})} \right] = \frac{\hbar^2}{2m_0} \left[1 + \sum_{\gamma}^B \frac{2p_{Y\gamma}^z p_{\gamma Y}^z}{m_0(E_0 - E_{\gamma})} \right] \\
M_3 &= \frac{\hbar^2}{2m_0} \left[1 + \sum_{\gamma}^B \frac{2p_{Z\gamma}^y p_{\gamma Z}^y}{m_0(E_0 - E_{\gamma})} \right] = \frac{\hbar^2}{2m_0} \left[1 + \sum_{\gamma}^B \frac{2p_{Z\gamma}^x p_{\gamma Z}^x}{m_0(E_0 - E_{\gamma})} \right] \\
N_1 &= \frac{\hbar^2}{m_0^2} \sum_{\gamma}^B \frac{p_{X\gamma}^x p_{\gamma Y}^y + p_{X\gamma}^y p_{\gamma Y}^x}{E_0 - E_{\gamma}} \\
N_2 &= \frac{\hbar^2}{m_0^2} \sum_{\gamma}^B \frac{p_{X\gamma}^x p_{\gamma Z}^z + p_{X\gamma}^z p_{\gamma Z}^x}{E_0 - E_{\gamma}} = \frac{\hbar^2}{m_0^2} \sum_{\gamma}^B \frac{p_{Y\gamma}^y p_{\gamma Z}^z + p_{Y\gamma}^z p_{\gamma Z}^y}{E_0 - E_{\gamma}}
\end{aligned} \tag{3.83}$$

The notation for matrix elements is the following:

$$\begin{aligned}\langle X | p_y | \gamma \rangle &\equiv p_{X\gamma}^y \\ |\langle X | p_y | \gamma \rangle|^2 &\equiv p_{X\gamma}^y p_{\gamma X}^y\end{aligned}\quad (3.84)$$

The terms (3.83) are related to experimental band structure parameters A_i which are known as parameters of Bir and Pikus:

$$\begin{aligned}\frac{\hbar^2}{2m_0} A_1 &= L_2 \\ \frac{\hbar^2}{2m_0} A_2 &= M_3 \\ \frac{\hbar^2}{2m_0} A_3 &= M_2 - L_2 \\ \frac{\hbar^2}{2m_0} A_4 &= \frac{L_1 + M_1}{2} - M_3 \\ \frac{\hbar^2}{2m_0} A_5 &= \frac{N_1}{2} \\ \frac{\hbar^2}{2m_0} A_6 &= \frac{N_2}{\sqrt{2}}\end{aligned}\quad (3.85)$$

3.2.2 Hamiltonian matrix in $|X\rangle |Y\rangle |Z\rangle$ basis

It is convenient to obtain the Hamiltonian matrix in $|X\rangle |Y\rangle |Z\rangle$ basis, which then helps to obtain matrix elements of Hamiltonian in u_j basis. The short notation and Hermitian symmetry properties used are the same as in section 3.1.2. The simplified notation is as follows:

$$\begin{aligned}L_1 &= D_{XX}^{xx} = D_{YY}^{yy} \\ L_2 &= D_{ZZ}^{zz} \\ M_1 &= D_{XX}^{yy} = D_{YY}^{xx} \\ M_2 &= D_{XX}^{zz} = D_{YY}^{zz} \\ M_3 &= D_{ZZ}^{xx} = D_{ZZ}^{yy} \\ N_1 &= 2D_{XY}^{xy} \\ N_2 &= 2D_{XZ}^{xz} = 2D_{YZ}^{yz} \\ \langle X | H | Y \rangle &\equiv D_{XY}\end{aligned}\quad (3.86)$$

where Hamiltonian D_{ab} has the following form:

$$D_{ab} = \sum_{\alpha\beta} D_{ab}^{\alpha\beta} k_{\alpha} k_{\beta} \quad (3.87)$$

where indices $a, b = |X\rangle, |Y\rangle, |Z\rangle$ and indices $\alpha, \beta = x, y, z$, $D_{ab}^{\alpha\beta}$ is given by (3.79). By substitution we obtain the following matrix elements (using (3.86)):

$$\begin{aligned} D_{XX} &= D_{XX}^{xx} k_x^2 + D_{XX}^{yy} k_y^2 + D_{XX}^{zz} k_z^2 = L_1 k_x^2 + M_1 k_y^2 + M_2 k_z^2 \\ D_{YY} &= D_{YY}^{xx} k_x^2 + D_{YY}^{yy} k_y^2 + D_{YY}^{zz} k_z^2 = L_1 k_y^2 + M_1 k_x^2 + M_2 k_z^2 \\ D_{ZZ} &= D_{ZZ}^{xx} k_x^2 + D_{ZZ}^{yy} k_y^2 + D_{ZZ}^{zz} k_z^2 = L_2 k_z^2 + M_3 (k_x^2 + k_y^2) \\ D_{XY} &= D_{XY}^{xy} k_x k_y + D_{XY}^{yx} k_y k_x = N_1 k_x k_y \\ D_{XZ} &= D_{XZ}^{xz} k_x k_z + D_{XZ}^{zx} k_z k_x = N_2 k_x k_z \\ D_{YZ} &= D_{YZ}^{yz} k_y k_z + D_{YZ}^{zy} k_z k_y = N_2 k_y k_z \end{aligned} \quad (3.88)$$

The explicit form of matrix Hamiltonian in $|X\rangle |Y\rangle |Z\rangle$ basis is the following:

$$D = \begin{bmatrix} L_1 k_x^2 + M_1 k_y^2 + M_2 k_z^2 & N_1 k_x k_y & N_2 k_x k_z \\ N_1 k_x k_y & L_1 k_y^2 + M_1 k_x^2 + M_2 k_z^2 & N_2 k_y k_z \\ N_2 k_x k_z & N_2 k_y k_z & L_2 k_z^2 + M_3 (k_x^2 + k_y^2) \end{bmatrix} \begin{matrix} |X\rangle \\ |Y\rangle \\ |Z\rangle \end{matrix} \quad (3.89)$$

3.2.3 Matrix in u_n basis

Calculations of explicit full matrix Hamiltonian in basis (3.71) is just a combination of matrix terms in $|X\rangle |Y\rangle |Z\rangle$ basis. In this section the following notation for matrix

elements is introduced¹²:

$$\begin{aligned}
F &= \Delta_1 + \Delta_2 + \lambda + \Theta \\
G &= \Delta_1 - \Delta_2 + \lambda + \Theta \\
\lambda &= \frac{\hbar^2}{2m_0} [A_1 k_z^2 + A_2 (k_x^2 + k_y^2)] \\
\Theta &= \frac{\hbar^2}{2m_0} [A_3 k_z^2 + A_4 (k_x^2 + k_y^2)] \\
K &= \frac{\hbar^2}{2m_0} A_5 (k_x - ik_y)^2 \\
H &= \frac{\hbar^2}{2m_0} A_6 (k_x - ik_y) k_z \\
\Delta &= \sqrt{2} \Delta_3
\end{aligned} \tag{3.90}$$

The following matrix elements were calculated using the above notation and the results of equation (3.89). Indices in $H_{jj'}$ run $j, j' = 1, \dots, 6$ which indicates the basis function $H_{jj'} \equiv \langle u_j | H | u_{j'} \rangle$ with double prime “''” dropped:

$$\begin{aligned}
H_{11} &= \langle u_1 | H | u_1 \rangle = \frac{1}{2} \langle (X - iY) \uparrow | H | (X + iY) \uparrow \rangle = \Delta_1 + \Delta_2 + \frac{1}{2} [D_{XX} + iD_{XY} - iD_{YX} + D_{YY}] \\
&= \Delta_1 + \Delta_2 + \frac{D_{XX} + D_{YY}}{2} = \Delta_1 + \Delta_2 + \frac{L_1 k_x^2 + M_1 k_y^2 + M_2 k_z^2 + L_1 k_y^2 + M_1 k_x^2 + M_2 k_z^2}{2} = F \\
H_{22} &= \langle u_2 | H | u_2 \rangle = \frac{1}{2} \langle (X + iY) \uparrow | H | (X - iY) \uparrow \rangle = \Delta_1 - \Delta_2 + \frac{1}{2} [D_{XX} - iD_{XY} + iD_{YX} + D_{YY}] \\
&= \Delta_1 - \Delta_2 + \frac{D_{XX} + D_{YY}}{2} = \Delta_1 - \Delta_2 + \frac{L_1 k_x^2 + M_1 k_y^2 + M_2 k_z^2 + L_1 k_y^2 + M_1 k_x^2 + M_2 k_z^2}{2} = G \\
H_{12} &= \langle u_1 | H | u_2 \rangle = -\frac{1}{2} \langle (X - iY) \uparrow | H | (X - iY) \uparrow \rangle = -\frac{1}{2} [D_{XX} - iD_{XY} - iD_{YX} - D_{YY}] \\
&= -\frac{1}{2} [L_1 k_x^2 + M_1 k_y^2 + M_2 k_z^2 - L_1 k_y^2 - M_1 k_x^2 - M_2 k_z^2 - 2iN_1 k_x k_y] \\
&= -\frac{1}{2} [(L_1 - M_1)(k_x^2 - k_y^2) - 2iN_1 k_x k_y] = -K^+ \\
H_{21} &= \langle u_2 | H | u_1 \rangle = -\frac{1}{2} \langle (X + iY) \uparrow | H | (X + iY) \uparrow \rangle = -\frac{1}{2} [D_{XX} + iD_{XY} + iD_{YX} - D_{YY}] \\
&= -\frac{1}{2} [L_1 k_x^2 + M_1 k_y^2 + M_2 k_z^2 - L_1 k_y^2 - M_1 k_x^2 - M_2 k_z^2 + 2iN_1 k_x k_y]
\end{aligned}$$

¹²Not to confuse matrix element H with the Hamiltonian and matrix element Θ with an angle θ .

$$\begin{aligned}
&= -\frac{1}{2}[(L_1 - M_1)(k_x^2 - k_y^2) + 2iN_1k_xk_y] = -K \\
H_{13} &= \langle u_1 | H | u_3 \rangle = -\frac{1}{\sqrt{2}} \langle (X - iY) \uparrow | H | Z \uparrow \rangle = -\frac{1}{\sqrt{2}}[D_{XZ} - iD_{YZ}] \\
&= -\frac{1}{\sqrt{2}}[N_2(k_xk_z) - iN_2(k_yk_z)] = -\frac{N_2}{\sqrt{2}}(k_x - ik_y)k_z = -H^+ \\
H_{31} &= \langle u_3 | H | u_1 \rangle = -\frac{1}{\sqrt{2}} \langle Z \uparrow | H | (X + iY) \uparrow \rangle = -\frac{1}{\sqrt{2}}[D_{XZ} + iD_{YZ}] \\
&= -\frac{1}{\sqrt{2}}[N_2(k_xk_z) + iN_2(k_yk_z)] = -\frac{N_2}{\sqrt{2}}(k_x + ik_y)k_z = -H
\end{aligned}$$

Due to spin relations (2.5) terms with opposite spins are:

$$H_{53} = \langle u_5 | H | u_3 \rangle = -\frac{1}{\sqrt{2}} \langle (X - iY) \downarrow | H | Z \uparrow \rangle = \sqrt{2}\Delta_3 = \Delta$$

$$H_{14} = H_{41} = \langle u_1 | H | u_4 \rangle = -\frac{1}{2} \langle (X - iY) \uparrow | H | (X - iY) \downarrow \rangle = 0$$

where superscript “+” means Hermitian conjugation.

Full explicit Luttinger Kohn Hamiltonian, denoted as \mathbf{H}^{LK} can be expressed in the following form:

$$\mathbf{H}^{LK} = - \begin{bmatrix} F & -K^+ & -H^+ & 0 & 0 & 0 \\ -K & G & H & 0 & 0 & \Delta \\ -H & H^+ & \lambda & 0 & \Delta & 0 \\ 0 & 0 & 0 & F & -K & H \\ 0 & 0 & \Delta & -K^+ & G & -H^+ \\ 0 & \Delta & 0 & H^+ & -H & \lambda \end{bmatrix} \quad (3.91)$$

where the notation in eq. (3.90) is used.

3.2.4 Strain effects on band structures

The introduction of strain for wurtzite structures is similar to zincblende (Sec. 3.1.4). The additional term will be added to Hamiltonian (3.91). This term is obtained by replacing wave vector terms $k_\alpha k_\beta$ by strain terms $\varepsilon_{\alpha\beta}$ as it was described in section 3.1.4 (vector \vec{k} and strain ε terms correspond to coordinate system axes, not the crystal axes, so for

hexagonal the same replacement as for cubic is used):

$$k_\alpha k_\beta \rightarrow \varepsilon_{\alpha\beta} \quad (3.92)$$

and replacing Bir and Pikus parameters A_i with the deformation potentials $D_i, i = 1, \dots, 6$. The deformation potentials have their analogs in cubic symmetry: D_1 and D_2 similar to hydrostatic deformation potential a_v ; D_3 and D_4 are similar to the shear deformation potential b . The modified matrix elements of the Hamiltonian (3.91) have the following form:

$$\begin{aligned} F &= \Delta_1 + \Delta_2 + \lambda + \Theta \\ G &= \Delta_1 - \Delta_2 + \lambda + \Theta \\ \lambda &= \frac{\hbar^2}{2m_0} [A_1 k_z^2 + A_2 (k_x^2 + k_y^2)] + \lambda_\varepsilon \\ \lambda_\varepsilon &= D_1 \varepsilon_{zz} + D_2 (\varepsilon_{xx} + \varepsilon_{yy}) \\ \Theta &= \frac{\hbar^2}{2m_0} [A_3 k_z^2 + A_4 (k_x^2 + k_y^2)] + \Theta_\varepsilon \\ \Theta_\varepsilon &= D_3 \varepsilon_{zz} + D_4 (\varepsilon_{xx} + \varepsilon_{yy}) \\ K &= \frac{\hbar^2}{2m_0} A_5 (k_x - ik_y)^2 + D_5 \varepsilon_+ \\ H &= \frac{\hbar^2}{2m_0} A_6 (k_x - ik_y) k_z + D_6 \varepsilon_{z+} \\ \Delta &= \sqrt{2} \Delta_3 \end{aligned} \quad (3.93)$$

where Chuang [29] notation is used:

$$\begin{aligned} \varepsilon_\pm &= \varepsilon_{xx} \pm 2i\varepsilon_{xy} - \varepsilon_{yy} \\ \varepsilon_{z\pm} &= \varepsilon_{zx} \pm i\varepsilon_{yz} \end{aligned} \quad (3.94)$$

The next relations allow to use only five band structure parameters A_1, A_2, A_5, Δ_1 and Δ_2 and three deformation potentials for the calculation of the valence band structures:

$$\begin{aligned} A_1 - A_2 &= -A_3 = 2A_4, & A_3 + 4A_5 &= \sqrt{2}A_6, & \Delta_2 &= \Delta_3, \\ D_1 - D_2 &= -D_3 = 2D_4, & D_3 + 4D_5 &= \sqrt{2}D_6. \end{aligned} \quad (3.95)$$

The stress τ and strain ε tensor for hexagonal crystal are related to each other through the matrix of elastic stiffness constants:

$$\begin{bmatrix} \tau_{xx} \\ \tau_{yy} \\ \tau_{zz} \\ \tau_{xy} \\ \tau_{yz} \\ \tau_{zx} \end{bmatrix} = \begin{bmatrix} C_{11} & C_{12} & C_{13} & 0 & 0 & 0 \\ C_{12} & C_{11} & C_{13} & 0 & 0 & 0 \\ C_{13} & C_{13} & C_{33} & 0 & 0 & 0 \\ 0 & 0 & 0 & C_{44} & 0 & 0 \\ 0 & 0 & 0 & 0 & C_{44} & 0 \\ 0 & 0 & 0 & 0 & 0 & \frac{C_{11} - C_{12}}{2} \end{bmatrix} \begin{bmatrix} \varepsilon_{xx} \\ \varepsilon_{yy} \\ \varepsilon_{zz} \\ 2\varepsilon_{yz} \\ 2\varepsilon_{zx} \\ 2\varepsilon_{xy} \end{bmatrix} \quad (3.96)$$

Assume that the strain tensor is diagonal:

$$\varepsilon_{xy} = \varepsilon_{yz} = \varepsilon_{zx} = 0 \quad (3.97)$$

Three cases are considered under the above approximation:

a: A strained-layer wurtzite crystal pseudomorphically grown along the (0001) direction of a sapphire substrate. The diagonal elements are similar to the ones that are expressed for lattice mismatch cubic crystal (3.68):

$$\varepsilon_{xx} = \varepsilon_{yy} = \frac{a_0 - a}{a} \quad \varepsilon_{zz} = -\frac{2C_{13}}{C_{33}}\varepsilon_{xx} \quad (3.98)$$

where a_0 and a are the lattice constants of the substrate and the well layer material.

b: A wurtzite crystal layer under an external biaxial in-plane stress $\tau_{xx} = \tau_{yy} = T$ and $\tau_{zz} = 0$. By substitution into (3.96) we obtain:

$$\begin{aligned} \varepsilon_{xx} = \varepsilon_{yy} &= \frac{C_{33}}{(C_{11} + C_{12})C_{33} - 2C_{13}^2} T \\ \varepsilon_{zz} &= -\frac{2C_{13}}{C_{33}}\varepsilon_{xx} \end{aligned} \quad (3.99)$$

c: A wurtzite crystal layer under an external uniaxial stress $\tau_{zz} = T$ and $\tau_{xx} = \tau_{yy} = 0$. By substitution into (3.96) we obtain:

$$\begin{aligned}\varepsilon_{xx} = \varepsilon_{yy} &= -\frac{C_{33}}{(C_{11} + C_{12})C_{33} - 2C_{13}^2}T \\ \varepsilon_{zz} &= \frac{C_{11} + C_{12}}{(C_{11} + C_{12})C_{33} - 2C_{13}^2}T\end{aligned}\tag{3.100}$$

Chapter 4

Luttinger-Kohn's model Hamiltonian for semiconductors on arbitrary-oriented substrates

4.1 Rotation of Luttinger-Kohn's Hamiltonian for hole states using angular momentum matrices (4×4) for zincblende crystal

4.1.1 Explanation of transformations

Let the three axes (1,2,3) of the rotated coordinate system be the following (Fig. 4.1): the axis 3 along the growth direction, the 1 and 3 axes in the $(\bar{1}10)$ plane, and the 2 axis in the $[\bar{1}10]$ direction. The angle between axis 3 and the x-y plane of the original coordinate system is denoted by θ ; thus when θ varies from 0 to $\pi/2$, the growth surface which is perpendicular to the 3 axis changes from (110) to (111), (112), (113), until (11∞) , i.e., (001) as shown on Fig. 4.2.

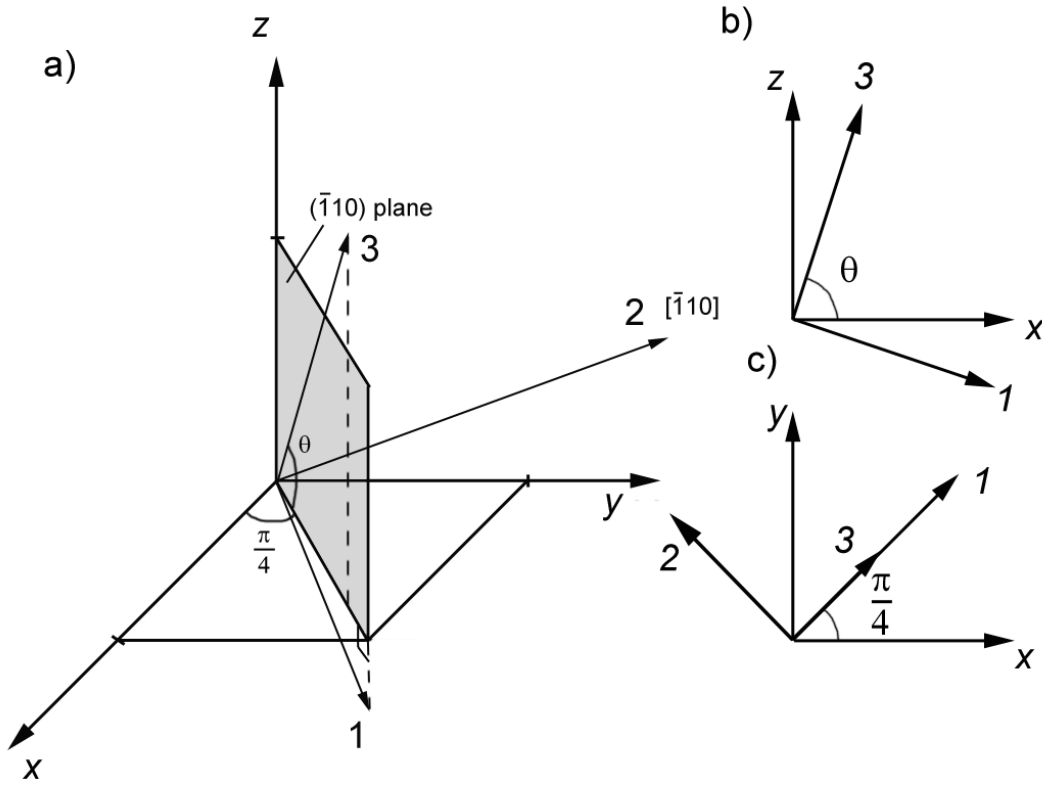


FIGURE 4.1: Rotation of coordinate system: a) x , y and z are axes of Cartesian coordinate system where z axis is perpendicular to (001) plane; 1, 2 and 3 are axes of rotated coordinate system; axis 2 is perpendicular to 1-3 plane which is parallel to $(\bar{1}10)$ plane; crystal is growing along axis 3; the system is rotated about axis 2 for angle θ ; b) side view of x - z and 1-3 planes; c) upside down view of x - y and 1-2 planes, coordinate system rotated to $\pi/4$ angle.

4.1.2 Coordinate transformations

In order to describe the above rotations and how they affect the Hamiltonian (which is written in (001) coordinate system), the following transformation has been introduced in ref. [44]. The components of wave vector \vec{k} transform in the same way as coordinates (Fig. 4.1):

$$\begin{aligned}
 k_x &= \frac{s}{\sqrt{2}}k_1 - \frac{1}{\sqrt{2}}k_2 + \frac{c}{\sqrt{2}}k_3 \\
 k_y &= \frac{s}{\sqrt{2}}k_1 + \frac{1}{\sqrt{2}}k_2 + \frac{c}{\sqrt{2}}k_3 \\
 k_z &= -ck_1 + sk_3
 \end{aligned} \tag{4.1}$$

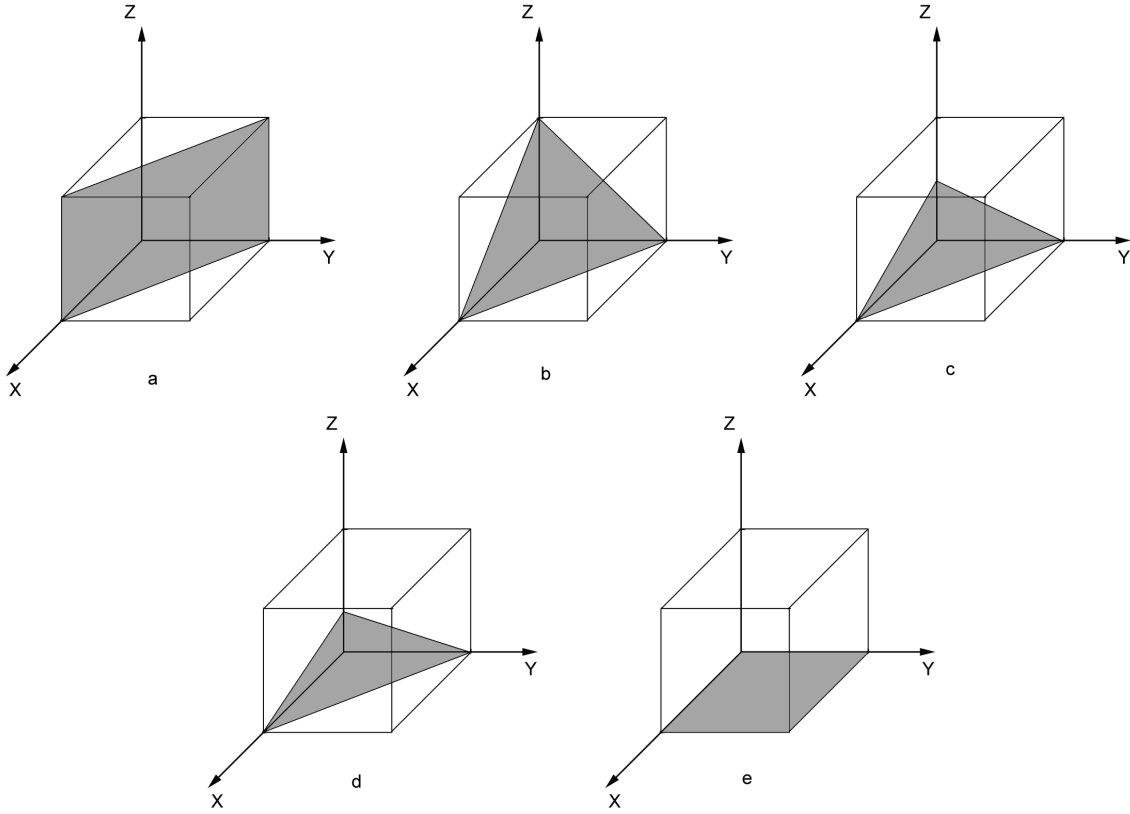


FIGURE 4.2: Growth surfaces in Miller indices notation: a - (110), b - (111), c - (112), d - (113), e - (11 ∞). Growth direction is perpendicular to plane which is colored gray.

$$\begin{aligned}
 J_x &= \frac{\mathbf{s}}{\sqrt{2}} J_1 - \frac{1}{\sqrt{2}} J_2 + \frac{\mathbf{c}}{\sqrt{2}} J_3 \\
 J_y &= \frac{\mathbf{s}}{\sqrt{2}} J_1 + \frac{1}{\sqrt{2}} J_2 + \frac{\mathbf{c}}{\sqrt{2}} J_3 \\
 J_z &= -\mathbf{c} J_1 + \mathbf{s} J_3
 \end{aligned} \tag{4.2}$$

where \mathbf{s} and \mathbf{c} represent $\sin \theta$ and $\cos \theta$, respectively. Matrices J_1 , J_2 and J_3 satisfy the commutation rules of angular momentum $(J_x, J_y) = iJ_z$ and are expressed in the following form:

$$J_1 = \begin{bmatrix} 0 & 0 & \frac{\sqrt{3}}{2} & 0 \\ 0 & 0 & 1 & \frac{\sqrt{3}}{2} \\ \frac{\sqrt{3}}{2} & 1 & 0 & 0 \\ 0 & \frac{\sqrt{3}}{2} & 0 & 0 \end{bmatrix} \tag{4.3}$$

$$J_2 = \begin{bmatrix} 0 & 0 & \frac{-\sqrt{3}i}{2} & 0 \\ 0 & 0 & i & \frac{-\sqrt{3}i}{2} \\ \frac{-\sqrt{3}i}{2} & -i & 0 & 0 \\ 0 & \frac{-\sqrt{3}i}{2} & 0 & 0 \end{bmatrix} \quad (4.4)$$

$$J_3 = \begin{bmatrix} \frac{3}{2} & 0 & 0 & 0 \\ 0 & -\frac{1}{2} & 0 & 0 \\ 0 & 0 & \frac{1}{2} & 0 \\ 0 & 0 & 0 & -\frac{3}{2} \end{bmatrix} \quad (4.5)$$

4.1.3 Solution for rotated Hamiltonian

Hole states are described by the following Luttinger effective-mass Hamiltonian [59], written in the x, y, z coordinate system:

$$H = \frac{1}{2m_0} \left[\left(\gamma_1 + \frac{5}{2}\gamma_2 \right) k^2 - 2\gamma_2 (k_x^2 J_x^2 + k_y^2 J_y^2 + k_z^2 J_z^2) - 4\gamma_3 (\{k_x, k_y\} \{J_x, J_y\} + \{k_y, k_z\} \{J_y, J_z\} + \{k_z, k_x\} \{J_z, J_x\}) \right] \quad (4.6)$$

where $k^2 = k_x^2 + k_y^2 + k_z^2$ and $\{k_x, k_y\}$ is the anticommutator. We want to transform vector \vec{k} and J matrices. To perform the transformation we substitute the expressions of the transformed \vec{k} (4.1) and J (4.2) into the equation (4.6) using symbolic software Maple 16 and we obtain the effective-mass Hamiltonian in the (1,2,3) coordinate system:

$$H = \frac{1}{2m_0} [\gamma_1 k^2 + \gamma_2 (Ak_1^2 + Bk_2^2 + Ck_3^2 + Dk_1k_2 + Ek_1k_3 + Fk_2k_3) + \gamma_3 (A'k_1^2 + B'k_2^2 + C'k_3^2 + D'k_1k_2 + E'k_1k_3 + F'k_2k_3)] \quad (4.7)$$

where A, B, C, \dots, E', F' are 4×4 matrices with matrix elements being functions of \mathbf{s} and \mathbf{c} , which all have the following form:

$$X = \begin{bmatrix} p & r & q & 0 \\ r^+ & -p & 0 & -q \\ q^+ & 0 & -p & r \\ 0 & -q^+ & r^+ & p \end{bmatrix} \quad (4.8)$$

where superscript "+" means Hermitian conjugation and the values of p, r and q for each matrix are provided in Ref. [44] (The values of p, r and q will not be needed in the further calculations).

4.1.4 Explicit form of rotated Luttinger effective-mass Hamiltonian

The Hamiltonian labeled as equation (4.7) in explicit form is a 4×4 matrix, which was calculated using Maple 16 (Appendix A) by substituting rotated expression for \vec{k} (4.1) and matrices J (4.2) into (4.6), and it is expressed as:

$$H = \frac{1}{2m_0} \begin{bmatrix} P_1 & R & Q & 0 \\ R^+ & P_2 & 0 & -Q \\ Q^+ & 0 & P_2 & R \\ 0 & -Q^+ & R^+ & P_1 \end{bmatrix} \quad (4.9)$$

Hamiltonian can be obtained for any (11N) orientation by the conversion formula for the angle of rotation θ (which is substituted into eq. (4.1) and (4.2)):

$$\theta = \tan^{-1} \frac{N}{\sqrt{2}} \quad (4.10)$$

For $N = 1$ we have $\theta = \tan^{-1} \frac{1}{\sqrt{2}}$ and we know the relations between sine, cosine and inverse tangent:

$$\sin(\tan^{-1} x) = \frac{x}{\sqrt{1+x^2}}, \quad \cos(\tan^{-1} x) = \frac{1}{\sqrt{1+x^2}} \quad (4.11)$$

so for $N = 1$ we set $\mathbf{s} = 1/\sqrt{3}$ and $\mathbf{c} = \sqrt{2/3}$ and the result for that case is:

$$\begin{aligned}
P_1 &= (\gamma_1 + \gamma_3)k_{\parallel}^2 + (\gamma_1 - 2\gamma_3)k_3^2 \\
P_2 &= (\gamma_1 - \gamma_3)k_{\parallel}^2 + (\gamma_1 + 2\gamma_3)k_3^2 \\
R &= -\frac{1}{\sqrt{3}}(\gamma_2 + 2\gamma_3)(k_1 - ik_2)^2 + \frac{2\sqrt{2}}{3}(\gamma_2 - \gamma_3)(k_1 + ik_2)k_3 \\
Q &= \sqrt{\frac{2}{3}}(\gamma_2 - \gamma_3)(k_1 + ik_2)^2 + \frac{2}{\sqrt{3}}(2\gamma_2 + \gamma_3)(k_1 - ik_2)k_3
\end{aligned} \tag{4.12}$$

where $k_{\parallel}^2 = k_x^2 + k_y^2$. Here we used Xia notation. More commonly used Chuang notation which is used later, is the following:

$$\begin{aligned}
-P_1 &\equiv P + Q \\
-P_2 &\equiv P - Q \\
-R &\equiv R \\
-Q &\equiv S
\end{aligned} \tag{4.13}$$

4.2 Rotation of Luttinger-Kohn's Hamiltonian for hole states using rotation matrix (4×4) for zincblende crystal

4.2.1 Introduction

In this section we describe rotations of Hamiltonian using different approach. It is based on the appropriate transformation of the initial Hamiltonian (4.6) expressed in a coordinate system (x, y, z) . The following transformation will transform it into new (transformed) coordinate system defined by axes $(1, 2, 3)$:

$$\begin{aligned}
k'_a &= U_{ac}k_c \\
H'_{ab} &= U_{ac}U_{bd}H_{cd} \\
k_c &= U_{ac}k'_a \\
H_{cd} &= U_{ac}U_{bd}H'_{ab}
\end{aligned} \tag{4.14}$$

where H' and k' represent any vectors and tensors in the transformed coordinate system and U is the rotation matrix; indices $a, b, c, d = 1, 2, 3$ indicates the corresponding components in the transformed system. The transformation of the form:

$$H' = U^{-1} H U \quad (4.15)$$

is called similarity (collineatory) transformation [60](p. 412). The rotation matrix approach is more general and with certain assumptions it reduces to one described in section 4.1. First, it is necessary to discuss how the rotation matrix is obtained and then describe the rotations (see Fig. 4.3). It will be shown later that rotation matrix approach and angular momentum matrices approach give the same result.

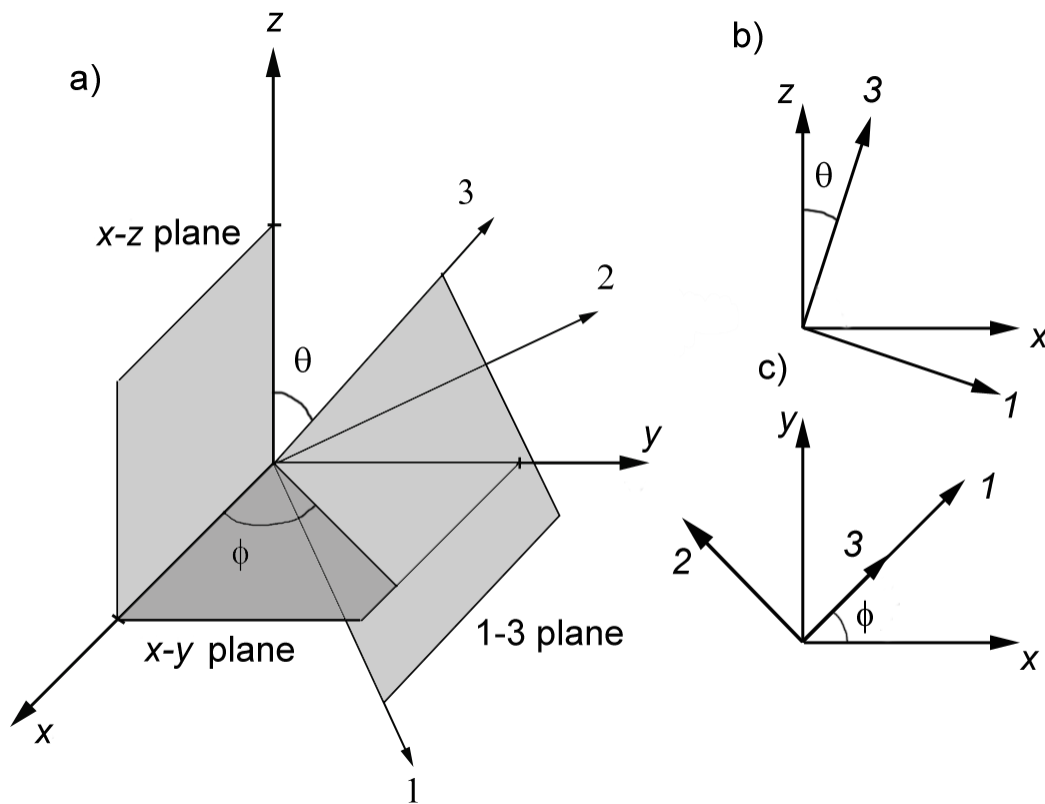


FIGURE 4.3: General transformation for arbitrary rotation from old to new rectangular coordinate system: a) axes x, y, z correspond to axes $1, 2, 3$ respectively, which are perpendicular to each other; $x-y, x-z$ and $1-3$ planes are indicated; angle ϕ is the angle between $x-z$ plane and $1-3$ plane; angle θ is the angle between z axis and 3 axis; both of the angles run from 0 to $\pi/2$; b) side view of $x-z$ and $1-3$ planes, angle of rotation θ indicated; c) upside down view of $x-y$ and $1-2$ planes, coordinate system rotated to angle ϕ .

4.2.2 Rotation matrix

To obtain rotation matrix we will use expressions for rotations of coordinate system about one of the axes of rectangular Cartesian system [60](p.471). We choose axes x, y, z so that they correspond to Miller indices h, k, l . Rotations are performed in spherical coordinate system; thus we rotate about axis 2 and z . Matrices which describe rotations about each of the axis are denoted as A_x, A_y and A_z for rotations about axes x, y and z respectively. Rotations about y and z axes are expressed in this form:

$$A_y(\theta) = \begin{bmatrix} \cos \theta & 0 & \sin \theta \\ 0 & 1 & 0 \\ -\sin \theta & 0 & \cos \theta \end{bmatrix} \quad (4.16)$$

$$A_z(\phi) = \begin{bmatrix} \cos \phi & -\sin \phi & 0 \\ \sin \phi & \cos \phi & 0 \\ 0 & 0 & 1 \end{bmatrix} \quad (4.17)$$

where angles θ and ϕ are right-handed rotations with Euler angles about the positive coordinate axes y and z . To obtain total rotation matrix, which gives the transformation for right-handed rotations about axes y and z together (two consecutive rotations - first about z and then about rotated y i.e. axis 2), it is necessary to perform matrix multiplication, and as a result we obtain the following matrix:

$$A = A_y \cdot A_z = \begin{bmatrix} \cos \theta \cos \phi & -\cos \theta \sin \phi & \sin \theta \\ \sin \phi & \cos \phi & 0 \\ -\sin \theta \cos \phi & \sin \theta \sin \phi & \cos \theta \end{bmatrix} \quad (4.18)$$

It represents the right-handed rotation first about axis z and then rotation about axis 2, which was axis y in the old coordinates [60](p. 476). This rotation matrix performs right-handed rotations. The spherical coordinate system has left handed angles. To obtain left-handed rotation matrix the angles should be reversed. By switching signs of angles θ and ϕ we can write our rotation matrix:

$$U = \begin{bmatrix} \cos \theta \cos \phi & \cos \theta \sin \phi & -\sin \theta \\ -\sin \phi & \cos \phi & 0 \\ \sin \theta \cos \phi & \sin \theta \sin \phi & \cos \theta \end{bmatrix} \quad (4.19)$$

where angles θ and ϕ defined for spherical coordinate system on the Fig. 4.3. This matrix leads to the following relation:

$$\begin{bmatrix} X' \\ Y' \\ Z' \end{bmatrix} = \begin{bmatrix} U \end{bmatrix} \begin{bmatrix} X \\ Y \\ Z \end{bmatrix} \quad (4.20)$$

The spins in the original coordinate system are assumed to be along the growth direction z . For rotated system, spins will be rotated by the rotation matrix for spins [61](p.125)¹:

$$M_s = \begin{bmatrix} e^{-i\frac{\phi}{2}} \cos \frac{\theta}{2} & e^{i\frac{\phi}{2}} \sin \frac{\theta}{2} \\ -e^{-i\frac{\phi}{2}} \sin \frac{\theta}{2} & e^{i\frac{\phi}{2}} \cos \frac{\theta}{2} \end{bmatrix} \quad (4.21)$$

which leads to the following relation:

$$\begin{bmatrix} \uparrow' \\ \downarrow' \end{bmatrix} = \begin{bmatrix} e^{-i\frac{\phi}{2}} \cos \frac{\theta}{2} & e^{i\frac{\phi}{2}} \sin \frac{\theta}{2} \\ -e^{-i\frac{\phi}{2}} \sin \frac{\theta}{2} & e^{i\frac{\phi}{2}} \cos \frac{\theta}{2} \end{bmatrix} \begin{bmatrix} \uparrow \\ \downarrow \end{bmatrix} \quad (4.22)$$

By combining matrices U and M_s we can relate basis functions in rotated coordinate system $[X', Y', Z']^T$ with spins $[\uparrow', \downarrow']^T$ and basis functions in original coordinate system $[X, Y, Z]^T$ with spins $[\uparrow, \downarrow]^T$. Combining matrices U and M_s , we can obtain the matrix that relates $[X' \uparrow', Y' \uparrow', Z' \uparrow', X' \downarrow', Y' \downarrow', Z' \downarrow']^T$ and $[X \uparrow, Y \uparrow, Z \uparrow, X \downarrow, Y \downarrow, Z \downarrow]^T$, where superscript T means transposition. The combined matrix is obtained as a Kronecker product \otimes (outer product for matrices) of matrices M_s and U :

$$M_c = M_s \otimes U = \quad (4.23)$$

$$= \begin{bmatrix} c\theta c\phi c\frac{\theta}{2} e^{-i\frac{\phi}{2}} & c\theta s\phi c\frac{\theta}{2} e^{-i\frac{\phi}{2}} & -s\theta c\frac{\theta}{2} e^{-i\frac{\phi}{2}} & c\theta c\phi s\frac{\theta}{2} e^{i\frac{\phi}{2}} & c\theta s\phi s\frac{\theta}{2} e^{i\frac{\phi}{2}} & -s\theta s\frac{\theta}{2} e^{i\frac{\phi}{2}} \\ -s\phi c\frac{\theta}{2} e^{-i\frac{\phi}{2}} & c\phi c\frac{\theta}{2} e^{-i\frac{\phi}{2}} & 0 & -s\phi s\frac{\theta}{2} e^{i\frac{\phi}{2}} & c\phi s\frac{\theta}{2} e^{i\frac{\phi}{2}} & 0 \\ s\theta c\phi c\frac{\theta}{2} e^{-i\frac{\phi}{2}} & s\theta s\phi c\frac{\theta}{2} e^{-i\frac{\phi}{2}} & c\theta c\frac{\theta}{2} e^{-i\frac{\phi}{2}} & s\theta c\phi s\frac{\theta}{2} e^{i\frac{\phi}{2}} & s\theta s\phi s\frac{\theta}{2} e^{i\frac{\phi}{2}} & c\theta s\frac{\theta}{2} e^{i\frac{\phi}{2}} \\ -c\theta c\phi s\frac{\theta}{2} e^{-i\frac{\phi}{2}} & -c\theta s\phi s\frac{\theta}{2} e^{-i\frac{\phi}{2}} & s\theta s\frac{\theta}{2} e^{-i\frac{\phi}{2}} & c\theta c\phi c\frac{\theta}{2} e^{i\frac{\phi}{2}} & c\theta s\phi c\frac{\theta}{2} e^{i\frac{\phi}{2}} & -s\theta c\frac{\theta}{2} e^{i\frac{\phi}{2}} \\ s\phi s\frac{\theta}{2} e^{-i\frac{\phi}{2}} & -c\phi s\frac{\theta}{2} e^{-i\frac{\phi}{2}} & 0 & -s\phi c\frac{\theta}{2} e^{i\frac{\phi}{2}} & c\phi c\frac{\theta}{2} e^{i\frac{\phi}{2}} & 0 \\ -s\theta c\phi s\frac{\theta}{2} e^{-i\frac{\phi}{2}} & -s\theta s\phi s\frac{\theta}{2} e^{-i\frac{\phi}{2}} & -c\theta s\frac{\theta}{2} e^{-i\frac{\phi}{2}} & s\theta c\phi c\frac{\theta}{2} e^{i\frac{\phi}{2}} & s\theta s\phi c\frac{\theta}{2} e^{i\frac{\phi}{2}} & c\theta c\frac{\theta}{2} e^{i\frac{\phi}{2}} \end{bmatrix}$$

¹The rotation matrix for spins is obtained by unitary transformation of Pauli spin matrix and provided by Wigner [62] in chapter 15.4.

where the notation $c\theta \equiv \cos \theta$ and $s\theta \equiv \sin \theta$ was used for convenience. The matrix M_c leads to the following relation between basis functions:

$$\begin{bmatrix} X' \uparrow \\ Y' \uparrow \\ Z' \uparrow \\ X' \downarrow \\ Y' \downarrow \\ Z' \downarrow \end{bmatrix} = \begin{bmatrix} & & & & & \\ & & & & & \\ & & & & & \\ & & & & & \\ & & & & & \\ & & & & & \\ & & & & & \end{bmatrix} M_c \begin{bmatrix} X \uparrow \\ Y \uparrow \\ Z \uparrow \\ X \downarrow \\ Y \downarrow \\ Z \downarrow \end{bmatrix} \quad (4.24)$$

where empty space in square brackets corresponds to matrix M_c . The matrix M_c was obtained by the following procedure using Maple 16 symbolic software:

```
with(LinearAlgebra); #the package for working with matrices in Maple 16

theta := 0; #defining angles (0 by default)
phi := 0;

#defining rotation matrix U
U := Matrix([[cos(theta)*cos(phi), cos(theta)*sin(phi), -sin(theta)], [-sin(phi),
cos(phi), 0], [sin(theta)*cos(phi), sin(theta)*sin(phi), cos(theta)]]);

#defining rotations of spin
M[s] := Matrix([[exp(-I*phi*(1/2))*cos((1/2)*theta), exp(I*phi*(1/2))*sin((1/2)
*theta)], [-exp(-I*phi*(1/2))*sin((1/2)*theta), exp(I*phi*(1/2))*cos((1/2)
*theta)]]);

#calculation of total rotation matrix Mc
M[c] := KroneckerProduct(M[s], U);
```

For electron wave vector \vec{k} the direct transformation is expressed as:

$$\vec{k}' = U\vec{k} \quad (4.25)$$

For vector \vec{k} we need inverse transformation:

$$\vec{k} = U^{-1}\vec{k}' \quad (4.26)$$

where U^{-1} is the inverse matrix² of matrix U which by simple manipulations[60](p.407) it is obtained as:

$$U^{-1} = \begin{bmatrix} \cos \theta \cos \phi & -\sin \phi & \sin \theta \cos \phi \\ \cos \theta \sin \phi & \cos \phi & \sin \theta \sin \phi \\ -\sin \theta & 0 & \cos \theta \end{bmatrix} \quad (4.27)$$

The corresponding Maple 16 code to this procedure is the following:

```
#calculating inverse matrix
Uk := simplify(MatrixInverse(U));

#calculation of rotated vector k components
K := VectorMatrixMultiply(Uk, Transpose(Matrix([[k[1], k[2], k[3]]]]));
```

4.2.3 Basis functions for arbitrary growth direction

We consider 4×4 Luttinger-Kohn's Hamiltonian. Basis functions for heavy hole and light hole bands for arbitrary growth direction are:

$$\begin{aligned} u'_{10}(\vec{r}) &= \left| \frac{3}{2}, \frac{3}{2} \right\rangle' = \frac{-1}{\sqrt{2}} |(X' + iY') \uparrow\rangle \\ u'_{20}(\vec{r}) &= \left| \frac{3}{2}, \frac{1}{2} \right\rangle' = \frac{-1}{\sqrt{6}} |(X' + iY') \downarrow\rangle + \sqrt{\frac{2}{3}} |Z' \uparrow\rangle \\ u'_{30}(\vec{r}) &= \left| \frac{3}{2}, \frac{-1}{2} \right\rangle' = \frac{1}{\sqrt{6}} |(X' - iY') \uparrow\rangle + \sqrt{\frac{2}{3}} |Z' \downarrow\rangle \\ u'_{40}(\vec{r}) &= \left| \frac{3}{2}, \frac{-3}{2} \right\rangle' = \frac{1}{\sqrt{2}} |(X' - iY') \downarrow\rangle \end{aligned} \quad (4.28)$$

where spherical harmonics were introduced in (2.12) and the “ ’ ” (“hatch”) is used to indicate rotated functions, whereas for coordinates the notation is x, y, z and $1, 2, 3$. New

²For rotation matrix the transpose and inverse operations gives the same results due to the fact that rotation matrix is orthogonal $U^T U = U U^T = I$, $U^T = U^{-1}$.

basis functions are obtained in terms of unrotated basis functions by substitution the rotated expressions in eq. (4.24) into (3.7). The explicit form of the functions is provided in Appendix D.

4.2.4 Matrix elements for rotated Luttinger-Kohn Hamiltonian

LKH (3.28) has the form which allows us to express total Hamiltonian in terms of four values (3.27) only, thus we need to find only these values. These four values expressed in Luttinger-Kohn's notation³ are [61](p.129):

$$\begin{aligned}
 P &= \frac{\hbar^2}{2m_0} \gamma_1 (k_x^2 + k_y^2 + k_z^2) = \frac{\hbar^2}{2m_0} \gamma_1 k^2 \\
 Q &= \frac{\hbar^2}{2m_0} \gamma_2 (k_x^2 + k_y^2 - 2k_z^2) \\
 R &= \frac{\hbar^2}{2m_0} [-\sqrt{3} \gamma_2 (k_x^2 - k_y^2) + i 2\sqrt{3} \gamma_3 k_x k_y] \\
 S &= \frac{\hbar^2}{m_0} \gamma_3 \sqrt{3} (k_x - i k_y) k_z
 \end{aligned} \tag{4.29}$$

All terms above are expressed in old unrotated coordinate system. To find matrix elements of Hamiltonian in the rotated system it is necessary to perform few steps. Consider matrix element $P+Q$. It corresponds to relation between u_{10}^* and u_{10} , thus we can write explicitly:

$$\begin{aligned}
 \langle u_{10}' | H | u_{10}' \rangle &= \frac{1}{2} \langle (X' - iY') \uparrow | H | (X' + iY') \uparrow \rangle \\
 &= \frac{1}{2} [\langle X' | H | X' \rangle + i \langle X' | H | Y' \rangle - i \langle Y' | H | X' \rangle + \langle Y' | H | Y' \rangle]
 \end{aligned} \tag{4.30}$$

After substituting the expressions given by equation (4.24) we obtain matrix element (the corresponding Maple 16 code is provided in appendix B), which is too large to write for arbitrary orientation. We will write it only for some particular directions, such as (001)⁴, (110) and (111). The convenient way to convert Miller indices (hkl) into angles θ and ϕ

³Each of the terms contains factor $\hbar^2/2m_0$ or $(2m_0)^{-1}$ as we set units where $\hbar = 1$, which is dropped below for convenience.

⁴For (001) orientation axes 1, 2, 3 coincide with x, y, z , but axes labels 1, 2, 3 instead of x, y, z used below for convenience.

for cubic systems is the following [37]:

$$\begin{aligned}\theta &= \arctan \frac{\sqrt{h^2 + k^2}}{l} \\ \phi &= \arctan \frac{k}{h}\end{aligned}\tag{4.31}$$

Set the angles θ and ϕ for each orientation as (001) - $\theta = 0$ and $\phi = 0$, (110) - $\theta = \frac{\pi}{2}$ and $\phi = \frac{\pi}{4}$, (111) - $\theta = \arccos \frac{1}{\sqrt{3}} \approx 0.955$ and $\phi = \frac{\pi}{4}$ and obtain:

$$P = (k_1^2 + k_2^2 + k_3^2)\gamma_1\tag{4.32}$$

$$Q^{(001)} = (k_1^2 + k_2^2 - 2k_3^2)\gamma_2$$

$$Q^{(110)} = \left(k_1^2 - \frac{k_2^2}{2} - \frac{k_3^2}{2}\right)\gamma_2 + 3\left(\frac{k_2^2}{2} - \frac{k_3^2}{2}\right)\gamma_3\tag{4.33}$$

$$Q^{(111)} = (k_1^2 + k_2^2 - 2k_3^2)\gamma_3$$

P term doesn't change during rotations. The same approach is used to obtain values of S and R . Corresponding matrix elements, that we are looking for, are:

$$\begin{aligned}\langle u'_{10} | H | u'_{20} \rangle &= \frac{1}{2\sqrt{3}} \langle (X' - iY') \uparrow | H | (X' + iY') \downarrow \rangle - \frac{1}{\sqrt{3}} \langle (X' - iY') \uparrow | H | Z' \uparrow \rangle \\ \langle u'_{10} | H | u'_{30} \rangle &= -\frac{1}{2\sqrt{3}} \langle (X' - iY') \uparrow | H | (X' - iY') \uparrow \rangle - \frac{1}{\sqrt{3}} \langle (X' - iY') \uparrow | H | Z' \downarrow \rangle\end{aligned}\tag{4.34}$$

The expressions of these matrix elements are obtained also for (001), (110) and (111) oriented substrates (code in Appendix B):

$$\begin{aligned}S^{(001)} &= -2\sqrt{3}\gamma_3(k_1 - ik_2)k_3 \\ S^{(110)} &= -2\sqrt{3}(k_1\gamma_3 - ik_2\gamma_2)k_3 \\ S^{(111)} &= \sqrt{\frac{2}{3}}(k_1^2 - k_2^2)(\gamma_2 - \gamma_3) + 2\sqrt{\frac{2}{3}}ik_1k_2(\gamma_2 - \gamma_3) + \frac{2}{\sqrt{3}}k_3(-k_1 + ik_2)(2\gamma_2 + \gamma_3) \\ &= \sqrt{\frac{2}{3}}(\gamma_2 - \gamma_3)(k_1 + ik_2)^2 - \frac{2}{\sqrt{3}}(2\gamma_2 + \gamma_3)(k_1 - ik_2)k_3\end{aligned}\tag{4.35}$$

$$\begin{aligned}
R^{(001)} &= -\sqrt{3}(\gamma_2(k_1^2 - k_2^2) - i2\gamma_3 k_1 k_2) \\
R^{(110)} &= \frac{\sqrt{3}}{2}(\gamma_2(-2k_1^2 + k_2^2 + k_3^2) + \gamma_3(k_2^2 - k_3^2 + 4ik_1 k_2)) \\
R^{(111)} &= -\frac{1}{\sqrt{3}}(\gamma_2 + 2\gamma_3)(k_1 - ik_2)^2 + \frac{2}{3}\sqrt{2}(\gamma_2 - \gamma_3)(k_1 + ik_2)k_3
\end{aligned} \tag{4.36}$$

Hamiltonian in matrix form is expressed as:

$$\mathbf{H} = -\frac{\hbar^2}{2m_0} \begin{bmatrix} P+Q & -S & R & 0 \\ -S^+ & P-Q & 0 & R \\ R^+ & 0 & P-Q & S \\ 0 & R^+ & S^+ & P+Q \end{bmatrix} \tag{4.37}$$

where superscript ”+” means Hermitian conjugation and the notation from section 4.2.4 is used. It is clear that this transformation gives the same result as angular momentum matrices approach (section 4.1.4).

4.3 Generalization of rotated (4×4) Hamiltonian to rotated (6×6) Hamiltonian for zincblende crystal

(6×6) Hamiltonian was determined in section 3.1.3 and it is obvious that it includes the terms, that are already calculated in section 4.2.4, except the term $P + \Delta$. The P term is already given above and it is invariant under rotations. Δ term, as it was noted in section 2.4, is a constant - spin-orbit split-off energy. Thus if we know rotations for 4-band Hamiltonian, we automatically know rotations for 6-band Hamiltonian. The additional two basis functions are:

$$\begin{aligned}
u'_{50}(\vec{r}) &= \left| \frac{1}{2}, \frac{1}{2} \right\rangle' = \frac{1}{\sqrt{3}} |(X' + iY') \downarrow\rangle + \frac{1}{\sqrt{3}} |Z' \uparrow\rangle \\
u'_{60}(\vec{r}) &= \left| \frac{1}{2}, \frac{-1}{2} \right\rangle' = \frac{1}{\sqrt{3}} |(X' - iY') \uparrow\rangle - \frac{1}{\sqrt{3}} |Z' \downarrow\rangle
\end{aligned} \tag{4.38}$$

Complete 6×6 matrix Hamiltonian has the following form:

$$\mathbf{H} = - \begin{bmatrix} P+Q & -S & R & 0 & -\frac{S}{\sqrt{2}} & \sqrt{2}R \\ -S^+ & P-Q & 0 & R & -\sqrt{2}Q & \sqrt{\frac{3}{2}}S \\ R^+ & 0 & P-Q & S & \sqrt{\frac{3}{2}}S^+ & \sqrt{2}Q \\ 0 & R^+ & S^+ & P+Q & -\sqrt{2}R^+ & -\frac{S^+}{\sqrt{2}} \\ -\frac{S^+}{\sqrt{2}} & -\sqrt{2}Q^+ & \sqrt{\frac{3}{2}}S & -\sqrt{2}R & P+\Delta & 0 \\ \sqrt{2}R^+ & \sqrt{\frac{3}{2}}S^+ & \sqrt{2}Q^+ & -\frac{S}{\sqrt{2}} & 0 & P+\Delta \end{bmatrix} \quad (4.39)$$

where the notation for rotated matrix elements (4.33), (4.36) and (4.35) is used.

4.4 Rotation of Luttinger-Kohn's Hamiltonian for conduction, hole and spin split off states using rotation matrix (8×8) for zincblende crystal

4.4.1 Basis functions and notation

In this section four-band (8 bands with both spin orientation) Luttinger-Kohn's model is considered. Using the same method as it is expressed in section 3.1 we have four bands of main interest as class A: conduction, heavy-hole, light-hole and spin-orbit split-off band all double degenerate. All other bands are in class B. Conduction band basis function $|S\rangle$ has symmetry properties as s-state wave function of hydrogen atom model, which is spherically symmetric. This implies that transformation for conduction band basis functions will include only transformation for spin:

$$\begin{aligned} |S'\rangle &= |S\rangle \\ \begin{bmatrix} S' \uparrow \\ S' \downarrow \end{bmatrix} &= \begin{bmatrix} e^{-i\frac{\phi}{2}} \cos \frac{\theta}{2} & e^{i\frac{\phi}{2}} \sin \frac{\theta}{2} \\ -e^{-i\frac{\phi}{2}} \sin \frac{\theta}{2} & e^{i\frac{\phi}{2}} \cos \frac{\theta}{2} \end{bmatrix} \begin{bmatrix} S \uparrow \\ S \downarrow \end{bmatrix} \end{aligned} \quad (4.40)$$

All notation and transformations for the other three bands are the same as discussed in section 4.2. The rotations of valence band matrix elements are already given above, so in this section only the rotations of conduction band interacting matrix elements are considered. The following expressions are based on the calculations, which are given in ref.[63]. The basic notation is expressed in terms of empirical Kane's parameters:

$$\begin{aligned}
A' &= \frac{\hbar^2}{m_0^2} \sum_{\gamma}^B \frac{p_{S\gamma}^x p_{\gamma S}^x}{E_g - E_{\gamma}} \\
B &= 2 \frac{\hbar^2}{m_0^2} \sum_{\gamma}^B \frac{p_{S\gamma}^x p_{\gamma Z}^x}{\frac{E_g}{2} - E_{\gamma}} \\
P_0 &= -i \frac{\hbar}{m_0} \langle S | p_x | X \rangle
\end{aligned} \tag{4.41}$$

where short notation is used:

$$\langle S | p_x | \gamma \rangle \equiv p_{S\gamma}^x \tag{4.42}$$

In this case constant parameter A' results from interaction of the conduction band with class-B states, parameter B results from the mixing interaction of conduction band and valence band with class-B states, and P_0 results from the interaction of conduction and valence bands.

4.4.2 (8×8) Luttinger-Kohn Hamiltonian for arbitrary growth direction

In this section we discuss matrix elements for interaction between conduction and valence bands. The order of basis functions is chosen as: $|S \uparrow\rangle, |S \downarrow\rangle, |u_{10}\rangle, \dots, |u_{60}\rangle$. Define matrix elements in the following form⁵:

$$\begin{aligned}
\langle S | H | S \rangle &= E_c + A'k^2 = A \\
\langle u_{20} | H | S \downarrow \rangle &= H_{S2} \\
\langle S \uparrow | H | u_{30} \rangle &= H_{S3} \\
\langle S \uparrow | H | u_{40} \rangle &= H_{S4} = 0 \\
\langle u_{50} | H | S \uparrow \rangle &= H_{S5} \\
\langle S \downarrow | H | u_{60} \rangle &= H_{S6}
\end{aligned} \tag{4.43}$$

⁵In ref.[63] basis functions have different form, thus the matrix elements are not the same as in this paper.

Using Maple 16 (see code in Appendix C - modified code of Appendix B) we obtain these matrix elements for some particular orientations (001), (110), (111):

$$\begin{aligned}
A^{(001)} &= E_c + \left(A' + \frac{\hbar^2}{2m_0} \right) k^2 \\
H_{S_2}^{(001)} &= -\frac{1}{\sqrt{6}}P_0(k_1 - ik_2) - \frac{1}{\sqrt{6}}B(k_1 + ik_2)k_3 \\
H_{S_3}^{(001)} &= \frac{1}{\sqrt{6}}P_0(k_1 - ik_2) - \frac{1}{\sqrt{6}}B(k_1 + ik_2)k_3 \\
H_{S_5}^{(001)} &= \frac{1}{\sqrt{3}}(P_0k_3 + iBk_1k_2) \\
H_{S_6}^{(001)} &= -\frac{1}{\sqrt{3}}(P_0k_3 - iBk_1k_2) \\
A^{(110)} &= E_c + \left(A' + \frac{\hbar^2}{2m_0} \right) k^2 \\
H_{S_2}^{(110)} &= -\frac{1}{\sqrt{6}}P_0(k_1 - ik_2) - \frac{1}{\sqrt{6}}B \left(k_1k_2 + \frac{i}{2}(k_2^2 - k_3^2) \right) \\
H_{S_3}^{(110)} &= \frac{1}{\sqrt{6}}P_0(k_1 - ik_2) - \frac{1}{\sqrt{6}}B \left(k_1k_2 + \frac{i}{2}(k_2^2 - k_3^2) \right) \\
H_{S_5}^{(110)} &= \frac{1}{\sqrt{3}}(P_0k_3 - iBk_1k_3) \\
H_{S_6}^{(110)} &= -\frac{1}{\sqrt{3}}(P_0k_3 + iBk_1k_3) \\
A^{(111)} &= E_c + \left(A' + \frac{\hbar^2}{2m_0} \right) k^2 \\
H_{S_2}^{(111)} &= -\frac{1}{\sqrt{6}}P_0(k_1 - ik_2) + \frac{1}{6}B (k_1^2 - ik_2^2 - 2k_1k_2 + \sqrt{2}(k_2 + ik_1)k_3) \\
H_{S_3}^{(111)} &= \frac{1}{\sqrt{6}}P_0(k_1 - ik_2) + \frac{1}{6}B (k_1^2 - ik_2^2 - 2k_1k_2 + \sqrt{2}(k_2 + ik_1)k_3) \\
H_{S_5}^{(111)} &= \frac{1}{\sqrt{3}}P_0k_3 - \frac{i}{6}B(k_1^2 + k_2^2 - 2k_3^2) \\
H_{S_6}^{(111)} &= -\frac{1}{\sqrt{3}}P_0k_3 - \frac{i}{6}B(k_1^2 + k_2^2 - 2k_3^2)
\end{aligned} \tag{4.44}$$

According to properties, discussed in Appendix F, it is necessary to set asymmetry parameter $B = 0$ in matrix elements (4.44) which leads to the same result as it is expressed

in ref.[64][46]. We set $B = 0$ in (4.44) and simplify the notation:

$$\begin{aligned}
H_{S2} &\rightarrow -T^+ = -\frac{1}{\sqrt{6}}P_0(k_1 - ik_2) \\
H_{S3} &\rightarrow T^+ = \frac{1}{\sqrt{6}}P_0(k_1 - ik_2) \\
H_{S5} &\rightarrow U = \frac{1}{\sqrt{3}}P_0k_3 \\
H_{S6} &\rightarrow -U = -\frac{1}{\sqrt{3}}P_0k_3
\end{aligned} \tag{4.45}$$

4.4.3 Hamiltonian matrix

The basis functions order here: $S \uparrow, S \downarrow, u_1 \dots u_6$. Hamiltonian matrix in explicit form for the notation (4.44) with $B \neq 0$ is expressed as:

$$H = \begin{bmatrix} A & 0 & -\sqrt{3}H_{S2}^+ & \sqrt{2}H_{S6} & H_{S3} & 0 & H_{S5}^+ & -\sqrt{2}H_{S3} \\ 0 & A & 0 & H_{S2}^+ & \sqrt{2}H_{S6} & -\sqrt{3}H_{S3} & \sqrt{2}H_{S2}^+ & H_{S6} \\ -\sqrt{3}H_{S2} & 0 & - & - & - & - & - & - \\ \sqrt{2}H_{S6}^+ & H_{S2} & - & - & - & - & - & - \\ H_{S3}^+ & \sqrt{2}H_{S6}^+ & - & - & - & - & - & - \\ 0 & -\sqrt{3}H_{S3}^+ & - & - & - & - & - & - \\ H_{S5} & \sqrt{2}H_{S2} & - & - & - & - & - & - \\ -\sqrt{2}H_{S3}^+ & H_{S6}^+ & - & - & - & - & - & - \end{bmatrix} \tag{4.46}$$

for the notation (4.45) with $B = 0$ is expressed as:

$$H = \begin{bmatrix} A & 0 & \sqrt{3}T & -\sqrt{2}U & T^+ & 0 & U & -\sqrt{2}T^+ \\ 0 & A & 0 & -T & -\sqrt{2}U & -\sqrt{3}T^+ & -\sqrt{2}T & -U \\ \sqrt{3}T^+ & 0 & - & - & - & - & - & - \\ -\sqrt{2}U & -T^+ & - & - & - & - & - & - \\ T & -\sqrt{2}U & - & - & - & - & - & - \\ 0 & -\sqrt{3}T & - & - & - & - & - & - \\ U & -\sqrt{2}T^+ & - & - & - & - & - & - \\ -\sqrt{2}T & -U & - & - & - & - & - & - \end{bmatrix} \tag{4.47}$$

where superscript ”+” means Hermitian conjugation and the empty space is the 6×6 matrix which was calculated in section 4.2 and expressed as equation (4.39). For 8×8 Hamiltonian the conduction band is also involved exactly as class A (the valence band is no longer the highest exact band) and its contribution should be subtracted off the original Luttinger parameters [65]:

$$\begin{aligned}\gamma_1 &= \gamma_1^L - \frac{1}{3} \frac{E_p}{E_g} \\ \gamma_2 &= \gamma_2^L - \frac{1}{6} \frac{E_p}{E_g} \\ \gamma_3 &= \gamma_3^L - \frac{1}{6} \frac{E_p}{E_g}\end{aligned}\tag{4.48}$$

where γ_i^L are Luttinger parameters, which are involved in the original 6×6 Hamiltonian (3.18), and γ_i are called modified Luttinger parameters. E_g is band gap and E_p is the energy in terms of Kane matrix element P_0 (4.41):

$$E_p = \frac{2m_0}{\hbar^2} P_0^2\tag{4.49}$$

The E_p/E_g terms appear as we run indices j in eq. (3.16) as $j = S, X, Y, Z$ and we get additional terms to eq. (3.17) of the form (above we set asymmetry parameter $B = 0$ as the terms $P_{S\gamma}^x$ are negligible):

$$\frac{P_{SX}^x P_{XS}^x}{E_c - E_v}\tag{4.50}$$

which is obviously the E_p/E_g term. For instance, consider γ_3 . The definition of γ_3 in eq. (3.18) may be rewritten in the form:

$$\gamma_3^L = -\frac{2m_0}{\hbar^2} \frac{C}{6}\tag{4.51}$$

where we redefine the C from eq. (3.17) to include the conduction band in the following form:

$$\tilde{C} = \frac{\hbar^2}{m_0^2} \sum_{\gamma}^B \frac{p_{X\gamma}^x p_{\gamma Y}^y + p_{X\gamma}^y p_{\gamma Y}^x}{E_0 - E_{\gamma}} + \frac{P_{SX}^x P_{XS}^x}{E_c - E_v} = C + \frac{P_0^2}{E_g}\tag{4.52}$$

We plug the definition of “new” \tilde{C} into the definition of γ_3 and obtain:

$$\gamma_3 = -\frac{2m_0}{\hbar^2} \frac{\tilde{C}}{6} = -\frac{2m_0}{\hbar^2} \frac{1}{6} \left(C + \frac{P_0^2}{E_g} \right) = -\frac{2m_0}{\hbar^2} \frac{C}{6} - \frac{1}{6} \frac{2m_0}{\hbar^2} \frac{P_0^2}{E_g} = \gamma_3^L - \frac{1}{6} \frac{E_p}{E_g}\tag{4.53}$$

4.5 Generalization of (8×8) Hamiltonian rotations to (10×10) Hamiltonian for zincblende crystal

10-bands Hamiltonians are discussed in ref. [46][66] and the result is the generalization of (8×8) Hamiltonian (4.46) by two additional nitrogen resonant levels with spins:

$$\begin{aligned} &|S_N \uparrow\rangle \\ &|S_N \downarrow\rangle \end{aligned} \quad (4.54)$$

Nitrogen level basis functions have the same symmetry properties as conduction band basis functions (section 4.4.1) which are spherically symmetric. This implies that transformation of conduction band basis functions will include only transformation for spin:

$$|S'_N\rangle = |S_N\rangle \quad (4.55)$$

Nitrogen level band interacts only with conduction band and both basis functions are spherically symmetric, so the matrix elements involving nitrogen level and conduction bands do not change during rotations of coordinate system. Explicit form of (10×10) Hamiltonian is the following:

$$H = \begin{bmatrix} E_N & 0 & V_{NC} & 0 & 0 & 0 & 0 & 0 & 0 & 0 \\ 0 & E_N & 0 & V_{NC} & 0 & 0 & 0 & 0 & 0 & 0 \\ V_{NC} & 0 & - & - & - & - & - & - & - & - \\ 0 & V_{NC} & - & - & - & - & - & - & - & - \\ 0 & 0 & - & - & - & - & - & - & - & - \\ 0 & 0 & - & - & - & - & - & - & - & - \\ 0 & 0 & - & - & - & - & - & - & - & - \\ 0 & 0 & - & - & - & - & - & - & - & - \\ 0 & 0 & - & - & - & - & - & - & - & - \\ 0 & 0 & - & - & - & - & - & - & - & - \end{bmatrix} \quad (4.56)$$

where the empty space is the 8×8 matrix which was calculated in section 4.4 and expressed as equation (4.46). The notation is used for nitrogen resonant level energy as E_N :

$$E_N = E_{N0} + N \quad (4.57)$$

For coupling between the nitrogen and conduction band:

$$V_{NC} = V_N + V \quad (4.58)$$

Coefficient N depends on nitrogen composition and the coupling coefficient in the band anti-crossing (BAC) model as V_N which is a constant, depending on the semiconductor matrix. The order of basis functions is the following: $|S_N \uparrow\rangle, |S_N \downarrow\rangle, |S \uparrow\rangle, |S \downarrow\rangle, |u_{10}\rangle, \dots, |u_{60}\rangle$ where $|u_{10}\rangle, \dots, |u_{60}\rangle$ basis functions explicitly expressed in sections 4.2.3 and 4.3.

4.6 Strain effects on band structures for arbitrary oriented zincblende crystal

The strain for arbitrary oriented crystal is described by strain tensor ε in the same way as described in section 3.1.4. To define the rotated strain tensor, the relations (4.14) are used:

$$\begin{aligned} \varepsilon'_{ab} &= U_{ac} U_{bd} \varepsilon_{cd} \\ \varepsilon_{cd} &= U_{ac} U_{bd} \varepsilon'_{ab} \end{aligned} \quad (4.59)$$

or the same in explicit form:

$$\begin{bmatrix} \varepsilon_{xx} & \varepsilon_{xy} & \varepsilon_{xz} \\ \varepsilon_{yx} & \varepsilon_{yy} & \varepsilon_{yz} \\ \varepsilon_{zx} & \varepsilon_{zy} & \varepsilon_{zz} \end{bmatrix} = U^T \begin{bmatrix} \varepsilon'_{xx} & \varepsilon'_{xy} & \varepsilon'_{xz} \\ \varepsilon'_{yx} & \varepsilon'_{yy} & \varepsilon'_{yz} \\ \varepsilon'_{zx} & \varepsilon'_{zy} & \varepsilon'_{zz} \end{bmatrix} U \quad (4.60)$$

where U is defined by (4.19) and U^T means matrix transposition. Strain tensor ε has the same behavior under transformation as tensor k^2 :

$$\begin{bmatrix} k_x k_x & k_x k_y & k_x k_z \\ k_y k_x & k_y k_y & k_y k_z \\ k_z k_x & k_z k_y & k_z k_z \end{bmatrix} = U^T \begin{bmatrix} k_1 k_1 & k_1 k_2 & k_1 k_3 \\ k_2 k_1 & k_2 k_2 & k_2 k_3 \\ k_3 k_1 & k_3 k_2 & k_3 k_3 \end{bmatrix} U \quad (4.61)$$

It was found in section 3.1.4 that strain perturbation operator has the same properties under rotation as the k -dependent perturbations. It allows us, instead of doing explicit rotations, to obtain rotated strain Hamiltonian terms by using (3.59), (3.61), (3.62),

(3.63) and similarity relations:

$$\begin{aligned} k'_i k'_j &\rightarrow \varepsilon'_{ij} & (i, j = x, y, z) \\ k'_i &\rightarrow -\sum_j \varepsilon'_{ij} k'_j & (i, j = x, y, z) \end{aligned} \quad (4.62)$$

In addition to the above, the strain terms for nitrogen resonant level introduce experimental parameter which have similar behavior as conduction band strain terms (3.59) and were discussed by [67]:

$$\begin{aligned} N_k &= \frac{\hbar^2}{2m_0} \gamma_N k^2 \\ N_\varepsilon &= a_N \text{Tr}(\varepsilon) \\ V_k &= \frac{\hbar^2}{2m_0} \gamma_{Nc} k^2 \\ V_\varepsilon &= a_{Nc} \text{Tr}(\varepsilon) \end{aligned} \quad (4.63)$$

The four terms of nitrogen resonant level are spherically symmetric and do not change their form during rotation. Moreover the influence of strain by nitrogen level is very small. Here γ_N and γ_{Nc} both vary at low nitrogen concentration as \sqrt{x} , and a_N is the nitrogen resonant level deformation potential. The a_{Nc} can be neglected as the effect of it is partially included in the a_N . Similar situation arises with conduction band strain terms with off-diagonal elements without their own deformation potentials:

$$\begin{aligned} A_\varepsilon &= a_c \text{Tr}(\varepsilon) \\ T_\varepsilon &= \frac{1}{\sqrt{6}} P_0 \sum_j (\varepsilon_{xj} + i\varepsilon_{yj}) k_j \\ U_\varepsilon &= \frac{1}{\sqrt{3}} P_0 \sum_j \varepsilon_{zj} k_j \end{aligned} \quad (4.64)$$

which do not change their form during rotations (The ε_{ij} terms may change, but the structure will remain the same).

The terms involving valence bands change during rotations are obtained by application of the replacement relation (4.62) on the expressions for rotated k-dependent terms (4.33),

(4.35) and (4.36) (only terms for (110) and (111) orientations are shown):

$$\begin{aligned}
Q_\varepsilon^{(110)} &= -\frac{b}{4}(2\varepsilon'_{xx} - \varepsilon'_{yy} - \varepsilon'_{zz}) - \frac{\sqrt{3}}{4}d(\varepsilon'_{yy} - \varepsilon'_{zz}) \\
Q_\varepsilon^{(111)} &= -\frac{d}{2\sqrt{3}}(\varepsilon'_{xx} + \varepsilon'_{yy} - 2\varepsilon'_{zz}) \\
S_\varepsilon^{(110)} &= d\varepsilon'_{xz} - ib\sqrt{3}\varepsilon'_{yz} \\
S_\varepsilon^{(111)} &= \frac{-b\sqrt{3} + d}{3\sqrt{2}}(\varepsilon'_{xx} - \varepsilon'_{yy} + 2i\varepsilon'_{xy}) - \frac{2\sqrt{3}b + d}{3}(\varepsilon'_{xz} - i\varepsilon'_{yz}) \\
R_\varepsilon^{(110)} &= \frac{\sqrt{3}b}{4}(2\varepsilon'_{xx} - \varepsilon'_{yy} - \varepsilon'_{zz}) - \frac{d}{4}(\varepsilon'_{yy} - \varepsilon'_{zz} + 4i\varepsilon'_{xy}) \\
R_\varepsilon^{(111)} &= \left(\frac{b}{2\sqrt{3}} + \frac{d}{3}\right)(\varepsilon'_{xx} - \varepsilon'_{yy} - i2\varepsilon'_{xy}) + \sqrt{\frac{2}{3}}\frac{d - \sqrt{3}b}{3}(\varepsilon'_{xz} + i\varepsilon'_{yz})
\end{aligned} \tag{4.65}$$

The explicit form of tensor ε is obtained from Hook's law:

$$\tau'_{ij} = C'_{ijkl}\varepsilon'_{kl} \tag{4.66}$$

where rotated strain related to stress by stiffness tensor, which also should be rotated:

$$\begin{aligned}
C'_{ijkl} &= U_{ip}U_{jq}U_{kr}U_{ls}C_{pqrs} \\
C' &= UUCU^T U^T
\end{aligned} \tag{4.67}$$

The general form of C' in Voigt notation is the following:

$$C' = \begin{bmatrix} C'_{11} & C'_{12} & C'_{13} & C'_{14} & C'_{15} & C'_{16} \\ C'_{21} & C'_{22} & C'_{23} & C'_{24} & C'_{25} & C'_{26} \\ C'_{31} & C'_{32} & C'_{33} & C'_{34} & C'_{35} & C'_{36} \\ C'_{41} & C'_{42} & C'_{43} & C'_{44} & C'_{45} & C'_{46} \\ C'_{51} & C'_{52} & C'_{53} & C'_{54} & C'_{55} & C'_{56} \\ C'_{61} & C'_{62} & C'_{63} & C'_{64} & C'_{65} & C'_{66} \end{bmatrix} \tag{4.68}$$

It has symmetric form $C_{ij} = C_{ji}$, which means that it is necessary to obtain only half of the terms. The example of the calculation is made for C'_{11} in general case by explicit

expansion of eq. (4.67) (product of rotation matrix U with four rank stiffness tensor C):

$$\begin{aligned}
C'_{11} \equiv C'_{1111} = & U_{1p}U_{1q}U_{1r}U_{1s}C_{pqrs} = U_{11}\{U_{11}[U_{11}(U_{11}C_{1111} + U_{12}C_{1112} + U_{13}C_{1113}) \\
& + U_{12}(U_{11}C_{1121} + U_{12}C_{1122} + U_{13}C_{1123}) + U_{13}(U_{11}C_{1131} + U_{12}C_{1132} + U_{13}C_{1133})] \\
& + U_{12}[U_{11}(U_{11}C_{1211} + U_{12}C_{1212} + U_{13}C_{1213}) + U_{12}(U_{11}C_{1221} + U_{12}C_{1222} + U_{13}C_{1223}) \\
& + U_{13}(U_{11}C_{1231} + U_{12}C_{1232} + U_{13}C_{1233})] + U_{13}[U_{11}(U_{11}C_{1311} + U_{12}C_{1312} + U_{13}C_{1313}) \\
& + U_{12}(U_{11}C_{1321} + U_{12}C_{1322} + U_{13}C_{1323}) + U_{13}(U_{11}C_{1331} + U_{12}C_{1332} + U_{13}C_{1333})]\} \\
& + U_{12}\{U_{11}[U_{11}(U_{11}C_{2111} + U_{12}C_{2112} + U_{13}C_{2113}) + U_{12}(U_{11}C_{2121} + U_{12}C_{2122} + U_{13}C_{2123}) \\
& + U_{13}(U_{11}C_{2131} + U_{12}C_{2132} + U_{13}C_{2133})] + U_{12}[U_{11}(U_{11}C_{2211} + U_{12}C_{2212} + U_{13}C_{2213}) \\
& + U_{12}(U_{11}C_{2221} + U_{12}C_{2222} + U_{13}C_{2223}) + U_{13}(U_{11}C_{2231} + U_{12}C_{2232} + U_{13}C_{2233})] \\
& + U_{13}[U_{11}(U_{11}C_{2311} + U_{12}C_{2312} + U_{13}C_{2313}) + U_{12}(U_{11}C_{2321} + U_{12}C_{2322} + U_{13}C_{2323}) \\
& + U_{13}(U_{11}C_{2331} + U_{12}C_{2332} + U_{13}C_{2333})] + \} + U_{13}\{U_{11}[U_{11}(U_{11}C_{3111} + U_{12}C_{3112} + U_{13}C_{3113}) \\
& + U_{12}(U_{11}C_{3121} + U_{12}C_{3122} + U_{13}C_{3123}) + U_{13}(U_{11}C_{3131} + U_{12}C_{3132} + U_{13}C_{3133})] \\
& + U_{12}[U_{11}(U_{11}C_{3211} + U_{12}C_{3212} + U_{13}C_{3213}) + U_{12}(U_{11}C_{3221} + U_{12}C_{3222} + U_{13}C_{3223}) \\
& + U_{13}(U_{11}C_{3231} + U_{12}C_{3232} + U_{13}C_{3233})] + U_{13}[U_{11}(U_{11}C_{3311} + U_{12}C_{3312} + U_{13}C_{3313}) \\
& + U_{12}(U_{11}C_{3321} + U_{12}C_{3322} + U_{13}C_{3323}) + U_{13}(U_{11}C_{3331} + U_{12}C_{3332} + U_{13}C_{3333})]\}
\end{aligned} \tag{4.69}$$

The original tensor C (3.67) has some zero terms and in rotation matrix U there is a zero term, thus the above general relation (4.69) may be reduced to the following particular term for cubic systems (using Voigt notation and explicit form of rotation matrix terms for convenience):

$$C'_{11} = C_{11}(c_{\theta}^4 c_{\phi}^4 + c_{\theta}^4 s_{\phi}^4 + s_{\theta}^4) + (2C_{12} + 4C_{44})(c_{\theta}^4 c_{\phi}^2 s_{\phi}^2 + c_{\theta}^2 c_{\phi}^2 s_{\theta}^2 + s_{\theta}^2 c_{\phi}^2 s_{\phi}^2)$$

where s and c are sine and cosine of the corresponding angle respectively. The other terms are obtained in a similar way and they have the form:

$$C'_{22} = C_{11}(s_{\phi}^4 + c_{\phi}^4) + (2C_{12} + 4C_{44})c_{\phi}^2 s_{\phi}^2$$

$$C'_{33} = C_{11}(s_{\theta}^4 c_{\phi}^4 + s_{\theta}^4 s_{\phi}^4 + c_{\theta}^4) + (2C_{12} + 4C_{44})(s_{\theta}^4 c_{\phi}^2 s_{\phi}^2 + c_{\theta}^2 c_{\phi}^2 s_{\theta}^2 + s_{\theta}^2 c_{\phi}^2 s_{\phi}^2)$$

$$C'_{44} = 2(C_{11} - C_{12})s_{\phi}^2 s_{\theta}^2 c_{\phi}^2 + C_{44}(s_{\phi}^4 s_{\theta}^2 - 2s_{\phi}^2 s_{\theta}^2 c_{\phi}^2 + s_{\phi}^2 c_{\theta}^2 + c_{\phi}^4 s_{\theta}^2 + c_{\phi}^2 c_{\theta}^2)$$

$$C'_{55} = C_{11}(c_{\theta}^2 c_{\phi}^4 s_{\theta}^2 + c_{\theta}^2 s_{\phi}^4 s_{\theta}^2 + s_{\theta}^2 c_{\theta}^2) + 2C_{12}(c_{\theta}^2 c_{\phi}^2 s_{\theta}^2 s_{\phi}^2 - c_{\theta}^2 c_{\phi}^2 s_{\theta}^2 - c_{\theta}^2 s_{\phi}^2 s_{\theta}^2)$$

$$+ C_{44}(4c_{\theta}^2 c_{\phi}^2 s_{\theta}^2 s_{\phi}^2 + c_{\theta}^4 c_{\phi}^2 - 2c_{\theta}^2 c_{\phi}^2 s_{\theta}^2 + c_{\theta}^4 s_{\phi}^2 - 2c_{\theta}^2 s_{\phi}^2 s_{\theta}^2 + s_{\theta}^4 c_{\phi}^2 + s_{\theta}^4 s_{\phi}^2)$$

$$\begin{aligned}
C'_{66} &= 2(C_{11} - C_{12})c_\phi^2 c_\theta^2 s_\phi^2 + C_{44}(c_\theta^4 c_\phi^2 - 2c_\phi^2 c_\theta^2 s_\phi^2 + s_\phi^4 c_\theta^2 + s_\phi^2 s_\theta^2 + c_\phi^2 s_\theta^2) \\
C'_{12} &= (2C_{11} + 4C_{44})c_\theta^2 c_\phi^2 s_\theta^2 + C_{12}(c_\theta^2 c_\phi^4 + c_\theta^2 s_\phi^4 + s_\theta^2 s_\phi^2 + s_\theta^2 c_\phi^2) \\
C'_{13} &= C_{11}(c_\theta^2 c_\phi^4 s_\theta^2 + c_\theta^2 s_\phi^4 s_\theta^2 + s_\theta^2 c_\phi^2) + C_{12}(2c_\theta^2 c_\phi^2 s_\theta^2 s_\phi^2 + c_\theta^4 c_\phi^2 + c_\theta^4 s_\phi^2 + s_\theta^4 c_\phi^2 + s_\theta^4 s_\phi^2) \\
&\quad + 4C_{44}(c_\theta^2 c_\phi^2 s_\theta^2 s_\phi^2 - c_\theta^2 c_\phi^2 s_\theta^2 - c_\theta^2 s_\phi^2 s_\theta^2) \\
C'_{14} &= (C_{11} - C_{12} - 2C_{44})(c_\theta^2 s_\phi^3 c_\phi s_\theta - c_\theta^2 c_\phi^3 s_\phi s_\theta) \\
C'_{15} &= C_{11}(c_\theta^3 c_\phi^4 s_\theta + c_\theta^3 s_\phi^4 s_\theta - s_\theta^3 c_\phi) + (C_{12} + 2C_{44})(2c_\theta^3 c_\phi^2 s_\theta^2 s_\phi - c_\theta^3 c_\phi^2 s_\theta - c_\theta^3 s_\phi^2 s_\theta + s_\theta^3 c_\phi c_\phi^2 + s_\theta^3 c_\theta s_\phi^2) \\
C'_{16} &= (C_{11} - C_{12} - 2C_{44})(c_\theta^3 s_\phi^3 c_\phi - c_\theta^3 c_\phi^3 s_\phi) \\
C'_{23} &= (2C_{11} - 4C_{44})s_\theta^2 s_\phi^2 c_\phi^2 + C_{12}(s_\theta^2 s_\phi^4 + c_\theta^2 s_\phi^2 + s_\theta^2 c_\phi^4 + c_\theta^2 c_\phi^2) \\
C'_{24} &= (C_{11} - C_{12} - 2C_{44})(c_\phi^3 s_\theta s_\phi - s_\phi^3 s_\theta c_\phi) \\
C'_{25} &= (2C_{11} - 4C_{44})s_\theta^2 c_\theta c_\phi^2 s_\theta + C_{12}(s_\phi^4 c_\theta s_\theta - s_\phi^4 s_\theta c_\theta + c_\phi^4 c_\theta s_\theta - c_\phi^4 s_\theta c_\theta) \\
C'_{26} &= (C_{11} - C_{12} - 2C_{44})(c_\phi^3 c_\theta s_\phi - s_\phi^3 c_\theta c_\phi) \\
C'_{34} &= (C_{11} - C_{12} - 2C_{44})(s_\theta^3 s_\phi^3 c_\phi - s_\theta^3 c_\phi^3 s_\phi) \\
C'_{35} &= C_{11}(s_\theta^3 c_\phi^4 c_\theta + s_\theta^3 s_\phi^4 c_\theta - c_\theta^3 s_\theta) + (C_{12} + 2C_{44})(2s_\theta^3 c_\phi^2 s_\theta^2 c_\theta - s_\theta^3 c_\phi^2 c_\theta - s_\theta^3 s_\phi^2 c_\theta + c_\theta^3 s_\theta c_\phi^2 + c_\theta^3 s_\theta s_\phi^2) \\
C'_{36} &= (C_{11} - C_{12} - 2C_{44})(s_\theta^2 s_\phi^3 c_\theta c_\phi - s_\theta^2 c_\phi^3 c_\theta s_\phi) \\
C'_{45} &\equiv C'_{36} = (C_{11} - C_{12} - 2C_{44})(s_\theta^2 s_\phi^3 c_\theta c_\phi - s_\theta^2 c_\phi^3 c_\theta s_\phi) \\
C'_{46} &= 2(C_{11} - C_{12})s_\theta^2 c_\theta c_\phi^2 s_\phi - C_{44}(2s_\theta^2 c_\phi^2 c_\theta - s_\phi^4 c_\theta s_\theta + s_\phi^2 s_\theta c_\theta - c_\phi^4 s_\theta c_\theta + c_\phi^2 s_\theta c_\theta) \\
C'_{56} &= (C_{11} - C_{12} - 2C_{44})(c_\theta^2 s_\phi^3 s_\theta c_\phi - c_\theta^2 c_\phi^3 s_\theta s_\phi)
\end{aligned}$$

By substituting the necessary angles we obtain the elastic stiffness components for (110) and (111) orientations in the following form:

$$\begin{aligned}
C_{11}^{(110)} &= C_{11} \\
C_{22}^{(110)} &= C_{33}^{(110)} = \frac{C_{11} + C_{12}}{2} + C_{44} \\
C_{44}^{(110)} &= \frac{C_{11} - C_{12}}{2} \\
C_{55}^{(110)} &= C_{66}^{(110)} = C_{44}
\end{aligned}$$

$$\begin{aligned}
C_{12}^{(110)} &= C_{13}^{(110)} = C_{12} \\
C_{23}^{(110)} &= \frac{C_{11} + C_{12}}{2} - C_{44} \\
C_{11}^{(111)} &= C_{22}^{(111)} = \frac{C_{11} + C_{12}}{2} + C_{44} \\
C_{33}^{(111)} &= \frac{C_{11} + 2C_{12} + 4C_{44}}{3} \\
C_{44}^{(111)} &= C_{55}^{(111)} = \frac{C_{11} - C_{12} + C_{44}}{3} \\
C_{66}^{(111)} &= \frac{C_{11} - C_{12} + 4C_{44}}{6} \\
C_{12}^{(111)} &= \frac{C_{11} + 5C_{12} - 2C_{44}}{6} \\
C_{13}^{(111)} &= C_{23}^{(111)} = \frac{C_{11} + 2C_{12} - 2C_{44}}{3} \\
C_{15}^{(111)} &= \frac{-C_{11} + C_{12} + 2C_{44}}{\sqrt{18}} \\
C_{25}^{(111)} &= C_{46}^{(111)} = \frac{C_{11} - C_{12} - 2C_{44}}{\sqrt{18}}
\end{aligned}$$

[Note: the terms which are not listed above are zero (for these two orientations only!)]

To obtain explicit form of ε' , three useful cases are discussed in details, those are ((110) and (111) orientations only):

a: The lattice-mismatched strain:

$$\varepsilon'_{xx} = \varepsilon'_{yy} = \frac{a_0 - a}{a} = \varepsilon_{\parallel} \quad (4.70)$$

where a_0 and a are the lattice constants of the substrate and the well layer material, ε_{\parallel} is in-plane fractional lattice mismatch⁶. The terms $\tau'_{xy} = \tau'_{yz} = \tau'_{zx} = 0$ which leads to ε off-diagonal terms to zero. There should be no stress in the z' -direction:

$$\begin{aligned}
0 &= \tau'_{zz} = C'_{13}\varepsilon'_{xx} + C'_{23}\varepsilon'_{xx} + C'_{33}\varepsilon'_{zz} \\
\varepsilon'_{zz} &= -\frac{C'_{13} + C'_{23}}{C'_{33}}\varepsilon'_{xx}
\end{aligned}$$

⁶The notation ε_{\parallel} is used for in-plane fractional lattice mismatch by some authors [68].

By substituting the explicit form for (110) and (111) orientations:

$$\begin{aligned}\varepsilon_{zz}^{(110)} &= -\frac{3C_{12} + C_{11} - 2C_{44}}{C_{11} + C_{12} + 2C_{44}}\varepsilon'_{xx} \\ \varepsilon_{zz}^{(111)} &= -2\frac{C_{11} + 2C_{12} - 2C_{44}}{C_{11} + 2C_{12} + 4C_{44}}\varepsilon'_{xx}\end{aligned}$$

b: A cubic crystal layer under an external biaxial in-plane stress $\tau'_{xx} = \tau'_{yy} = T$ and $\tau'_{zz} = 0$. The system of equations leads to the following for both (110) and (111) orientations:

$$\varepsilon'_{yz} = \varepsilon'_{zx} = \varepsilon'_{xy} = 0$$

The leftover system with three unknowns:

$$\begin{cases} T &= C'_{11}\varepsilon'_{xx} + C'_{12}\varepsilon'_{yy} + C'_{13}\varepsilon'_{zz} \\ T &= C'_{12}\varepsilon'_{xx} + C'_{22}\varepsilon'_{yy} + C'_{23}\varepsilon'_{zz} \\ 0 &= C'_{13}\varepsilon'_{xx} + C'_{23}\varepsilon'_{yy} + C'_{33}\varepsilon'_{zz} \end{cases}$$

By elementary manipulations the ε' terms are obtained:

$$\begin{aligned}\varepsilon'_{xx} &= \frac{C'_{13}C'_{23} - C'^2_{23} + C'_{22}C'_{33} - C'_{12}C'_{33}}{C'_{11}C'_{22}C'_{33} - C'_{11}C'^2_{23} - C'_{22}C'^2_{13} - C'^2_{12}C'_{33} + 2C'_{23}C'_{13}C'_{12}}T \\ \varepsilon'_{yy} &= \frac{C'_{13}C'_{23} - C'^2_{13} + C'_{11}C'_{33} - C'_{12}C'_{33}}{C'_{11}C'_{22}C'_{33} - C'_{11}C'^2_{23} - C'_{22}C'^2_{13} - C'^2_{12}C'_{33} + 2C'_{23}C'_{13}C'_{12}}T \\ \varepsilon'_{zz} &= \frac{C'_{12}C'_{23} - C'_{11}C'_{23} - C'_{13}C'_{22} + C'_{12}C'_{13}}{C'_{11}C'_{22}C'_{33} - C'_{11}C'^2_{23} - C'_{22}C'^2_{13} - C'^2_{12}C'_{33} + 2C'_{23}C'_{13}C'_{12}}T\end{aligned}$$

For (110) and (111) oriented substrates the above terms are converted to:

$$\begin{aligned}\varepsilon_{xx}^{(110)} &= \frac{C_{11}}{C^2_{11} + C_{11}C_{12} - 2C^2_{12}}T \\ \varepsilon_{yy}^{(110)} &= \frac{1}{4}\frac{C^2_{11} + C_{11}C_{12} + 2C_{11}C_{44} - 4C_{12}C_{44} - 2C^2_{12}}{C_{44}(C^2_{11} + C_{11}C_{12} - 2C^2_{12})}T \\ \varepsilon_{zz}^{(110)} &= -\frac{1}{4}\frac{C^2_{11} + C_{11}C_{12} - 2C_{11}C_{44} + 4C_{12}C_{44} - 2C^2_{12}}{C_{44}(C^2_{11} + C_{11}C_{12} - 2C^2_{12})}T \\ \varepsilon_{xx}^{(111)} &= \varepsilon_{yy}^{(111)} = \frac{1}{6}\frac{C_{11} + 2C_{12} + 4C_{44}}{C_{44}(C_{11} + 2C_{12})}T\end{aligned}$$

$$\varepsilon_{zz}^{(111)} = -\frac{1}{3} \frac{C_{11} + 2C_{12} - 2C_{44}}{C_{44}(C_{11} + 2C_{12})} T$$

c: A cubic crystal layer under an external uniaxial stress along growth direction $\tau'_{zz} = T$ and $\tau'_{xx} = \tau'_{yy} = 0$. The system of equations leads to the following, for both (110) and (111) orientations:

$$\varepsilon'_{yz} = \varepsilon'_{zx} = \varepsilon'_{xy} = 0$$

The leftover system with three unknowns:

$$\begin{cases} 0 &= C'_{11}\varepsilon'_{xx} + C'_{12}\varepsilon'_{yy} + C'_{13}\varepsilon'_{zz} \\ 0 &= C'_{12}\varepsilon'_{xx} + C'_{22}\varepsilon'_{yy} + C'_{23}\varepsilon'_{zz} \\ T &= C'_{13}\varepsilon'_{xx} + C'_{23}\varepsilon'_{yy} + C'_{33}\varepsilon'_{zz} \end{cases}$$

By elementary manipulations the ε' terms are obtained:

$$\varepsilon'_{xx} = \frac{C'_{12}C'_{23} - C'_{13}C'_{22}}{C'_{11}C'_{22}C'_{33} - C'_{11}C'_{23}{}^2 - C'_{22}C'_{13}{}^2 - C'_{12}{}^2C'_{33} + 2C'_{23}C'_{13}C'_{12}} T$$

$$\varepsilon'_{yy} = \frac{C'_{12}C'_{13} - C'_{11}C'_{23}}{C'_{11}C'_{22}C'_{33} - C'_{11}C'_{23}{}^2 - C'_{22}C'_{13}{}^2 - C'_{12}{}^2C'_{33} + 2C'_{23}C'_{13}C'_{12}} T$$

$$\varepsilon'_{zz} = \frac{C'_{11}C'_{22} - C'_{12}{}^2}{C'_{11}C'_{22}C'_{33} - C'_{11}C'_{23}{}^2 - C'_{22}C'_{13}{}^2 - C'_{12}{}^2C'_{33} + 2C'_{23}C'_{13}C'_{12}} T$$

For (110) and (111) oriented substrates the above terms are converted to:

$$\varepsilon_{xx}^{(110)} = -\frac{C_{12}}{C_{11}^2 + C_{11}C_{12} - 2C_{12}^2} T$$

$$\varepsilon_{yy}^{(110)} = -\frac{1}{4} \frac{C_{11}^2 + C_{11}C_{12} - 2C_{11}C_{44} - 2C_{12}^2}{C_{44}(C_{11}^2 + C_{11}C_{12} - 2C_{12}^2)} T$$

$$\varepsilon_{zz}^{(110)} = \frac{1}{4} \frac{C_{11}^2 + C_{11}C_{12} + 2C_{11}C_{44} - 2C_{12}^2}{C_{44}(C_{11}^2 + C_{11}C_{12} - 2C_{12}^2)} T$$

$$\varepsilon_{xx}^{(111)} = \varepsilon_{yy}^{(111)} = -\frac{1}{6} \frac{C_{11} + 2C_{12} - 2C_{44}}{C_{44}(C_{11} + 2C_{12})} T$$

$$\varepsilon_{zz}^{(111)} = \frac{1}{3} \frac{C_{11} + 2C_{12} + C_{44}}{C_{44}(C_{11} + 2C_{12})} T$$

4.7 Rotation of Luttinger-Kohn's Hamiltonian for hole states using rotation matrix (6×6) for wurtzite crystal

4.7.1 Introduction

The method of rotating hexagonal Hamiltonian is similar to the one discussed in section 4.2 with small differences, which are going to be discussed in this section.

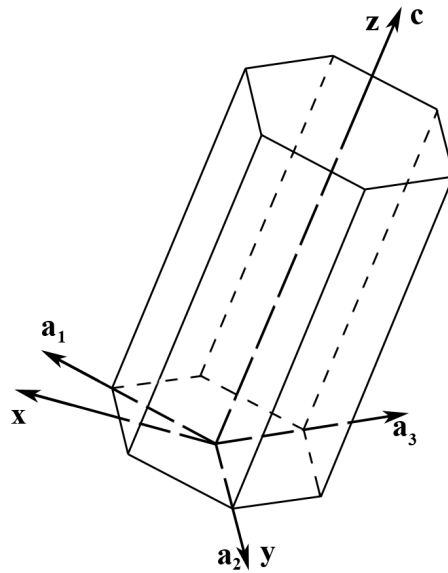


FIGURE 4.4: The Cartesian coordinate system in wurtzite primitive cell.

The first and major difference is that the axes of Cartesian coordinate system (x, y, z) do not coincide with the crystallographic axes of hexagon (a_1, a_2, a_3, c), and the convenient way to orient the crystal and coordinate system is the one that is shown on Fig. 4.4 [32] [36], due to the fact that the rotation is performed about y/a_2 and z/c axes. The coordinate system is rotated by using the same transformation as for cubic systems. The growth direction is assumed along c/z -axis.

4.7.2 Basis functions

We consider 6×6 Luttinger-Kohn's Hamiltonian for wurtzite crystal [29]. Basis functions for arbitrary growth direction are:

$$\begin{aligned}
 u'_1 &= \frac{-1}{\sqrt{2}} |(X' + iY') \uparrow\rangle \\
 u'_2 &= \frac{1}{\sqrt{2}} |(X' - iY') \uparrow\rangle \\
 u'_3 &= |Z' \uparrow\rangle \\
 u'_4 &= \frac{1}{\sqrt{2}} |(X' - iY') \downarrow\rangle \\
 u'_5 &= \frac{-1}{\sqrt{2}} |(X' + iY') \downarrow\rangle \\
 u'_6 &= |Z' \downarrow\rangle
 \end{aligned} \tag{4.71}$$

where the notation used is the same as in section 4.2.3. The explicit form of basis functions after rotation is given in Appendix D.

4.7.3 Matrix elements for rotated Luttinger-Kohn Hamiltonian

LKH has the form which allows us to express total Hamiltonian in terms of four values (by inspection of wurtzite LKH (3.91) it is found, that independent parameters are λ , Θ , K and H) only [29] for (0001), i.e. $\theta = 0$, $\phi = 0$, orientation:

$$\begin{aligned}
 \lambda &= \frac{\hbar^2}{2m_0} [A_1 k_z^2 + A_2 (k_x^2 + k_y^2)] \\
 \Theta &= \frac{\hbar^2}{2m_0} [A_3 k_z^2 + A_4 (k_x^2 + k_y^2)] \\
 K &= \frac{\hbar^2}{2m_0} A_5 (k_x - ik_y)^2 \\
 H &= \frac{\hbar^2}{2m_0} A_6 (k_x - ik_y) k_z
 \end{aligned} \tag{4.72}$$

The rotated matrix elements are obtained by Maple 16 program (code is provided in Appendix B). The matrix elements below are written for two particular orientations⁷, as the terms for other angles are too big and inconvenient to provide here (the same orientations are used in ref. [32]):

$$\theta = \frac{\pi}{2}, \phi = 0$$

$$\begin{aligned}\lambda &= \frac{\hbar^2}{2m_0} [(A_1 + A_3)k_1^2 + (A_2 + A_4)(k_2^2 + k_3^2) + A_5(k_2^2 - k_3^2)] \\ \Theta &= \frac{\hbar^2}{2m_0} \left[-A_3 \frac{k_1^2}{2} - A_4 \frac{k_2^2 + k_3^2}{2} + A_5 \frac{3(k_2^2 - k_3^2)}{2} \right] \\ K &= \frac{\hbar^2}{2m_0} \left[-A_3 \frac{k_1^2}{2} - A_4 \frac{k_2^2 + k_3^2}{2} - A_5 \frac{k_2^2 - k_3^2}{2} + i\sqrt{2}A_6 k_1 k_2 \right] \\ H &= \frac{\hbar^2}{2m_0} (A_6 k_1 + i\sqrt{2}A_5 k_2) k_3\end{aligned}\tag{4.73}$$

$$\theta = \frac{\pi}{4}, \phi = 0$$

$$\begin{aligned}\lambda &= \frac{\hbar^2}{2m_0} \left[\left(A_1 + \frac{A_3}{2} \right) \left(\frac{k_1^2}{2} + \frac{k_3^2}{2} - k_1 k_3 \right) + \left(A_2 + \frac{A_4}{2} \right) \left(\frac{k_1^2}{2} + \frac{k_3^2}{2} + k_1 k_3 + k_2^2 \right) \right. \\ &\quad \left. + A_5 \left(\frac{k_1^2}{4} + \frac{k_3^2}{4} + \frac{k_1 k_3}{2} - \frac{k_2^2}{2} \right) \right] \\ \Theta &= \frac{\hbar^2}{2m_0} \left[\frac{A_3}{4} \left(\frac{k_1^2}{2} + \frac{k_3^2}{2} - k_1 k_3 \right) + \frac{A_4}{4} \left(\frac{k_1^2}{2} + \frac{k_3^2}{2} + k_1 k_3 + k_2^2 \right) \right. \\ &\quad \left. - \frac{3A_5}{4} \left(\frac{k_1^2}{2} + \frac{k_3^2}{2} + k_1 k_3 - k_2^2 \right) + \frac{3\sqrt{2}A_6}{4} (k_1^2 - k_3^2) \right] \\ K &= \frac{\hbar^2}{2m_0} \left[-\frac{A_3}{4} \left(\frac{k_1^2}{2} + \frac{k_3^2}{2} - k_1 k_3 \right) - \frac{A_4}{4} \left(\frac{k_1^2}{2} + \frac{k_3^2}{2} + k_2^2 + k_1 k_3 \right) \right. \\ &\quad \left. + \frac{3A_5}{4} \left(\frac{k_1^2}{2} + \frac{k_3^2}{2} - k_2^2 + k_1 k_3 + ik_1 k_2 + ik_2 k_3 \right) + \frac{\sqrt{2}A_6}{2} \left(\frac{k_1^2}{2} + \frac{k_3^2}{2} + ik_1 k_2 - ik_2 k_3 \right) \right] \\ H &= \frac{\hbar^2}{2m_0} \frac{\sqrt{2}}{8} [A_3(k_1^2 + k_3^2 - k_1 k_3) + A_4(k_1^2 + k_3^2 + 2k_2^2 + 2k_1 k_3) \\ &\quad + A_5(k_1^2 + k_3^2 - 2k_2^2 + 2k_1 k_3 + i4k_1 k_2 + i4k_2 k_3) + i2\sqrt{2}A_6(k_2 k_3 - k_1 k_2)]\end{aligned}\tag{4.74}$$

⁷The orientations are expressed in terms of angles due to the fact that conversion of angles into Miller-Bravais indices depends on the lattice constants for each material.

4.8 Strain effects on band structures for arbitrary oriented wurtzite crystal

The strain effects on band structure for rotated wurtzite crystals are introduced by the same method as for cubic. We obtain rotated elastic stiffness tensor C' by the eq. (4.67). The general form of rotated elastic stiffness tensor C' (symmetric $C'_{ij} = C'_{ji}$) for wurtzite in Voigt notation is the following:

$$C' = \begin{bmatrix} C'_{11} & C'_{12} & C'_{13} & 0 & C'_{15} & 0 \\ C'_{21} & C'_{22} & C'_{23} & 0 & C'_{25} & 0 \\ C'_{31} & C'_{32} & C'_{33} & 0 & C'_{35} & 0 \\ 0 & 0 & 0 & C'_{44} & 0 & C'_{46} \\ C'_{51} & C'_{52} & C'_{53} & 0 & C'_{55} & 0 \\ 0 & 0 & 0 & C'_{64} & 0 & C'_{66} \end{bmatrix} \quad (4.75)$$

where the elastic stiffness tensor components for arbitrary oriented substrate have the following form (obtained by similar to eq. (4.69) procedure):

$$C'_{11} = C_{11}c_{\theta}^4 + C_{33}(s_{\theta}^2 - c_{\theta}^2 + c_{\theta}^4) + (2C_{13} + 4C_{44})(c_{\theta}^2 - c_{\theta}^4)$$

$$C'_{22} = C_{11}$$

$$C'_{33} = C_{11}(s_{\theta}^2 - c_{\theta}^2 + c_{\theta}^4) + C_{33}c_{\theta}^4 + (2C_{13} + 4C_{44})(c_{\theta}^2 - c_{\theta}^4)$$

$$C'_{44} = (C_{11} - C_{12})\frac{s_{\theta}^2}{2} + C_{44}c_{\theta}^2$$

$$C'_{55} = (C_{11} + C_{33} - 2C_{13} - 4C_{44})(c_{\theta}^2 - c_{\theta}^4) + C_{44}$$

$$C'_{66} = C_{44}s_{\theta}^2 + (C_{11} - C_{12})\frac{c_{\theta}^2}{2}$$

$$C'_{12} = C_{12}c_{\theta}^2 + C_{13}s_{\theta}^2$$

$$C'_{13} = (C_{11} + C_{33} - 4C_{44})(c_{\theta}^2 - c_{\theta}^4) + C_{13}(s_{\theta}^2 - c_{\theta}^2 + 2c_{\theta}^4)$$

$$C'_{15} = [C_{11}c_{\theta}^2 - C_{33}s_{\theta}^2 + (C_{13} + 2C_{44})(s_{\theta}^2 - c_{\theta}^2)] s_{\theta}c_{\theta}$$

$$C'_{23} = C_{12}s_{\theta}^2 + C_{13}c_{\theta}^2$$

$$C'_{25} = (C_{12} - C_{13})c_{\theta}s_{\theta}$$

$$C'_{35} = [C_{11}s_\theta^2 - C_{33}c_\theta^2 + (C_{13} + 2C_{44})(c_\theta^2 - s_\theta^2)] s_\theta c_\theta$$

$$C'_{46} = (C_{11} - C_{12} - 2C_{44}) \frac{C_\theta s_\theta}{2}$$

It is obvious that elastic stiffness is dependent on angle θ only. For particular orientations the expression for elastic stiffness tensor components may be simplified by inserting the proper angle:

$$C_{11}^{\theta=\pi/2} = C_{33}$$

$$C_{22}^{\theta=\pi/2} = C_{11}$$

$$C_{33}^{\theta=\pi/2} = C_{11}$$

$$C_{44}^{\theta=\pi/2} = \frac{C_{11} - C_{12}}{2}$$

$$C_{55}^{\theta=\pi/2} = C_{44}$$

$$C_{66}^{\theta=\pi/2} = C_{44}$$

$$C_{12}^{\theta=\pi/2} = C_{13}$$

$$C_{13}^{\theta=\pi/2} = C_{13}$$

$$C_{23}^{\theta=\pi/2} = C_{12}$$

$$C_{11}^{\theta=\pi/4} = \frac{C_{11} + C_{33} + 2C_{13} + 4C_{44}}{4}$$

$$C_{22}^{\theta=\pi/4} = C_{11}$$

$$C_{33}^{\theta=\pi/4} = \frac{C_{11} + C_{33} + 2C_{13} + 4C_{44}}{4}$$

$$C_{44}^{\theta=\pi/4} = \frac{C_{11} - C_{12} + 2C_{44}}{4}$$

$$C_{55}^{\theta=\pi/4} = \frac{C_{11} + C_{33} - 2C_{13}}{4}$$

$$C_{66}^{\theta=\pi/4} = \frac{C_{11} - C_{12} + 2C_{44}}{4}$$

$$C_{12}^{\theta=\pi/4} = \frac{C_{12} + C_{13}}{2}$$

$$C_{13}^{\theta=\pi/4} = \frac{C_{11} + C_{33} + 2C_{13} - 4C_{44}}{4}$$

$$C_{15}^{\theta=\pi/4} = \frac{C_{11} + C_{33}}{4}$$

$$\begin{aligned}
C_{23}^{\theta=\pi/4} &= \frac{C_{12} + C_{13}}{2} \\
C_{25}^{\theta=\pi/4} &= \frac{C_{12} - C_{13}}{2} \\
C_{35}^{\theta=\pi/4} &= \frac{C_{11} - C_{33}}{4} \\
C_{46}^{\theta=\pi/4} &= \frac{C_{11} - C_{12} - 2C_{44}}{4}
\end{aligned}$$

We obtain matrix elements for Bir and Bikus strain Hamiltonian by using the correspondences (4.62) on matrix elements (4.73) and (4.74) which are allowed as we work in the same coordinate system as for cubic. We replace Bir and Pikus parameters A_i with deformation potentials D_i , $i = 1, \dots, 6$. The explicit form of rotated Bir and Pikus strain Hamiltonian terms:

$$\theta = \frac{\pi}{2}, \phi = 0$$

$$\begin{aligned}
\lambda &= (D_1 + D_3)\varepsilon'_{xx} + (D_2 + D_4)(\varepsilon'_{yy} + \varepsilon'_{zz}) + D_5(\varepsilon'_{yy} - \varepsilon'_{zz}) \\
\Theta &= -D_3 \frac{\varepsilon'_{xx}}{2} - D_4 \frac{\varepsilon'_{yy} + \varepsilon'_{zz}}{2} + D_5 \frac{3(\varepsilon'_{yy} - \varepsilon'_{zz})}{2} \\
K &= -D_3 \frac{\varepsilon'_{xx}}{2} - D_4 \frac{\varepsilon'_{yy} + \varepsilon'_{zz}}{2} - D_5 \frac{\varepsilon'_{yy} - \varepsilon'_{zz}}{2} + i\sqrt{2}D_6\varepsilon'_{xy} \\
H &= D_6\varepsilon'_{xz} + i\sqrt{2}D_5\varepsilon'_{yz}
\end{aligned} \tag{4.76}$$

$$\theta = \frac{\pi}{4}, \phi = 0$$

$$\begin{aligned}
\lambda &= \left(D_1 + \frac{D_3}{2}\right) \left(\frac{\varepsilon'_{xx}}{2} + \frac{\varepsilon'_{zz}}{2} - \varepsilon'_{xz}\right) + \left(D_2 + \frac{D_4}{2}\right) \left(\frac{\varepsilon'_{xx}}{2} + \frac{\varepsilon'_{zz}}{2} + \varepsilon'_{xz} + \varepsilon'_{yy}\right) \\
&\quad + D_5 \left(\frac{\varepsilon'_{xx}}{4} + \frac{\varepsilon'_{zz}}{4} + \frac{\varepsilon'_{xz}}{2} - \frac{\varepsilon'_{yy}}{2}\right) \\
\Theta &= \frac{D_3}{4} \left(\frac{\varepsilon'_{xx}}{2} + \frac{\varepsilon'_{zz}}{2} - \varepsilon'_{xz}\right) + \frac{D_4}{4} \left(\frac{\varepsilon'_{xx}}{2} + \frac{\varepsilon'_{zz}}{2} + \varepsilon'_{xz} + \varepsilon'_{yy}\right) \\
&\quad - \frac{3D_5}{4} \left(\frac{\varepsilon'_{xx}}{2} + \frac{\varepsilon'_{zz}}{2} + \varepsilon'_{xz} - \varepsilon'_{yy}\right) + \frac{3\sqrt{2}D_6}{4} (\varepsilon'_{xx} - \varepsilon'_{zz}) \\
K &= -\frac{D_3}{4} \left(\frac{\varepsilon'_{xx}}{2} + \frac{\varepsilon'_{zz}}{2} - \varepsilon'_{xz}\right) - \frac{D_4}{4} \left(\frac{\varepsilon'_{xx}}{2} + \frac{\varepsilon'_{zz}}{2} + \varepsilon'_{yy} + \varepsilon'_{xz}\right) \\
&\quad + \frac{3D_5}{4} \left(\frac{\varepsilon'_{xx}}{2} + \frac{\varepsilon'_{zz}}{2} - \varepsilon'_{yy} + \varepsilon'_{xz} + i\varepsilon'_{xy} + i\varepsilon'_{yz}\right) + \frac{\sqrt{2}D_6}{2} \left(\frac{\varepsilon'_{xx}}{2} + \frac{\varepsilon'_{zz}}{2} + i\varepsilon'_{xy} - i\varepsilon'_{yz}\right) \\
H &= \frac{\sqrt{2}}{8} [D_3(\varepsilon'_{xx} + \varepsilon'_{zz} - \varepsilon'_{xz}) + D_4(\varepsilon'_{xx} + \varepsilon'_{zz} + 2\varepsilon'_{yy} + 2\varepsilon'_{xz}) \\
&\quad + D_5(\varepsilon'_{xx} + \varepsilon'_{zz} - 2\varepsilon'_{yy} + 2\varepsilon'_{xz} + i4\varepsilon'_{xy} + i4\varepsilon'_{yz}) + i2\sqrt{2}D_6(\varepsilon'_{yz} - \varepsilon'_{xy})]
\end{aligned} \tag{4.77}$$

where the rotated strain tensor ε components are obtained for three particular strain situations:

a: Lattice-mismatched strain, using the same assumptions as for cubic:

$$\varepsilon'_{xx} = \varepsilon'_{yy} = \frac{a_0 - a}{a} = \varepsilon_{\parallel} \tag{4.78}$$

where a_0 and a are the lattice constants of the substrate and the well layer material. There should be no stress in the growth direction and there are no diagonal stresses, so $\tau'_{zz} = \tau'_{xy} = \tau'_{yz} = \tau'_{zx} = 0$ which leads to the system of equations:

$$\begin{cases} 0 = C'_{13}\varepsilon'_{xx} + C'_{23}\varepsilon'_{yy} + C'_{33}\varepsilon'_{zz} + 2C'_{35}\varepsilon'_{zx} \\ 0 = 2C'_{44}\varepsilon'_{yz} + 2C'_{46}\varepsilon'_{xy} \\ 0 = C'_{15}\varepsilon'_{xx} + C'_{25}\varepsilon'_{yy} + C'_{35}\varepsilon'_{zz} + 2C'_{55}\varepsilon'_{zx} \\ 0 = 2C'_{46}\varepsilon'_{yz} + 2C'_{66}\varepsilon'_{xy} \end{cases} \Rightarrow \begin{cases} -\varepsilon_{\parallel}(C'_{13} + C'_{23}) = C'_{33}\varepsilon'_{zz} + 2C'_{35}\varepsilon'_{zx} \\ -C'_{44}\varepsilon'_{yz} = C'_{46}\varepsilon'_{xy} \\ -\varepsilon_{\parallel}(C'_{15} + C'_{25}) = C'_{35}\varepsilon'_{zz} + 2C'_{55}\varepsilon'_{zx} \\ -C'_{46}\varepsilon'_{yz} = C'_{66}\varepsilon'_{xy} \end{cases} \tag{4.79}$$

The solution is difficult to provide in general so the solution is provided for particular cases:

$$\varepsilon'_{zz}{}^{\theta=\pi/2} = -\frac{C_{12} + C_{13}}{C_{11}}\varepsilon_{\parallel} \tag{4.80}$$

$$\varepsilon_{zx}^{\theta=\pi/2} = \varepsilon_{yz}^{\theta=\pi/2} = \varepsilon_{xy}^{\theta=\pi/2} = 0 \quad (4.81)$$

$$\varepsilon_{zz}^{\theta=\pi/4} = \frac{(C_{11} - C_{33})^2 - 4C_{55}(C_{11} + C_{33} + 2C_{12} + 4C_{13} - 4C_{44}) + 2(C_{11} - C_{33})(C_{12} - C_{13})}{-(C_{11} - C_{33})^2 + 4C_{55}(C_{11} + C_{33} + 2C_{13} + 4C_{44})} \varepsilon_{\parallel} \quad (4.82)$$

$$\varepsilon_{zx}^{\theta=\pi/4} = \frac{2C_{33}C_{12} + 4C_{44}(C_{11} - C_{33} + C_{12} - C_{13} - 4C_{44}) - 2C_{13}(C_{11} - C_{12} + C_{13})}{(C_{11} - C_{33})^2 - 4C_{55}(C_{11} + C_{33} + 2C_{13} + 4C_{44})} \varepsilon_{\parallel} \quad (4.83)$$

$$\varepsilon_{yz}^{\theta=\pi/4} = \varepsilon_{xy}^{\theta=\pi/4} = 0 \quad (4.84)$$

b: A hexagonal crystal under an external biaxial in-plane stress $\tau'_{xx} = \tau'_{yy} = T$ and $\tau'_{zz} = 0$. The system of equations is expressed as:

$$\begin{cases} T = C'_{11}\varepsilon'_{xx} + C'_{12}\varepsilon'_{yy} + C'_{13}\varepsilon'_{zz} + 2C'_{15}\varepsilon'_{zx} \\ T = C'_{12}\varepsilon'_{xx} + C'_{22}\varepsilon'_{yy} + C'_{23}\varepsilon'_{zz} + 2C'_{25}\varepsilon'_{zx} \\ 0 = C'_{13}\varepsilon'_{xx} + C'_{23}\varepsilon'_{yy} + C'_{33}\varepsilon'_{zz} + 2C'_{35}\varepsilon'_{zx} \\ 0 = 2C'_{44}\varepsilon'_{yz} + 2C'_{46}\varepsilon'_{xy} \\ 0 = C'_{15}\varepsilon'_{xx} + C'_{25}\varepsilon'_{yy} + C'_{35}\varepsilon'_{zz} + 2C'_{55}\varepsilon'_{zx} \\ 0 = 2C'_{46}\varepsilon'_{yz} + 2C'_{66}\varepsilon'_{xy} \end{cases} \quad (4.85)$$

Solving this system of equations for particular orientations we obtain:

$$\varepsilon_{xx}^{\theta=\pi/2} = \frac{C_{11} + C_{12} - C_{13}}{C_{33}(C_{11} + C_{12}) - 2C_{13}^2} T \quad (4.86)$$

$$\varepsilon_{yy}^{\theta=\pi/2} = \frac{C_{11}C_{33} - C_{13}(C_{11} - C_{12} + C_{13})}{(C_{11} - C_{12})(C_{33}(C_{11} + C_{12}) - 2C_{13}^2)} T \quad (4.87)$$

$$\varepsilon_{zz}^{\theta=\pi/2} = \frac{-C_{12}C_{33} - C_{13}(C_{11} - C_{12} - C_{13})}{(C_{11} - C_{12})(C_{33}(C_{11} + C_{12}) - 2C_{13}^2)} T \quad (4.88)$$

$$\varepsilon_{zx}^{\theta=\pi/2} = \varepsilon_{yz}^{\theta=\pi/2} = \varepsilon_{xy}^{\theta=\pi/2} = 0 \quad (4.89)$$

$$\varepsilon_{xx}^{\theta=\pi/4} = \frac{1}{4C_{44}} \frac{C_{44}(C_{11}(C_{33} + C_{11} - 4C_{13}) + C_{12}(2C_{33} - C_{12} + 4C_{13}) + C_{13}^2)}{(C_{11} - C_{12})(C_{33}(C_{11} + C_{12}) - 2C_{13}^2)} + \frac{C_{11}(C_{11}C_{33} - 2C_{13}^2) + C_{12}(2C_{13}^2 - C_{12}C_{33})}{4C_{44}} T \quad (4.90)$$

$$\varepsilon_{yy}^{\theta=\pi/4} = \frac{1}{2} \frac{C_{12}(C_{13} - C_{33}) - C_{11}(C_{13} - 2C_{33}) - C_{13}^2}{(C_{11} - C_{12})(C_{33}(C_{11} + C_{12}) - 2C_{13}^2)} T \quad (4.91)$$

$$\varepsilon_{zz}^{\theta=\pi/4} = \frac{1}{4C_{44}} \frac{C_{44}(C_{11}(C_{33} + C_{11} - 4C_{13}) + C_{12}(2C_{33} - C_{12} + 4C_{13}) + C_{13}^2)}{(C_{11} - C_{12})(C_{33}(C_{11} + C_{12}) - 2C_{13}^2)}$$

$$\frac{-C_{11}(C_{11}C_{33} - 2C_{13}^2) - C_{12}(2C_{13}^2 - C_{12}C_{33})}{2}T \quad (4.92)$$

$$\varepsilon_{zx}^{\theta=\pi/4} = \frac{1}{2} \frac{C_{11}C_{33} - C_{11}^2 + C_{12}^2 + C_{13}^2 + 2(C_{11}C_{13} - C_{12}C_{13} - C_{12}C_{33})}{(C_{11} - C_{12})(C_{33}(C_{11} + C_{12}) - 2C_{13}^2)}T \quad (4.93)$$

$$\varepsilon_{yz}^{\theta=\pi/4} = \varepsilon_{xy}^{\theta=\pi/4} = 0 \quad (4.94)$$

c: A hexagonal crystal under an external uniaxial stress along growth direction $\tau'_{xx} = \tau'_{yy} = 0$ and $\tau'_{zz} = T$. The system of equations is expressed as:

$$\begin{cases} 0 = C'_{11}\varepsilon'_{xx} + C'_{12}\varepsilon'_{yy} + C'_{13}\varepsilon'_{zz} + 2C'_{15}\varepsilon'_{zx} \\ 0 = C'_{12}\varepsilon'_{xx} + C'_{22}\varepsilon'_{yy} + C'_{23}\varepsilon'_{zz} + 2C'_{25}\varepsilon'_{zx} \\ T = C'_{13}\varepsilon'_{xx} + C'_{23}\varepsilon'_{yy} + C'_{33}\varepsilon'_{zz} + 2C'_{35}\varepsilon'_{zx} \\ 0 = 2C'_{44}\varepsilon'_{yz} + 2C'_{46}\varepsilon'_{xy} \\ 0 = C'_{15}\varepsilon'_{xx} + C'_{25}\varepsilon'_{yy} + C'_{35}\varepsilon'_{zz} + 2C'_{55}\varepsilon'_{zx} \\ 0 = 2C'_{46}\varepsilon'_{yz} + 2C'_{66}\varepsilon'_{xy} \end{cases} \quad (4.95)$$

Solving this system of equation for particular orientations we obtain:

$$\varepsilon_{xx}^{\theta=\pi/2} = \frac{-C_{13}}{C_{33}(C_{11} + C_{12}) - 2C_{13}^2}T \quad (4.96)$$

$$\varepsilon_{yy}^{\theta=\pi/2} = \frac{C_{13}^2 - C_{12}C_{33}}{(C_{11} - C_{12})(C_{33}(C_{11} + C_{12}) - 2C_{13}^2)}T \quad (4.97)$$

$$\varepsilon_{zz}^{\theta=\pi/2} = \frac{C_{11}C_{33} - C_{13}^2}{(C_{11} - C_{12})(C_{33}(C_{11} + C_{12}) - 2C_{13}^2)}T \quad (4.98)$$

$$\varepsilon_{zx}^{\theta=\pi/2} = \varepsilon_{yz}^{\theta=\pi/2} = \varepsilon_{xy}^{\theta=\pi/2} = 0 \quad (4.99)$$

$$\varepsilon_{xx}^{\theta=\pi/4} = \frac{1}{4C_{44}} \frac{C_{44}(C_{11}(C_{33} + C_{11} - 2C_{13}) + 2C_{12}C_{13} - C_{12}^2 - C_{13}^2)}{(C_{11} - C_{12})(C_{33}(C_{11} + C_{12}) - 2C_{13}^2)} - \frac{C_{11}(C_{11}C_{33} - 2C_{13}^2) - C_{12}(2C_{13}^2 - C_{12}C_{33})}{2}T \quad (4.100)$$

$$\varepsilon_{yy}^{\theta=\pi/4} = \frac{1}{2} \frac{C_{12}(C_{13} - C_{33}) - C_{11}C_{13} + C_{13}^2}{(C_{11} - C_{12})(C_{33}(C_{11} + C_{12}) - 2C_{13}^2)}T \quad (4.101)$$

$$\varepsilon_{zz}^{\theta=\pi/4} = \frac{1}{4C_{44}} \frac{C_{44}(C_{11}(C_{33} + C_{11} - 2C_{13}) + 2C_{12}C_{13} - C_{12}^2 - C_{13}^2)}{(C_{11} - C_{12})(C_{33}(C_{11} + C_{12}) - 2C_{13}^2)} + \frac{C_{11}(C_{11}C_{33} - 2C_{13}^2) + C_{12}(2C_{13}^2 - C_{12}C_{33})}{2}T \quad (4.102)$$

$$\varepsilon_{zx}^{\theta=\pi/4} = \frac{1}{2} \frac{C_{11}C_{33} - C_{11}^2 + C_{12}^2 - C_{13}^2}{(C_{11} - C_{12})(C_{33}(C_{11} + C_{12}) - 2C_{13}^2)} T \quad (4.103)$$

$$\varepsilon_{yz}^{\theta=\pi/4} = \varepsilon_{xy}^{\theta=\pi/4} = 0 \quad (4.104)$$

Chapter 5

Numerical method for band structure calculations

In this chapter we describe one of the most commonly used methods for numerical calculations of band structure of QW. The method is called Plane Wave Expansion or Fourier Series solution of LKH. In general, a finite number of plane wave functions are used as a basis set. A finite sum of plane waves approximates a true envelop function. Considered QW of the length L . We solve Schrödinger equation with LKH in rectangular potential of QW. QW has the form as shown on Fig. 5.1. LKH describes a number of types of coupled particles. We start with a basis of plane waves for each subband envelope function, and each envelope function will be a sum of a number of plane waves:

$$F_\nu(z) = \sum_{n=-M}^M f_{\nu n} e^{ik_n z}$$

where $k_n = 2\pi n/L$ and number of plane waves is $2M + 1$. This is a truncated Fourier series representation of the wave function. The other quantities can be represented also as truncated Fourier series if they depended on z . The following quantities (Luttinger parameters, potential, spin split-off energy, band-edge energies etc.) are approximated the same way:

$$\gamma_\zeta(z) = \sum_{l=-2M}^{2M} \gamma_{\zeta l} e^{ik_l z}$$

$$V(z) = \sum_{l=-2M}^{2M} v_l e^{ik_l z}$$

$$U(z) = \sum_{l=-2M}^{2M} u_l e^{ik_l z}$$

$$\Delta(z) = \sum_{l=-2M}^{2M} \Delta_l e^{ik_l z}$$

$$\alpha(z) = \sum_{l=-2M}^{2M} \alpha_l e^{ik_l z}$$

where $k_l = 2\pi l/L$. Fourier series have been written in symmetric form to ensure that Hamiltonian is Hermitian. We insert Fourier series into the LKH and look for the solution of the eigenvalue problem:

$$\mathbf{H} \sum_n f_{\nu n} e^{ik_n z} = E \sum_n f_n e^{ik_n z} \quad (5.1)$$

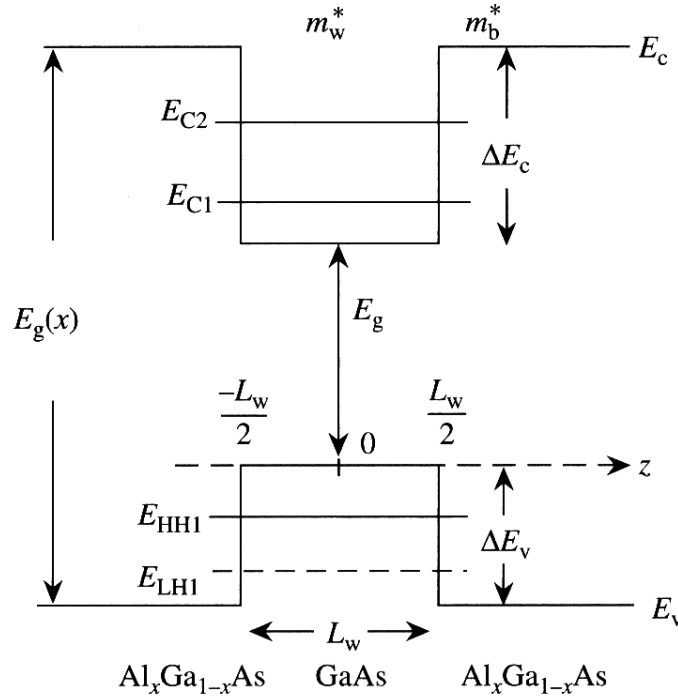


FIGURE 5.1: QW profiles for the conduction and valence bands of a GaAs/AlGaAs system.

5.1 Plane wave expansion method for 4×4 Hamiltonian

The example calculation of the eigenvalue problem above is implemented in Matlab and divided into sections corresponding to the subroutines of the program.

5.1.1 Reading initial data

As a starting point we define the following numerical parameters:

- L_w - length of the QW region measured in angstroms;
- L_b - length of barrier region;
- N_{pw} - number of plane waves used for Plane wave expansion;
- x, y - parameters for material composition;
- k_{pt} - number of points discretizing wave vector \vec{k} ;
- k_{ran} - range of wave vector \vec{k} ;
- T - uniaxial external stress (optional).

5.1.2 Material parameters

Using this initial data, the parameters of material composition are defined using Vegard's interpolation formula [69], for example for $Al_{1-x}Ga_xAs/GaAs$ QW:

$$E_{gap} = E_{gap}^{GaAs}(1-x) + E_{gap}^{AlAs}x - x(1-x)(1.31x - 0.127) \quad (5.2)$$

$$\mathbf{Q} = \mathbf{Q}^{GaAs}(1-x) + \mathbf{Q}^{AlAs}x \quad (5.3)$$

where E_{gap} is a band gap for corresponding material and \mathbf{Q} represents the parameter such as: γ_i - Luttinger parameters, m_e - effective mass, a - lattice constant, a_c, a_v, b - deformation potentials, etc. Band edges are defined depending on the region:

- For barrier regions the conduction band edge set as the size of bandgap, heavy and light hole band edges set as zero for programming convenience, strain terms do not exist in barrier region.

- For well region heavy and light hole band edges defined by using model-solid theory [70][71][72][73]. The idea is to set up the absolute reference energy level. All energies can be put on an absolute energy scale and band lineups are derived. The estimation of band offsets is based on the average energy $E_{v,av}$ which is the average of three uppermost valence bands (heavy, light holes and spin split-off bands). For various materials the $E_{v,av}$ already calculated [73] and tabulated in Table E.1. The position of valence band edge then is obtained by:

$$E_v = E_{v,av} + \frac{\Delta}{3} \quad (5.4)$$

but as we define barrier region energy as zero it should be subtracted from the above energy:

$$E_v = E_{v,av} + \frac{\Delta}{3} - \left(E_{v,av}^{sub} + \frac{\Delta^{sub}}{3} \right) \quad (5.5)$$

where superscript “sub” refers to “substrate”. The conduction band edge is calculated by adding the band-gap energy to the valence band:

$$E_c = E_v + E_g \quad (5.6)$$

If the strain exists (lattice constants of well and substrate materials do not match or external pressure applied) the additional terms, shifting band edges, are introduced and the each band edge energy is obtained by:

$$E_c = E_v^0 + E_g + P_c \quad (5.7)$$

$$E_{HH} = E_v^0 - P_\varepsilon - Q_\varepsilon \quad (5.8)$$

$$E_{LH} = E_v^0 - P_\varepsilon - \frac{\Delta}{2} + \frac{Q_\varepsilon}{2} + \frac{1}{2} \sqrt{\Delta^2 + 2\Delta Q_\varepsilon + 9Q_\varepsilon^2} \quad (5.9)$$

where $P_c = a_c \text{Tr}(\varepsilon)$, P_ε and Q_ε are defined in the strain discussion sections.

5.1.3 Fourier transform and matrix of Fourier coefficients

Using the geometry of the system L_w and L_b from initial data one dimensional spatial grid is constructed. The variable of the grid is labeled as z . All material parameters including strain related terms are calculated for each plane wave using Fourier transformation:

$$\mathbf{Q}_{ij} = \frac{1}{\sqrt{L}} \int_0^L \mathbf{Q} e^{-iK_m z} dz \quad (5.10)$$

where $i, j = -N_{pw}, \dots, N_{pw}$ - plane wave index, \mathbf{Q} - is the vector of values of the material parameters and matrix elements of LKH, $K_m = 2\pi(i - j)/L$, L - the length of the structure, the integral is normalized with $\frac{1}{\sqrt{L}}$ factor. For 4×4 Hamiltonian the matrix of Fourier coefficients is created with size $4(2N_{pw} + 1)$. The following parameters corresponds to matrix elements in LKH (each of them creates a matrix of the size $(2N_{pw} + 1) \times (2N_{pw} + 1)$):

$$\begin{aligned} f_{ij}^Q &= Q(k_{ij}) \\ f_{ij}^{hh} &= P(k_{ij}) + Q(k_{ij}) \\ f_{ij}^{lh} &= P(k_{ij}) - Q(k_{ij}) \\ f_{ij}^R &= R(k_{ij}) \\ f_{ij}^S &= S(k_{ij}) \end{aligned} \quad (5.11)$$

Each of the above parameters evaluated by cyclic operation, for instance, we show f^Q for 2 plane waves $N_{pw} = 2$ it will have the size 5×5 :

$$\begin{aligned} f_{11}^Q &= \frac{\hbar^2}{2m_0} \left(k_x^2 + k_y^2 - 2 \left(\frac{2\pi}{L} \right)^2 \cdot 4 \right) \cdot \frac{1}{\sqrt{L}} \int_0^L \gamma_2 e^{-i \frac{2\pi(-2+2)}{L} z} dz \\ f_{12}^Q &= \frac{\hbar^2}{2m_0} \left(k_x^2 + k_y^2 - 2 \left(\frac{2\pi}{L} \right)^2 \cdot 2 \right) \cdot \frac{1}{\sqrt{L}} \int_0^L \gamma_2 e^{-i \frac{2\pi(-2+1)}{L} z} dz \\ &\dots \\ f_{54}^Q &= \frac{\hbar^2}{2m_0} \left(k_x^2 + k_y^2 - 2 \left(\frac{2\pi}{L} \right)^2 \cdot 2 \right) \cdot \frac{1}{\sqrt{L}} \int_0^L \gamma_2 e^{-i \frac{2\pi(2-1)}{L} z} dz \\ f_{55}^Q &= \frac{\hbar^2}{2m_0} \left(k_x^2 + k_y^2 - 2 \left(\frac{2\pi}{L} \right)^2 \cdot 4 \right) \cdot \frac{1}{\sqrt{L}} \int_0^L \gamma_2 e^{-i \frac{2\pi(2-2)}{L} z} dz \end{aligned} \quad (5.12)$$

so the matrix f^Q will have the following form:

$$f^Q = \begin{bmatrix} f_{11}^Q & f_{12}^Q & f_{13}^Q & f_{14}^Q & f_{15}^Q \\ f_{21}^Q & f_{22}^Q & f_{23}^Q & f_{24}^Q & f_{25}^Q \\ f_{31}^Q & f_{32}^Q & f_{33}^Q & f_{34}^Q & f_{35}^Q \\ f_{41}^Q & f_{42}^Q & f_{43}^Q & f_{44}^Q & f_{45}^Q \\ f_{51}^Q & f_{52}^Q & f_{53}^Q & f_{54}^Q & f_{55}^Q \end{bmatrix} \quad (5.13)$$

The resulting matrices are constructing the matrix of Fourier coefficients which has similar to LKH matrix form:

$$H^{LK} = \begin{bmatrix} f^{hh} & -f^S & f^R & 0 \\ -f^{S+} & f^{lh} & 0 & f^R \\ f^{R+} & 0 & f^{lh} & f^S \\ 0 & f^{R+} & f^{S+} & f^{hh} \end{bmatrix} \quad (5.14)$$

Each element of the matrix is divided by $e_0\sqrt{L}$ normalization factor where e_0 is elementary charge. The program then evaluates eigenvalues and eigenvectors for the H^{LK} matrix by using the appropriate in Matlab routine. The eigenvalues are sorted to provide the array of envelope functions for each band. The resulting vectors for each envelope functions represent vectors of energy values with respect to wave vector. Explicit examples of band structure for some materials are provided in the next chapter. Also the arrays for envelope functions are used in matrix elements for optical transitions to evaluate overlap integrals.

5.2 Generalization plane wave expansion for 4×4 Hamiltonian to 6 - 14 band Hamiltonians

The addition of extra calculating parameters generalize the method to higher number of bands.

5.2.1 6×6 Hamiltonian

For 6 band LKH the only additional material parameter - spin split-off band edge energy, should be evaluated:

$$E_{SO} = E_v^0 - P_\varepsilon - \frac{\Delta}{2} + \frac{Q_\varepsilon}{2} - \frac{1}{2}\sqrt{\Delta^2 + 2\Delta Q_\varepsilon + 9Q_\varepsilon^2} \quad (5.15)$$

The matrix of Fourier coefficients (the size of $6(2N_{pw} + 1) \times 6(2N_{pw} + 1)$) with additional split-off terms is expressed:

$$H^{LK} = \begin{bmatrix} f^{hh} & -f^S & f^R & 0 & -f^S/\sqrt{2} & \sqrt{2}f^R \\ -f^{S+} & f^{lh} & 0 & f^R & -\sqrt{2}f^Q & \sqrt{3/2}f^S \\ f^{R+} & 0 & f^{lh} & f^S & \sqrt{3/2}f^{S+} & \sqrt{2}f^Q \\ 0 & f^{R+} & f^{S+} & f^{hh} & -\sqrt{2}f^{R+} & -f^{S+}/\sqrt{2} \\ -f^{S+}/\sqrt{2} & -\sqrt{2}f^{Q+} & \sqrt{3/2}f^S & -\sqrt{2}f^R & f^{so} & 0 \\ \sqrt{2}f^{R+} & \sqrt{3/2}f^{S+} & \sqrt{2}f^{Q+} & -f^S/\sqrt{2} & 0 & f^{so} \end{bmatrix} \quad (5.16)$$

where

$$\begin{aligned} f_{ij}^Q &= Q(k_{ij}) \\ f_{ij}^{so} &= P(k_{ij}) + \Delta(k_{ij}) \end{aligned} \quad (5.17)$$

5.2.2 8×8 Hamiltonian

8 band LKH has conduction band treated exactly so the modified Luttinger parameters used (4.48). The additional material parameters (conduction band edge energy and Kane's parameter) for conduction band result in the following matrix:

$$H^{LK}$$

$$= \begin{bmatrix} f^{cb} & 0 & \sqrt{3}f^T & -\sqrt{2}f^U & f^{T+} & 0 & f^U & -\sqrt{2}f^{T+} \\ 0 & f^{cb} & 0 & -f^T & -\sqrt{2}f^U & -\sqrt{3}f^{T+} & -\sqrt{2}f^T & -f^U \\ \sqrt{3}f^{T+} & 0 & f^{hh} & -f^S & f^R & 0 & -f^S/\sqrt{2} & \sqrt{2}f^R \\ -\sqrt{2}f^U & -f^{T+} & -f^{S+} & f^{lh} & 0 & f^R & -\sqrt{2}f^Q & \sqrt{3/2}f^S \\ f^T & -\sqrt{2}f^U & f^{R+} & 0 & f^{lh} & f^S & \sqrt{3/2}f^{S+} & \sqrt{2}f^Q \\ 0 & -\sqrt{3}f^T & 0 & f^{R+} & f^{S+} & f^{hh} & -\sqrt{2}f^{R+} & -f^{S+}/\sqrt{2} \\ f^U & -\sqrt{2}f^{T+} & -f^{S+}/\sqrt{2} & -\sqrt{2}f^{Q+} & \sqrt{3/2}f^S & -\sqrt{2}f^R & f^{so} & 0 \\ -\sqrt{2}f^T & -f^U & \sqrt{2}f^{R+} & \sqrt{3/2}f^{S+} & \sqrt{2}f^{Q+} & -f^S/\sqrt{2} & 0 & f^{so} \end{bmatrix} \quad (5.18)$$

5.2.3 10 × 10 Hamiltonian

For 10 bands, as it evaluates band structure for four compound material $In_xGa_{1-x}As_{1-y}N_y$, the interpolation formula for four compound material is used [74][66]:

$$\mathbf{Q} = \mathbf{Q}^{GaAs}(1-x)(1-y) + \mathbf{Q}^{InAs}x(1-y) + \mathbf{Q}^{GaN}y(1-x) + \mathbf{Q}^{GaN}xy \quad (5.19)$$

The material parameters for nitrogen band are estimated by:

$$\begin{aligned} E_N &= 1.65(1-x) + 1.44x - 0.38x(1-x) \\ V_{NC} &= 2.7(1-x) + 2x - 3.5x(1-x) \end{aligned} \quad (5.20)$$

or:

$$\begin{aligned} E_N &= 1.65 + 0.25x - 0.56x \\ V_{NC} &= 2.4(1-x) + 1.75x \end{aligned} \quad (5.21)$$

depending on the In concentrations.

5.2.4 14 × 14 Hamiltonian

For 14 band the interpolation formula is similar to 10 band and as some parameter of bismuth are unknown they are estimated by plots available in ref. [48] [75](band edges positions depends on Bi composition), [47](bandgap).

Chapter 6

Band structure calculations results

In this chapter our band structures results are shown and compared with published ones. The parameters used in calculations are listed in the tables [E.1](#) for Zincblende and [E.2](#) for Wurtzite semiconductors (parameters in published papers may vary).

6.1 Band structures for zincblende semiconductors

6.1.1 4×4 Hamiltonian

The calculations for 4×4 Hamiltonian are compared with the paper published by Xia [\[44\]](#)(the original Xia's results are presented here also for convenience). The band structure were calculated for unstrained and uniaxially strained $GaAs/Al_{0.2}Ga_{0.8}As$ QW with barrier $L_B = 50\text{\AA}$ and well $L_W = 100\text{\AA}$. The directions and orientations as well as stress are listed on the corresponding figures. Figures [6.1](#) and [6.3](#) represent the original Xia's results and figures [6.2](#) and [6.4](#) represent our work results. For convenience our results are presented with the same scales and the directions.

6.1.2 6×6 Hamiltonian

The calculations for 6×6 Hamiltonian are compared to the paper published by Seo et al. [\[45\]](#)(the original Seo's results are presented here also for convenience). The band

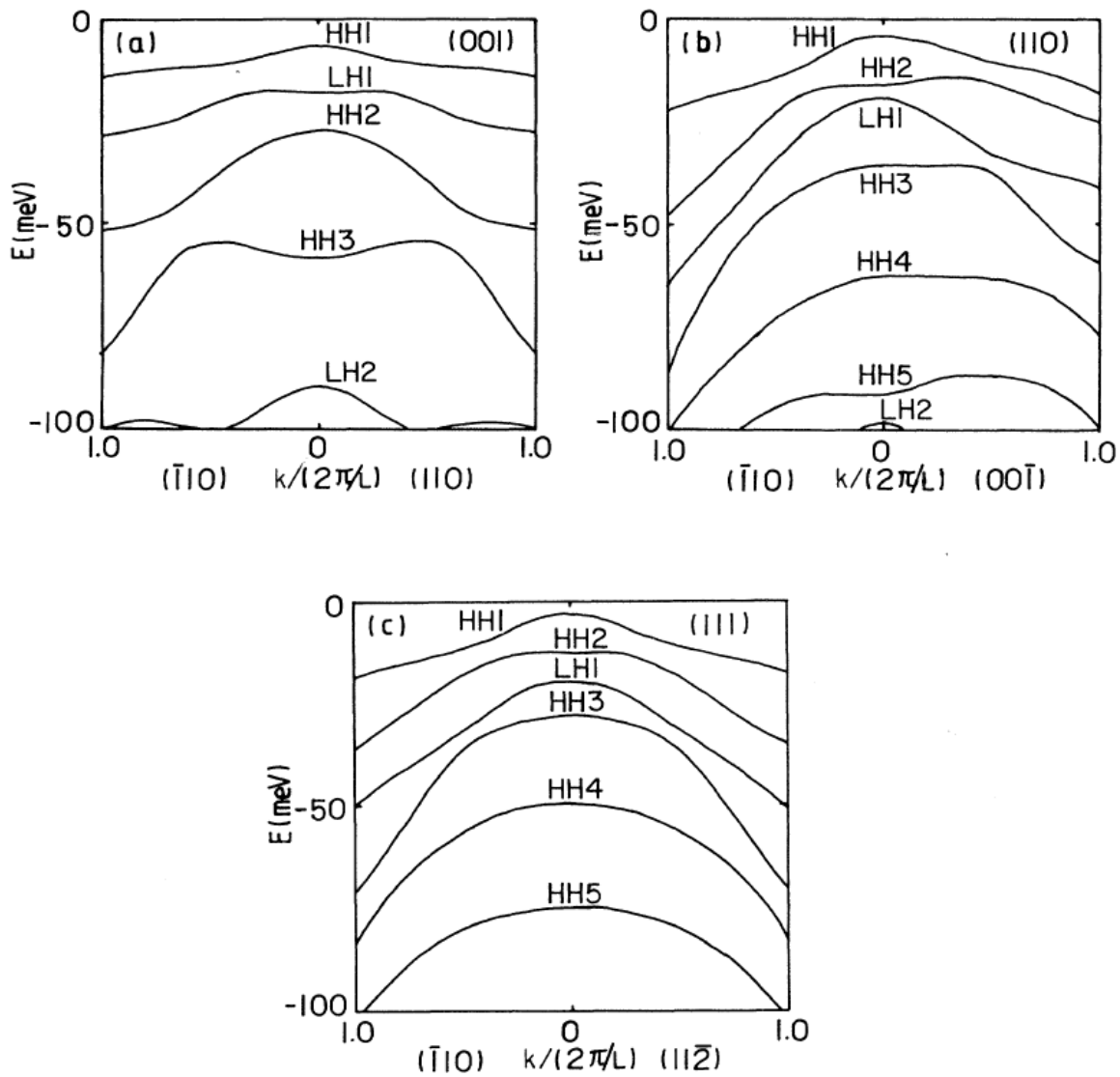


FIGURE 6.1: Hole subband for unstrained superlattices grown on (11N)-oriented substrates with (a) $N = \infty$, (b) $N = 0$, (c) $N = 1$. [44]

structure were determined for unstrained and uniaxially strained $In_{0.53}Ga_{0.47}As/InP$ QW with barrier $L_B = 50\text{\AA}$ ¹ and well $L_W = 60\text{\AA}$. The directions and orientations as well as stress are listed on the corresponding figures. Figure 6.5 and 6.7 represent the original Seo's results and figure 6.6 and 6.8 represent this work results. We present our results in the same scales and the directions as the compared paper for convenience.

¹In the original Seo [45] paper many of the parameters are not listed, so for comparing there were chosen arbitrary values.

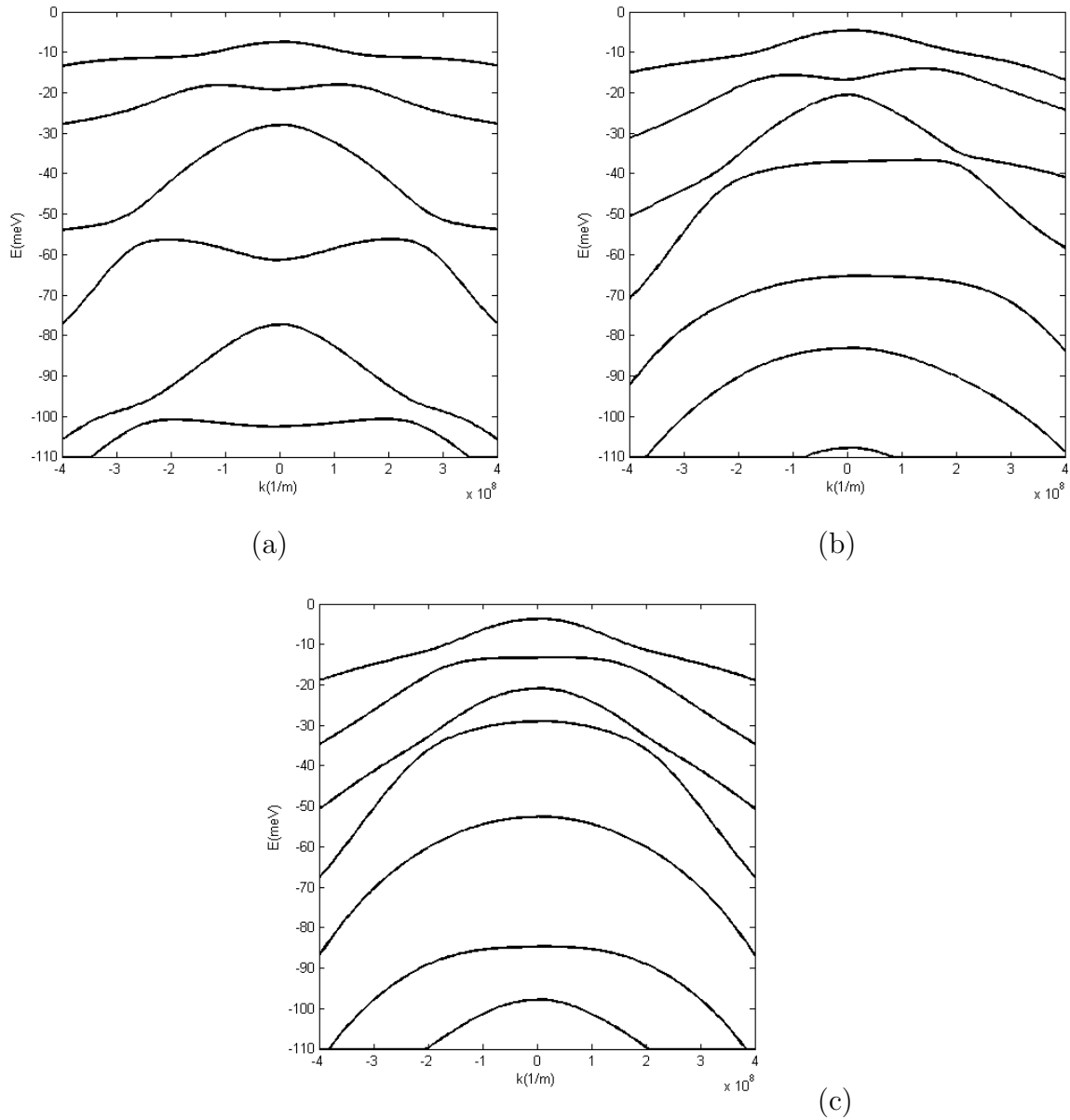


FIGURE 6.2: Hole subband for unstrained superlattices grown on (11N)-oriented substrates with (a) $N = \infty$, (b) $N = 0$, (c) $N = 1$. [this work]

6.1.3 8×8 Hamiltonian

It is difficult to compare band structures for non-(001) oriented QWs, calculated by 8×8 Hamiltonian, due to the fact that the sample results are not presented in the literature, but the standalone results are calculated for $Al_xGa_{1-x}As/In_xGa_{1-x}As$ with the compositions

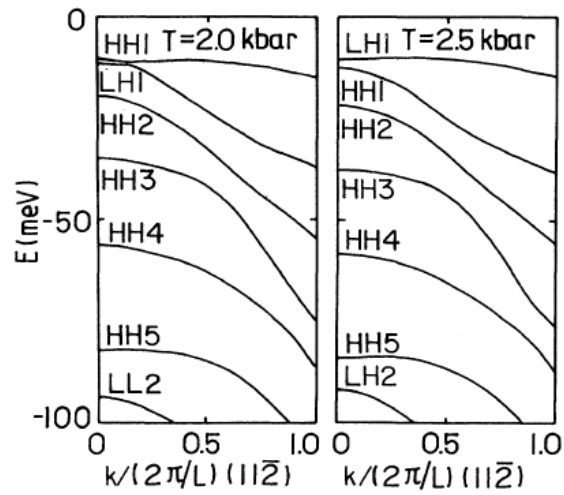


FIGURE 6.3: Hole subband for (111)-oriented superlattices under the uniaxial stresses $T = 2.0$ and 2.5 kbar. [44]

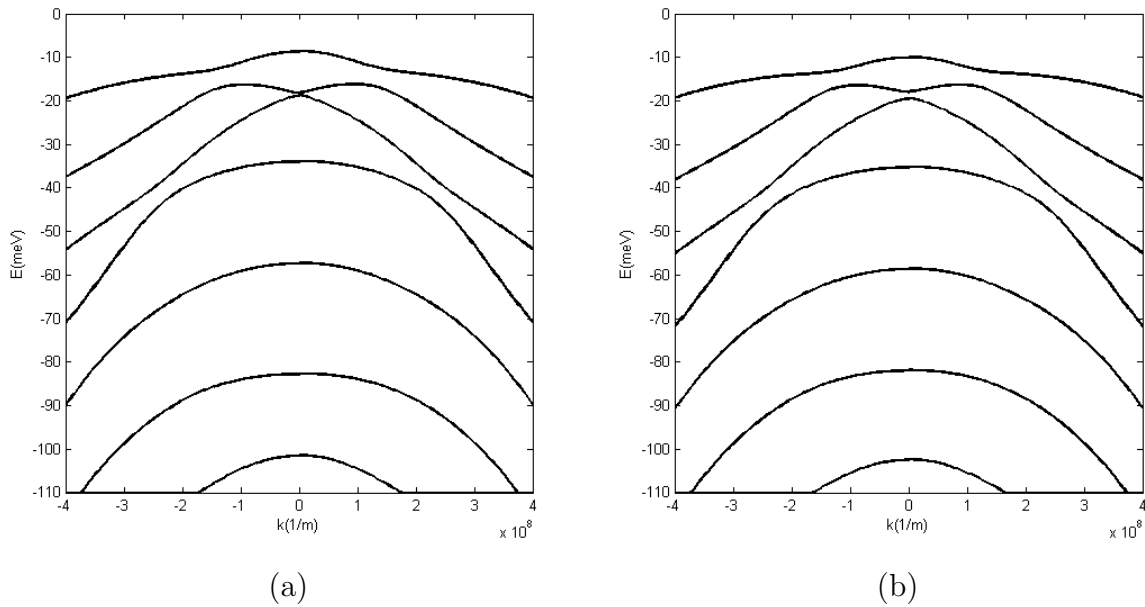


FIGURE 6.4: Hole subband for (111)-oriented superlattices under the uniaxial stresses (a) $T = 2.0$ and (b) 2.5 kbar.[this work]

of $x = 0.5$ for both compounds. The size of well and barriers are chosen to be $L_W = 100\text{\AA}$ and $L_B = 50\text{\AA}$. The final result is shown on Figure 6.9.

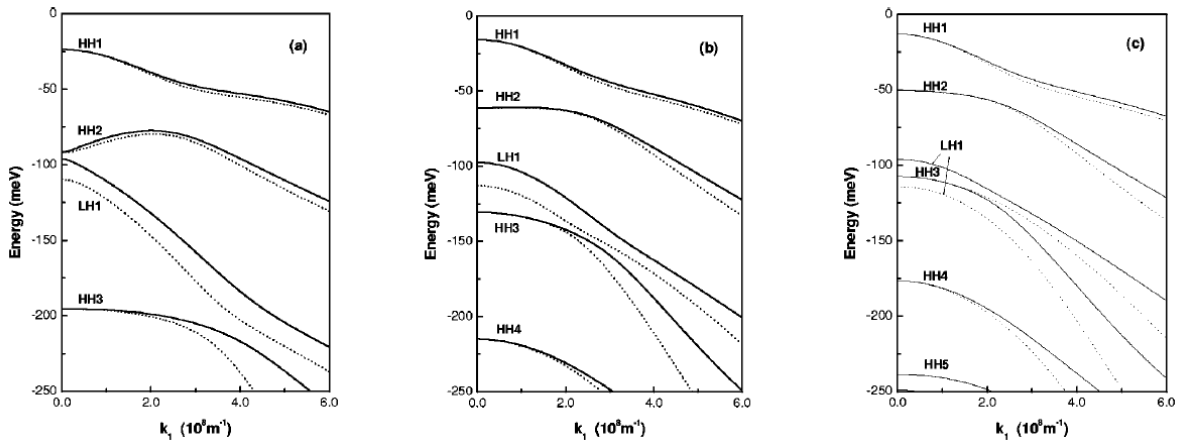


FIGURE 6.5: Hole subband for unstrained superlattices grown on (11N)-oriented substrates with (a) $N = \infty$, (b) $N = 0$, (c) $N = 1$. [45]

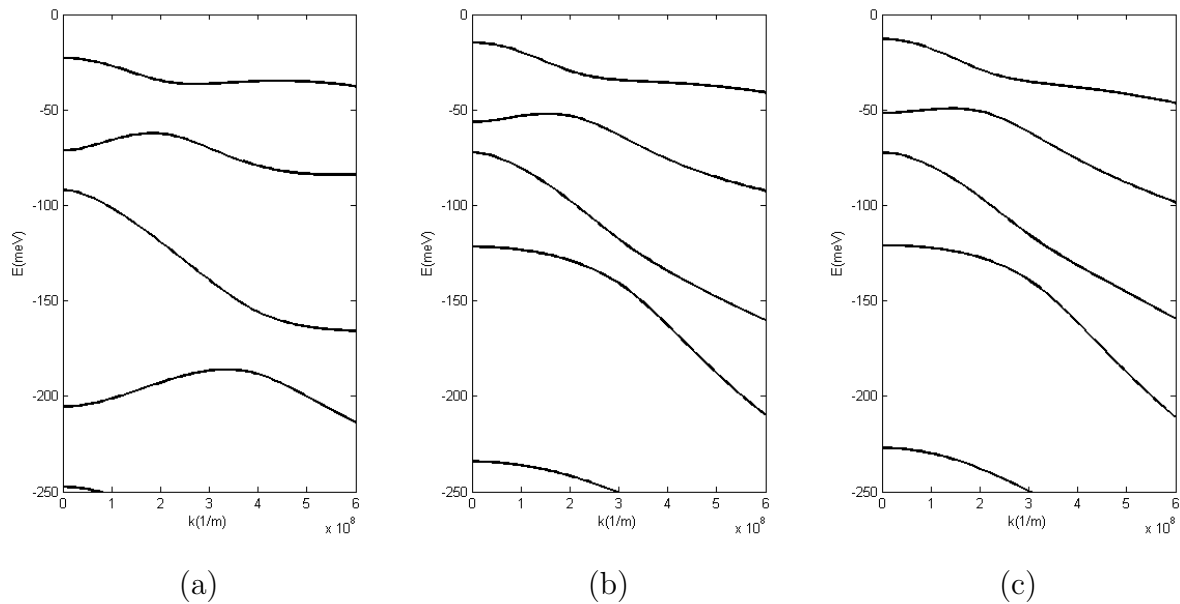


FIGURE 6.6: Hole subband for unstrained superlattices grown on (11N)-oriented substrates with (a) $N = \infty$, (b) $N = 0$, (c) $N = 1$. [this work]

6.1.4 10×10 Hamiltonian

The calculations for 10×10 Hamiltonian are compared to the paper published by Fan [46] (the original Fan's results presented here also for convenience). The band structure calculated for unstrained and uniaxially strained $In_{0.36}Ga_{0.64}As_{0.973}N_{0.027}/GaAs$ QW with barrier $L_B = 100 \text{\AA}$ and well $L_W = 70 \text{\AA}$. The directions and orientations are listed on the corresponding figures. Figure 6.10 represents the original Fan's results and figure 6.11

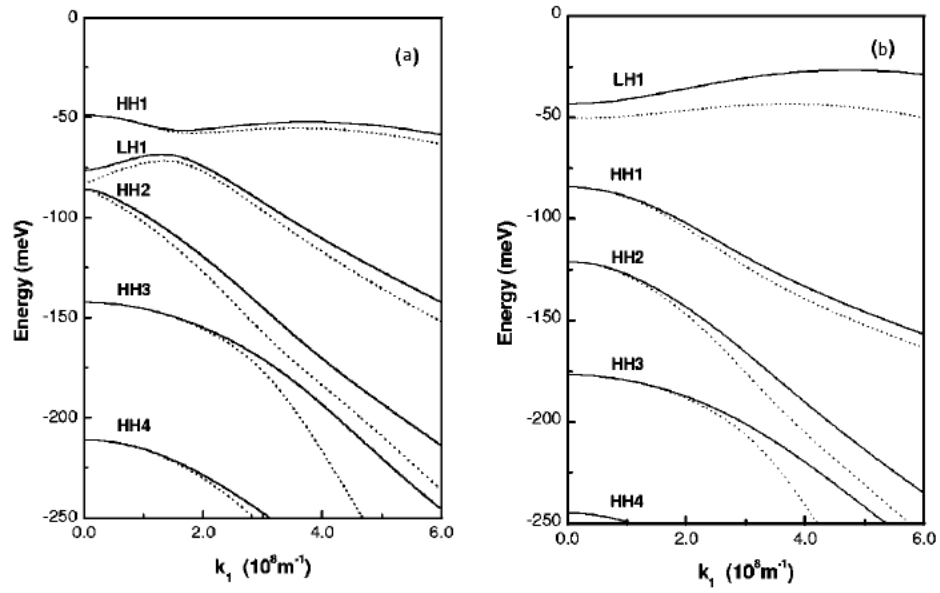


FIGURE 6.7: Hole subband for (111)-oriented superlattices under the uniaxial stresses (a) $T = 1.0 \cdot 10^9 \text{Pa}$ and (b) $T = 2.0 \cdot 10^9 \text{Pa}$. [45]

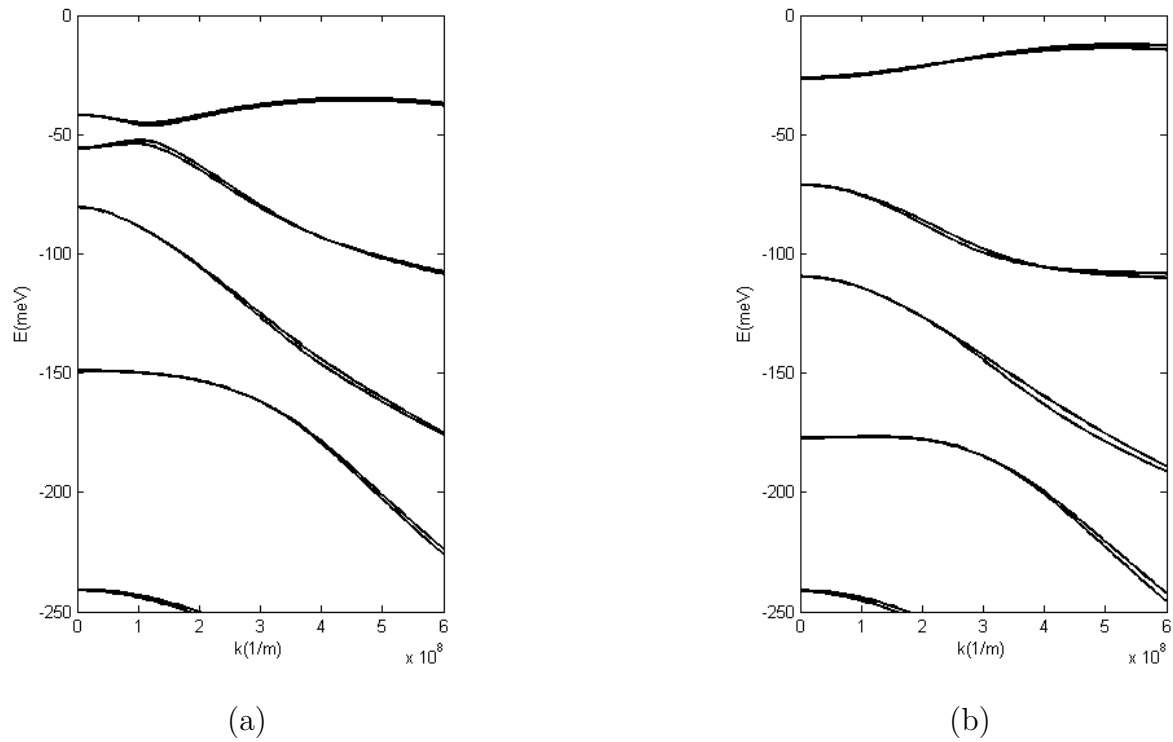


FIGURE 6.8: Hole subband for (111)-oriented superlattices under the uniaxial stresses (a) $T = 1.0 \cdot 10^9 \text{Pa}$ and (b) $T = 2.0 \cdot 10^9 \text{Pa}$. [this work]

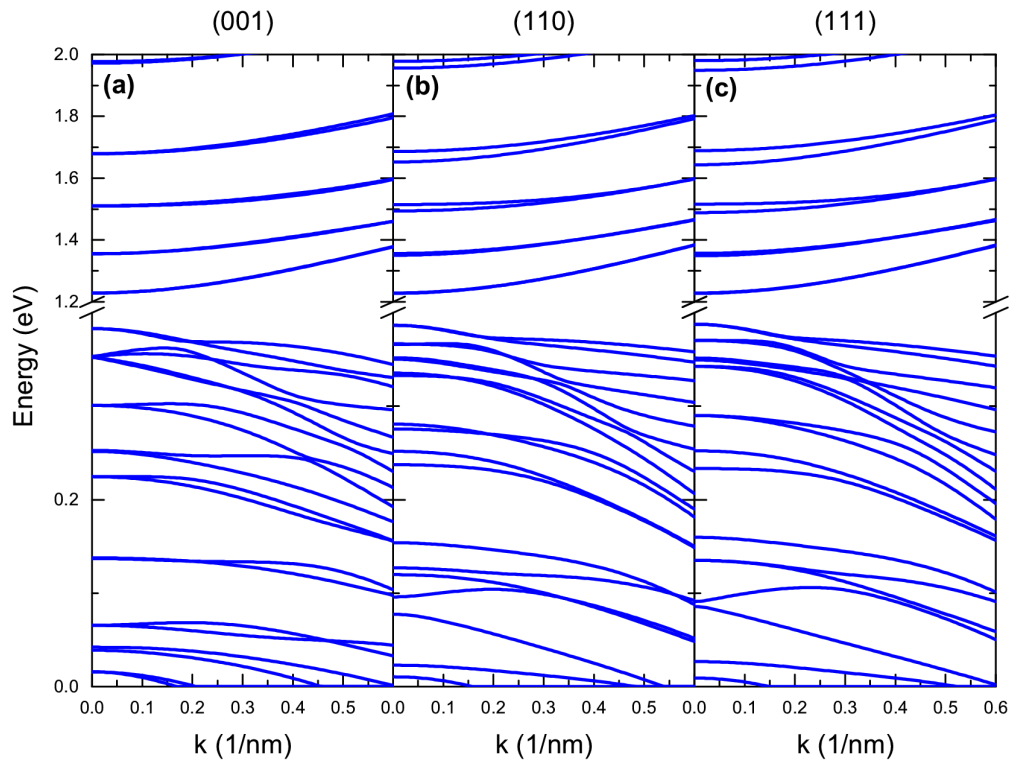


FIGURE 6.9: Band structure for unstrained AlGaAs/InGaAs QWs grown on (11N)-oriented substrates with (a) $N = \infty$, (b) $N = 0$, (c) $N = 1$.

represents this work results. This work results made in the same directions for convenience. We made another figure 6.12 with additional orientation for the same QW.

6.1.5 14×14 Hamiltonian

There is no reference to compare the band structure calculated by 14×14 Hamiltonian so the results are presented standalone. The materials are used GaAsBi/GaAs with 0.05 composition of Bi. The size of well and barriers are chosen to be $L_W = 100\text{\AA}$ and $L_B = 50\text{\AA}$. The final result shown on Figure 6.13.

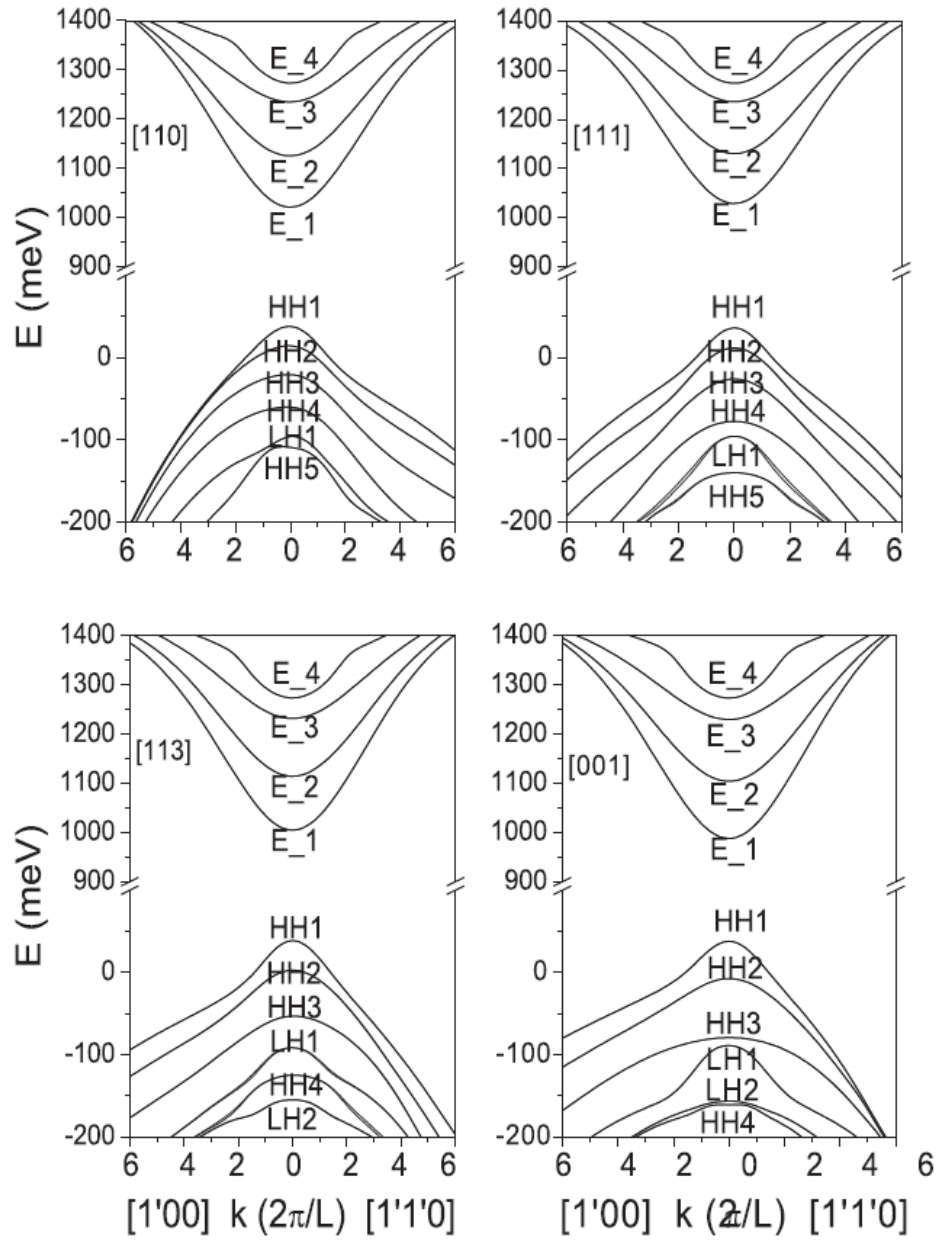


FIGURE 6.10: Electron and hole energy dispersion curves of the unstrained (110)-, (111)-, (113), and (001)-oriented QWs. [46]

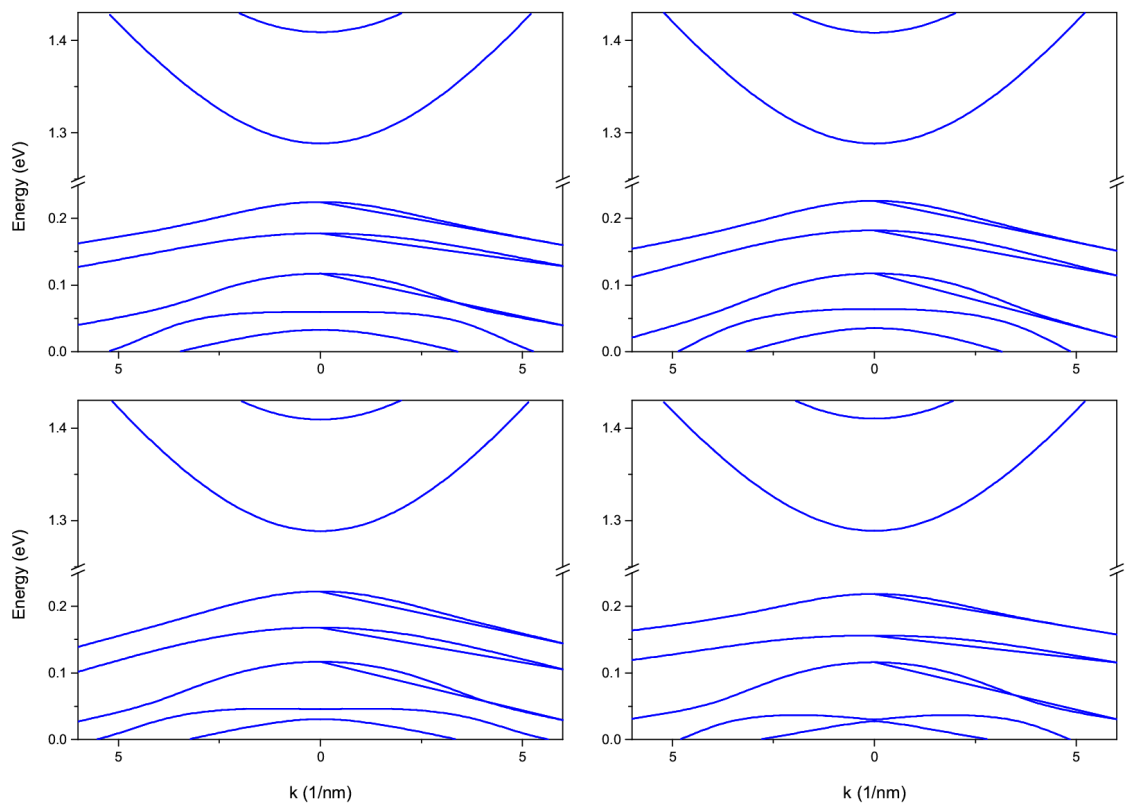


FIGURE 6.11: Band structure for unstrained InGaAsN/GaAs QWs grown on (a) (110)-, (b) (111)-, (c) (113), and (d) (001)-oriented QWs.[this work]

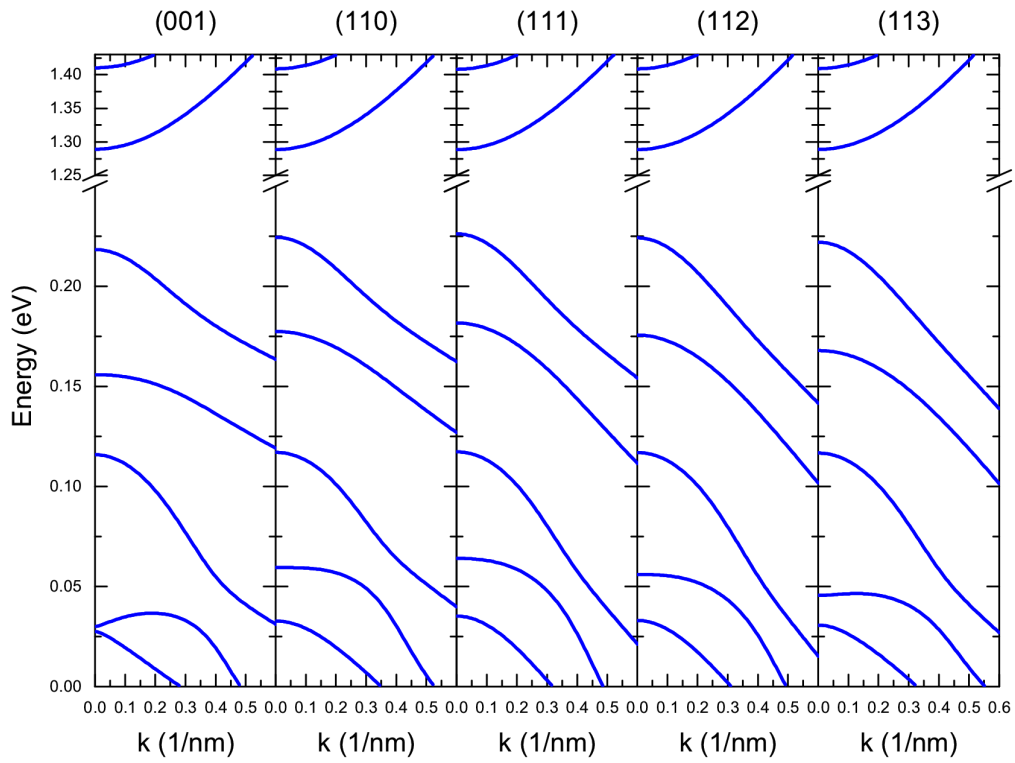


FIGURE 6.12: Band structure for unstrained InGaAsN/GaAs QWs grown on (a) (001)-, (b) (110)-, (c) (111), (d) (112), and (e) (113)-oriented QWs.[this work]

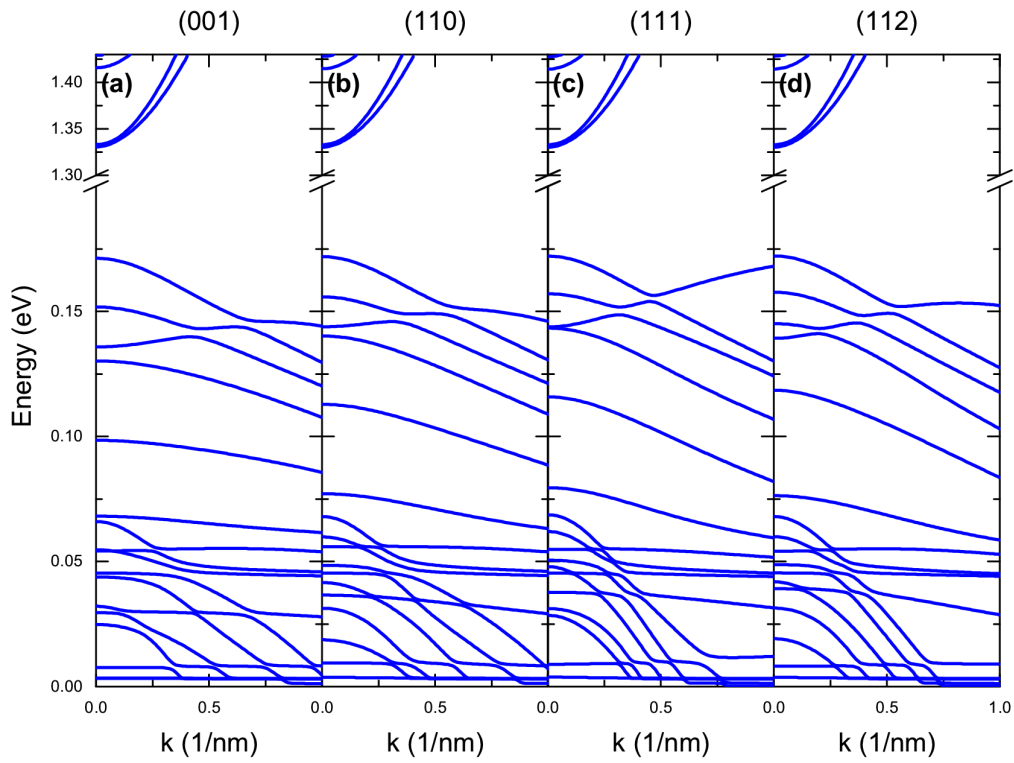


FIGURE 6.13: Band structure for unstrained GaAsBi/GaAs QWs grown on (11N)-oriented substrates with (a) $N = \infty$, (b) $N = 0$, (c) $N = 1$, (d) $N = 2$.

Chapter 7

Optical applications

7.1 Matrix elements in optical transitions

7.1.1 Wave functions

Matrix elements in optical transitions (or just optical) appear in the gain calculation. Optical transition rates strongly depend on the matrix elements. The matrix element of the momentum operator is evaluated between initial and final states. The states are given as wave functions which are the product of the envelope function and the cell periodic functions. Wave functions are expressed for each state in conduction band:

$$\Psi_{n\vec{k}_t}^{CB^\sigma}(\vec{r}) = \frac{e^{i\vec{k}_t \cdot \vec{\rho}}}{\sqrt{A}} f_n^{(CB)}(z) u_{CB}^\sigma(\vec{r}) \quad (7.1)$$

and in valence band for split-off:

$$\Psi_{n\vec{k}_t}^{SO^\sigma}(\vec{r}) = \frac{e^{i\vec{k}_t \cdot \vec{\rho}}}{\sqrt{A}} f_n^{(SO)}(z) u_{SO}^\sigma(\vec{r}) \quad (7.2)$$

and heavy/light hole (will be used below) subbands:

$$\Psi_{n\vec{k}_t}^{HL^\sigma}(\vec{r}) = \frac{e^{i\vec{k}_t \cdot \vec{\rho}}}{\sqrt{A}} \sum_{j=HH^\sigma, LH^\sigma} f_n^{(j)}(\vec{k}_t, z) u_j(\vec{r}) \quad (7.3)$$

where n - subband index, $\sigma = \pm$ - spin index, k_t - transverse (xy-plane) wave vector, which is forced to satisfy periodic boundary conditions over an area A , $\vec{\rho}$ - transverse (xy-plane) position vector. Here the heavy and light holes go together as they are strongly coupled near $\vec{k} = 0$.

If the Bloch functions are written in the following way:

$$\Psi_{n\vec{k}}(\vec{r}) = \frac{e^{i\vec{k}\cdot\vec{r}}}{\sqrt{\Omega}} u_{n\vec{k}}(\vec{r}) \quad (7.4)$$

then the properties of the cell periodic functions are defined by the following relation [55](p. 129):

$$\langle \Psi_{n\vec{k}} | \Psi_{n'\vec{k}'} \rangle = \frac{1}{\Omega} \int_{\Omega} d\vec{r} e^{-i(\vec{k}-\vec{k}')\cdot\vec{r}} u_{n\vec{k}}^*(\vec{r}) u_{n'\vec{k}'}(\vec{r}) = \delta_{nn'} \delta_{\vec{k}\vec{k}'} \quad (7.5)$$

Here the functions are required to be orthonormal when integrated over the full crystal volume $\Omega = L_x L_y L_z$ (L_i - is the length of the crystal in x , y and z directions). Eq. (7.5) is forcing cell periodic functions $u_{n\vec{k}}$ to satisfy a particular normalization. The cell periodic function $u_{n\vec{k}}$ is a periodic in the direct lattice vectors \vec{R} , therefore the following combination of u functions can be expanded as a Fourier series in vectors from the inverse lattice \vec{G} (more on that [76] chapter 5):

$$u_{n\vec{k}}^*(\vec{r}) u_{n'\vec{k}'}(\vec{r}) = \sum_{\vec{G}} e^{i\vec{G}\cdot\vec{r}} B_{\vec{G}}^{n\vec{k},n'\vec{k}'} \quad (7.6)$$

The cell periodic function has the same value in each real space unit cell with volume v_{cell} . The expansion coefficient $B_{\vec{G}}^{n\vec{k},n'\vec{k}'}$ is obtained using the generalized Fourier inversion relation:

$$B_{\vec{G}}^{n\vec{k},n'\vec{k}'} = \frac{1}{v_{cell}} \int_{v_{cell}} d\vec{r} e^{-i\vec{G}\cdot\vec{r}} u_{n\vec{k}}^*(\vec{r}) u_{n'\vec{k}'}(\vec{r}) \quad (7.7)$$

Substituting (7.6) into (7.5) gives:

$$\frac{1}{\Omega} \sum_{\vec{G}} B_{\vec{G}}^{n\vec{k},n'\vec{k}'} \int_{\Omega} d\vec{r} e^{-i(\vec{k}-\vec{k}'-\vec{G})\cdot\vec{r}} = \sum_{\vec{G}} B_{\vec{G}}^{n\vec{k},n'\vec{k}'} \delta_{\vec{k}-\vec{k}',\vec{G}} = \delta_{nn'} \delta_{\vec{k}\vec{k}'} \quad (7.8)$$

From here it is obvious that Kronecker delta $\delta_{\vec{k}-\vec{k}',\vec{G}}$ is non zero only if $\vec{k} - \vec{k}' = \vec{G}$, but both \vec{k} values are restricted to the first Brillouin zone, while \vec{G} is non zero outside the

zone¹, so the condition $\vec{k} - \vec{k}' = \vec{G}$ satisfied when $\vec{G} = 0$ which leads to $\vec{k} = \vec{k}'$, and the last equivalence reduces to:

$$B_0^{n\vec{k}, n'\vec{k}'} \delta_{\vec{k}\vec{k}'} = \delta_{nn'} \delta_{\vec{k}\vec{k}'} \quad (7.9)$$

The equation turns to zero when \vec{k} vectors are not equal, but for $\vec{k} = \vec{k}'$ one has:

$$\delta_{nn'} = B_0^{n\vec{k}, n'\vec{k}} = \frac{1}{v_{cell}} \int_{v_{cell}} d\vec{r} u_{n\vec{k}}^*(\vec{r}) u_{n'\vec{k}}(\vec{r}) \quad (7.10)$$

which is the normalization condition for cell periodic functions. So cell periodic functions $u_{n\vec{k}}$ are orthogonal if they belongs to the same \vec{k} and to different bands.

7.1.2 Optical momentum matrix element

Optical momentum matrix elements are directly involved in optical gain calculations and it is a very important parameter of control optical gain in QW (apart from carrier concentration etc.). Consider two single band states:

$$\Psi_1(\vec{r}) = F_\alpha^{(1)}(\vec{r}) u_\alpha(\vec{r}) \quad (7.11)$$

$$\Psi_2(\vec{r}) = F_\beta^{(2)}(\vec{r}) u_\beta(\vec{r}) \quad (7.12)$$

where Greek letters indicates bands which may be equal or different, and F_i ($i = \alpha, \beta$) are the envelope functions, defined in general form as:

$$F_i(\vec{r}) = \sum_{\vec{k} \in BZ} \frac{e^{i\vec{k} \cdot \vec{r}}}{\sqrt{\Omega}} a_i(\vec{k}) \quad (7.13)$$

where BZ means first Brillouin zone, Ω is the crystal volume, $a_i(\vec{k})$ are the solutions to effective mass equation written in momentum space. The momentum matrix element between these two states may be written as (using product rule):

$$\begin{aligned} \langle \Psi_1 | \vec{p} | \Psi_2 \rangle &= \langle F_\alpha^{(1)}(\vec{r}) u_\alpha(\vec{r}) | \vec{p} | F_\beta^{(2)}(\vec{r}) u_\beta(\vec{r}) \rangle \\ &= \langle F_\alpha^{(1)}(\vec{r}) | F_\beta^{(2)}(\vec{r}) \rangle \cdot \langle u_\alpha(\vec{r}) | \vec{p} | u_\beta(\vec{r}) \rangle + \langle F_\alpha^{(1)}(\vec{r}) | \vec{p} | F_\beta^{(2)}(\vec{r}) \rangle \cdot \langle u_\alpha(\vec{r}) | u_\beta(\vec{r}) \rangle \end{aligned}$$

¹By definition first Brillouin zone is the “volume” in inverse lattice space constructed by faces which are located on the equal distance from the particular inverse lattice site to the adjacent sites.

$$= \int_{\Omega} d\vec{r} F_{\alpha}^{(1)*}(\vec{r}) F_{\beta}^{(2)}(\vec{r}) [u_{\alpha}^*(\vec{r}) \vec{p} u_{\beta}(\vec{r})] + \int_{\Omega} d\vec{r} \left[F_{\alpha}^{(1)*}(\vec{r}) \vec{p} F_{\beta}^{(2)}(\vec{r}) \right] u_{\alpha}^*(\vec{r}) u_{\beta}(\vec{r}) \quad (7.14)$$

where $\vec{p} = \frac{\hbar}{i} \frac{\partial}{\partial \vec{r}}$. Here both cell periodic terms are periodic in the direct lattice vector \vec{R} , so they both can be expanded as a Fourier series in vectors of inverse lattice \vec{G} as in Eq. (7.6):

$$u_{\alpha}^*(\vec{r}) \vec{p} u_{\beta}(\vec{r}) = \sum_{\vec{G}} e^{i\vec{G}\cdot\vec{r}} D_{\vec{G}}^{\alpha\beta} \quad (7.15)$$

$$u_{\alpha}^*(\vec{r}) u_{\beta}(\vec{r}) = \sum_{\vec{G}} e^{i\vec{G}\cdot\vec{r}} B_{\vec{G}}^{\alpha\beta} \quad (7.16)$$

where the expansion coefficients $D_{\vec{G}}^{\alpha\beta}$ and $B_{\vec{G}}^{\alpha\beta}$ are defined using generalized Fourier expansion formulas as:

$$D_{\vec{G}}^{\alpha\beta} = \frac{1}{v_{\text{cell}}} \int_{v_{\text{cell}}} d\vec{r} e^{-i\vec{G}\cdot\vec{r}} u_{\alpha}^*(\vec{r}) \vec{p} u_{\beta}(\vec{r}) \quad (7.17)$$

$$B_{\vec{G}}^{\alpha\beta} = \frac{1}{v_{\text{cell}}} \int_{v_{\text{cell}}} d\vec{r} e^{-i\vec{G}\cdot\vec{r}} u_{\alpha}^*(\vec{r}) u_{\beta}(\vec{r}) \quad (7.18)$$

where v_{cell} is the volume of real-space unit cell. The same expansions can be done for $F_{\alpha}^{(1)}$ and $F_{\beta}^{(2)}$:

$$F_{\alpha}^{(1)}(\vec{r}) = \sum_{\vec{k} \in BZ} \frac{e^{i\vec{k}\cdot\vec{r}}}{\sqrt{\Omega}} a_{\alpha}(\vec{k}) \quad (7.19)$$

$$F_{\beta}^{(2)}(\vec{r}) = \sum_{\vec{k} \in BZ} \frac{e^{i\vec{k}\cdot\vec{r}}}{\sqrt{\Omega}} b_{\beta}(\vec{k}) \quad (7.20)$$

Now the (7.14) may be rewritten by inserting (7.15), (7.16), (7.19) and (7.20) into it (also the replacement $\vec{p} = \hbar \vec{k}$ is made):

$$\begin{aligned} \langle \Psi_1 | \vec{p} | \Psi_2 \rangle &= \left[\sum_{\vec{k} \in BZ} a_{\alpha}^*(\vec{k}) b_{\beta}(\vec{k}) \right] \times \frac{1}{v_{\text{cell}}} \int_{v_{\text{cell}}} d\vec{r} u_{\alpha}^*(\vec{r}) \vec{p} u_{\beta}(\vec{r}) \quad (7.21) \\ &+ \left[\sum_{\vec{k} \in BZ} a_{\alpha}^*(\vec{k}) \hbar \vec{k} b_{\beta}(\vec{k}) \right] \times \frac{1}{v_{\text{cell}}} \int_{v_{\text{cell}}} d\vec{r} u_{\alpha}^*(\vec{r}) u_{\beta}(\vec{r}) \end{aligned}$$

where the exponent term integrates to 1 due to the following relation (Parseval's Theorem²):

$$\int_{\Omega} d\vec{r} F_{\alpha}^{(1)*}(\vec{r}) F_{\beta}^{(2)}(\vec{r}) = \sum_{\vec{k}, \vec{k}' \in BZ} a_{\alpha}^*(\vec{k}) b_{\beta}(\vec{k}') \times \frac{1}{\Omega} \int_{\Omega} d\vec{r} e^{-i(\vec{k}-\vec{k}') \cdot \vec{r}} = \sum_{\vec{k} \in BZ} a_{\alpha}^*(\vec{k}) b_{\beta}(\vec{k}) \quad (7.22)$$

where the integral of exponent gives a Kronecker delta $\delta_{\vec{k}\vec{k}'}$ according to (7.5) which is consistent with “vertical” transitions statement. The (7.22) leads to the normalizations of the envelopes (using eq. (7.19)):

$$\begin{aligned} \int_{\Omega} d\vec{r} |\Psi(\vec{r})|^2 &= \sum_{jj' \in A} \sum_{\vec{k}, \vec{k}' \in BZ} a_j^*(\vec{k}) a_{j'}(\vec{k}') \times \frac{1}{\Omega} \int_{\Omega} d\vec{r} e^{-i(\vec{k}-\vec{k}') \cdot \vec{r}} u_j^*(\vec{k}) u_{j'}(\vec{k}') \\ &= \sum_{j \in A} \sum_{\vec{k} \in BZ} |a_j(\vec{k})|^2 = \sum_{j \in A} \int_{\Omega} d\vec{r} |F_j(\vec{r})|^2 \end{aligned} \quad (7.23)$$

From quantum mechanics it is known that the wave function represents probability distribution, thus the integral of $|\Psi|^2$ over the entire space should be equal to 1, which leads to normalization condition:

$$\sum_{j \in A} \int_{\Omega} d\vec{r} |F_j(\vec{r})|^2 = 1 \quad (7.24)$$

where A is the “class A” states which are the states of interest used in Löwdin's perturbation method application. Cell periodic functions u both correspond to $\vec{k} = 0$ so (7.10) may be inserted into (7.21) and keeping in mind (7.22) gives:

$$\langle \Psi_1 | \vec{p} | \Psi_2 \rangle = \left[\int_{\Omega} d\vec{r} F_{\alpha}^{(1)*}(\vec{r}) \vec{p} F_{\beta}^{(2)}(\vec{r}) \right] \delta_{\alpha\beta} + \left[\int_{\Omega} d\vec{r} F_{\alpha}^{(1)*}(\vec{r}) F_{\beta}^{(2)}(\vec{r}) \right] \times \langle u_{\alpha} | \vec{p} | u_{\beta} \rangle \quad (7.25)$$

where:

$$\frac{1}{v_{cell}} \int_{v_{cell}} d\vec{r} u_{\alpha}^*(\vec{r}) \vec{p} u_{\beta}(\vec{r}) = \langle u_{\alpha} | \vec{p} | u_{\beta} \rangle \quad (7.26)$$

In the equation (7.25) only one term is non zero. If $\alpha \neq \beta$ then the first term is zero. If $\alpha = \beta$ then the second term is zero because matrix element of \vec{p} between equal u functions vanish.

²Parseval's Theorem claims that Fourier transform is unitary, in other words the sum or integral of the square of a function is equal to the sum or integral of the square of its transform.

7.1.3 Application of the optical momentum matrix element

Consider matrix element between conduction and split-off subband using the definitions of wave functions (7.1) and (7.2):

$$\left\langle \Psi_{n\vec{k}_t}^{SO\sigma} \left| \vec{p} \right| \Psi_{n'\vec{k}'_t}^{CB\sigma'} \right\rangle = \frac{1}{A} \int d\vec{\rho} e^{-i(\vec{k}_t - \vec{k}'_t) \cdot \vec{\rho}} \int dz f_n^{(SO)*}(z) f_{n'}^{(CB)}(z) \cdot \left\langle u_{SO}^\sigma \left| \vec{p} \right| u_{CB}^{\sigma'} \right\rangle \quad (7.27)$$

The first integral evaluates to Kronecker delta $\delta_{\vec{k}_t \vec{k}'_t}$ due to the orthonormality of the plane waves over the area A , which restricts the system to transverse momentum conserving transitions, \vec{p} - transverse position vector. It means that transition occurs only if initial and final \vec{k}_t vectors are equal to each other, in other words the transition may be called “vertical” since it occur “vertically” in \vec{k} -space. The second integral may be rewritten in “bra-ket” notation:

$$\int dz f_n^{(SO)*}(z) f_{n'}^{(CB)}(z) \equiv \langle f_n^{SO} | f_{n'}^{CB} \rangle \quad (7.28)$$

Substitution of (7.28) and Kronecker delta back into (7.27) gives:

$$\left\langle \Psi_{n\vec{k}_t}^{SO\sigma} \left| \vec{p} \right| \Psi_{n'\vec{k}'_t}^{CB\sigma'} \right\rangle = \delta_{\vec{k}_t \vec{k}'_t} \langle f_n^{SO} | f_{n'}^{CB} \rangle \left\langle u_{SO}^\sigma \left| \vec{p} \right| u_{CB}^{\sigma'} \right\rangle \quad (7.29)$$

For heavy and light hole subband levels the same relation (transition between heavy/light (HL) hole and conduction subband levels) may be obtained:

$$\left\langle \Psi_{n\vec{k}_t}^{HL\sigma} \left| \vec{p} \right| \Psi_{n'\vec{k}'_t}^{CB\sigma'} \right\rangle = \delta_{\vec{k}_t \vec{k}'_t} \sum_{j=HH^\sigma, LH^\sigma} \left\langle f_{n\vec{k}_t}^j \left| f_{n'}^{CB} \right\rangle \left\langle u_j \left| \vec{p} \right| u_{CB}^{\sigma'} \right\rangle \quad (7.30)$$

For the sum part the short notation may be introduced:

$$\sum_{j=HH^\sigma, LH^\sigma} \left\langle f_{n\vec{k}_t}^j \left| f_{n'}^{CB} \right\rangle \left\langle u_j \left| \vec{p} \right| u_{CB}^{\sigma'} \right\rangle \equiv \vec{P}_{nn'}^{\sigma\sigma'}(\vec{k}_t) \quad (7.31)$$

It is obvious that the optical matrix elements strongly dependent on the momentum matrix elements $\langle u_j | \vec{p} | u_{j'} \rangle$ between the zone-center cell-periodic, i.e. basis functions for the conduction and valence subbands. These matrix elements contain a non-zero term (introduced earlier in discussions of Kane’s model):

$$\langle S | p_x | X \rangle = i \frac{m_0}{\hbar} P_0 \hat{\mathbf{x}} = \frac{m_0}{\hbar} P_x \quad \langle S | p_y | Y \rangle = i \frac{m_0}{\hbar} P_0 \hat{\mathbf{y}} \quad \langle S | p_z | Z \rangle = i \frac{m_0}{\hbar} P_0 \hat{\mathbf{z}} \quad (7.32)$$

where $\hat{\mathbf{x}}$ represent a unit vector along x axis.

7.1.4 Expressions for matrix elements $\mathbf{M}_{c-hh, lh, so}$

The more important is the squared absolute value of the matrix element $\langle u_j | \vec{p} | u_{j'} \rangle$ as it is involved directly in gain calculations. Usually \vec{k} is chosen to be parallel with the spin (along z axis), but since there is no preferred spin direction we must average over the spin. As soon as the matrix element will be averaged over the solid angle for bulk semiconductor and over the x - y plane for quantum wells, the \vec{k} should be expressed in general coordinates:

$$\vec{k} = k \sin \theta \cos \phi \hat{\mathbf{x}} + k \sin \theta \sin \phi \hat{\mathbf{y}} + k \cos \theta \hat{\mathbf{z}} \quad (7.33)$$

Then the cell periodic functions u_j (3.7) should also be expressed in arbitrary coordinates in terms of spherical harmonics:

$$\begin{aligned} |S'\rangle &= |S\rangle \\ |X'\rangle &= |\cos \theta \cos \phi X + \cos \theta \sin \phi Y - \sin \theta Z\rangle \\ |Y'\rangle &= |-\sin \phi X + \cos \phi Y\rangle \\ |Z'\rangle &= |\sin \theta \cos \phi X + \sin \theta \sin \phi Y + \cos \theta Z\rangle \end{aligned} \quad (7.34)$$

In order to perform the average, the matrix elements \mathbf{M}_{c-v} ($v = hh, lh, so$) are necessary:

$$\mathbf{M}_{c-v} = \langle u_c | \vec{p} | u_v \rangle = \hat{\mathbf{x}} \left\langle u_c \left| \frac{\hbar}{i} \frac{\partial}{\partial x} \right| u_v \right\rangle + \hat{\mathbf{y}} \left\langle u_c \left| \frac{\hbar}{i} \frac{\partial}{\partial y} \right| u_v \right\rangle + \hat{\mathbf{z}} \left\langle u_c \left| \frac{\hbar}{i} \frac{\partial}{\partial z} \right| u_v \right\rangle \quad (7.35)$$

where \mathbf{M}_{c-v} includes transitions with both spin orientations. The expressions for all possible transitions are as follows (terms with opposite spins³ are zero):

Heavy holes:

$$\begin{aligned} \left\langle iS \uparrow \left| \vec{p} \right| \frac{3}{2}, \frac{3}{2} \right\rangle' &= -\frac{1}{\sqrt{2}} [\langle iS \uparrow | p_x | X \uparrow \rangle (\cos \theta \cos \phi - i \sin \phi) \\ &+ \langle iS \uparrow | p_y | Y \uparrow \rangle (\cos \theta \sin \phi + i \cos \phi) - \langle iS \uparrow | p_z | Z \uparrow \rangle \sin \theta] \end{aligned}$$

³Spin terms \uparrow and \downarrow are not necessary to consider explicitly, so the spins are provided in implicit form.

$$= -\frac{P_x}{\sqrt{2}} [(\cos \theta \cos \phi - i \sin \phi) \hat{\mathbf{x}} + (\cos \theta \sin \phi + i \cos \phi) \hat{\mathbf{y}} - \sin \theta \hat{\mathbf{z}}] \quad (7.36)$$

$$\begin{aligned} \left\langle iS \downarrow' \left| \vec{p} \right| \frac{3}{2}, -\frac{3}{2} \right\rangle' &= \frac{1}{\sqrt{2}} [\langle iS \downarrow' | p_x | X \downarrow' \rangle (\cos \theta \cos \phi + i \sin \phi) \\ &+ \langle iS \downarrow' | p_y | Y \downarrow' \rangle (\cos \theta \sin \phi - i \cos \phi) - \langle iS \downarrow' | p_z | Z \downarrow' \rangle \sin \theta] \\ &= \frac{P_x}{\sqrt{2}} [(\cos \theta \cos \phi + i \sin \phi) \hat{\mathbf{x}} + (\cos \theta \sin \phi - i \cos \phi) \hat{\mathbf{y}} - \sin \theta \hat{\mathbf{z}}] \end{aligned} \quad (7.37)$$

$$\left\langle iS \downarrow' \left| \vec{p} \right| \frac{3}{2}, \frac{3}{2} \right\rangle' = 0 \quad (7.38)$$

$$\left\langle iS \uparrow' \left| \vec{p} \right| \frac{3}{2}, -\frac{3}{2} \right\rangle' = 0 \quad (7.39)$$

Light holes:

$$\left\langle iS \uparrow' \left| \vec{p} \right| \frac{3}{2}, \frac{1}{2} \right\rangle' = P_x \sqrt{\frac{2}{3}} (\sin \theta \cos \phi \hat{\mathbf{x}} + \sin \theta \sin \phi \hat{\mathbf{y}} + \cos \theta \hat{\mathbf{z}}) \quad (7.40)$$

$$\left\langle iS \downarrow' \left| \vec{p} \right| \frac{3}{2}, -\frac{1}{2} \right\rangle' = P_x \sqrt{\frac{2}{3}} (\sin \theta \cos \phi \hat{\mathbf{x}} + \sin \theta \sin \phi \hat{\mathbf{y}} + \cos \theta \hat{\mathbf{z}}) \quad (7.41)$$

$$\left\langle iS \downarrow' \left| \vec{p} \right| \frac{3}{2}, \frac{1}{2} \right\rangle' = -\frac{P_x}{\sqrt{6}} [(\cos \theta \cos \phi - i \sin \phi) \hat{\mathbf{x}} + (\cos \theta \sin \phi + i \cos \phi) \hat{\mathbf{y}} - \sin \theta \hat{\mathbf{z}}] \quad (7.42)$$

$$\left\langle iS \uparrow' \left| \vec{p} \right| \frac{3}{2}, -\frac{1}{2} \right\rangle' = \frac{P_x}{\sqrt{6}} [(\cos \theta \cos \phi + i \sin \phi) \hat{\mathbf{x}} + (\cos \theta \sin \phi - i \cos \phi) \hat{\mathbf{y}} - \sin \theta \hat{\mathbf{z}}] \quad (7.43)$$

Spin-orbit split-off:

$$\left\langle iS \uparrow' \left| \vec{p} \right| \frac{1}{2}, \frac{1}{2} \right\rangle' = \frac{P_x}{\sqrt{3}} (\sin \theta \cos \phi \hat{\mathbf{x}} + \sin \theta \sin \phi \hat{\mathbf{y}} + \cos \theta \hat{\mathbf{z}}) \quad (7.44)$$

$$\left\langle iS \downarrow' \left| \vec{p} \right| \frac{1}{2}, -\frac{1}{2} \right\rangle' = -\frac{P_x}{\sqrt{3}} (\sin \theta \cos \phi \hat{\mathbf{x}} + \sin \theta \sin \phi \hat{\mathbf{y}} + \cos \theta \hat{\mathbf{z}}) \quad (7.45)$$

$$\left\langle iS \downarrow' \left| \vec{p} \right| \frac{1}{2}, \frac{1}{2} \right\rangle' = \frac{P_x}{\sqrt{3}} [(\cos \theta \cos \phi - i \sin \phi) \hat{\mathbf{x}} + (\cos \theta \sin \phi + i \cos \phi) \hat{\mathbf{y}} - \sin \theta \hat{\mathbf{z}}] \quad (7.46)$$

$$\left\langle iS \uparrow' \left| \vec{p} \right| \frac{1}{2}, -\frac{1}{2} \right\rangle' = \frac{P_x}{\sqrt{3}} [(\cos \theta \cos \phi + i \sin \phi) \hat{\mathbf{x}} + (\cos \theta \sin \phi - i \cos \phi) \hat{\mathbf{y}} - \sin \theta \hat{\mathbf{z}}] \quad (7.47)$$

7.1.5 Cell periodic functions part for bulk semiconductor

To be involved in gain calculations the above matrix elements should be averaged over the spin as there is no way to determine the spin of particular state. For bulk semiconductor the average over spin is performed with respect to solid angle $d\Omega$ which in spherical coordinates includes the Jacobian $d\Omega = dx dy dz = \sin\theta d\theta d\phi$ ⁴. For example, for TE polarization (where $\hat{\mathbf{e}} = \hat{\mathbf{x}}$), due to transition from the conduction band $|iS\rangle$ to heavy hole bands $|u'_1\rangle$ and $|u'_4\rangle$ the average over the spin (spin direction defined by angles) is performed using the formula:

$$|\hat{\mathbf{x}} \cdot \mathbf{M}_{c-hh}|^2 = \left| \left\langle iS \uparrow \left| p_x \left| \frac{3}{2}, \frac{3}{2} \right\rangle \right\rangle \right|^2 + \left| \left\langle iS \uparrow \left| p_x \left| \frac{3}{2}, -\frac{3}{2} \right\rangle \right\rangle \right|^2 \quad (7.48)$$

where due to spin orientation (u_1 and u_4 have opposite spins) only one of the two transitions is non zero. The average over the solid angle is the following:

$$\langle |\hat{\mathbf{x}} \cdot \langle u_c | \vec{p} | u_{hh} \rangle|^2 \rangle = \frac{1}{4\pi} \int_{\theta=0}^{\pi} \int_{\phi=0}^{2\pi} |\hat{\mathbf{x}} \cdot \mathbf{M}_{c-hh}|^2 \sin\theta d\theta d\phi \quad (7.49)$$

Consider squared absolute value first⁵:

$$\begin{aligned} |\hat{\mathbf{x}} \cdot \mathbf{M}_{c-hh}|^2 &= \hat{\mathbf{x}} \cdot \mathbf{M}_{c-hh}^* \cdot \hat{\mathbf{x}} \cdot \mathbf{M}_{c-hh} = \left[-\frac{P_x}{\sqrt{2}} (\cos\theta \cos\phi + i \sin\phi) \right] \cdot \left[-\frac{P_x}{\sqrt{2}} (\cos\theta \cos\phi - i \sin\phi) \right] \\ &= \frac{P_x^2}{2} (\cos^2\theta \cos^2\phi - i \cos\theta \cos\phi \sin\phi + i \cos\theta \cos\phi \sin\phi + \sin^2\phi) \\ &= \frac{P_x^2}{2} (\cos^2\theta \cos^2\phi + \sin^2\phi) \end{aligned} \quad (7.50)$$

Substitute this back into (7.49) and obtain:

$$\frac{1}{4\pi} \int_0^{\pi} \sin\theta d\theta \int_0^{2\pi} d\phi (\cos^2\theta \cos^2\phi + \sin^2\phi) \frac{P_x^2}{2} \quad (7.51)$$

⁴By definition of spherical coordinates $dx dy dz = r^2 \sin\theta dr d\theta d\phi$, but the expressions does not depend on r so the integration over r is dropped.

⁵ $\hat{\mathbf{x}}$ is a unit vector and multiplied by $\hat{\mathbf{x}}$ gives 1, multiplied by $\hat{\mathbf{y}}$ or $\hat{\mathbf{z}}$ gives 0.

The goal is the evaluate definite double integral. Consider integral of ϕ first:

$$\int_0^{2\pi} (\cos^2 \theta \cos^2 \phi + \sin^2 \phi) d\phi = \cos^2 \theta \int_0^{2\pi} \cos^2 \phi d\phi + \int_0^{2\pi} \sin^2 \phi d\phi \quad (7.52)$$

Integrals above easily obtained:

$$\int_0^{2\pi} \cos^2 \phi d\phi = \frac{1}{2} \int_0^{2\pi} (1 + \cos 2\phi) d\phi = \frac{1}{2} \int_0^{2\pi} (1 + \cos 2\phi) \frac{d(2\phi)}{2} = \frac{1}{4} (2\phi + \sin 2\phi) \Big|_0^{2\pi} = \pi \quad (7.53)$$

$$\int_0^{2\pi} \sin^2 \phi d\phi = \frac{1}{2} \int_0^{2\pi} (1 - \cos 2\phi) d\phi = \frac{1}{2} \int_0^{2\pi} (1 - \cos 2\phi) \frac{d(2\phi)}{2} = \frac{1}{4} (2\phi - \sin 2\phi) \Big|_0^{2\pi} = \pi \quad (7.54)$$

Then (7.51) converts to:

$$\frac{1}{4\pi} \frac{P_x^2}{2} \int_0^\pi \sin \theta (\cos^2 \theta + 1) \pi d\theta = \frac{P_x^2}{8} \int_0^\pi \sin \theta \cos^2 \theta d\theta + \int_0^\pi \sin \theta d\theta \quad (7.55)$$

where the integrals are (substitution $u = \cos \theta \Rightarrow du = -\sin \theta d\theta$):

$$\int_0^\pi \sin \theta \cos^2 \theta d\theta = - \int_0^\pi u^2 du = -\frac{u^3}{3} \Big|_0^\pi = -\frac{\cos^3 \theta}{3} \Big|_0^\pi = \frac{2}{3} \quad (7.56)$$

$$\int_0^\pi \sin \theta d\theta = -\cos \theta \Big|_0^\pi = 2 \quad (7.57)$$

Then the result for the matrix element is:

$$\langle |\hat{\mathbf{e}} \cdot \langle u_c | \vec{p} | u_{hh} \rangle|^2 \rangle = \frac{P_x^2}{8} \left(2 + \frac{2}{3} \right) = \frac{P_x^2}{8} \frac{8}{3} = \frac{1}{3} P_x^2 \equiv M_b^2 \quad (7.58)$$

where M_b is the **bulk Momentum** matrix element. It is may be expressed trough the Kane's experimental energy parameter:

$$E_p = \frac{2m_0}{\hbar^2} P_0^2 \quad (7.59)$$

$$M_b^2 = \frac{m_0}{6} E_p \quad (7.60)$$

The result is going to be the same for the other spin in conduction band as well as if polarization would be $\hat{\mathbf{e}} = \hat{\mathbf{y}}$ or $\hat{\mathbf{z}}$ the result will still be the same due to fact that bulk crystal is isotropic (i.e. the direction is doesn't matter). In gain calculations factor of 2 is added to include both spin orientations.

7.1.6 Cell periodic functions part for quantum well

For quantum wells the cavity direction is perpendicular to x - y plane, so the matrix elements are polarization dependent and averaged over the angle ϕ (spin direction here is defined by angle ϕ only), which lies on the x - y plane [77].

For TE polarization ($\hat{\mathbf{e}} = \hat{\mathbf{x}}$):

$$\langle |\hat{\mathbf{x}} \cdot \mathbf{M}_{c-hh}|^2 \rangle = \frac{1}{2\pi} \int_0^{2\pi} |\hat{\mathbf{x}} \cdot \mathbf{M}_{c-hh}|^2 d\phi \quad (7.61)$$

The integral of this form was already calculated in the previous section (7.50) and using that result we can write down:

$$\frac{1}{2\pi} \int_0^{2\pi} d\phi (\cos^2 \theta \cos^2 \phi + \sin^2 \phi) \frac{P_x^2}{2} = \frac{P_x^2}{4} (1 + \cos^2 \theta) = \frac{3}{4} (1 + \cos^2 \theta) M_b^2 \quad (7.62)$$

The same for light-holes:

$$\langle |\hat{\mathbf{x}} \cdot \mathbf{M}_{c-lh}|^2 \rangle = \frac{1}{2\pi} \int_0^{2\pi} |\hat{\mathbf{x}} \cdot \mathbf{M}_{c-lh}|^2 d\phi \quad (7.63)$$

Here the light hole absolute value consists of two parts:

$$\begin{aligned} |\hat{\mathbf{x}} \cdot \mathbf{M}_{c-lh}|^2 &= \left| \left\langle iS \uparrow \left| p_x \left| \frac{3}{2}, \frac{1}{2} \right\rangle \right\rangle \right|^2 + \left| \left\langle iS \uparrow \left| p_x \left| \frac{3}{2}, -\frac{1}{2} \right\rangle \right\rangle \right|^2 \\ &= \left[P_x \sqrt{\frac{2}{3}} \sin \theta \cos \phi \right] \cdot \left[P_x \sqrt{\frac{2}{3}} \sin \theta \cos \phi \right] \\ &+ \left[\frac{P_x}{\sqrt{6}} (\cos \theta \cos \phi - i \sin \phi) \right] \cdot \left[\frac{P_x}{\sqrt{6}} (\cos \theta \cos \phi + i \sin \phi) \right] \end{aligned} \quad (7.64)$$

$$= \frac{2}{3} P_x^2 \sin^2 \theta \cos^2 \phi + \frac{P_x^2}{6} (\cos^2 \theta \cos^2 \phi + \sin^2 \phi) = \frac{P_x^2}{6} [(4 \sin^2 \theta + \cos^2 \theta) \cos^2 \phi + \sin^2 \phi]$$

The averaging integral of the above is:

$$\begin{aligned} & \frac{1}{2\pi} \frac{P_x^2}{6} \int_0^{2\pi} [(4 \sin^2 \theta + \cos^2 \theta) \cos^2 \phi + \sin^2 \phi] d\phi \\ &= \frac{1}{2\pi} \frac{P_x^2}{6} \left[(4 \sin^2 \theta + \cos^2 \theta) \int_0^{2\pi} \cos^2 \phi d\phi + \int_0^{2\pi} \sin^2 \phi d\phi \right] = \frac{1}{2\pi} \frac{P_x^2}{6} [(4 \sin^2 \theta + \cos^2 \theta) \pi + \pi] \\ &= \frac{P_x^2}{12} (4 \sin^2 \theta + \cos^2 \theta + 1) = \frac{P_x^2}{12} (4 - 4 \cos^2 \theta + \cos^2 \theta + 1) = \frac{P_x^2}{12} (5 - 3 \cos^2 \theta) \quad (7.65) \end{aligned}$$

Taking into account (7.58):

$$\langle |\hat{\mathbf{x}} \cdot \mathbf{M}_{c-lh}|^2 \rangle = \frac{1}{4} (5 - 3 \cos^2 \theta) M_b^2 \quad (7.66)$$

For split-off the result is much more simpler than the light and heavy holes:

$$\langle |\hat{\mathbf{x}} \cdot \mathbf{M}_{c-so}|^2 \rangle = \frac{1}{2\pi} \int_0^{2\pi} |\hat{\mathbf{x}} \cdot \mathbf{M}_{c-so}|^2 d\phi \quad (7.67)$$

Here the split-off absolute value also consists of two parts:

$$\begin{aligned} |\hat{\mathbf{x}} \cdot \mathbf{M}_{c-so}|^2 &= \left| \left\langle iS \uparrow \left| p_x \left| \frac{1}{2}, \frac{1}{2} \right\rangle \right\rangle \right|^2 + \left| \left\langle iS \uparrow \left| p_x \left| \frac{1}{2}, -\frac{1}{2} \right\rangle \right\rangle \right|^2 \\ &= \left[\frac{P_x}{\sqrt{3}} \sin \theta \cos \phi \right] \cdot \left[\frac{P_x}{\sqrt{3}} \sin \theta \cos \phi \right] + \left[\frac{P_x}{\sqrt{3}} (\cos \theta \cos \phi - i \sin \phi) \right] \cdot \left[\frac{P_x}{\sqrt{3}} (\cos \theta \cos \phi + i \sin \phi) \right] \\ &= \frac{P_x^2}{3} \sin^2 \theta \cos^2 \phi + \frac{P_x^2}{3} (\cos^2 \theta \cos^2 \phi + \sin^2 \phi) = \frac{P_x^2}{3} [(\sin^2 \theta + \cos^2 \theta) \cos^2 \phi + \sin^2 \phi] \\ &= \frac{P_x^2}{3} (\cos^2 \phi + \sin^2 \phi) = \frac{P_x^2}{3} \quad (7.68) \end{aligned}$$

The averaging integral of the above is:

$$\frac{1}{2\pi} \frac{P_x^2}{3} \int_0^{2\pi} d\phi = \frac{1}{2\pi} \frac{P_x^2}{3} \cdot 2\pi = \frac{P_x^2}{3} = M_b^2 \quad (7.69)$$

For TM polarization ($\hat{\mathbf{e}} = \hat{\mathbf{z}}$):

$$\langle |\hat{\mathbf{z}} \cdot \mathbf{M}_{c-hh}|^2 \rangle = \frac{1}{2\pi} \int_0^{2\pi} |\hat{\mathbf{z}} \cdot \mathbf{M}_{c-hh}|^2 d\phi \quad (7.70)$$

Using the same method as for TE:

$$|\hat{\mathbf{z}} \cdot \mathbf{M}_{c-hh}|^2 = \hat{\mathbf{z}} \cdot \mathbf{M}_{c-hh}^* \cdot \hat{\mathbf{z}} \cdot \mathbf{M}_{c-hh} = \left[\frac{P_z}{\sqrt{2}} \sin \theta \right] \cdot \left[\frac{P_z}{\sqrt{2}} \sin \theta \right] = \frac{P_z^2}{2} \sin^2 \theta \quad (7.71)$$

The average of the above gives:

$$\frac{1}{2\pi} \frac{P_z^2}{2} \sin^2 \theta \int_0^{2\pi} d\phi = \frac{1}{2\pi} \frac{P_z^2}{2} \sin^2 \theta \cdot 2\pi = \frac{P_z^2}{2} \sin^2 \theta = \frac{3}{2} \sin^2 \theta M_b^2 \quad (7.72)$$

The same for light holes:

$$\langle |\hat{\mathbf{z}} \cdot \mathbf{M}_{c-lh}|^2 \rangle = \frac{1}{2\pi} \int_0^{2\pi} |\hat{\mathbf{z}} \cdot \mathbf{M}_{c-lh}|^2 d\phi \quad (7.73)$$

Here the light hole absolute value also consists of two parts:

$$\begin{aligned} |\hat{\mathbf{z}} \cdot \mathbf{M}_{c-lh}|^2 &= \left| \left\langle iS \uparrow \left| p_z \left| \frac{3}{2}, \frac{1}{2} \right\rangle \right\rangle \right|^2 + \left| \left\langle iS \uparrow \left| p_z \left| \frac{3}{2}, -\frac{1}{2} \right\rangle \right\rangle \right|^2 \\ &= \left[P_z \sqrt{\frac{2}{3}} \cos \theta \right] \cdot \left[P_z \sqrt{\frac{2}{3}} \cos \theta \right] + \left[\frac{P_z}{\sqrt{6}} (-\sin \theta) \right] \cdot \left[\frac{P_z}{\sqrt{6}} (-\sin \theta) \right] \\ &= \frac{2}{3} P_z^2 \cos^2 \theta + \frac{P_z^2}{6} \sin^2 \theta = \frac{P_z^2}{6} (4 \cos^2 \theta + \sin^2 \theta) \end{aligned} \quad (7.74)$$

The averaging integral of the above is:

$$\frac{1}{2\pi} \frac{P_z^2}{6} (4 \cos^2 \theta + \sin^2 \theta) \int_0^{2\pi} d\phi = \frac{P_z^2}{6} (4 \cos^2 \theta + \sin^2 \theta) = \frac{P_z^2}{6} (1 + 3 \cos^2 \theta) = \frac{1 + 3 \cos^2 \theta}{2} M_b^2 \quad (7.75)$$

The same for split-off:

$$\langle |\hat{\mathbf{z}} \cdot \mathbf{M}_{c-so}|^2 \rangle = \frac{1}{2\pi} \int_0^{2\pi} |\hat{\mathbf{z}} \cdot \mathbf{M}_{c-so}|^2 d\phi \quad (7.76)$$

$$\begin{aligned} |\hat{\mathbf{z}} \cdot \mathbf{M}_{c-so}|^2 &= \left| \left\langle iS \uparrow \left| p_z \left| \frac{1}{2}, \frac{1}{2} \right\rangle \right\rangle \right|^2 + \left| \left\langle iS \uparrow \left| p_z \left| \frac{1}{2}, -\frac{1}{2} \right\rangle \right\rangle \right|^2 \\ &= \left[\frac{P_z}{\sqrt{3}} \cos \theta \right] \cdot \left[\frac{P_z}{\sqrt{3}} \cos \theta \right] + \left[\frac{P_z}{\sqrt{3}} (-\sin \theta) \right] \cdot \left[\frac{P_z}{\sqrt{3}} (-\sin \theta) \right] \\ &= \frac{P_z^2}{3} \cos^2 \theta + \frac{P_z^2}{3} \sin^2 \theta = \frac{P_z^2}{3} (\cos^2 \theta + \sin^2 \theta) = \frac{P_z^2}{3} \end{aligned} \quad (7.77)$$

The averaging integral of the above is:

$$\frac{1}{2\pi} \frac{P_z^2}{3} \int_0^{2\pi} d\phi = \frac{1}{2\pi} \frac{P_z^2}{3} \cdot 2\pi = \frac{P_z^2}{3} = M_b^2 \quad (7.78)$$

The angular factor above may be expressed in terms of wave vectors:

$$\cos^2 \theta = \frac{k_z^2}{k^2} \quad (7.79)$$

Chapter 8

Conclusions

We summarize the goals that we have achieved during the preparation of this manuscript:

- we discussed Kane's parabolic four band model for semiconductors with zincblende crystal structure, and provided the detailed description of this approach;
- we described $k \cdot p$ method for degenerate bands based on Luttinger-Kohn's model for zincblende crystals;
- we expanded the original Luttinger Hamiltonian by using band anticrossing model, which describes the important properties of dilute nitride compounds;
- we generalized Luttinger-Kohn's and Kane's approaches on semiconductors with wurtzite crystal structure;
- we introduced the influence of strain on band structures using Bir and Pikus method both for zincblende and wurtzite crystals, and discussed three typical strain situations;
- we derived a method for calculating band structure for QWs grown away from natural (001) direction for semiconductors with both zincblende and wurtzite crystal structures, and provided a source code for rotation of Hamiltonian to any arbitrary orientation;
- we used plane wave expansion method for numerical implementation of Luttinger-Kohn's theory to evaluate band structures in QW;

- we calculated the examples of band structures;
- we obtained the behavior of band structure under orientation of growth and under internal and external stresses and compared our calculations with published papers;
- we derived optical transition matrix elements;
- we provided a short note on a point group theory as $k \cdot p$ method strongly relies on that.

The methods which were described in this thesis can be used in calculations of band structures around extremum Γ point for any new material compositions with zincblende and wurtzite crystal structures. We provided the theory only for three typical strain situations, in some cases it can be expanded to other strain situations to achieve the necessary properties of a particular composition in QW.

We presented the theory of evaluating matrix elements for optical transitions which can be used for straightforward numerical implementation. Further extension should include the theory on calculations of optical gain as matrix elements are directly involved in optical gain calculation methodology. It can be extended to provide the theory on momentum matrix elements for arbitrary oriented substrates.

Our method can be used for well researched materials based on *GaAs* or *InP*, dilute nitride compounds, bismuth compounds which have attract attention for past couple of years and expect to grow, and compounds with wurtzite primitive cell already used in blue-violet lasers, which makes it almost universal. The extensive calculations for any future materials with special properties are almost straightforward, based on the discussion presented in this Thesis.

Appendix A

Maple 16 code used in calculations of rotated Luttinger effective-mass Hamiltonian

In this appendix Maple 16 code for obtaining rotated Hamiltonian (4.7) in matrix form (4.9) is provided. The only input for the program is specify sine s and cosine c of the rotation angle, as we follow the Xia's methodology. The output of the program is denoted in the code as H and gives a rotated Hamiltonian in matrix form. In Maple 16 symbol $\#$ means the text after it is a comment.

```
with(LinearAlgebra); #the package for working with matrices in Maple 16

c := 0; #defining Cos and Sin of the angle of rotation (default is 90 deg)
s := 1;

#defining three J(1,2,3) matrices
J[1] := Matrix([[0, 0, (1/2)*sqrt(3), 0], [0, 0, 1, (1/2)*sqrt(3)], [(1/2)*sqrt(3), 1, 0, 0], [0, (1/2)*sqrt(3), 0, 0]]);
J[2] := Matrix([[0, 0, (-I*sqrt(3))*(1/2), 0], [0, 0, I, (-I*sqrt(3))*(1/2)], [I*sqrt(3)*(1/2), -I, 0, 0], [0, I*sqrt(3)*(1/2), 0, 0]]);
J[3] := Matrix([[3/2, 0, 0, 0], [0, -1/2, 0, 0], [0, 0, 1/2, 0], [0, 0, 0, -3
```

```

/2]]);

#calculating J(x,y,z) matrices
J[x] := Typesetting[delayDotProduct](s/sqrt(2), J[1], true)-Typesetting
[delayDotProduct](1/sqrt(2), J[2], true)+Typesetting[delayDotProduct]
(c/sqrt(2), J[3], true);
J[y] := Typesetting[delayDotProduct](s/sqrt(2), J[1], true)+Typesetting
[delayDotProduct](1/sqrt(2), J[2], true)+Typesetting[delayDotProduct]
(c/sqrt(2), J[3], true);
J[z] := -c*J[1]+s*J[3];

#defining rotations for components of k
k[x] := s*k[1]/sqrt(2)-k[2]/sqrt(2)+c*k[3]/sqrt(2);
k[y] := s*k[1]/sqrt(2)+k[2]/sqrt(2)+c*k[3]/sqrt(2);
k[z] := -c*k[1]+s*k[3];

#calculation of k squared
ksq := collect(k[x]^2+k[y]^2+k[z]^2, [k[1], k[2], k[3]]);

#calculation of J(x,y,z) matrices squared
Jxsq := simplify(MatrixMatrixMultiply(J[x], J[x]));
Jysq := simplify(MatrixMatrixMultiply(J[y], J[y]));
Jzsq := simplify(MatrixMatrixMultiply(J[z], J[z]));

#calculation of multiplication of k squared and J squared
kxJx := simplify(MatrixScalarMultiply(k[x]^2, Jxsq));
kyJy := simplify(MatrixScalarMultiply(k[y]^2, Jysq));
kzJz := simplify(MatrixScalarMultiply(k[z]^2, Jzsq));

#calculation of sum of product kJ squared multiplied by -2
Bra10 := simplify(MatrixAdd(kxJx, kyJy));
Bra1 := simplify(MatrixAdd(Bra10, kzJz));
Bra21 := collect(MatrixScalarMultiply(-2, Bra1), [k[1], k[2], k[3]]);

```

```

#calculation of factor after gamma2
Gam2 := collect(MatrixAdd((5/2)*ksq, Bra21), [k[1], k[2], k[3]]);

#calculation of factor after gamma3 including anticommutators
JxJy := MatrixScalarMultiply(-2*k[x]*k[y], MatrixAdd(MatrixMatrixMultiply(J
  [x], J[y]), MatrixMatrixMultiply(J[y], J[x])));
JyJz := MatrixScalarMultiply(-2*k[y]*k[z], MatrixAdd(MatrixMatrixMultiply(J
  [y], J[z]), MatrixMatrixMultiply(J[z], J[y])));
JzJx := MatrixScalarMultiply(-2*k[z]*k[x], MatrixAdd(MatrixMatrixMultiply(J
  [z], J[x]), MatrixMatrixMultiply(J[x], J[z])));
Gam3 := collect(MatrixAdd(MatrixAdd(JxJy, JyJz), JzJx), [k[1], k[2], k[3]]);

#calculation of final rotated Hamiltonian matrix
H := collect(simplify(MatrixAdd(MatrixAdd(gamma[1]*ksq, MatrixScalarMulti
  ply(gamma[2], Gam2)), MatrixScalarMultiply(gamma[3], Gam3))), [gamma[1],
  gamma[2], gamma[3]]);

```

Appendix B

Maple 16 code used in matrix elements rotations 4×4 zinblende and 6×6 wurtzite

In this appendix Maple 16 code for obtaining matrix elements for rotated LKH is expressed.

B.1 Zinblende

The input of this program is only angles of rotation θ and ϕ , which are found in terms of Miller indices by eq. (4.31). The output result is denoted in the code as Q , S and R for each matrix element respectively. Program determines three terms (4.33), (4.36) and (4.35) at the same time and do not need external intervention. By default angles set as 0.

```
with(LinearAlgebra); #the package for working with matrices in Maple 16
```

```
theta := 0; #defining angles of rotation(0 by default)
```

```
phi := 0;
```

```

#defining rotation matrix U
U := Matrix([[cos(theta)*cos(phi), cos(theta)*sin(phi), -sin(theta)], [-sin(phi),
cos(phi), 0], [sin(theta)*cos(phi), sin(theta)*sin(phi), cos(theta)]]);

Uk := simplify(MatrixInverse(U));#calculating inverse matrix

#defining rotations of spin
M[s] := Matrix([[exp(-I*phi*(1/2))*cos((1/2)*theta), exp(I*phi*(1/2))*sin((1/2)
*theta)], [-exp(-I*phi*(1/2))*sin((1/2)*theta), exp(I*phi*(1/2))*cos((1/2)
*theta)]]);

M[c] :=KroneckerProduct(M[s], U);#calculation of total rotation matrix Mc

M[t] := simplify(MatrixInverse(M[c]));#calculating inverse matrix

#matrix in X,Y,Z basis
H[o] := Matrix([[A*k[x]^2+B*k[y]^2+B*k[z]^2, C*k[x]*k[y], C*k[x]*k[z]],
[C*k[x]*k[y], B*k[x]^2+A*k[y]^2+B*k[z]^2, C*k[y]*k[z]], [C*k[x]*k[z],
C*k[y]*k[z], B*k[x]^2+B*k[y]^2+A*k[z]^2]]);
H[a] := KroneckerProduct(Matrix([[1, 0], [0, 1]]), H[o]);

#calculation of rotated vector k components
K := VectorMatrixMultiply(Uk, Transpose(Matrix([[k[1], k[2], k[3]]]]));
k[x] := K(1);
k[y] := K(2);
k[z] := K(3);

#transformation U^T H U
H[n] := simplify(MatrixMatrixMultiply(MatrixMatrixMultiply(M[c], H[a]), M[t]));
Q[1] := simplify(-(H[n](1, 1)+H[n](2, 2))*(1/2));
S[1] := simplify((H[n](1, 4)+I*H[n](1, 5)+H[n](2, 5)-I*H[n](4, 2))/sqrt(12)
-(H[n](1, 3)-I*H[n](2, 3))/sqrt(3));
R[1] := simplify((H[n](1, 1)-I*H[n](1, 2)-H[n](2, 2)-I*H[n](1, 2))/sqrt(12)
+(H[n](1, 6)-I*H[n](2, 6))/sqrt(3));

```

```
#result
Q[2] := collect(simplify(subs({A = -gamma[1]-4*gamma[2], B = 2*gamma[2]
-gamma[1], C = -6*gamma[3]}, Q[1])-gamma[1]*(k[x]^2+k[y]^2+k[z]^2)),
  [gamma[1], gamma[2], gamma[3]]);
S[2] := collect(simplify(subs({A = -gamma[1]-4*gamma[2], B = 2*gamma[2]
-gamma[1], C = -6*gamma[3]}, S[1])), [gamma[1], gamma[2], gamma[3]]);
R[2] := collect(simplify(subs({A = -gamma[1]-4*gamma[2], B = 2*gamma[2]
-gamma[1], C = -6*gamma[3]}, R[1])), [gamma[1], gamma[2], gamma[3]]);
```

B.2 Wurtzite

The input of this program is only angles of rotation θ and ϕ , which is difficult to find in terms of Miller-Bravais indices for wurtzite. The output of the program denoted in code as F, lambda, X and K (Theta found by simple F-lambda relation), which corresponds to rotated matrix elements (4.73) and (4.74).

```
with(LinearAlgebra);

theta := 0;#input angles of rotation
phi := 0;

U := Matrix([[cos(theta)*cos(phi), cos(theta)*sin(phi), -sin(theta)], [-sin(phi),
  cos(phi), 0], [sin(theta)*cos(phi), sin(theta)*sin(phi), cos(theta)]]);

Uk := simplify(MatrixInverse(U));

M[s] := Matrix([[exp(-I*phi*(1/2))*cos((1/2)*theta), exp(I*phi*(1/2))*sin((1/2)
*theta)], [-exp(-I*phi*(1/2))*sin((1/2)*theta), exp(I*phi*(1/2))*cos((1/2)
*theta)]]);

M[c] := KroneckerProduct(M[s], U);

M[t] := simplify(MatrixInverse(M[c]));
```

```

H[o] := Matrix([[L[1]*k[x]^2+M[1]*k[y]^2+M[2]*k[z]^2, N[1]*k[x]*k[y],
N[2]*k[x]*k[z]], [N[1]*k[x]*k[y], M[1]*k[x]^2+L[1]*k[y]^2+M[2]*k[z]^2,
N[2]*k[y]*k[z]], [N[2]*k[x]*k[z], N[2]*k[y]*k[z], M[3]*k[x]^2+M[3]*k[y]^2
+L[2]*k[z]^2]]);

H[a] := KroneckerProduct(Matrix([[1, 0], [0, 1]]), H[o]);

K := VectorMatrixMultiply(Uk, Transpose(Matrix([[k[1], k[2], k[3]]]]));
k[x] := K(1);
k[y] := K(2);
k[z] := K(3);

H[n] := simplify(MatrixMatrixMultiply(MatrixMatrixMultiply(M[c], H[a]), M[t]));

F[1] := simplify((H[n](1, 1)+H[n](2, 2))*(1/2));

lambda[1] := simplify(H[n](3, 3));

X[1] := simplify((H[n](1, 3)+I*H[n](2, 3))/sqrt(2));

K[1] := simplify((H[n](1, 1)-H[n](2, 2)+(2*I)*H[n](1, 2))*(1/2));

#resulting matrix elements
F[2] := collect(simplify(subs({L[1] = A[2]+A[4]+A[5], L[2] = A[1], M[1] =
A[2]+A[4]-A[5], M[2] = A[1]+A[3], M[3] = A[2], N[1] = 2*A[5], N[2] =
sqrt(2)*A[6]}, F[1])), [A[1], A[2], A[3], A[4], A[5], A[6]]);

lambda[2] := collect(simplify(subs({L[1] = A[2]+A[4]+A[5], L[2] = A[1],
M[1] = A[2]+A[4]-A[5], M[2] = A[1]+A[3], M[3] = A[2], N[1] = 2*A[5],
N[2] = sqrt(2)*A[6]}, lambda[1])), [A[1], A[2], A[3], A[4], A[5], A[6]]);

X[2] := collect(simplify(subs({L[1] = A[2]+A[4]+A[5], L[2] = A[1], M[1]
= A[2]+A[4]-A[5], M[2] = A[1]+A[3], M[3] = A[2], N[1] = 2*A[5], N[2]

```

```
= sqrt(2)*A[6]}, X[1])), [A[1], A[2], A[3], A[4], A[5], A[6]]);
```

```
K[2] := collect(simplify(subs({L[1] = A[2]+A[4]+A[5], L[2] = A[1], M[1]  
= A[2]+A[4]-A[5], M[2] = A[1]+A[3], M[3] = A[2], N[1] = 2*A[5], N[2]  
= sqrt(2)*A[6]}, K[1])), [A[1], A[2], A[3], A[4], A[5], A[6]]);
```

```
Theta := collect(F[2]-lambda[2], [A[1], A[2], A[3], A[4], A[5], A[6]]);
```

Appendix C

Maple 16 code used in matrix elements calculations 8×8

In this appendix Maple 16 code for obtaining rotated matrix elements is provided. The program start with angles of rotation θ and ϕ and end with result which is denoted in code as $H0$, $H2$, $H3$, $H5$ and $H6$ for each term in eq. (4.44) respectively. Program determines all terms at the same time. By default angles set as 0.

```
with(LinearAlgebra); #the package for working with matrices in Maple 16

theta := 0; #defining angles of rotation(0 by default)
phi := 0;

#defining rotation matrix U
U := Matrix([[cos(theta)*cos(phi), cos(theta)*sin(phi), -sin(theta)], [-sin(phi),
  cos(phi), 0], [sin(theta)*cos(phi), sin(theta)*sin(phi), cos(theta)]]);

#calculating inverse matrix
Uk := simplify(MatrixInverse(U));

#defining rotations of spin
M[s] := Matrix([[exp(-I*phi*(1/2))*cos((1/2)*theta), exp(I*phi*(1/2))*sin((1/2)
```

```

*theta)], [-exp(-I*phi*(1/2))*sin((1/2)*theta), exp(I*phi*(1/2))*cos((1/2)
*theta)]]);

#calculation of total rotation matrix Mc
M[c] := KroneckerProduct(M[s], U);

#Calculation of valence rotated basis functions
New := MatrixVectorMultiply(M[c], Transpose(Matrix([[X[u], Y[u], Z[u], X[d], Y[d],
Z[d]]]])));

#Calculation of rotated conduction basis functions
NewS := MatrixVectorMultiply(M[s], Transpose(Matrix([[S[u], S[d]]]])));

#define basis functions
s[1] := I*NewS(1);
s[2] := I*NewS(2);
u[2] := -(New(4)+I*New(5))/sqrt(6)+sqrt(2/3)*New(3);
u[3] := (New(1)-I*New(2))/sqrt(6)+sqrt(2/3)*New(6);
u[5] := (New(4)+I*New(5))/sqrt(3)+New(3)/sqrt(3);
u[6] := (New(1)-I*New(2))/sqrt(3)-New(6)/sqrt(3);
n[2] := subs({I = -I}, u[2]);
n[5] := subs({I = -I}, u[5]);
s[3] := subs({I = -I}, s[1]);
s[4] := subs({I = -I}, s[2]);

#calculation matrix elements
H0 := simplify(collect(s[1]*s[3], [S[u], S[d]]));
H2 := simplify(collect(n[2]*s[2], [S[u], S[d]]));
H3 := simplify(collect(s[3]*u[3], [S[u], S[d]]));
H5 := simplify(collect(s[1]*n[5], [S[u], S[d]]));
H6 := simplify(collect(u[6]*s[4], [S[u], S[d]]));

#calculation of rotated vector k components
K := VectorMatrixMultiply(Uk, Transpose(Matrix([[k[1], k[2], k[3]]]])));

```

```

#substitution
H01 := collect(simplify(subs({S[d]^2 = E[c]+A*(K(1)^2+K(2)^2+K(3)^2)
+h^2*(K(1)^2+K(2)^2+K(3)^2)/(2*m[0]), S[u]^2 = E[c]+A*(K(1)^2+
K(2)^2+K(3)^2)+h^2*(K(1)^2+K(2)^2+K(3)^2)/(2*m[0])}, H2)), [S[u]
, S[d]]);
H11 := collect(simplify(subs({S[d]^2 = E[c]+A*(K(1)^2+K(2)^2+K(3)^2)
+h^2*(K(1)^2+K(2)^2+K(3)^2)/(2*m[0]), S[u]^2 = E[c]+A*(K(1)^2+
K(2)^2+K(3)^2)+h^2*(K(1)^2+K(2)^2+K(3)^2)/(2*m[0])}, H2)), [S[u]
, S[d]]);
H41 := collect(simplify(subs({S[d]^2 = E[c]+A*(K(1)^2+K(2)^2+K(3)^2)
+h^2*(K(1)^2+K(2)^2+K(3)^2)/(2*m[0]), S[u]^2 = E[c]+A*(K(1)^2+
K(2)^2+K(3)^2)+h^2*(K(1)^2+K(2)^2+K(3)^2)/(2*m[0])}, H3)), [S[u]
, S[d]]);
H51 := collect(simplify(subs({S[d]^2 = E[c]+A*(K(1)^2+K(2)^2+K(3)^2)
+h^2*(K(1)^2+K(2)^2+K(3)^2)/(2*m[0]), S[u]^2 = E[c]+A*(K(1)^2+
K(2)^2+K(3)^2)+h^2*(K(1)^2+K(2)^2+K(3)^2)/(2*m[0])}, H5)), [S[u]
, S[d]]);
H61 := collect(simplify(subs({S[d]^2 = E[c]+A*(K(1)^2+K(2)^2+K(3)^2)
+h^2*(K(1)^2+K(2)^2+K(3)^2)/(2*m[0]), S[u]^2 = E[c]+A*(K(1)^2+
K(2)^2+K(3)^2)+h^2*(K(1)^2+K(2)^2+K(3)^2)/(2*m[0])}, H6)), [S[u]
, S[d]]);

H02 := collect(simplify(subs({S[d] = X[d], S[u] = X[u]}, H01)), [X[u], X[d]]);
H12 := collect(simplify(subs({S[d] = X[d], S[u] = X[u]}, H11)), [X[u], X[d]]);
H42 := collect(simplify(subs({S[d] = X[d], S[u] = X[u]}, H41)), [X[u], X[d]]);
H52 := collect(simplify(subs({S[d] = X[d], S[u] = X[u]}, H51)), [X[u], X[d]]);
H62 := collect(simplify(subs({S[d] = X[d], S[u] = X[u]}, H61)), [X[u], X[d]]);

H03 := subs({X[d]^2 = B*K(2)*K(3)+I*P[0]*K(1), X[u]^2 = B*K(2)*K(3)+
I*P[0]*K(1)}, H02);
H13 := subs({X[d]^2 = B*K(2)*K(3)-I*P[0]*K(1), X[u]^2 = B*K(2)*K(3)-
I*P[0]*K(1)}, H12);
H43 := subs({X[d]^2 = B*K(2)*K(3)+I*P[0]*K(1), X[u]^2 = B*K(2)*K(3)+

```

```

I*P[0]*K(1)}, H42);
H53 := subs({X[d]^2 = B*K(2)*K(3)-I*P[0]*K(1), X[u]^2 = B*K(2)*K(3)-
I*P[0]*K(1)}, H52);
H63 := subs({X[d]^2 = B*K(2)*K(3)+I*P[0]*K(1), X[u]^2 = B*K(2)*K(3)+
I*P[0]*K(1)}, H62);

H04 := collect(subs({X[d] = Y[d], X[u] = Y[u]}, H03), [Y[u], Y[d]]);
H14 := collect(subs({X[d] = Y[d], X[u] = Y[u]}, H13), [Y[u], Y[d]]);
H44 := collect(subs({X[d] = Y[d], X[u] = Y[u]}, H43), [Y[u], Y[d]]);
H54 := collect(subs({X[d] = Y[d], X[u] = Y[u]}, H53), [Y[u], Y[d]]);
H64 := collect(subs({X[d] = Y[d], X[u] = Y[u]}, H63), [Y[u], Y[d]]);

H05 := subs({Y[d]^2 = B*K(1)*K(3)+I*P[0]*K(2), Y[u]^2 = B*K(1)*K(3)
+I*P[0]*K(2)}, H04);
H15 := subs({Y[d]^2 = B*K(1)*K(3)-I*P[0]*K(2), Y[u]^2 = B*K(1)*K(3)
-I*P[0]*K(2)}, H14);
H45 := subs({Y[d]^2 = B*K(1)*K(3)+I*P[0]*K(2), Y[u]^2 = B*K(1)*K(3)
+I*P[0]*K(2)}, H44);
H55 := subs({Y[d]^2 = B*K(1)*K(3)-I*P[0]*K(2), Y[u]^2 = B*K(1)*K(3)
-I*P[0]*K(2)}, H54);
H65 := subs({Y[d]^2 = B*K(1)*K(3)+I*P[0]*K(2), Y[u]^2 = B*K(1)*K(3)
+I*P[0]*K(2)}, H64);

H06 := collect(subs({Y[d] = Z[d], Y[u] = Z[u]}, H05), [Z[u], Z[d]]);
H16 := collect(subs({Y[d] = Z[d], Y[u] = Z[u]}, H15), [Z[u], Z[d]]);
H46 := collect(subs({Y[d] = Z[d], Y[u] = Z[u]}, H45), [Z[u], Z[d]]);
H56 := collect(subs({Y[d] = Z[d], Y[u] = Z[u]}, H55), [Z[u], Z[d]]);
H66 := collect(subs({Y[d] = Z[d], Y[u] = Z[u]}, H65), [Z[u], Z[d]]);

H07 := subs({Z[d]^2 = B*K(1)*K(2)+I*P[0]*K(3), Z[u]^2 = B*K(1)*K(2)
+I*P[0]*K(3)}, H06);
H17 := subs({Z[d]^2 = B*K(1)*K(2)-I*P[0]*K(3), Z[u]^2 = B*K(1)*K(2)-
I*P[0]*K(3)}, H16);
H47 := subs({Z[d]^2 = B*K(1)*K(2)+I*P[0]*K(3), Z[u]^2 = B*K(1)*K(2)+

```

```
I*P[0]*K(3)}, H46);
H57 := subs({Z[d]^2 = B*K(1)*K(2)-I*P[0]*K(3), Z[u]^2 = B*K(1)*K(2)-
I*P[0]*K(3)}, H56);
H67 := subs({Z[d]^2 = B*K(1)*K(2)+I*P[0]*K(3), Z[u]^2 = B*K(1)*K(2)+
I*P[0]*K(3)}, H66);

#output
Hs0 := combine(collect(expand(simplify(subs({Z[d] = 0, Z[u] = 0}, H07))),
[B, P[0], A, h, E[c]]), radical);
Hs2 := combine(collect(expand(simplify(subs({Z[d] = 0, Z[u] = 0}, H17))),
[B, P[0], A, h, E[c]]), radical);
Hs3 := combine(collect(expand(simplify(subs({Z[d] = 0, Z[u] = 0}, H47))),
[B, P[0], A, h, E[c]]), radical);
Hs5 := combine(collect(expand(simplify(subs({Z[d] = 0, Z[u] = 0}, H57))),
[B, P[0], A, h, E[c]]), radical);
Hs6 := combine(collect(expand(simplify(subs({Z[d] = 0, Z[u] = 0}, H67))),
[B, P[0], A, h, E[c]]), radical);
```

Appendix D

Basis functions for 6×6 LKH for arbitrary orientation

The basis functions for 6×6 LKH for arbitrary orientation are expressed in terms of old basis functions:

D.1 Zincblende

$$u'_{10} = -\frac{1}{\sqrt{2}} \left[(c\theta \, c\phi \, c\frac{\theta}{2} \, e^{-i\frac{\phi}{2}} - ic\frac{\theta}{2} \, s\phi \, e^{-i\frac{\phi}{2}})X \uparrow + (c\theta \, s\phi \, c\frac{\theta}{2} \, e^{-i\frac{\phi}{2}} + ic\frac{\theta}{2} \, c\phi \, e^{-i\frac{\phi}{2}})Y \uparrow \right. \\ \left. - (s\theta \, c\frac{\theta}{2} \, e^{-i\frac{\phi}{2}})Z \uparrow + (c\theta \, c\phi \, s\frac{\theta}{2} \, e^{i\frac{\phi}{2}} - is\frac{\theta}{2} \, s\phi \, e^{i\frac{\phi}{2}})X \downarrow + (c\theta \, s\phi \, s\frac{\theta}{2} \, e^{i\frac{\phi}{2}} + is\frac{\theta}{2} \, c\phi \, e^{i\frac{\phi}{2}})Y \downarrow \right. \\ \left. - (s\theta \, s\frac{\theta}{2} \, e^{i\frac{\phi}{2}})Z \downarrow \right] \quad (D.1)$$

$$u'_{20} = -\frac{1}{\sqrt{6}} \left[(-c\theta \, c\phi \, s\frac{\theta}{2} \, e^{-i\frac{\phi}{2}} + is\frac{\theta}{2} \, s\phi \, e^{-i\frac{\phi}{2}})X \uparrow - (-c\theta \, s\phi \, s\frac{\theta}{2} \, e^{-i\frac{\phi}{2}} - is\frac{\theta}{2} \, c\phi \, e^{-i\frac{\phi}{2}})Y \uparrow \right. \\ \left. + (s\theta \, s\frac{\theta}{2} \, e^{-i\frac{\phi}{2}})Z \uparrow + (c\theta \, c\phi \, c\frac{\theta}{2} \, e^{i\frac{\phi}{2}} - ic\frac{\theta}{2} \, s\phi \, e^{i\frac{\phi}{2}})X \downarrow + (c\theta \, s\phi \, c\frac{\theta}{2} \, e^{i\frac{\phi}{2}} + ic\frac{\theta}{2} \, c\phi \, e^{i\frac{\phi}{2}})Y \downarrow \right. \\ \left. - (s\theta \, c\frac{\theta}{2} \, e^{i\frac{\phi}{2}})Z \downarrow \right] + \sqrt{\frac{2}{3}} \left[s\theta \, c\phi \, c\frac{\theta}{2} \, e^{-i\frac{\phi}{2}}X \uparrow + s\theta \, s\phi \, c\frac{\theta}{2} \, e^{-i\frac{\phi}{2}}Y \uparrow + c\theta \, c\frac{\theta}{2} \, e^{-i\frac{\phi}{2}}Z \uparrow \right. \\ \left. + s\theta \, c\phi \, s\frac{\theta}{2} \, e^{i\frac{\phi}{2}}X \downarrow + s\theta \, s\phi \, s\frac{\theta}{2} \, e^{i\frac{\phi}{2}}Y \downarrow - c\theta \, s\frac{\theta}{2} \, e^{i\frac{\phi}{2}}Z \downarrow \right] \quad (D.2)$$

$$\begin{aligned}
u'_{30} = & \frac{1}{\sqrt{6}} \left[(-c\theta c\phi c\frac{\theta}{2} e^{-i\frac{\phi}{2}} + ic\frac{\theta}{2} s\phi e^{-i\frac{\phi}{2}})X \uparrow + (c\theta s\phi c\frac{\theta}{2} e^{-i\frac{\phi}{2}} - ic\frac{\theta}{2} c\phi e^{-i\frac{\phi}{2}})Y \uparrow \right. \\
& - (s\theta c\frac{\theta}{2} e^{-i\frac{\phi}{2}})Z \uparrow + (c\theta c\phi s\frac{\theta}{2} e^{i\frac{\phi}{2}} + is\frac{\theta}{2} s\phi e^{i\frac{\phi}{2}})X \downarrow + (c\theta s\phi s\frac{\theta}{2} e^{i\frac{\phi}{2}} - is\frac{\theta}{2} c\phi e^{i\frac{\phi}{2}})Y \downarrow \\
& \left. - (s\theta s\frac{\theta}{2} e^{i\frac{\phi}{2}})Z \downarrow \right] + \sqrt{\frac{2}{3}} \left[-s\theta c\phi s\frac{\theta}{2} e^{-i\frac{\phi}{2}}X \uparrow - s\theta s\phi s\frac{\theta}{2} e^{-i\frac{\phi}{2}}Y \uparrow - c\theta s\frac{\theta}{2} e^{-i\frac{\phi}{2}}Z \uparrow \right. \\
& \left. + s\theta c\phi c\frac{\theta}{2} e^{i\frac{\phi}{2}}X \downarrow + s\theta s\phi c\frac{\theta}{2} e^{i\frac{\phi}{2}}Y \downarrow + c\theta c\frac{\theta}{2} e^{i\frac{\phi}{2}}Z \downarrow \right]
\end{aligned} \tag{D.3}$$

$$\begin{aligned}
u'_{40} = & \frac{1}{\sqrt{2}} \left[(-c\theta c\phi s\frac{\theta}{2} e^{-i\frac{\phi}{2}} - is\frac{\theta}{2} s\phi e^{-i\frac{\phi}{2}})X \uparrow + (-c\theta s\phi s\frac{\theta}{2} e^{-i\frac{\phi}{2}} + is\frac{\theta}{2} c\phi e^{-i\frac{\phi}{2}})Y \uparrow \right. \\
& + (s\theta c\frac{\theta}{2} e^{-i\frac{\phi}{2}})Z \uparrow + (c\theta c\phi c\frac{\theta}{2} e^{i\frac{\phi}{2}} + ic\frac{\theta}{2} s\phi e^{i\frac{\phi}{2}})X \downarrow + (c\theta s\phi c\frac{\theta}{2} e^{i\frac{\phi}{2}} - ic\frac{\theta}{2} c\phi e^{i\frac{\phi}{2}})Y \downarrow \\
& \left. - (s\theta c\frac{\theta}{2} e^{i\frac{\phi}{2}})Z \downarrow \right]
\end{aligned} \tag{D.4}$$

$$\begin{aligned}
u'_{50} = & \frac{1}{\sqrt{3}} \left[(-c\theta c\phi s\frac{\theta}{2} e^{-i\frac{\phi}{2}} + is\frac{\theta}{2} s\phi e^{-i\frac{\phi}{2}})X \uparrow - (-c\theta s\phi s\frac{\theta}{2} e^{-i\frac{\phi}{2}} - is\frac{\theta}{2} c\phi e^{-i\frac{\phi}{2}})Y \uparrow \right. \\
& + (s\theta s\frac{\theta}{2} e^{-i\frac{\phi}{2}})Z \uparrow + (c\theta c\phi c\frac{\theta}{2} e^{i\frac{\phi}{2}} - ic\frac{\theta}{2} s\phi e^{i\frac{\phi}{2}})X \downarrow + (c\theta s\phi c\frac{\theta}{2} e^{i\frac{\phi}{2}} + ic\frac{\theta}{2} c\phi e^{i\frac{\phi}{2}})Y \downarrow \\
& \left. - (s\theta c\frac{\theta}{2} e^{i\frac{\phi}{2}})Z \downarrow \right] + \frac{1}{\sqrt{3}} \left[s\theta c\phi c\frac{\theta}{2} e^{-i\frac{\phi}{2}}X \uparrow + s\theta s\phi c\frac{\theta}{2} e^{-i\frac{\phi}{2}}Y \uparrow + c\theta c\frac{\theta}{2} e^{-i\frac{\phi}{2}}Z \uparrow \right. \\
& \left. + s\theta c\phi s\frac{\theta}{2} e^{i\frac{\phi}{2}}X \downarrow + s\theta s\phi s\frac{\theta}{2} e^{i\frac{\phi}{2}}Y \downarrow - c\theta s\frac{\theta}{2} e^{i\frac{\phi}{2}}Z \downarrow \right]
\end{aligned} \tag{D.5}$$

$$\begin{aligned}
u'_{60} = & \frac{1}{\sqrt{3}} \left[(-c\theta c\phi c\frac{\theta}{2} e^{-i\frac{\phi}{2}} + ic\frac{\theta}{2} s\phi e^{-i\frac{\phi}{2}})X \uparrow + (c\theta s\phi c\frac{\theta}{2} e^{-i\frac{\phi}{2}} - ic\frac{\theta}{2} c\phi e^{-i\frac{\phi}{2}})Y \uparrow \right. \\
& - (s\theta c\frac{\theta}{2} e^{-i\frac{\phi}{2}})Z \uparrow + (c\theta c\phi s\frac{\theta}{2} e^{i\frac{\phi}{2}} + is\frac{\theta}{2} s\phi e^{i\frac{\phi}{2}})X \downarrow + (c\theta s\phi s\frac{\theta}{2} e^{i\frac{\phi}{2}} - is\frac{\theta}{2} c\phi e^{i\frac{\phi}{2}})Y \downarrow \\
& \left. - (s\theta s\frac{\theta}{2} e^{i\frac{\phi}{2}})Z \downarrow \right] - \frac{1}{\sqrt{3}} \left[-s\theta c\phi s\frac{\theta}{2} e^{-i\frac{\phi}{2}}X \uparrow - s\theta s\phi s\frac{\theta}{2} e^{-i\frac{\phi}{2}}Y \uparrow - c\theta s\frac{\theta}{2} e^{-i\frac{\phi}{2}}Z \uparrow \right. \\
& \left. + s\theta c\phi c\frac{\theta}{2} e^{i\frac{\phi}{2}}X \downarrow + s\theta s\phi c\frac{\theta}{2} e^{i\frac{\phi}{2}}Y \downarrow + c\theta c\frac{\theta}{2} e^{i\frac{\phi}{2}}Z \downarrow \right]
\end{aligned} \tag{D.6}$$

where s and c represents sine and cosine of appropriate angle.

D.2 Wurtzite

$$\begin{aligned}
u'_1 = & -\frac{1}{\sqrt{2}} \left[(c\theta c\phi c\frac{\theta}{2} e^{-i\frac{\phi}{2}} - ic\frac{\theta}{2} s\phi e^{-i\frac{\phi}{2}})X \uparrow + (c\theta s\phi c\frac{\theta}{2} e^{-i\frac{\phi}{2}} + ic\frac{\theta}{2} c\phi e^{-i\frac{\phi}{2}})Y \uparrow \right. \\
& - (s\theta c\frac{\theta}{2} e^{-i\frac{\phi}{2}})Z \uparrow + (c\theta c\phi s\frac{\theta}{2} e^{i\frac{\phi}{2}} - is\frac{\theta}{2} s\phi e^{i\frac{\phi}{2}})X \downarrow + (c\theta s\phi s\frac{\theta}{2} e^{i\frac{\phi}{2}} + is\frac{\theta}{2} c\phi e^{i\frac{\phi}{2}})Y \downarrow \\
& \left. - (s\theta s\frac{\theta}{2} e^{i\frac{\phi}{2}})Z \downarrow \right]
\end{aligned} \tag{D.7}$$

$$\begin{aligned}
u'_2 = \frac{1}{\sqrt{2}} & \left[(-c\theta c\phi c\frac{\theta}{2} e^{-i\frac{\phi}{2}} + ic\frac{\theta}{2} s\phi e^{-i\frac{\phi}{2}})X \uparrow + (c\theta s\phi c\frac{\theta}{2} e^{-i\frac{\phi}{2}} - ic\frac{\theta}{2} c\phi e^{-i\frac{\phi}{2}})Y \uparrow \right. \\
& - (s\theta c\frac{\theta}{2} e^{-i\frac{\phi}{2}})Z \uparrow + (c\theta c\phi s\frac{\theta}{2} e^{i\frac{\phi}{2}} + is\frac{\theta}{2} s\phi e^{i\frac{\phi}{2}})X \downarrow + (c\theta s\phi s\frac{\theta}{2} e^{i\frac{\phi}{2}} - is\frac{\theta}{2} c\phi e^{i\frac{\phi}{2}})Y \downarrow \\
& \left. - (s\theta s\frac{\theta}{2} e^{i\frac{\phi}{2}})Z \downarrow \right]
\end{aligned} \tag{D.8}$$

$$\begin{aligned}
u'_3 = s\theta c\phi c\frac{\theta}{2} e^{-i\frac{\phi}{2}}X \uparrow + s\theta s\phi c\frac{\theta}{2} e^{-i\frac{\phi}{2}}Y \uparrow + c\theta c\frac{\theta}{2} e^{-i\frac{\phi}{2}}Z \uparrow + s\theta c\phi s\frac{\theta}{2} e^{i\frac{\phi}{2}}X \downarrow \\
+ s\theta s\phi s\frac{\theta}{2} e^{i\frac{\phi}{2}}Y \downarrow - c\theta s\frac{\theta}{2} e^{i\frac{\phi}{2}}Z \downarrow
\end{aligned} \tag{D.9}$$

$$\begin{aligned}
u'_4 = \frac{1}{\sqrt{2}} & \left[(-c\theta c\phi s\frac{\theta}{2} e^{-i\frac{\phi}{2}} - is\frac{\theta}{2} s\phi e^{-i\frac{\phi}{2}})X \uparrow + (-c\theta s\phi s\frac{\theta}{2} e^{-i\frac{\phi}{2}} + is\frac{\theta}{2} c\phi e^{-i\frac{\phi}{2}})Y \uparrow \right. \\
& + (s\theta c\frac{\theta}{2} e^{-i\frac{\phi}{2}})Z \uparrow + (c\theta c\phi c\frac{\theta}{2} e^{i\frac{\phi}{2}} + ic\frac{\theta}{2} s\phi e^{i\frac{\phi}{2}})X \downarrow + (c\theta s\phi c\frac{\theta}{2} e^{i\frac{\phi}{2}} - ic\frac{\theta}{2} c\phi e^{i\frac{\phi}{2}})Y \downarrow \\
& \left. - (s\theta c\frac{\theta}{2} e^{i\frac{\phi}{2}})Z \downarrow \right]
\end{aligned} \tag{D.10}$$

$$\begin{aligned}
u'_5 = -\frac{1}{\sqrt{2}} & \left[(-c\theta c\phi s\frac{\theta}{2} e^{-i\frac{\phi}{2}} + is\frac{\theta}{2} s\phi e^{-i\frac{\phi}{2}})X \uparrow - (-c\theta s\phi s\frac{\theta}{2} e^{-i\frac{\phi}{2}} - is\frac{\theta}{2} c\phi e^{-i\frac{\phi}{2}})Y \uparrow \right. \\
& + (s\theta s\frac{\theta}{2} e^{-i\frac{\phi}{2}})Z \uparrow + (c\theta c\phi c\frac{\theta}{2} e^{i\frac{\phi}{2}} - ic\frac{\theta}{2} s\phi e^{i\frac{\phi}{2}})X \downarrow + (c\theta s\phi c\frac{\theta}{2} e^{i\frac{\phi}{2}} + ic\frac{\theta}{2} c\phi e^{i\frac{\phi}{2}})Y \downarrow \\
& \left. - (s\theta c\frac{\theta}{2} e^{i\frac{\phi}{2}})Z \downarrow \right]
\end{aligned} \tag{D.11}$$

$$\begin{aligned}
u'_6 = -s\theta c\phi s\frac{\theta}{2} e^{-i\frac{\phi}{2}}X \uparrow - s\theta s\phi s\frac{\theta}{2} e^{-i\frac{\phi}{2}}Y \uparrow - c\theta s\frac{\theta}{2} e^{-i\frac{\phi}{2}}Z \uparrow + s\theta c\phi c\frac{\theta}{2} e^{i\frac{\phi}{2}}X \downarrow \\
+ s\theta s\phi c\frac{\theta}{2} e^{i\frac{\phi}{2}}Y \downarrow + c\theta c\frac{\theta}{2} e^{i\frac{\phi}{2}}Z \downarrow
\end{aligned} \tag{D.12}$$

where s and c represents sine and cosine of appropriate angle.

Appendix E

Tables of material parameters for various semiconductor materials

The recommended material parameters are listed in the tables below.

TABLE E.1: Important band structure parameters for zincblende GaAs, AlAs, InAs, InP and GaP [61](p. 803)

Parameters	Materials				
	GaAs	AlAs	InAs	InP	GaP
$a_0(\text{\AA})$	5.6533	5.6600	6.0584	5.8688	5.4505
$E_g(\text{eV})$	1.424	3.03	0.354	1.344	2.78
$\Delta(\text{eV})$	0.34	0.28	0.38	0.11	0.08
$E_{v,av}(\text{eV})$	-6.92	-7.49	-6.67	-7.04	-7.40
$E_p(\text{eV})$	25.7	21.1	22.2	20.7	22.2
$a_c(\text{eV})$	-7.17	-5.64	-5.08	-5.04	-7.14
$a_v(\text{eV})$	1.16	2.47	1.00	1.27	1.70
$b(\text{eV})$	-1.7	-1.5	-1.8	-1.7	-1.8
$d(\text{eV})$	-4.55	-3.4	-3.6	-5.6	-4.5
$C_{11}(10^{11}\text{dyne/cm}^2)$	11.879	12.5	8.329	10.11	14.05
$C_{12}(10^{11}\text{dyne/cm}^2)$	5.376	5.34	4.526	5.61	6.203
$C_{44}(10^{11}\text{dyne/cm}^2)$	5.94	5.42	3.96	4.56	7.033
m_e^*/m_0	0.067	0.15	0.023	0.077	0.25
m_{hh}^*/m_0	0.50	0.79	0.40	0.60	0.67
m_{lh}^*/m_0	0.087	0.15	0.026	0.12	0.17
$m_{hh,z}^*/m_0 = 1/(\gamma_1 - 2\gamma_2)$	0.333	0.478	0.263	0.606	0.326
$m_{lh,z}^*/m_0 = 1/(\gamma_1 + 2\gamma_2)$	0.094	0.208	0.027	0.121	0.199
γ_1	6.85	3.45	20.4	4.95	4.05
γ_2	2.1	0.68	8.3	1.65	0.49
γ_3	2.9	1.29	9.1	2.35	1.25

TABLE E.2: Important band structure parameters for wurtzite GaN, AlN and InN [61](p. 807)

Parameters	Materials		
	GaN	AlN	InN
$a(\text{\AA})$	3.189	3.112	3.545
$c(\text{\AA})$	5.185	4.982	5.703
$E_g(eV)$	3.44	6.16	0.64
$\Delta_{cr}(eV)$	0.010	-0.169	0.040
$\Delta_{so}(eV)$	0.017	0.019	0.005
m_e^{\parallel}/m_0	0.20	0.32	0.07
m_e^{\perp}/m_0	0.20	0.30	0.07
A_1	-7.21	-3.86	-8.21
A_2	-0.44	-0.25	-0.68
A_3	6.68	3.58	7.57
A_4	-3.46	-1.32	-5.23
A_5	-3.40	-1.47	-5.11
A_6	-4.90	-1.64	-5.96
$a_1(eV)$	-4.9	-3.4	-3.5
$a_2(eV)$	-11.3	-11.8	-3.5
D_1	-3.7	-17.1	-3.7
D_2	4.5	7.9	4.5
D_3	8.2	8.8	8.2
D_4	-4.1	-3.9	-4.1
D_5	-4.0	-3.4	-4.0
D_6	-5.5	-3.4	-5.5
C_{11} (GPa)	390	396	223
C_{12} (GPa)	145	137	115
C_{13} (GPa)	106	108	92
C_{33} (GPa)	398	373	224
C_{44} (GPa)	105	116	48

Appendix F

Notes on point group theory

In this Appendix we write a short note on point group theory and its consequences. Group theory properties related to $k \cdot p$ method found in Loehr book [55], a list of publications and explanations of symmetry properties is presented by Knox and Gold [78], the full group theory of solid state as provided by its elaborator Wigner [62], the properties of deformation and theory of invariants are described by Bir and Pikus [56].

Point group is a group of rotations and reflections leaving specific point invariant. The axes of rotations meet at this point and this point lies on the planes of reflections. All the point groups are the subgroups of three dimensional rotations and reflections.

The rotation axis, typically called as an axis of n -th order if it allows the rotation around the axis by the angle $2\pi k/n$ where $n \geq k$ and they are both integers. The two axes of point group are equivalent if the group contains an element, which translates one axis to the other. Two reflection planes are equivalent if the group contains similar translation element. Rotations of the same angle around equivalent axes or reflections in equivalent planes create class. Clockwise and counterclockwise rotations are of the same class if the axis of rotation lies in the plane of symmetry or group has one more turn to angle π around the axis, which is perpendicular to the given one. The core of classification of the point groups and their classes is the list of not equivalent axes and planes corresponding to a given symmetry.

It should be noted that in group theory there exist a variety of notations which makes it difficult to read. In our work we use Schoenflies notation for point groups and list them below.

C_n group is a cyclic group of the n -th order which includes rotations of angles $2\pi k/n$ around n -th order axis. It may be elaborated with horizontal symmetry plane, perpendicular to the axis of rotation (C_{nh}) or with the symmetry plane passing through the axis of rotation (C_{nv}) with both in the order of $2n$ ¹.

D_n group made by addition the 2-nd order axis to group C_n , where 2-nd order axis is perpendicular to n -th order axis.

T group - tetrahedron group consists of the symmetries of regular tetrahedron. It is included in so called cubic group, as the elements of cubic groups are taken directly from the elements of the symmetry of the cube. In particular, group T has second order axes passing through the centers of the opposite faces of the cube and third order axes are the diagonals of the cube. In total, group T has 12 elements.

T_d group is full tetrahedron group, which may be obtained from T group by addition of the symmetry planes with each of them include one 2-nd axis and one 3-rd order axis. Each of the planes includes two opposite edges of a cube and two diagonals connecting vertexes of these edges. The group T_d has 24 elements.

T_h group is a direct product of groups T and C_i ($T_h = T \times C_i$). It adds three more symmetry planes to T group, dividing cube to octants (1/8 part). The group T_h has 24 elements.

O group is a group of regular octahedron (two 4-face pyramids joined by bases) which consists of rotations translating octahedron into itself. It includes axes of cube: 4-th order axes passing through the centers of opposite faces of a cube, 3-rd order axes are the diagonals of a cube, 2-nd order axes are pass through the middles of the opposite edges. The group O has 24 elements.

O_h group is a full cubic group which includes all symmetries of a cube and is obtained as a direct product $O_h = O \times C_i$. It includes the elements of groups T_d and T_h . The group O_h has 48 elements.

¹There may be added a superscript such as C_{6v}^4 which is the index of space group, but in our discussion this index is useless.

Crystal has translation symmetry which restricts the types and quantity of symmetry axes in solid state. For crystal, the n -th order rotation axis with n taking $n = 1, 2, 3, 4, 6$ values only.

In the quantum mechanics, group theory comes from considering the symmetry group of the Hamiltonian, which is a set of all symmetry operations that do not change the functional form of the Hamiltonian. In solid state, the Hamiltonian depends only on the locations of atoms in crystal. The locations are invariant under the transformations of a crystal point group, so the Hamiltonian is also invariant under these transformations.

Mathematically, the group is a coordinate transformation \mathbf{T} that transform \vec{r} to another \vec{r}' set of coordinates $\mathbf{T}\vec{r} = \vec{r}'$. Explicitly the transformation \mathbf{T}_U of the group element U is 3×3 matrix. The symmetry operation τ_U on a function f is defined by:

$$\tau_U [f(\vec{r})] \equiv f(\mathbf{T}_U^{-1}\vec{r}) \quad (\text{F.1})$$

The symmetry operation applied on Hamiltonian:

$$\tau_U [H(\vec{r})] = H(\mathbf{T}_U^{-1}\vec{r}) = H(\vec{r}) \quad (\text{F.2})$$

If we apply the symmetry operation on the equation of the form:

$$H(\vec{r}) f(\vec{r}) = E f(\vec{r}) \quad (\text{F.3})$$

we obtain:

$$\tau_U [H(\vec{r}) f(\vec{r})] = E \tau_U [f(\vec{r})] \Rightarrow H(\vec{r}) f(\mathbf{T}_U^{-1}\vec{r}) = E f(\mathbf{T}_U^{-1}\vec{r}) \quad (\text{F.4})$$

Recall that new function $f(\mathbf{T}_U^{-1}\vec{r})$ as $g(\vec{r})$, so the f is transformed into g by the symmetry operation τ_U . Both functions f and g are the eigenfunctions of H with the same eigenvalue E , so now E is double degenerate.

A representation Γ of the group is a set of finite-dimensional square matrices $\Gamma(A), \Gamma(B), \dots$ that obey the same multiplication table as the corresponding group elements A, B, \dots . The dimension of representation is the dimension of its matrix. A representation is irreducible if no similarity transformation exists that simultaneously reduces all its matrices to a simpler block-diagonal form. Finite groups have a finite number of elements and have

finite number of distinct irreducible representations. Consider a particular l -dimensional representation $\Gamma^{(\nu)}$. A set of l independent functions $f_1^{(\nu)}, \dots, f_l^{(\nu)}$ are basis function for representation $\Gamma^{(\nu)}$ or belongs to $\Gamma^{(\nu)}$ or transforms like $\Gamma^{(\nu)}$ if for each element U of the group:

$$\tau_U \left[f_i^{(\nu)}(\vec{r}) \right] = \sum_{j=1}^l \Gamma_{ji}^{(\nu)}(U) f_j^{(\nu)}(\vec{r}) \quad (\text{F.5})$$

where $\Gamma_{ji}^{(\nu)}(U)$ is the ij -th element of matrix $\Gamma^{(\nu)}(U)$. The set of distinct irreducible representations of any group is complete, so any function h may be written as a sum of functions $f^{(\nu)}$, each belonging to a particular irreducible representation of the group:

$$h = \sum_{\nu} f^{(\nu)} \quad (\text{F.6})$$

The Hamiltonian H_0 (3.2) is the unperturbed Hamiltonian. The Schrödinger equation with this Hamiltonian gives the eigenfunctions u_{n0} and corresponding energies $E_n(0)$ at $\vec{k} = 0$, i.e. the band edge. The Hamiltonian H_0 has the symmetry of the crystal point group, therefore the zone center energies $E_n(0) \equiv E_n$ and wave functions $u_{n0} \equiv u_n$ must belong to one of the irreducible representations Γ_i of the crystal point group. But away from the band edge, the Hamiltonian (3.1) does not have the symmetry of the crystal point group since the energies $E_n(\vec{k})$ and wave functions $u_{n\vec{k}}$ do not belong to distinct point group representations.

We tabulate the representations of some point groups in tables F.1 and F.2². Here we should note that the notation of most authors of a group theory related works does not match with each other completely, which makes it very confusing and difficult to compare.

Zincblende elementary cell has a symmetry of a regular tetrahedron, but unlike diamond or rock salt it has no inversion symmetry, because it consists of two atoms, where anion and cation are different. Diamond structure has all atoms the same and therefore it has inversion symmetry. The diamond is described by point group O_h and zincblende is described by point group T_d . In the table F.1 the representations for diamond split the representations of zincblende into two separate representations of even and odd parity. The even parity is labeled with plus sign “+” and odd parity is labeled with minus sign “-”. T_d does not need to have parity defined and any linear combination of the even and

² J_z is pseudovector along z direction.

TABLE F.1: Representations for cubic crystals

T_d	O_h	Degeneracy	Basis functions
Γ_1	Γ_1^+	1	r^2
Γ_2	$\Gamma_{2'}^-$	1	xyz
	Γ_2^+		$x^4(y^2 - z^2) + y^4(z^2 - x^2) + z^4(x^2 - y^2)$
Γ_3	$\Gamma_{1'}^-$	2	$xyz[x^4(y^2 - z^2) + y^4(z^2 - x^2) + z^4(x^2 - y^2)]$
	Γ_{12}^+		$\{3z^2 - r^2, \sqrt{3}(x^2 - y^2)\}$
Γ_4	$\Gamma_{12'}^-$	3	$\{xyz(3z^2 - r^2), xyz\sqrt{3}(x^2 - y^2)\}$
	$\Gamma_{15'}^+$		$\{xy(x^2 - y^2), yz(y^2 - z^2), zx(z^2 - x^2)\}$
Γ_5	Γ_{25}^-	3	$\{z(x^2 - y^2), x(y^2 - z^2), y(z^2 - x^2)\}$
	$\Gamma_{25'}^+$		$\{xy, yz, zx\}$
	Γ_{15}^-		$\{x, y, z\}$

TABLE F.2: Representations for wurtzite crystals

C_{6v}	Basis functions
Γ_1	z
Γ_2	J_z
Γ_3	$x^3 - 3xy^2$
Γ_4	$y^3 - 3yx^2$
Γ_5	$\{x, y\}$
Γ_6	$\Gamma_3 \otimes \Gamma_5$

odd O_h representations forms a representation for T_d . Each representation possesses basis functions that transform into each other under the symmetry operations as the functions in the last column. From the careful comparison the experiment data and the theory it is established that in zincblende semiconductors conduction band edge belongs to Γ_1 representation and the valence band edge belongs to Γ_5 representation [79]. In diamond semiconductors, the conduction band edge has odd parity and valence band edge has even parity. The zincblende has not defined parity so there is some mixing of even parity into the conduction band and odd parity states into valence band which results in the asymmetry terms (B in eq. (4.41)), but the terms are small so we neglect them. As we neglect the asymmetry terms we assume that zincblende wave functions transform like diamond functions and have the same parity.

Wurtzite elementary cell has a C_{6v} symmetry of a regular hexagon with vertical axis. The representations for wurtzite are listed in table F.2 and from the table we can see that the representations for x, y and representation for z are separated. Vertical axis behaves as one dimensional Γ_1 representation, while the x, y axes have the basis of a special

form. The axes a_1, a_2 and a_3 of hexagon lie on the $x-y$ plane and have a symmetry of group C_3 . To obtain the behavior (the behavior means that functions will have the same transformations under operations of crystal point group, they do not have to be these actual functions) of basis for wurtzite we apply explicit form of group element C_3 [56] (table 11.1 - C_3 part) on \vec{r} :

$$\begin{bmatrix} x'' \\ y'' \\ z'' \end{bmatrix} = C_3 \begin{bmatrix} x \\ y \\ z \end{bmatrix} = \begin{bmatrix} \frac{1}{2} & \frac{\sqrt{3}}{2} & 0 \\ -\frac{\sqrt{3}}{2} & \frac{1}{2} & 0 \\ 0 & 0 & 1 \end{bmatrix} \begin{bmatrix} x \\ y \\ z \end{bmatrix} = \begin{bmatrix} \frac{1}{2}x + \frac{\sqrt{3}}{2}y \\ -\frac{\sqrt{3}}{2}x + \frac{1}{2}y \\ z \end{bmatrix} \quad (\text{F.7})$$

Under this basis the Hamiltonian is invariant under the symmetry operations of C_{6v} point group. C_3 matrix is obtained from matrix (4.17), which describes right-handed rotation around vertical axis, by reversing the angles to make it left-handed and substitute $\phi = 2\pi/3$.

Bibliography

- [1] C. A. Chang. Interface morphology of epitaxial growth of Ge on GaAs and GaAs on Ge by molecular beam epitaxy. *J. Appl. Phys.*, 53:1253–1255, 1982.
- [2] C. A. Chang. Interface morphology studies of (110) and (111) *Ge – GaAs* grown by molecular beam epitaxy. *Appl. Phys. Lett.*, 40:1037–1039, 1982.
- [3] S. L. Wright, H. Kroemer, and M. Inada. Molecular beam epitaxial growth of GaP on Si. *J. Appl. Phys.*, 55:2916–2927, 1984.
- [4] P. N. Uppal, H. Kroemer. Molecular beam epitaxial growth of GaAs on Si (211). *J. Appl. Phys.*, 58:2195–2203, 1985.
- [5] J. McKenna, F. K. Reinhart. Double-heterostructure *GaAs – Al_xGa_{1-x}As* [110] p-n-junction-diode modulator. *J. Appl. Phys.*, 47:2069–2078, 1976.
- [6] T. P. Pearsall, F. Capasso, R. E. Nahory, M. A. Pollack, J. R. Chelikowsky. The band structure dependence of impact ionization by hot carriers in semiconductors: GaAs. *Solid-State Electron.*, 21:297–302, 1978.
- [7] W. I. Wang. Novel crystal growth of AlGaAs/GaAs heterostructures on polar surfaces. *Surf. Sci.*, 174:31–37, 1986.
- [8] S. Subbanna, H. Kroemer, J. L. Merz. Molecular-beam-epitaxial growth and selected properties of GaAs layers and GaAs/(Al, Ga) As superlattices with the (211) orientation. *J. Appl. Phys.*, 59:488–494, 1986.
- [9] L. T. P. Allen, E. R. Weber, J. Washburn, Y. C. Pao. Device quality growth and characterization of (110) GaAs grown by molecular beam epitaxy. *Appl. Phys. Lett.*, 51:670–672, 1987.

- [10] T. Hayakawa, K. Takahashi, M. Kondo, T. Suyama, S. Yamamoto, T. Hijikata. Enhancement in optical transition in (111)-oriented GaAs-AlGaAs quantum well structures. *Phys. Rev. Lett.*, 60:349, 1988.
- [11] T. Hayakawa, K. Takahashi, M. Kondo, T. Suyama, S. Yamamoto, T. Hijikata. Observation of the 2s state excitons in (111)-oriented GaAs/Al_xGa_{1-x}As quantum-well structures. *Phys. Rev. B*, 38:1526, 1988.
- [12] L. W. Molenkamp, G. E. W. Bauer, R. Eppenga, C. T. Foxon. Exciton binding energy in (Al, Ga) As quantum wells: Effects of crystal orientation and envelope-function symmetry. *Phys. Rev. B*, 38:6147, 1988.
- [13] G. E. W. Bauer, T. Ando. Exciton mixing in quantum wells. *Phys. Rev. B*, 38:6015, 1988.
- [14] B. Gil, Y. El Khalifi, H. Mathieu, C. De Paris, J. Massies, G. Neu, T. Fukunaga, H. Nakashima. Line-shape analysis of the reflectivity spectra of GaAs/(Ga, Al) As single quantum wells grown on (001)-and (311)-oriented substrates. *Phys. Rev. B*, 41:2885, 1990.
- [15] Z. Y. Xu, Z. L. Yuan, J. Z. Xu, B. Z. Zheng, B. S. Wang, D. S. Jiang, R. Nötzel, K. Ploog. Exciton localization in corrugated GaAs/AlAs superlattices grown on (311) GaAs substrates. *Phys. Rev. B*, 51:7024, 1995.
- [16] M. Henini, S. Sanguinetti, L. Brusaferrri, E. Grilli, M. Guzzi, M. D. Upward, P. Moriarty, P. H. Beton. Structural and optical characterization of self-assembled InAs-GaAs quantum dots grown on high index surfaces. *Microelectron. J.*, 28:933–938, 1997.
- [17] A. Polimeni, A. Patane, M. Henini, L. Eaves, P. C. Main, S. Sanguinetti, M. Guzzi. Influence of high-index GaAs substrates on the growth of highly strained (InGa) As/GaAs heterostructures. *J. Cryst. Grow.*, 201:276–279, 1999.
- [18] R. Nötzel, K. H. Ploog. Quantum wires and quantum dots on high-index substrates. *Phys. E: Low-dimens. Syst. and Nanostruc.*, 8:117–124, 2000.
- [19] Y. F. Li, X. L. Ye, F. Q. Liu, B. Xu, D. Ding, W. H. Jiang, Z. Z. Sun, H. Y. Liu, Y. C. Zhang, Z. G. Wang. Structural and optical characterization of InAs nanostructures grown on (001) and high index InP substrates. *Appl. Surf. Sci.*, 167:191–196, 2000.

- [20] S. L. S. Freire, J. E. T. Reis, L. A. Cury, F. M. Matinaga, J. F. Sampaio, F. E. G. Guimaraes. Optical studies of strain effects in quantum wells grown on (311) and (100) GaAs substrates. *Phys. Rev. B*, 64:195325, 2001.
- [21] S. Tomić, E. P. O'Reilly. Gain characteristics of ideal dilute nitride quantum well lasers. *Phys. E: Low-dimens. Syst. and Nanostruc.*, 13:1102–1105, 2002.
- [22] S. Tomić, E. P. O'Reilly, R. Fehse, S. J. Sweeney, A. R. Adams, A. D. Andreev, S. A. Choulis, T. J. C. Hosea, and H. Riechert. Theoretical and experimental analysis of 1.3- μm InGaAsN/GaAs lasers. *J. of Sel. Top. in Quantum Electron., IEEE*, 9: 1228–1238, 2003.
- [23] J. Ibáñez, R. Kudrawiec, J. Misiewicz, M. Schmidbauer, M. Henini, M. Hopkinson. Nitrogen incorporation into strained (In, Ga)(As, N) thin films grown on (100),(511),(411),(311), and (111) GaAs substrates studied by photoreflectance spectroscopy and high-resolution x-ray diffraction. *J. Appl. Phys.*, 100:093522, 2006.
- [24] S. Blanc, A. Arnoult, H. Carrere, C. Fontaine. GaAsN and GaInAsN/GaAs quantum wells grown on $\{111\}$ substrates: growth conditions and optical properties. *Phys. E: Low-dimens. Syst. and Nanostruc.*, 17:252–254, 2003.
- [25] J. Miguel-Sánchez, A. Guzmán, J. M. Ulloa, A. Hierro, E. Muñoz. Effect of nitrogen on the optical properties of InGaAsN pin structures grown on misoriented (111) B GaAs substrates. *Appl. Phys. Lett.*, 84:2524–2526, 2004.
- [26] J. Miguel-Sánchez, A. Guzmán, J. M. Ulloa, M. Montes, A. Hierro, E. Muñoz. Room-temperature laser emission of GaInNAs-GaAs quantum wells grown on GaAs (111) B. *Photon. Tech. Lett., IEEE*, 17:2271–2273, 2005.
- [27] J. Miguel-Sánchez, A. Guzmán, J. M. Ulloa, M. Montes, A. Hierro, E. Muñoz. MBE growth and processing of diluted nitride quantum well lasers on GaAs (111) B. *Microelectron. J.*, 37:1442–1445, 2006.
- [28] M. Latkowska, R. Kudrawiec, G. Sęk, J. Misiewicz, J. Ibanez, M. Hopkinson, M. Henini. Micro-photoluminescence of GaInNAs layers grown on GaAs substrates of various crystallographic orientations. *Phys. Status Solidi*, 8:1655–1658, 2011.
- [29] S. L. Chuang, C. S. Chang. k-p method for strained wurtzite semiconductors. *Phys. Rev. B*, 54:2491–2504, 1996.

-
- [30] S. L. Chuang, C. S. Chang. A band-structure model of strained quantum-well wurtzite semiconductors. *Semicond. Sci. Technol.*, 12:252–263, 1996.
- [31] S. L. Chuang. Optical gain of strained wurtzite GaN quantum-well lasers. *J. Quantum Electron.*, 32:1791–1800, 1996.
- [32] S.-H. Park and S. L. Chuang. Crystal-orientation effects on the piezoelectric field and electronic properties of strained wurtzite semiconductors. *Phys. Rev. B*, 59:4725–4737, 1999.
- [33] F. Mireles, S. E. Ulloa. Strain and crystallographic orientation effects on the valence subbands of wurtzite quantum wells. *Phys. Rev. B*, 62:2562–2572, 2000.
- [34] S.-H. Park, S. L. Chuang. Crystal orientation dependence of many-body optical gain in wurtzite GaN/AlGa_N quantum-well lasers. *Semicond. Sci. Technol.*, 17:686–691, 2002.
- [35] S.-H. Park, D. Ahn. Crystal orientation effects on electronic and optical properties of the wurtzite ZnO/MgZnO quantum well lasers. *Opt. Quantum Electron.*, 38:935–952, 2006.
- [36] S.-H. Park, D. Ahn. Electronic and optical properties of a- and m-plane wurtzite InGa_N-Ga_N quantum wells. *J. Quantum Electron.*, 43:1175–1182, 2007.
- [37] K. H. Yoo, J. D. Albrecht, L. R. Ram-Mohan. Strain in layered zinc blende and wurtzite semiconductor structures grown along arbitrary crystallographic directions. *Am. J. Phys.*, 78:589–597, 2010.
- [38] P. Waltereit, O. Brandt, A. Trampert, H. T. Grahn, J. Menniger, M. Ramsteiner, M. Reiche, K. H. Ploog. Nitride semiconductors free of electrostatic fields for efficient white light-emitting diodes. *Nature*, 406:865–868, 2000.
- [39] Y. J. Sun, O. Brandt, S. Cronenberg, S. Dhar, H. T. Grahn, K. H. Ploog, P. Waltereit, J. S. Speck. Nonpolar $In_xGa_{1-x}N/GaN$ ($1\bar{1}00$) multiple quantum wells grown on $\gamma - LiAlO_2$ (100) by plasma-assisted molecular-beam epitaxy. *Phys. Rev. B*, 67:041306, 2003.
- [40] H. M. Ng. Molecular-beam epitaxy of $GaN/Al_xGa_{1-x}N$ multiple quantum wells on R-plane ($10\bar{2}2$) sapphire substrates. *Appl. Phys. Lett.*, 80:4369–4371, 2002.

-
- [41] M. D. Craven, P. Waltereit, F. Wu, J. S. Speck, S. P. DenBaars, Steven P. Characterization of a-plane GaN/(Al, Ga) N multiple quantum wells grown via metalorganic chemical vapor deposition. *Jap. J. Appl. Phys.*, 42:L235, 2003.
- [42] A. Chitnis, C. Chen, V. Adivarahan, M. Shatalov, E. Kuokstis, V. Mandavilli, J. Yang, M. A. Khan. Visible light-emitting diodes using a-plane GaN–InGaN multiple quantum wells over r-plane sapphire. *Appl. Phys. Lett.*, 84:3663–3665, 2004.
- [43] K. Domen, K. Horino, A. Kuramata, T. Tanahashi. Optical gain for wurtzite GaN with anisotropic strain in c plane. *Appl. Phys. Lett.*, 70:987–989, 1997.
- [44] J.-B. Xia. Effective-mass theory for superlattices grown on (11N)-oriented substrates. *Phys. Rev. B*, 43:9856–9864, 1991.
- [45] W.-H. Seo and J. F. Donegan. 6×6 effective mass Hamiltonian for heterostructures grown on (11N)-oriented substrates. *Phys. Rev. B*, 68:075318, 2003.
- [46] W. J. Fan. Orientational dependence of electronic structure and optical gain of (11N)-oriented III-V-N quantum wells. *J. Appl. Phys.*, 113:83102, 2013.
- [47] C. A. Broderick, M. Usman, E. P. O’Reilly. Derivation of 12-and 14-band $k \cdot p$ Hamiltonians for dilute bismide and bismide-nitride semiconductors. *Semicond. Sci. Tech.*, 28:125025, 2013.
- [48] M. Gladysiewicz, R. Kudrawiec, M. S. Wartak. 8-band and 14-band kp modeling of electronic band structure and material gain in Ga (In) AsBi quantum wells grown on GaAs and InP substrates. *J. Appl. Phys.*, 118:055702, 2015.
- [49] E. O. Kane. Band structure of indium antimonide. *J. Phys. Chem. Solids*, 1:249–261, 1957.
- [50] P. Y. Yu, M. Cardona. *Fundamentals of Semiconductors: Physics And Materials Properties, Volume 3*. Springer, Berlin, 2005.
- [51] P. Löwdin. A note on the quantum-mechanical perturbation theory. *J. Chem. Phys.*, 19:1396–1401, 1951.
- [52] I. M. Tsidilkovski. *Band structure of semiconductors*. Pergamon Press, Oxford, 1982.

-
- [53] G. L. Bir and G. E. Pikus. Effects of deformation on the hole energy spectrum of germanium and silicon. *Sov. Phys. Solid State*, 1:1502–1517, 1960.
- [54] Y. Sun, S. E. Thompson, T. Nishida. *Strain Effect in Semiconductors: Theory and Device Applications*. Springer, New York, 2010.
- [55] John P. Loehr. *Physics of strained quantum well lasers*. Kluwer, Boston, 1998.
- [56] G. L. Bir and G. E. Pikus. *Symmetry and Strain-induced Effects in Semiconductors*. Wiley, New York, 1974.
- [57] J. F. Nye. *Physical properties of crystals: their representation by tensors and matrices*. Clarendon Press, Oxford, 1985.
- [58] W. Voigt. *Lehrbuch der Kristallphysik: mit Ausschluss der Kristalloptik*. B.G. Teubner, Leipzig, Berlin, 1910.
- [59] J. M. Luttinger. Quantum Theory of Cyclotron Resonance in Semiconductors: General Theory. *Phys. Rev.*, 102:1030–1041, 1956.
- [60] G. A. Korn and T. M. Korn. *Mathematical handbook for scientists and engineers: definitions, theorems, and formulas for reference and review*. McGraw-Hill, New York, 1968.
- [61] S. L. Chuang. *Physics of photonic devices*. Wiley, New Jersey, 2nd edition, 2009.
- [62] E. P. Wigner. *Group theory and its application to the quantum mechanics of atomic spectra*. Academic Press, New York, expanded and improved edition, 1959.
- [63] T. B. Bahder. Eight-band kp model of strained zinc-blende crystals. *Phys. Rev. B*, 41:11992–12001, 1990.
- [64] T. E. Ostromek. Evaluation of matrix elements of the 8x8 kp Hamiltonian with k-dependent spin-orbit contributions for the zinc-blende structure of GaAs. *Phys. Rev. B*, 54:14467–14479, 1996.
- [65] C. R. Pidgeon and R. N. Brown. Interband magneto-absorption and Faraday rotation in InSb. *Phys. Rev.*, 146:575–583, 1966.

- [66] M. Gladysiewicz, R. Kudrawiec, J. M. Miloszewski, P. Weetman, J. Misiewicz and M. S. Wartak. Band structure and the optical gain of GaInNAs/GaAs quantum wells modeled within 10-band and 8-band kp model. *J. Appl. Phys.*, 113:63514, 2013.
- [67] S. Tomić. Electronic structure of $In_yGa_{1-y}As_{1-x}N_x/GaAs(N)$ quantum dots by ten-band $k \cdot p$ theory. *Phys. Rev. B*, 73:125348, 2006.
- [68] R. H. Henderson and E. Towe. Strain and crystallographic orientation effects on interband optical matrix elements and band gaps of [111]-oriented III-V epilayers. *J. Appl. Phys.*, 78:2447–2455, 1995.
- [69] L. Vegard. Die Konstitution der Mischkristalle und die Raumfüllung der Atome. *Zeitschrift für Physik*, 5:17–26, 1921.
- [70] C. G. Van de Walle and R. M. Martin. Theoretical calculations of semiconductor heterojunction discontinuities. *J. Vac. Sci. Technol. B*, 4:1055–1059, 1986.
- [71] C. G. Van de Walle and R. M. Martin. Theoretical study of band offsets at semiconductor interfaces. *Phys. Rev. B*, 35:8154–8165, 1987.
- [72] C. G. Van de Walle, K. Shahzad, and D. J. Olego. Strained-layer interfaces between II-VI compound semiconductors. *J. Vac. Sci. Technol. B*, 6:1350–1353, 1988.
- [73] C. G. Van de Walle. Band lineups and deformation potentials in the model-solid theory. *Phys. Rev. B*, 39:1871–1883, 1989.
- [74] S. T. Ng, W. J. Fan, Y. X. Dang, S. F. Yoon. Comparison of electronic band structure and optical transparency conditions of $In_xGa_{1-x}As_{1-y}N_y/GaAs$ quantum wells calculated by 10-band, 8-band, and 6-band k·p models. *Phys. Rev. B*, 72:115341, 2005.
- [75] M. Gladysiewicz, I. Ivashev, M. S. Wartak. Theoretical investigations of optical properties of Ga(In)AsBi quantum well systems using 8-band and 14-band models. *Proc. SPIE*, 9742:974218, 2016.
- [76] N. W. Ashcroft, N. D. Mermin. *Solid state physics*. Holt, Rinehart and Winston, 1976.
- [77] M. Asada, A. Kameyama, and Y. Suematsu. Gain and intervalence band absorption in quantum-well lasers. *J. of Quantum Electron., IEEE*, 20:745–753, 1984.

- [78] R. S. Knox and A. Gold. *Symmetry in the solid state*. W. A. Benjamin, New York, 1964.
- [79] G. Dresselhaus, A. F. Kip, and C. Kittel. Cyclotron resonance of electrons and holes in silicon and germanium crystals. *Phys. Rev.*, 98:368–384, 1955.